Diverse Mechanisms of Regulating the Mitotic Cell Cycle

Thesis by

Wenying Shou

In Partial Fulfillment of the Requirements

For the Degree of

Doctor of Philosophy

California Institute of Technology

Pasadena, California

May 16, 2001

To my parents and Pomona College

with love

Acknowledgements

HHMI, NIH, and the Division of Biology financially supported my graduate work.

I thank the many people who have shaped me during my graduate life at Caltech. My advisors Ray Deshaies and Bill Dunphy contributed enormously to my scientific maturity. Initial rigorous training at Dunphy Lab enabled me to rapidly acquire many critical molecular biology and biochemistry skills, and my first paper was born shortly afterwards. Later training at Deshaies Lab further transformed me into a combination of geneticist and biochemist. In addition to providing incessant "what's new" reminders, 100 potential models, brilliant insights, and pivotal support to my work, Ray has also taught me many things beyond science, including making slides, giving talks, putting a spin on a paper, dealing with collaborators, handling students, backpacking, and investment "strategies" that I'll be many years in remembrance. I am very privileged to have worked with both of them.

Professors on my committee have all given me their time and insight: I have discussed ideas with Barbara Wold, Paul Sternberg, and Elliot Meyerowitz, and learned in situ hybridization from David Anderson's lab. Though not on my committee, Bruce Hay, Kai Zinn, Mel Simon, David Chan, Ed Lewis, and Ray Owen have all helped me. I want to thank Bruce in particular for his insights and encouragement.

Many colleagues have influenced or contributed to my research. Akiko Kumagai and Paul Mueller from Dunphy lab and Rati Verma from Deshaies lab have contributed the most to my experimental style and skills. By revising my HHMI predoctoral fellowship essay, Renny Feldman taught me an invaluable lesson on how to write a proposal. It is a great pleasure to form collaborations with Jae Hong Seol, and labs of H. Charbonneau, D. Moazed, A. Schevchenco, M. Nomura, and S. Carr. I loved working with Mitotic Exit Network (MEN) consortium members, especially Ramzi Azzam and Kathleen Sakamoto, and greatly appreciate the help of two technicians – Bill Reynolds and Greg Reynard. Members of Deshaies Lab have also been consistently putting up with me.

Friends at Caltech have made my life more colorful: John DeModena and Te-Yi Kung brought me food, juice, and cheers; Rati Verma took me out for delicious Indian lunches, and Yong Chi gave me rides to Chinese stores.

Special thanks to my adorable pet pig Dill, and to my sister Yan and brother Frank for the many tears and laughter and dreams that we shared.

Finally, many thanks to Mom and Dad – my first teachers of sciences and literature - for their love, support, and insight, and to my alma mater Pomona College – for accepting an imperfect me, giving me an opportunity to study in the US, supporting me with a full scholarship, and spoiling me with superb lectures.

Abstract

The mitotic cell cycle – a process in which one cell divides into two - is carefully regulated in response to signals. Organisms as diverse as yeast and human all drive their cell cycles by turning cyclin-dependent kinases (Cdks) on and off. We have examined Cdk regulation in two systems. First, we isolated a relatively general Cdk inhibitor (CKI) $p28^{Kix1}$ in *Xenopus laevis*. $p28^{Kix1}$ binds to and directly inhibits multiple Cdks, and retards DNA replication and mitosis when added to *Xenopus* egg extracts. Remarkably, the protein level of $p28^{Kix1}$ is dramatically upregulated around late gastrulation, suggesting that it is induced in response to a developmental signal and in turn functions to establish a somatic type of cell cycle. Second, we examined how Cdk inactivation is achieved during mitotic exit in the yeast *S. cerevisiae*. We found that mutants in at least six linkage groups bypassed the mitotic arrest in *cdc15Δ* cells. The *net1-1* mutant was studied further. Net1 inhibits mitotic exit by inhibiting Cdc14, an essential protein phosphatase, using two parallel mechanisms: by binding and inactivating Cdc14, and by tethering Cdc14 to the nucleolus. Correct orientation of the mitotic spindle activates Cdc15, which evicts Cdc14 from the nucleolus into the entire cell. Cdc14 subsequently inactivates Cdks by promoting cyclin degradation and CKI induction, and mitotic exit ensues. Unexpectedly, Net1 also regulates the structure and function of the nucleolus: it tethers the transcriptional silencing protein Sir2 to the nucleolus, regulates proper localization of multiple nucleolar antigens and rDNA morphology, and directly binds to and stimulates the activity of RNA Pol I. In summary, we observe that different signals regulate cell cycle progression by controlling Cdk activity, that cell cycle regulators may play important roles in other biological processes, and that localization of a protein to a subcellular structure could imply that it is sequestered instead of employed there.

Table of Contents

Chapter I – Introduction: Cell Cycle Progression and its Regulation

Overview: Cyclin-dependent kinases drive cell cycle transitions

Cell cycle progression is orchestrated by the oscillating activities of the cyclin-dependent kinases (Cdks), each containing a catalytic subunit (Cdk) and a regulatory partner (cyclin). In the budding yeast *S. cerevisiae*, a single Cdk (Cdc28) controls all cell cycle stages by complexing initially with G1 cyclins (Clns1– 3), followed by S cyclins (Clbs 5 and 6), and finally with mitotic cyclins (Clbs 1 – 4) (reviewed by Deshaies, 1997). Mammalian cells have adopted a more elaborate system of Cdks: Cdk4 and Cdk6 complexed with D-type cyclins (D1, D2, and D3) promote passage through START and entry into a new cell cycle; Cdk2 partnered with cyclins E and A promote G1/S transition and S phase progression; and finally, Cdc2/cyclin B catalyzes mitosis and its inactivation promotes mitotic exit (for reviews, see Coleman and Dunphy, 1994; Sherr and Roberts, 1999).

Cdk activities are strictly regulated to ensure that a cell undergoes cell division cycles only under the appropriate circumstances and that the division cycle is executed with high precision. The Cdks are regulated by at least three distinct mechanisms: cyclin binding and degradation, subunit phosphorylations that either activate or inactivate the Cdks, and association with Cdk inhibitors. This thesis focuses on 1. how $p28^{Kix1}$, a *Xenopus* Cdk inhibitor, slows down cell cycle progression; 2. how cyclin degradation and Cdk inhibitor induction are regulated during mitotic exit in *S. cerevisiae*; and 3. how does

Net1, a regulator of mitotic exit in yeast, is intimately involved in the regulation of the structure and function of the nucleolus.

Cdk inhibitors

Cdk inhibitors in mammalian cells

To date, two families of Cdk inhibitors have been identified in mammalian cells (for review, see Sherr and Roberts, 1999). The INK4 (Inhibitors of Cdk4) family includes $p16^{INK4a}$ (Serrano *et al.*, 1993), $p15^{INK4b}$ (Hannon and Beach, 1994), $p18^{INK4c}$ (Guan *et al.*, 1994), and $p19^{INK4d}$ (Chan *et al.*, 1995). Ink4 proteins have multiple ankryin repeats, and exclusively associate with and inhibit D-type Cdks, and appear to play a role in cellular differentiation and tumor suppression (reviewed in Elledge and Harper, 1994). D-type Cdks phosphorylate and consequently inactivate Rb, a major tumor suppressor protein. Thus, by inhibiting D-type Cdks, INK proteins allow Rb to exert its growth suppression functions such as sequestering E2F family transcription factors in an inactive state (for a review, see Dyson, 1998).

The Cip/Kip family of Cdk inhibitors include p21 (also known as CIP1, WAF1, CAP20, SDI1) (El-Deiry *et al.*, 1993; Gu *et al.*, 1993; Harper *et al.*, 1993; Xiong *et al.*, 1993; Noda *et al.*, 1994), $p27^{Kip1}$(Polyak *et al*, 1994a, b; Toyoshima and Hunter, 1994), and $p57^{Kip2}$ (Lee *et al.*, 1995; Matsuoka *et al.*, 1995). The N-terminal regions of these three proteins share a Cdk inhibition domain which binds to and inhibits Cdk2/cyclin E, Cdk2/cyclin A, and, to a lesser extent, Cdk4/cyclin D and Cdc2/cyclin B. Except for a bipartite nuclear localization signal, the C-terminal domains of these proteins are not

strongly conserved: $p21^{Cip1}$ binds proliferating cell nuclear antigen (PCNA, a DNA polymerase δ-subunit), while $p27^{Kip1}$ and $p57^{Kip2}$ do not (Waga *et al.*, 1994; Chen *et al.*, 1995; Luo *et al.*, 1995). The structural diversity among $p21^{Cip1}$, $p27^{Kip1}$, and $p57^{Kip2}$ suggests that these proteins may play distinct roles in cell cycle regulation.

Interestingly, p21 and p27 are not strict Cdk inhibitors. cyclin D – Cdks not only are relatively resistant to inhibition by p21 and p27, but also depend on p21 and p27 for efficient assembly *in vitro* (Labaer et al., 1997). In mouse embryo fibroblast cells from animals lacking both p21 and p27, the level of cyclin D1/Cdk complex was reduced by more than 10 fold, and immunoprecipitable cyclin D-Cdk - dependent kinase activity toward Rb was undetectable (Cheng et al., 1999). However, the reduction in D-type Cdk activity had no overall effect on the cell cycle, presumably due to compensation by elevated E- and A- types of Cdks. Thus, the significance of D-type Cdk assembly activity of p21 and p27 is still unclear.

$p21^{Cip1}$ transmits various growth inhibitory signals to the cell cycle engine. p21 mRNA levels are up-regulated by the tumor suppressor protein p53 following radiation-induced DNA damage (El-Deiry *et al.*, 1993). By inhibiting Cdk2/cyclin E, p21 blocks S phase initiation and progression. Although the C-terminal domain of p21 associates with PCNA and blocks PCNA-dependent DNA replication, it does not inhibit PCNA-dependent DNA repair (Li *et al.*, 1994). Thus, irradiated cells arrest in G1 and repair their DNA. Consistent with these observations, embryonic fibroblasts derived from $p21^{-/-}$ mice are significantly deficient in their ability to arrest in G1 in response to DNA damage (Deng *et al.*, 1995). Besides playing a role in the G1 checkpoint, p21 may also

be involved in cellular differentiation under normal circumstances. For example, MyoD, a skeletal-muscle-specific transcriptional regulator, activates the expression of p21 during differentiation in a p53-independent fashion (Halevy *et al.*, 1995). However, $p21^{-/-}$ mice undergo normal development, and do not develop spontaneous tumors (Deng *et al.*, 1995), implying the existence of redundant pathways that ensure proper development and tumor prevention in this organism.

$P27^{Kip1}$ responds to a variety of signals, depending on the cell type. For example, in TGFβ-arrested or contact-inhibited mink epithelial cells, p27 dissociates from Cdk4/cyclin D, and binds to and prevents activation of Cdk2/cyclin E (Polyak *et al.*, 1994a and b). In macrophages, cAMP exerts its anti-mitogenic effects by raising the level of p27 (Kato *et al.*, 1994). Mice lacking p27 display enhanced growth, multiple organ hyperplasia, and pituitary tumors (Fero et al., 1996; Kiyokawa et al., 1996; Nakayama et al., 1996). In addition, low expression of p27 occurs frequently in many types of human tumors, and correlates strongly with tumor aggression (reviewed in Tsihlias et al., 1999). These observations point to a critical role of p27 in tumor suppression, at least in certain cell types.

The functions of $p57^{Kip2}$ are still enigmatic. Most $p57^{Kip2}$ null mice die after birth, and display severe developmental defects associated with extensive apoptosis (Yan et al., 1997; Zhang et al., 1997). However, $p57^{Kip2}$ mutant mice show no neoplastic development (Yan et al., 1997), and embryonic fibroblasts prepared from $p57^{Kip2}$-deficient mice showed no differences in the proliferation rate and saturation density (Takahashi et al., 2000). It is still debatable if $p57^{Kip2}$ is a tumor suppressor.

Cdk inhibitors in yeast

Yeast also utilizes Cdk inhibitors to regulate Cdk activities. Two Cdk inhibitors from *S. cerevisiae* (the Cdc28/Cln inhibitor Far1 and the Cdc28/Clb2,5,6 inhibitor Sic1) and one from *S. pombe* (the Cdc2/Cdc13 inhibitor Rum1) have been identified, but these show little homology with p15/p16 or p21/p27 Cdk inhibitors (for review, see Elledge and Harper, 1994).

Although considerable information about Cdk inhibitors has emerged recently, much remains to be learned about the evolution of these families, the diversity of their functions, and the mechanisms of their regulation. The isolation and characterization of $p28^{Kix1}$, a new member of the Cip/Kip family Cdk inhibitors, is reported in Chapter II.

Exit from mitosis in the budding yeast *S. cerevisiae*

Inactivation of mitotic Cdk activities lies at the heart of mitotic exit

Mitotic exit, the transition from anaphase to G1, is realized when mitotic Cdk activity is eliminated. In the budding yeast, mitotic Cdks consist of the Cdc28 kinase complexed with mitotic cyclins Clbs 1-4. Proteolysis of the major mitotic cyclin Clb2 and/or accumulation of the Cdc28/Clb inhibitor Sic1 is sufficient to inactivate Cdc28 and to promote transition to G1 (Schwab et al., 1997; Visintin et al., 1998).

Clb2 proteolysis occurs in two stages: at the metaphase-anaphase transition and at the mitotic exit. Anaphase Promoting Complex/Cyclosome ubiquitin ligase (APC/C)

complexed with activator Cdc20 (APC^{Cdc20}) initiates Clb2 ubiquitination at metaphase when the level of Clb2 is high, whereas APC^{Hct1} ubiquitinates the residual amount of Clb2 at mitotic exit (Yeong et al., 2000; Baumer et al., 2000). Ubiquitinated Clb2 is targeted to the 26S proteasome for degradation. Sic1 accumulation in late mitosis requires resumption of transcription mediated by the Swi5 transcription factor and protection of Sic1 from the constitutively active SCF^{Cdc4} ubiquitin ligase (reviewed by Deshaies, 1999).

Cells devoid of Hct1/Cdh1 fail to completely degrade Clb2 but are viable (Schwab et al., 1997; Visintin et al., 1997), probably because Sic1 accumulates and turns off Cdc28 activity. Whereas cells devoid of Sic1 can degrade Clb2 and exit mitosis, cells devoid of both Hct1 and Sic1 are inviable, presumably due to their inability to extinguish Cdc28 activity during mitotic exit (Schwab et al., 1997).

The mitotic exit network (MEN) is required for exit from mitosis

The mitotic exit network (MEN) plays a pivotal role in exit from mitosis. Identified components of MEN include *TEM1*, *LTE1*, *CDC15*, *DBF2/DBF20*, *CDC5*, *MOB1*, *CDC14*, and *NUD1* (reviewed in Deshaies, 1997; Luca and Winey, 1998; Gruneberg et al., 2000). When cells that harbor conditional-lethal temperature-sensitive (ts) mutations in any of these genes are shifted to the restrictive temperature, they uniformly arrest in late anaphase/telophase as large-budded cells with segregated chromosomes, fully elongated microtubule spindles, and in all tested cases, elevated Cdc28/Clb2 protein kinase activity. Clb2 proteolysis is not completed, and *SIC1*

transcripts and protein fail to accumulate to high levels (Surana et al., 1993; Shirayama et al., 1994b; Toyn and Johnston, 1994; Irniger et al., 1995; Charles et al., 1998; Jaspersen et al., 1998; Visintin et al., 1998). Furthermore, manipulation of Sic1 and Clb2 levels has dramatic effects on these mutants (Donovan et al., 1994; Shirayama et al., 1994b; Toyn et al., 1997; Charles et al., 1998; Jaspersen et al., 1998): overexpression of Clb2 or deletion of Sic1 typically exacerbates their phenotype, whereas overexpression of Sic1 has the opposite effect (reviewed by Morgan, 1999).

Most of these proteins required for exit from mitosis resemble components of signaling pathways: Tem1 is a GTP-binding protein (Shirayama et al., 1994b), *LTE1* encodes a putative guanine nucleotide exchange factor (Shirayama et al., 1994a), Dbf2/Dbf20, Cdc15, and Cdc5 are protein kinases (Toyn and Johnston, 1994; Jaspersen et al., 1998; Hardy and Pautz, 1996), Mob1 is a novel protein that associates with Dbf2 (Komarnitsky et al., 1998; Luca and Winey, 1998) and Cdc14 is a dual specificity protein phosphatase (Taylor et al., 1997). Consistent with the notion that these proteins constitute elements of a signaling pathway, the corresponding genes display a variety of genetic interactions with each other (Parkes and Johnston, 1992; Kitada et al., 1993; Shirayama et al., 1994b; Shirayama et al., 1996; Jaspersen et al., 1998; Komarnitsky et al., 1998; Luca and Winey, 1998; Visintin et al., 1998).

cAMP and PKA negatively regulate mitotic exit. Lowering cAMP levels is sufficient to allow *cdc5*, *cdc15* and *dbf2* cells to exit mitosis (Spevak et al., 1993; Anghileri et al., 1999; Irniger et al., 2000). How does PKA inhibit mitotic exit? One possibility is that PKA inactivates APC through phosphorylation, and this inhibition is

dominant over APC activation by the Polo kinase Cdc5 (Kotani et al., 1998). Thus, by preventing the degradation of mitotic cyclins, PKA holds cells hostage in late mitosis.

Recent work suggests that the protein phosphatase Cdc14 might act directly on cell cycle regulators to promote mitotic exit. First, overexpression of Cdc14 can activate ectopic degradation of Clb2 and accumulation of Sic1 (Visintin et al., 1998). Second, mutation of Cdk consensus phosphorylation sites in Swi5 and Hct1 activates their ability to promote *SIC1* transcription and Clb2 degradation, respectively (Moll et al., 1991; Zachariae et al., 1998), and Cdc14 antagonizes the phosphorylation of both proteins (Visintin et al., 1998; Jaspersen et al., 1999). These data suggest that Cdc14 is required to dephosphorylate Swi5 and Hct1 as cells exit mitosis. However, how MEN is organized and regulated is largely unknown.

Multiple checkpoint pathways control MEN

The DNA damage checkpoint and the spindle position checkpoint pathways have recently been demonstrated to inhibit mitotic exit.

After cells suffered DNA damage in mitosis, multiple pathways are activated to delay cell cycle progression. First, Pds1, an anaphase inhibitor (Yamamoto et al., 1996), is stabilized (Sanchez et al., 1999; Tinker-Kulberg and Morgan, 1999). Pds1 inhibits anaphase by sequestering Esp1, a protease that promotes sister chromosome segregation by cleaving cohesins that "glue" sister chromosomes together (reviewed by Nasmyth et al., 2000). In addition, if DNA damages occurred in late mitosis, cells would respond by increasing the protein level of Pds1, which inhibits Clb2 degradation and Sic1

accumulation and thereby blocks mitotic exit (Tinker-Kulberg and Morgan, 1999; Cohen-Fix and Koshland, 1999). Second, Cdc5, a polo – kinase in MEN, is inactivated (Sanchez et al., 1999). By inactivating Cdc5, both anaphase entry and mitotic exit are inhibited (Song and Lee, 2001, and references therein). Interestingly, Plk1, a mouse homologue of Cdc5, is also inhibited after DNA damage (Smits et al., 2000). Third, Clb5, an S-phase cyclin, is stabilized (Germain et al., 1997). Cdc28/Clb5 inhibits mitotic exit by counteracting Cdc14, the most downstream member of MEN (Shirayama et al., 1999), and *clb5Δclb6Δ* cells are hypersensitive to DNA damage (Meyn and Holoway, 2000). Fourth, the two-component GTPase-activating protein Bub2/Bfa1 inactivates Tem1, the Ras-like GTP-binding protein in MEN, and *bub2Δ bfa1Δ* cells exit mitosis despite DNA damage (Wang et al., 2000). The combined efforts of multiple pathways ensure that cells do not exit mitosis when their DNA has been damaged.

Spindle orientation also plays a critical role in signaling mitotic exit. In order to distribute sister chromosomes equally between the mother and the daughter cells, the mitotic spindle has to thrust through the mother-daughter neck. If the mitotic spindle lingers within the mother cell, then cells undergo nuclear division but not mitotic exit (Yeh et al., 1995). How do cells monitor whether the mitotic spindle has aligned properly? Recent studies have shown that Bub2/Bfa1 anchors Tem1 to the cytoplasmic face of the spindle pole body (the yeast equivalent of centrosome) that enters the daughter cell, and presumably keeps Tem1 in an inactive state. The guanine nucleotide exchange factor Lte1 is localized in the daughter cell, and is likely to activate Tem1 once Tem1 on the spindle pole body is sent into the daughter cell (Bardin et al., 2000; Pereira et al.,

2000). However, it is surprising that Lte1 is only essential at cold temperature, suggesting that alternative pathways relieve the inhibition of Tem1 by Bub2/Bfa1 at mitotic exit (Shirayama et al., 1994a).

Proteins of the mitotic exit network also regulate cytokinesis

In the fission yeast *S. pombe*, the SIN (Septation INitiation) pathway promotes cytokinesis and septum formation. SIN and MEN share striking similarity: *spg1*, *plo1*, *cdc7*, *sid2*, *mob1*, *clp1*, *byr4* and *cdc16* in *S.pombe* are homologous to *TEM1*, *CDC5*, *CDC15*, *DBF2*, *MOB1*, *CDC14*, *BFA1* and *BUB2* in *S. cerevisiae*, respectively (reviewed by McCollum and Gould, 2001). The phenotypes of SIN mutants are: normal assembly of the medial ring, but failure to initiate ring contraction and septum formation. This raises the possibility that MEN may also play an active role in cytokinesis. In fact, *cdc15(lyt1)* cells form long chains indicative of multiple rounds of cell cycle without cytokinesis (Jimenez et al., 1998). Tem1 is required for the contraction (but not formation) of the actomyosin ring during cytokinesis (Lippincott et al., 2001). Both Dbf2 and Cdc5 localize to spindle pole bodies and at the end of mitosis, to the bud neck, and both have been implicated in cytokinesis (Frenz et al., 2000; Song and Lee, 2001). Thus, MEN promotes both mitotic exit and cytokinesis.

The nucleolus

The yeast nucleolus, which contains ~150 consecutive repeats of the rDNA, is the center for ribosomal RNA synthesis and ribosome assembly (reviewed in Shaw and Jordan,

1995). The chromatin structure in the nucleolus silences transcription by RNA polymerase II without interfering with highly active transcription by RNA polymerase I (Pol I) (Bryk et al., 1997; Fritze et al., 1997; Smith and Boeke, 1997). This restriction, termed "nucleolar silencing," may be the consequence of a mechanism that evolved to suppress recombination amongst rDNA repeats and thereby reduce the production of rDNA circles which have been shown to cause cellular senescence (reviewed in Guarente, 2000). Sir2, an essential regulator of silencing, mediates silencing, suppression of recombination, and extension of longevity through its NAD-dependent histone deacetylase activity (reviewed by Gottschling, 2000; Guarente, 2000) and/or other mechanisms such as NAD breakdown and generation of O-acetyl-ADP-ribose (Tanner et al., 2000; Tanny and Moazed, 2000). Despite the key role of the nucleolus in cellular metabolism, the molecular basis for nucleolar assembly/organization and the role of Net1 in this process remain mysterious.

Concluding remarks

In Chapter III, we present the *telophase-arrest-bypassed* (*tab*) screen aimed at isolating both positive and negative regulators of MEN. Characterization of the *tab2-1* (*net1-1*) mutant from this screen (Chapter IV) has led to the discovery of a novel nucleolar RENT complex in which Net1 is a core component (Shou et al., 1999), and the delineation of how RENT controls mitotic exit (Chapter IV, Shou et al., 1999; Visintin et al., 1999) and nucleolar silencing (Straight et al., 1999). Remarkably, Net1 also stimulates RNA Pol I, and is required for the proper localization of multiple nucleolar antigens and normal

rDNA morphology (submitted; Chapter V). Characterization of the *TAB6-1* mutant, a gain-of-function allele of *CDC14*, demonstrates that the nucleolar and cell cycle functions of Net1 can be uncoupled (submitted; Chapter V).

References

Anghileri, P., Branduardi, P., Sternieri, F., Monti, P., Visintin, R., Bevilacqua, A., Alberghina, L., Martegani, E., and Baroni, M.D. (1999). Chromosome separation and exit from mitosis in budding yeast: dependence on growth revealed by cAMP-mediated inhibition. Exp Cell Res *250*:510-523.

Bardin, A.J., Visintin, R., and Amon, A. (2000) A mechanism for coupling exit from mitosis to partitioning of the nucleus. Cell 102:21-31.

Baumer, M., Braus, G.H., Irniger, S. (2000). Two different modes of cyclin Clb2 proteolysis during mitosis in Saccharomyces cerevisiae. FEBS Lett *468*:142-148.

Bryk, M., Banerjee, M., Murphy, M., Knudsen, K. E., Garfinkel, D. J., and Curcio, M. J. (1997). Transcriptional silencing of Ty1 elements in the RDN1 locus of yeast. Genes Dev *11*, 255-69.

Chan, F.K.M., Zhang, J., Cheng, L., Shapiro, D.N., and Winoto, A. (1995). Identification of human and mouse p19, a novel Cdk4 and Cdk6 inhibitor with homology to $p16^{Ink4}$. Mol. Cell. Biol. *15*, 2682–2688.

Chen, J., Jackson, P.K., Kirschner, M.W., and Dutta, A. (1995). Separate domains of p21 involved in the inhibition of Cdk kinase and PCNA. Nature *374*, 386–388.

Cheng M, Olivier P, Diehl JA, Fero M, Roussel MF, Roberts JM, and Sherr CJ. (1999). The p21(Cip1) and p27(Kip1) CDK 'inhibitors' are essential activators of cyclin D-dependent kinases in murine fibroblasts. EMBO J *18*: 1571-83

Charles, J.F., Jaspersen, S.L., Tinker-Kulberg, R.L., Hwang, L., Szidon, A. and Morgan, D.O. (1998). The Polo-related kinase Cdc5 activates and is destroyed by the mitotic cyclin destruction machinery in *S. cerevisiae*. Curr Biol *8*, 497-507.

Cohen-Fix, O., and Koshland, D. (1999). Pds1p of budding yeast has dual roles: inhibition of anaphase initiation and regulation of mitotic exit. Genes Dev *13*:1950-1959.

Coleman, T.R. and Dunphy, W.G. (1994) Cdc2 regulatory factors. Curr Opin Cell Biol *6*: 877-882.

Deng, C., Zhang, P., Harper, J.W., Elledge, S.J., and Leder, P. (1995). Mice lacking $P21^{CIP1/WAF1}$ undergo normal development, but are defective in G1 checkpoint control. Cell *82*, 675–684.

Deshaies, R.J. (1997). Phosphorylation and proteolysis: partners in the regulation of cell division in budding yeast. Curr Opin Genet Dev *7*, 7-16.

Deshaies, R.J. (1999). SCF and Cullin/Ring H2-based ubiquitin ligases. Annu Rev Cell Dev Biol 15:435-467.

Donovan, J.D., Toyn, J.H., Johnson, A.L. and Johnston, L.H. (1994). $p40^{SDB25}$, a putative CDK inhibitor, has a role in the M/G1 transition in *Saccharomyces cerevisiae*. Genes & Development *8*, 1640-1653.

Dyson, N. (1998). The regulation of E2F by pRB-family proteins. Genes Dev *12*, 2245-2262.

El-Deiry, W.S., Tokino, T., Velculescu, V.E., Levy, D.B., Parsons, R., Trent, J.M., Lin, D., Mercer, W.E., Kinzler, K.W., and Vogelstein, B. (1993). WAF1, a potential mediator of p53 tumor suppression. Cell *75*, 817–825.

Elledge, S.J., and Harper, J.W. (1994). Cdk inhibitors: on the threshold of checkpoints and development. Curr. Opin. Cell Biol. *6*, 847–852.

Fero ML, Rivkin M, Tasch M, Porter P, Carow CE, Firpo E, Polyak K, Tsai LH, Broudy V, Perlmutter RM, Kaushansky K, and Roberts JM. (1996). A syndrome of multiorgan hyperplasia with features of gigantism, tumorigenesis, and female sterility in $p27^{Kip1}$-deficient mice. Cell *85*, 733-44.

Frenz LM, Lee SE, Fesquet D, and Johnston LH. (2000). The budding yeast Dbf2 protein kinase localises to the centrosome and moves to the bud neck in late mitosis. J Cell Sci *113*:3399-3408.

Fritze, C. E., Verschueren, K., Strich, R., and Easton, E. R. (1997). Direct evidence for SIR2 modulation of chromatin structure in yeast rDNA. Embo J *16*, 6495-509.

Germain, D., Hendley, J., and Futcher, B. (1997). DNA damage inhibits proteolysis of the B-type cyclin Clb5 in *S. cerevisiae*. J Cell Sci *110*:1813-1820.

Gottschling, D. E. (2000). Gene silencing: two faces of SIR2. Curr Biol *10*, R708-11.

Gruneberg, U., Campbell, K., Simpson, C., Grindlay, J., Schiebel, E. (2000). Nud1p links astral microtubule organization and the control of exit from mitosis. EMBO J *19*, 6475-88

Gu, Y., Turck, C.W., and Morgan, D.O. (1993). Inhibition of Cdk2 activity *in vivo* by an associated 20K regulatory subunit. Nature *366*, 707–710.

Guan, K.-L., Jenkins, C.W., Li, Y., Nichols, M.A., Wu, X., O'Keefe, C.L., Matera, A.G., and Xiong, Y. (1994). Growth suppression by p18, a $p16^{INK4/MTS1}$ and $p14^{INK4B/MTS2}$-related CDK6 inhibitor, correlates with wild-type pRb function. Genes & Develop. *8*, 2939–2952.

Guarente, L. (2000). Sir2 links chromatin silencing, metabolism, and aging. Genes Dev *14*, 1021-6.

Halevy, O., Novitch, B.G., Spicer, D.B., Skapek, S.X., Rhee, J., Hannon, G.J., Beach, D., and Lassar, A.B. (1995). Correlation of terminal cell-cycle arrest of skeletal-muscle with induction of p21 by MyoD. Science *267*, 1018–1021.

Hannon, G.J., and Beach, D. (1994). $p15^{INK4B}$ is a potential effector of TGFβ-induced cell cycle arrest. Nature *371*, 257–261.

Hardy, C. F., and Pautz, A. (1996). A novel role for Cdc5p in DNA replication. Mol Cell Biol *16*, 6775-82.

Harper, J.W., Adami, G., Wei, N., Keyomarsi, K., Elledge, S.J. (1993). The p21 Cdk-interacting protein Cip1 is a potent inhibitor of G1 cyclin-dependent kinases. Cell *75*, 805–816.

Irniger S, Baumer M, Braus GH. (2000). Glucose and ras activity influence the ubiquitin ligases APC/C and SCF in *Saccharomyces cerevisiae*. Genetics *154*:1509-1521.

Irniger, S., Piatti, S., Michaelis, C. and Nasmyth, K. (1995). Genes involved in sister chromatid separation are needed for B-type cyclin proteolysis in budding yeast. Cell *81*, 269-277.

Jackson, P.K., Chevalier, S., Philippe, M., and Kirschner, M.W. (1995). Early events in DNA replication require cyclin E and are blocked by $p21^{CIP1}$. J. Cell Biol. *130*, 755–769.

Jaspersen, S.L., Charles, J.F., Tinker-Kulberg, R.L. and Morgan, D.O. (1998). A late mitotic regulatory network controlling cyclin destruction in *Saccharomyces cerevisiae*. Mol Biol Cell *9*, 2803-17.

Jaspersen, S.L., Charles, J.F., and Morgan, D.O. (1999). Inhibitory phosphorylation of the APC regulator Hct1 is controlled by the kinase Cdc28 and the phosphatase Cdc14. Curr Biol *9*, 227-236.

Jimenez J, Cid VJ, Cenamor R, Yuste M, Molero G, Nombela C, and Sanchez M (1998). Morphogenesis beyond cytokinetic arrest in Saccharomyces cerevisiae. J Cell Biol *143*:1617-1634.

Kato, J.-Y., Matsuoka, M., Polyak, K., Massagué, J., and Sherr, C.J. (1994). Cyclic AMP-induced G1 phase arrest mediated by an inhibitor ($p27^{KIP1}$) of cyclin-dependent kinase-4 activation. Cell *79*, 487–496.

Kitada, K., Johnson, A.L., Johnston, L.H. and Sugino, A. (1993). A multicopy suppressor gene of the *Saccharomyces cerevisiae* G1 cell cycle mutant gene dbf4 encodes a protein kinase and is identified as CDC5. Mol Cell Biol *13*, 4445-57.

Kiyokawa H, Kineman RD, Manova-Todorova KO, Soares VC, Hoffman ES, Ono M, Khanam D, Hayday AC, Frohman LA, and Koff A. (1996). Enhanced growth of mice lacking the cyclin-dependent kinase inhibitor function of $p27^{Kip1}$. Cell *85*:721-32.

Komarnitsky, S.I., Chiang, Y.C., Luca, F.C., Chen, J., Toyn, J.H., Winey, M., Johnston, L.H. and Denis, C.L. (1998). DBF2 protein kinase binds to and acts through the cell cycle-regulated MOB1 protein. Mol Cell Biol *18*, 2100-7.

Kotani S, Tugendreich S, Fujii M, Jorgensen PM, Watanabe N, Hoog C, Hieter P, Todokoro K. (1998). PKA and MPF-activated polo-like kinase regulate anaphase-promoting complex activity and mitosis progression. Mol Cell *1*:371-380.

LaBaer J, Garrett MD, Stevenson LF, Slingerland JM, Sandhu C, Chou HS, Fattaey A, and Harlow E. (1997). New functional activities for the p21 family of CDK inhibitors. Genes Dev 11:847-862.

Lee, M.-H., Reynisdottir, I., and Massagué, J. (1995). Cloning of $p57^{KIP2}$, a cyclin-dependent kinase inhibitor with unique domain structure and tissue distribution. Genes & Develop. *9*, 639–649.

Li, R., Waga, S., Hannon, G.J., Beach, D., and Stillman, B. (1994). Differential effects by the p21 Cdk inhibitor on PCNA-dependent DNA replication and repair. Nature *371*, 534–537.

Lippincott J, Shannon KB, Shou W, Deshaies RJ, and Li R. (2001). The Tem1 small GTPase controls actomyosin and septin dynamics during cytokinesis. J Cell Sci *114*:1379-1386.

Luca, F.C. and Winey, M. (1998). MOB1, an essential yeast gene required for completion of mitosis and maintenance of ploidy. Mol Biol Cell *9*, 29-46.

Luo, Y., Hurwitz, J., and Massagué, J. (1995). Cell-cycle inhibition by independent Cdk and PCNA binding domains in $p21^{CIP1}$. Nature *375*, 159–161.

Meyn, M.A. 3rd, and Holloway, S.L. (2000). S-phase cyclins are required for a stable arrest at metaphase. Curr Biol *10*:1599-1602.

Moll, T., Tebb, G., Surana, U., Robitsch, H. and Nasmyth, K. (1991). The role of phosphorylation and the CDC28 protein kinase in cell cycle-regulated nuclear import of the *S. cerevisiae* transcription factor SWI5. Cell *66*, 743-58.

Morgan, D.O. (1999). Regulation of the APC and the exit from mitosis. Nat Cell Biol. *1*, E47-53.

Matsuoka, S., Edwards, M.C., Bai, C., Parker, S., Zhang, P., Baldini, A., Harper, J.W., and Elledge, S.J. (1995). $p57^{KIP2}$, a structurally distinct member of the $p21^{CIP1}$ Cdk inhibitor family, is a candidate tumor-suppressor gene. Genes & Develop. *9*, 650–662.

McCollum, D., and Gould, K.L. (2001). Timing is everything: regulation of mitotic exit and cytokinesis by the MEN and SIN. Trends Cell Biol *11*:89-95.

Nakayama K, Ishida N, Shirane M, Inomata A, Inoue T, Shishido N, Horii I, Loh DY, and Nakayama K. (1996). Mice lacking $p27^{Kip1}$ display increased body size, multiple organ hyperplasia, retinal dysplasia, and pituitary tumors. Cell *85*, 707-720.

Nasmyth, K., Peters, J.M., and Uhlmann, F. (2000) Splitting the chromosome: cutting the ties that bind sister chromatids. Science *288*, 1379-85

Noda, A., Ning, Y., Venable, S.F., Pereira-Smith, O.M., and Smith, J.R. (1994). Cloning of senescent cell-derived inhibitors of DNA synthesis using an expression screen. Exp. Cell Res. *211*, 90–98.

Parkes, V. and Johnston, L.H. (1992). SPO12 and SIT4 suppress mutations in DBF2, which encodes a cell cycle protein kinase that is periodically expressed. Nucleic Acids Res *20*, 5617-23.

Pereira G, Hofken T, Grindlay J, Manson C, Schiebel E. (2000). The Bub2p spindle checkpoint links nuclear migration with mitotic exit. Mol Cell *6*:1-10.

Polyak, K., Kato, J.-Y., Solomon, M.J., Sherr, C.J., Massagué, J., Roberts, J.M., and Koff, A. (1994a). $p27^{KIP1}$, a cyclin-cdk inhibitor, links transforming growth factor-β and contact inhibition to cell cycle arrest. Genes Dev. *8*, 9–22.

Polyak, K., Lee, M.-H., Erdjument-Bromage, H., Koff, A., Roberts, J.M., Tempst, P., and Massagué, J. (1994b). Cloning of $p27^{KIP1}$, a cyclin-dependent kinase inhibitor and a potential mediator of extracellular antimitogenic signals. Cell *78*, 59–66.

Smith, J. S., and Boeke, J. D. (1997). An unusual form of transcriptional silencing in yeast ribosomal DNA. Genes Dev *11*, 241-54.

Sanchez, Y., Bachant, J., Wang ,H., Hu, F., Liu, D., Tetzlaff, M., and Elledge, S.J. (1999). Control of the DNA damage checkpoint by Chk1 and Rad53 protein kinases through distinct mechanisms. Science *286*,1166-1171.

Schwab, M., Lutum, A.S. and Seufert, W. (1997). Yeast Hct1 is a regulator of Clb2 cyclin proteolysis. Cell *90*, 683-93.

Serrano, M., Hannon, G.J., and Beach, D. (1993). A new regulatory motif in cell-cycle control causing specific inhibition of cyclin D/Cdk4. Nature *366*, 704–707.

Shaw, P. J., and Jordan, E. G. (1995). The nucleolus. Annu Rev Cell Dev Biol *11*, 93-121.

Sherr, C.J. and Roberts, J.M. (1999) CDK inhibitors: positive and negative regulators of G1-phase progression. Genes Dev *13*:1501-1512.

Shirayama, M., Matsui, Y., Tanaka, K., and Toh-e, A. (1994a). Isolation of a CDC25 family gene, MSI2/LTE1, as a multicopy suppressor of ira1. Yeast *10*, 451-61.

Shirayama, M., Matsui, Y. and Toh-e, A. (1994b). The yeast TEM1 gene, which encodes a GTP-binding protein, is involved in termination of M phase. Molecular and Cellular Biology *14*, 7476-7482.

Shirayama, M., Matsui, Y. and Toh-e, A. (1996). Dominant mutant alleles of yeast protein kinase gene CDC15 suppress the lte1 defect in termination of M phase and genetically interact with CDC14. Mol Gen Genet *251*, 176-85.

Shirayama, M., Toth, A., Galova, M., Nasmyth, K. (1999). APC(Cdc20) promotes exit from mitosis by destroying the anaphase inhibitor Pds1 and cyclin Clb5. Nature *402*: 203-207.

Shirayama, M., Zachariae, W., Ciosk, R., and Nasmyth, K. (1998). The Polo-like kinase Cdc5p and the WD-repeat protein Cdc20p/fizzy are regulators and substrates of the anaphase promoting complex in *Saccharomyces cerevisiae*. Embo J *17*, 1336-49.

Shou W, Seol JH, Shevchenko A, Baskerville C, Moazed D, Chen ZW, Jang J, Shevchenko A, Charbonneau H, Deshaies RJ. (1999). Exit from mitosis is triggered by Tem1-dependent release of the protein phosphatase Cdc14 from nucleolar RENT complex. Cell *97*: 233-244.

Smits, V.A., Klompmaker, R., Arnaud, L., Rijksen, G., Nigg, E.A., and Medema, R.H. (2000). Polo-like kinase-1 is a target of the DNA damage checkpoint. Nat Cell Biol 2:672-676.

Song, S., and Lee, K. (2001). A Novel Function of Saccharomyces cerevisiae CDC5 in Cytokinesis. J Cell Biol *152*, 451-470.

Spevak W, Keiper BD, Stratowa C, Castanon MJ. (1993). Saccharomyces cerevisiae cdc15 mutants arrested at a late stage in anaphase are rescued by *Xenopus* cDNAs encoding N-ras or a protein with beta-transducin repeats. Mol Cell Biol *13*, 4953-4966.

Surana, U., Amon, A., Dowzer, C., McGrew, J., Byers, B. and Nasmyth, K. (1993). Destruction of the CDC28/CLB mitotic kinase is not required for the metaphase to anaphase transition in budding yeast. Embo J *12*, 1969-1978.

Takahashi, K., Nakayama, Ki., and Nakayama, K. (2000) Mice lacking a CDK inhibitor, p57Kip2, exhibit skeletal abnormalities and growth retardation. J Biochem (Tokyo) *127*:73-83.

Tanner, K. G., Landry, J., Sternglanz, R., and Denu, J. M. (2000). Silent information regulator 2 family of NAD- dependent histone/protein deacetylases generates a unique product, 1-O-acetyl-ADP-ribose. Proc Natl Acad Sci U S A *97*, 14178-82.

Tanny, J. C., and Moazed, D. (2000). Coupling of histone deacetylation to NAD breakdown by the yeast silencing protein Sir2: Evidence for acetyl transfer from substrate to an NAD breakdown product. Proc Natl Acad Sci U S A. *98*, 415-420

Taylor, G.S., Liu, Y., Baskerville, C. and Charbonneau, H. (1997). The activity of Cdc14p, an oligomeric dual specificity protein phosphatase from *Saccharomyces cerevisiae*, is required for cell cycle progression. J Biol Chem *272*, 24054-63.

Tinker-Kulberg, R.L., Morgan, D.O. (1999). Pds1 and Esp1 control both anaphase and mitotic exit in normal cells and after DNA damage. Genes Dev *13*,1936-1949.

Toyoshima, H., and Hunter, T. (1994). p27, a novel inhibitor of G1 cyclin-Cdk protein kinase activity, is related to p21. Cell *78*, 67–74.

Toyn, J.H., Johnson, A.L., Donovan, J.D., Toone, W.M. and Johnston, L.H. (1997). The Swi5 transcription factor of *Saccharomyces cerevisiae* has a role in exit from mitosis through induction of the cdk-inhibitor Sic1 in telophase. Genetics *145*, 85-96.

Toyn, J.H. and Johnston, L.H. (1994). The Dbf2 and Dbf20 protein kinases of budding yeast are activated after the metaphase to anaphase cell cycle transition. Embo J *13*, 1103-1113.

Tsihlias, J., Kapusta, L., and Slingerland, J. (1999). The prognostic significance of altered cyclin-dependent kinase inhibitors in human cancer. Annu Rev Med *50*:401-423.

Visintin, R., Craig, K., Hwang, E.S., Prinz, S., Tyers, M. and Amon, A. (1998). The phosphatase Cdc14 triggers mitotic exit by reversal of Cdk-dependent phosphorylation. Molecular Cell *2*, 709-718.

Visintin R, Hwang ES, and Amon A. (1999). Cfi1 prevents premature exit from mitosis by anchoring Cdc14 phosphatase in the nucleolus. Nature *398*:818-823.

Visintin, R., Prinz, S. and Amon, A. (1997). CDC20 and CDH1: a family of substrate-specific activators of APC-dependent proteolysis. Science *278*, 460-3.

Waga, S., Hannon, G.J., Beach, D., and Stillman, B. (1994). The p21 inhibitor of cyclin-dependent kinases controls DNA replication by interaction with PCNA. Nature *369*, 574–578.

Wang, Y., Hu, F., and Elledge, S.J. (2000). The Bfa1/Bub2 GAP complex comprises a universal checkpoint required to prevent mitotic exit. Curr Biol *10*: 1379-1382.

Xiong, Y., Hannon, G.J., Zhang, H., Casso, D., Kobayashi, R., and Beach, D. (1993). p21 is a universal inhibitor of cyclin kinases. Nature *366*, 701–704.

Yamamoto, A., Guacci, V., and Koshland, D. (1996). Pds1p, an inhibitor of anaphase in budding yeast, plays a critical role in the APC and checkpoint pathway(s). J Cell Biol *133*: 99-110.

Yan, Y., Lee M.H., Massague, J., and Barbacid, M. (1997). Ablation of the CDK inhibitor p57Kip2 results in increased apoptosis and delayed differentiation during mouse development. Genes Dev *11*: 973-983.

Yeh, E., Skibbens, R.V., Cheng, J.W., Salmon, E.D., and Bloom, K. (1995). Spindle dynamics and cell cycle regulation of dynein in the budding yeast, Saccharomyces cerevisiae. J Cell Biol *130*, 687-700.

Yeong, F.M., Lim, H.H., Padmashree, C.G., and Surana, U. (2000). Exit from mitosis in budding yeast: biphasic inactivation of the Cdc28-Clb2 mitotic kinase and the role of Cdc20. Mol Cell *5*:501-511.

Zachariae, W., Schwab, M., Nasmyth, K. and Seufert, W. (1998). Control of cyclin ubiquitination by CDK-regulated binding of Hct1 to the anaphase promoting complex. Science *282*, 1721-4

Zhang, P., Liegeois, N.J., Wong, C., Finegold, M., Hou, H., Thompson, J.C., Silverman, A., Harper, J.W., DePinho, R.A., and Elledge, S.J. (1997). Altered cell differentiation and proliferation in mice lacking p57KIP2 indicates a role in Beckwith-Wiedemann syndrome. Nature *387*:151-158.

Chapter II – Cell Cycle Control by *Xenopus* $p28^{Kix1}$, a Developmentally Regulated Inhibitor of Cyclin-dependent Kinases

(Wenying Shou and William G. Dunphy. Published in Molecular Biology of the Cell, 7:457-469, 1996; Appendix I)

Abstract

We have isolated *Xenopus* $p28^{Kix1}$, a member of the $p21^{CIP1}/p27^{KIP1}/p57^{KIP2}$ family of Cdk inhibitors. Members of this family negatively regulate cell cycle progression in mammalian cells by inhibiting the activities of cyclin-dependent kinases (Cdks). p28 shows significant sequence homology with p21, p27, and p57 in its N-terminal region, where the Cdk inhibition domain is known to reside. In contrast, the C-terminal domain of p28 is distinct from that of p21, p27, and p57. In co-immunoprecipitation experiments, p28 was found to be associated with Cdk2, cyclin E, and cyclin A, but not the Cdc2/cyclin B complex in *Xenopus* egg extracts. *Xenopus* p28 associates with the proliferating cell nuclear antigen (PCNA), but with a substantially lower affinity than human p21. In kinase assays with recombinant Cdks, p28 inhibits pre-activated Cdk2/cyclin E and Cdk2/cyclin A, but not Cdc2/cyclin B. However, at high concentrations, p28 does prevent the activation of Cdc2/cyclin B by the Cdk-activating kinase (CAK). Consistent with the role of p28 as a Cdk inhibitor, recombinant p28 elicits an inhibition of both DNA replication and mitosis upon addition to egg extracts, indicating that it can regulate multiple cell cycle

transitions. The level of p28 protein shows a dramatic developmental profile: it is low in *Xenopus* oocytes, eggs, and embryos up to stage 11, but increases ~100 fold between stages 12 and 13, and remains high thereafter. The induction of p28 expression temporally coincides with late gastrulation. Thus, although p28 may play only a limited role during the early embryonic cleavages, it may function later in development to establish a somatic type of cell cycle. Taken together, our results indicate that *Xenopus* p28 is a new member of the p21/p27/p57 class of Cdk inhibitors, and that it may play a role in developmental processes.

Introduction

Progression through the cell cycle is controlled by the cyclin dependent kinases (Cdks), which comprise a family containing various catalytic subunits and regulatory partners called cyclins. In mammalian cells, Cdk4/cyclin D, Cdk2/cyclin E, Cdk2/cyclin A, and Cdc2/cyclin B act sequentially at different points in the cell cycle (for review, see Draetta, 1993; Sherr, 1993). Although particular details vary, the central mechanisms of cell cycle regulation by Cdks are conserved from yeast to vertebrates.

Cdk activities are strictly controlled to ensure that a cell undergoes cell division cycles only under the appropriate circumstances. The Cdks are regulated by at least three distinct mechanisms: cyclin binding, subunit phosphorylation, and association with Cdk inhibitors. To date, two classes of Cdk inhibitors have been identified in mammalian cells (for review, see Elledge and Harper, 1994; Massagué and Polyak, 1995). The p15/p16 class includes $p15^{INK4B}$ (Hannon and Beach, 1994), $p16^{INK4}$ (Serrano *et al.*,

1993), p18 (Guan *et al.*, 1994), and p19 (Chan *et al.*, 1995). Proteins in this class share considerable sequence homology with each other. They exclusively associate with and inhibit D-type Cdks, and appear to play a role in cellular differentiation and tumor suppression (reviewed in Elledge and Harper, 1994). A second class of Cdk inhibitors includes p21 (also known as CIP1, WAF1, CAP20, SDI1) (Xiong *et al.*, 1993; Harper *et al.*, 1993; El-Deiry *et al.*, 1993; Gu *et al.*, 1993; Noda *et al.*, 1994), $p27^{KIP1}$(Polyak *et al*, 1994b; Toyoshima and Hunter, 1994), and $p57^{KIP2}$ (Lee *et al.*, 1995; Matsuoka *et al.*, 1995). The N-terminal regions of these three proteins share significant homology; this domain can bind to and inhibit Cdk2/cyclin E, Cdk2/cyclin A, Cdk4/cyclin D, and, to a lesser extent, Cdc2/cyclin B. Although p21 and p27 do not directly inhibit Cdk-activating kinase (CAK), they can associate with Cdks and prevent them from being phosphorylated and activated by CAK (Polyak *et al.*, 1994b; Aprelikova *et al.*, 1995). Except for a bipartite nuclear localization signal, the C-terminal domains of these proteins are not strongly conserved: $p21^{CIP1}$ binds proliferating cell nuclear antigen (PCNA, a DNA polymerase δ-subunit), while $p27^{KIP1}$ and $p57^{KIP2}$ do not (Waga *et al.*, 1994; Chen *et al.*, 1995; Luo *et al.*, 1995). Moreover, in the central regions, human $p57^{KIP2}$ has PAPA repeats while mouse $p57^{KIP2}$ has a proline-rich domain followed by acidic repeats (Lee *et al.*, 1995; Matsuoka *et al.*, 1995). The structural diversity among $p21^{CIP1}$, $p27^{KIP1}$, and $p57^{KIP2}$ suggests that these proteins may play distinct roles in cell cycle regulation.

p21 and p27 participate in diverse regulatory responses. Following radiation-induced DNA damage, the tumor suppressor protein p53 up-regulates p21 mRNA levels (El-Deiry *et al.*, 1993). p21 inhibits Cdk2/cyclin E activity, and thereby prevents DNA replication (Jackson *et al.*, 1995). Although the C-terminal domain of p21 associates with PCNA and blocks PCNA-dependent DNA replication, it does not inhibit PCNA-dependent DNA repair (Li *et al.*, 1994), giving irradiated cells the opportunity to remain in G1 and repair their DNA. Consistent with these observations, embryonic fibroblasts derived from $p21^{-/-}$ mice are significantly deficient in their ability to arrest in G1 in response to DNA damage (Deng *et al.*, 1995). Besides playing a role in the G1 checkpoint, p21 may also be involved in cellular differentiation under normal circumstances. For example, p21 mRNA levels increase in senescent cells (Noda *et al.*, 1994). Also, MyoD, a skeletal-muscle-specific transcriptional regulator, activates the expression of p21 during differentiation in a p53-independent fashion (Halevy *et al.*, 1995). The expression pattern of p21 in the mouse correlates with terminal differentiation and cell cycle withdrawal, suggesting roles in development (Parker *et al.*, 1995). However, $p21^{-/-}$ mice undergo normal development, and do not develop spontaneous tumors (Deng *et al.*, 1995), implying the existence of redundant pathways that ensure proper development and tumor prevention in this organism.

Although the functions of p27 and p57 are less well understood, they appear to play a role in differentiation-mediated cell cycle arrest and possibly in tumor prevention. In the mouse, most of the p57-expressing cells are terminally differentiated (Matsuoka *et al.*, 1995). The human p57 gene is located at a chromosomal region implicated in both

sporadic cancers and a familial cancer syndrome, suggesting that p57 is a candidate tumor suppressor (Matsuoka *et al.*, 1995). The regulation of p27 appears to be cell-type dependent. In TGFβ-arrested or contact-inhibited mink epithelial cells, p27 dissociates from Cdk4/cyclin D, and binds to and prevents the CAK-mediated activation of Cdk2/cyclin E (Polyak *et al.*, 1994a and b). In macrophages, cAMP exerts its anti-mitogenic effects by raising the level of p27, which then associates with Cdk4/cyclin D and prevents its activation by CAK (Kato *et al.*, 1994). During T cell mitogenesis, IL-2 signaling activates Cdk2/cyclin E complexes by eliminating the p27 protein, whereas p27 levels fail to drop when the immunosuppressant rapamycin is present (Nourse *et al.*, 1994). In at least some human cell lines, proliferating cells have a lower level of p27 due to an elevated p27-ubiquitinating activity that targets p27 to the ubiquitin-dependent proteasome degradation pathway (Pagano *et al.*, 1995).

Although considerable information about Cdk inhibitors has emerged recently, much remains to be learned about the evolution of these families and the diversity of their functions. Two Cdk inhibitors from *S. cerevisiae* (the Cdc28/Cln inhibitor Far1 and the Cdc28/Clb2,5,6 inhibitor $p40^{SIC1}$) and one from *S. pombe* (the Cdc2/Cdc13 inhibitor Rum1) have been identified, but these show little homology with p15/p16 or p21/p27 Cdk inhibitors (for review, see Elledge and Harper, 1994). Since cell-free extracts from *Xenopus* eggs faithfully recapitulate many cell cycle events including DNA replication, mitosis, and various checkpoint mechanisms (Leno and Laskey, 1991; Murray, 1991; Dasso and Newport, 1990; Minshull *et al.*, 1994; Kumagai and Dunphy, 1995), it will be

valuable to ascertain the extent to which Cdk inhibitors contribute to the regulation of the various Cdks present in this system. Because *Xenopus* embryos are readily available and easy to manipulate, it is also an attractive organism for the study of developmental regulatory mechanisms. Isolation of Cdk inhibitors from *Xenopus* and characterization of their upstream regulators, downstream targets, and expression during embryogenesis will contribute to our understanding of cell cycle regulation and its dynamic changes during development. With these goals in mind, we have searched for Cdk inhibitors in *Xenopus laevis* using a polymerase chain reaction (PCR)-based approach. Here, we report the isolation and initial characterization of *Xenopus* $p28^{Kix1}$, a p21/p27-class Cdk inhibitor.

Materials and Methods

Cloning of Xenopus p28

An internal fragment of *Xenopus* p28 was isolated by PCR using degenerate primers specific to conserved regions among human $p21^{CIP1}$, mouse $p21^{CIP1}$, and human $p27^{KIP1}$ (see Figure 1A). The 5' primer was (5') CGCGGATCCTG(C/T)(A/C)G(I/C)(I/C)(G/A)(I/C)(T/C)T(I/C)TT(C/T) GG(I/C)CC(I/C)GT (3'), and the 3' primer was (5') CGGGGTACCT(G/C)(I/C)IT(I/C)I(G/C) IAA(G/A)TC(G/A)AA(A/G)TTCCA (3'). The 5' end of each primer contains nine extra nucleotides (underlined) to provide restriction sites for BamHI or KpnI, respectively. PCR reactions (50 μl) contained 15 ng of *Xenopus* oocyte cDNA as template (Mueller *et al.*, 1995) and 50 pmol of each primer. PCR reactions were carried out as described (Mueller *et al.*, 1995), except that the first

five cycles were: 94°C for 1 min, 54°C for 2 min, and 72°C for 1 min, and that the remaining 30 cycles were: 94°C for 1 min, 57°C for 2 min, and 72°C for 1 min. An ~130 bp DNA fragment was isolated and cloned into the TA cloning vector (Invitrogen, San Diego, CA). After the fragment was sequenced to confirm its identity, it was radiolabeled by PCR and used to screen a *Xenopus* oocyte cDNA library by colony hybridization (Mueller *et al.*, 1995; Sambrook *et al.*, 1989). Approximately 1.2 million colonies were screened. Four positives were identified, two of which encoded the full-length *Xenopus* p28 gene. The entire cDNA was sequenced on both strands by primer walking using Sequenase (U.S. Biochemical, Cleveland, OH) with the dideoxy chain termination method. The GenBank accession number is U38844.

Subcloning of Xenopus p28 into Protein Expression Vectors

The pAX-NMT plasmid (Mueller *et al.*, 1995) harboring the full-length *Xenopus* p28 cDNA was mutagenized by PCR to create an NdeI site at the initiation codon. Briefly, the 5' primer (5') GGAAGTCCATATGGCTGCTTTCCACATCGC (3') containing an NdeI site (underlined) and the 3' primer (5') CTAGATTCGATTGGTGCCATGG (3') containing an NcoI site (underlined) were used to amplify 10 ng of the pAX-NMT-p28 plasmid in the presence of 2.5 units of Pfu DNA polymerase and dNTPs in the buffer supplied by the manufacturer (Stratagene, La Jolla, CA). The reactions were heated to 94°C for 2.5 min and 95°C for 0.5 min followed by 20 cycles at: 94°C for 1 min, 56°C for 2 min, and 75°C for 5 min. In addition, an extra 5 min at 75°C was added to the last

cycle. After verification by sequencing, the PCR product was digested with NdeI and NcoI, generating fragment A (~650 bp), which included the entire coding region of *Xenopus* p28. Fragment B (~1 kb) containing the 3' untranslated region of *Xenopus* p28 was obtained by digesting *Xenopus* p28 in the pBlueScript vector (Stratagene) with NcoI and EcoRI. Finally, the bacterial expression vector pET9-His6 (Kumagai and Dunphy, 1995) and the insect cell expression vector pVL1393-His6 (Tang *et al.*, 1993) were digested with NdeI and EcoRI, and were ligated with fragments A and B through a three-piece ligation. The resulting plasmids pET9-His6-p28 and pVL1393-His6-p28 were used for production of recombinant proteins. Sequence alignments were performed using the PILEUP program.

Antibody Production

Rabbits were immunized either with a C-terminal peptide from *Xenopus* p28 (CPLEQTPRKKIR) coupled to keyhole limpet hemocyanin or with purified *Xenopus* p28 protein expressed in bacteria (see below). Anti-peptide antibodies were affinity-purified on Affi-Gel 10 columns (Bio-Rad, Hercules, CA) containing covalently-attached peptides. Anti-p28 protein antibodies were affinity purified on purified p28 protein coupled to CNBr-activated Sepharose 4B columns (Pharmacia Biotech, Uppsala, Sweden). Affinity-purified anti-*Xenopus* cyclin E1 antibodies and anti-*Xenopus* Cdk2 antibodies were a generous gift from J. Maller (University of Colorado, Denver, CO). Purified monoclonal anti-human PCNA antibodies and polyclonal rabbit anti-human p21 antibodies were purchased from PharMingen (San Diego, CA). Affinity-purified rabbit

anti-mouse IgG antibodies were purchased from Cappel (West Chester, PA). Antibodies to *Xenopus* Cdc2, cyclin A1, and cyclin B2 were generously provided by A. Kumagai (Kumagai and Dunphy, 1995; A. Kumagai and W.G.D., unpublished results).

Production and Purification of Proteins from Insect Cells and Bacteria

The pET9-His6-p28 and pET3d-His6-human p21 (Xiong *et al.*, 1993) plasmids were transformed into BL21(DE3)pLysS bacteria. The bacteria were grown to mid-log phase and then induced, harvested, and lysed as described (Kumagai and Dunphy, 1991). The lysates were clarified and the p28 protein was purified by nickel-IDA Sepharose chromatography (Kumagai and Dunphy, 1995). In the case of *Xenopus* p28, the protein was further purified using SDS-PAGE followed by electro-eluting in an Elutrap (Schleicher and Schuell, Keene, NH). The pure protein was used to produce rabbit anti-*Xenopus* p28 protein antibodies.

Histidine-tagged *Xenopus* p28, histidine-tagged human cyclin B1 (Kumagai and Dunphy, 1995), and histidine-tagged human cyclin A and cyclin E (Desai *et al.*, 1992; Koff *et al.*, 1992) were purified from insect cell lysates using established protocols (Desai *et al.*, 1992). *Xenopus* Cdc2- or human Cdk2-containing lysates were aliquoted, drop frozen in liquid nitrogen, and stored at -80^{o}C. ^{35}S-Labeled His6-p28 was purified from metabolically labeled insect cells using a standard protocol (Kumagai and Dunphy, 1995).

In vitro Cdk Inhibition Assays

Active Cdk2/cyclin A, Cdk2/cyclin E, and Cdc2/cyclin B complexes were prepared essentially as described previously (Kumagai and Dunphy, 1995). Briefly, 20 μl of histidine-tagged cyclins bound to nickel-IDA beads were agitated with 100 μl of Cdk2- or Cdc2-containing insect cell lysates in the presence of 0.5 mM ATP and 10 mM $MgCl_2$ for 20 min at room temperature. The beads were then washed four times with ice-cold HBS (150 mM NaCl, 10 mM Hepes, pH 7.5), and eluted with 20 μl of 300 mM imidazole in HBS. All kinase assays were performed in the linear range. Kinase complexes were mixed with increasing amounts of *Xenopus* p28 or human p21, preincubated on ice for 5 min, and finally histone H1 assays were performed as described in Dunphy and Newport (1989). To assess the effect of *Xenopus* p28 on the activation of the Cdc2/cyclin B complex in insect cell lysates, increasing amounts of p28 were incubated with Cdc2-containing insect cell lysates (2 μl) and purified cyclin B (0.3 μl) at room temperature for 20 min, and the histone H1 kinase activity measured. Quantitation of kinase assays was performed with a PhosphorImager (Molecular Dynamics, Sunnyvale, CA).

Preparation of Extracts from Xenopus Eggs, Embryos, Oocytes, and Tissue Culture Cells

Xenopus cytostatic factor (CSF)-arrested egg extracts were prepared as described by Murray (1991). Interphase extracts were obtained by activation of CSF extracts with 0.4 mM $CaCl_2$. Freshly squeezed eggs were fertilized *in vitro* to obtain synchronously developing embryos (Newport and Kirschner, 1982a). Embryos were maintained in 0.2X MMR (Murray, 1991) for the first six hours, and in 0.1X MMR thereafter. Embryos were staged according to Nieuwkoop and Faber (1967). Typically, 20 embryos were

homogenized in 200 μl of ice cold EB (80 mM β-glycerol phosphate, pH 7.3, 20 mM EGTA, and 15 mM $MgCl_2$) containing 1 mM DTT, and 10 μg/ml each of leupeptin, pepstatin, and chymostatin. The homogenate was clarified by centrifugation at 16,000g for 5 min at 4°C. The crude cytoplasmic fraction was aliquoted and drop frozen in liquid nitrogen. Oocytes were separated from ovary tissue by treatment with collagenase (Cyert and Kirschner, 1988). Oocytes at different stages were manually selected and homogenized as described above for embryos. *Xenopus* tissue culture (XTC) cells were cultured using standard methods (Smith and Tata, 1991). Proliferating cells were harvested, and cell pellets were dissolved in SDS gel sample buffer.

Immunoprecipitation and Western Blotting

Affinity purified anti-p28 protein antibodies (2 μg) or control rabbit anti-mouse IgG antibodies (2 μg) were incubated with protein A beads (Sigma, St. Louis, MO) in HBS for 1 hr at 4°C. In the case of p21 immunoprecipitation, 2 μl of rabbit anti-human p21 antibodies were used. The antibody-coated beads were then incubated with mitotic extracts or interphase extracts for 1 hr at 4°C. In some cases, recombinant p28 was added to the extracts, and in these experiments, cycloheximide was also included. Following incubation with the extracts, the beads were collected by centrifugation and washed four times with EB containing 0.1% NP-40, 25 μg/ml aprotinin, 1 mM PMSF, 1 mM benzamidine, and 10 μg/ml each of pepstatin, chymostatin, and leupeptin (PCL), and then three times with HBS. All washes were done at 4°C. Similar washes were carried

out for nickel-IDA beads recovered from the extracts (which had been diluted one-fold in EB containing PCL), except that 20 mM EGTA was included in the first four washes. To recover p28 using p13 beads, CSF extracts were incubated with a 25% volume of p13 beads (5 mg p13/ml beads) or control beads lacking p13 for 1 hour at 4°C. Beads were removed by centrifugation, and the extracts were re-incubated with fresh beads. The p13 beads or the control beads were pooled, and washed as described for protein A beads. Immunoblotting using ^{125}I-labeled protein A (ICN, Irvine, CA) or ^{125}I-labeled sheep anti-mouse IgG antibodies (Amersham, Arlington Heights, IL) was performed as described (Coleman *et al.*, 1993). Alternatively, ECL (Amersham) was performed using horseradish peroxidase conjugated goat anti-rabbit IgG antibodies (Bio-Rad).

Replication Assays

Replication assays were performed essentially as described previously (Dasso and Newport, 1990). Briefly, 40 μl of CSF extracts containing 100 μg/ml cycloheximide, 10 μCi [α-^{32}P]-dCTP (ICN), and demembranated sperm nuclei (500 per μl) were incubated with 10 μl of Cdk inhibitors for 5 minutes at room temperature prior to activation with $CaCl_2$. At various time points, 3 μl aliquots were taken, mixed with replication sample buffer, and frozen at -20°C. The samples were digested with proteinase K (Boehringer Mannheim, Germany) and separated on a 0.8% agarose gel. Quantitation was performed using a PhosphorImager (Molecular Dynamics).

Results

Isolation of Xenopus p28

To search for Cdk inhibitors from *Xenopus laevis*, we designed degenerate PCR primers based upon conserved residues in the Cdk inhibition domain of human and mouse $p21^{CIP1}$ as well as human $p27^{KIP1}$ (Figure II-1A). PCR amplification of *Xenopus* oocyte cDNA yielded a ~130 bp fragment, which was used to isolate the corresponding full-length cDNA from an oocyte library. Several positive clones were identified; the longest (~1.7 kb) encodes a protein of 209 amino acids with a predicted molecular weight of 23,460 D (Figure II-1A). Since the endogenous protein in *Xenopus* extracts migrated at 28 kD during SDS gel electrophoresis (see below), we have designated this protein as $p28^{Kix1}$ (for cyclin-dependent kinase inhibitor from *Xenopus*).

The N-terminal region of p28 is 35% identical to p21/p27-class Cdk inhibitors (Figure II-1A). The most noticeable conservation is within the Cdk inhibition domain (the hatched box in Figure II-1B; residues 30-90 in p28) which, in the cases of p21, p27, and p57, is sufficient to bind and inhibit Cdks (Polyak *et al.*, 1994b; Luo *et al.*, 1995). The C-terminal regions of p28, p21, and p27/p57 are less well conserved (21%-25% identical), but they all have a putative nuclear localization signal (NLS). In the case of p28, residues 166-182 (KREITTPITDYFPKRKK; the black box in Figure II-1B) fit the consensus for the bipartite NLS first found in nucleoplasmin (Dingwall and Laskey, 1991). Moreover, p28 has several Ser/Thr-Pro motifs (stars in Figure II-1B) that are potential sites for phosphorylation by various mitotic kinases. Recently, Su et al. (1995) have cloned a distinct *Xenopus* Cdk inhibitor (Xic1) that is 90% identical to Kix1 at the

amino acid level, indicating that multiple genes for Cdk inhibitors are expressed in this organism.

Recombinant p28 Can Inhibit Cdks Via Two Mechanisms

To characterize its biochemical properties, p28 was expressed as a histidine-tagged fusion protein in baculovirus-infected insect cells, and purified using nickel-IDA affinity chromatography (Figure II-2). His6-p28 migrated with an apparent molecular weight of 28 kD, slightly larger than the endogenous *Xenopus* p28 (see Figure II-6A).

Since p28 possesses a Cdk inhibition domain similar to that of other p21/p27 Cdk inhibitors, we examined if p28 could inhibit various recombinant Cdk complexes. In particular, the effect of p28 upon Cdk2/cyclin E, Cdk2/cyclin A, and Cdc2/cyclin B was examined. Active Cdk complexes were prepared by mixing insect cell lysates containing the individual Cdk components under conditions that allowed formation of the complex and its activation by an endogenous insect cell Cdk-activating kinase (CAK). After Cdk complexes were purified by nickel-IDA chromatography and mixed with either human p21 or *Xenopus* p28, their activities were measured with histone H1 as the substrate (Figure II-3A). As expected, p21 inhibited Cdk2/cyclin E in a dose-dependent manner (Figures II-3A and B). In parallel experiments, p28 effectively inhibited the kinase activity of both Cdk2/cyclin E and Cdk2/cyclin A when present in only a five-fold molar excess of the Cdk (Figures II-3A and B). In contrast, p28 displayed little inhibitory activity toward Cdc2/cyclin B even at molar concentrations ~800-fold higher than the Cdk complex. Finally, like p21 and p27, *Xenopus* p28 is heat-stable: heating p28 to

100°C for 5 min had little effect upon its capacity to inhibit Cdk2/cyclin E (Figure II-3C). Taken together, these data suggest that p28 is a Cdk inhibitor with a striking preference for the G1/S Cdks over the mitotic Cdk in these *in vitro* assays.

In addition to directly inhibiting Cdk activity, both the p21/p27 and p15/p16 classes of inhibitors have been observed to exert their effects by preventing CAK-mediated activation of Cdks (Polyak *et al.*, 1994b; Aprelikova *et al.*, 1995). To investigate the possibility that p28 might have a similar function, we added p28 during the step at which the active Cdk complex was prepared. Whereas p28 did not inhibit pre-activated Cdc2/cyclin B, it nevertheless blocked the formation of the activated Cdc2/cyclin B complex. At a concentration of 160 nM, p28 elicited a 90% reduction in the H1 kinase activity generated by mixing insect cell lysates containing Cdc2 and cyclin B (Figure II-3D). This inhibition coincided with a reduction in the level of the threonine-161-phosphorylated (active) form of Cdc2 (our unpublished results), indicating that p28 can interfere with CAK-mediated activation of Cdc2/cyclin B.

p28 Associates with Cyclin-Dependent Kinases in Xenopus Extracts

Having characterized the effect of p28 upon recombinant Cdks, we examined whether p28 might associate with any of these Cdks in *Xenopus* egg extracts. As an initial method to monitor the association of p28 with Cdks in egg extracts, we utilized p13-agarose beads, an affinity matrix that binds Cdc2, Cdk2, and associated proteins. p28 was recovered efficiently by p13 beads but not control beads (Figure II-4A), suggesting that endogenous p28 is associated with Cdks in egg extracts. To identify which Cdks

associate with p28, we immunoprecipitated p28 from egg extracts with anti-p28 whole protein antibodies, and subsequently subjected the immunoprecipitates to immunoblotting with various antibodies. Cyclin E1 and cyclin A1 (Figure II-4B), but not cyclin B2, co-immunoprecipitated with p28. We also probed the immunoprecipitates with anti-p28 antibodies to monitor the endogenous p28 protein (Figure II-4B). Using recombinant p28 as a standard, we estimated that p28 was present at a rather low concentration (0.05 ng/μl, or 2 nM) in *Xenopus* egg extracts (our unpublished results). In control experiments with ^{35}S-labeled p28, we verified that the anti-p28 antibodies immunoprecipitated p28 quantitatively under these conditions. In accompanying studies, recombinant p28 was incubated with extracts, and then immunoprecipitated (Figure II-4C). Immunoblotting of these immunoprecipitates revealed a significant association of p28 with cyclin E1 and Cdk2, but not cyclin B2. In addition, only small amounts of Cdc2 (perhaps complexed with cyclin A1 or A2) were detected in the anti-p28 immunoprecipitates.

Next, we tested whether p28 was modified during the cell cycle, and if so, whether this could affect its association with Cdks. Radiolabeled recombinant p28 was incubated with either mitotic or interphase extracts. The electrophoretic mobility of p28 incubated in mitotic extracts was reduced compared with p28 from interphase extracts (Figure II-4D). Furthermore, the up-shifted form of p28 could be shifted down by protein phosphatase 2A (our unpublished results), suggesting that certain kinase(s) in mitotic extracts can phosphorylate p28. Although p28 was differentially phosphorylated during

the cell cycle, its association with Cdk complexes did not vary discernibly (Figure II-4B and C).

The C-terminal domain of human p21 associates with the replication and repair factor PCNA (Waga *et al.*, 1994; Chen *et al.*, 1995; Luo *et al.*, 1995). To determine whether p28 could bind PCNA, equivalent amounts (0.12 μg) of recombinant p28 or human p21 (as a positive control) were added to extracts, immunoprecipitated with their respective antibodies, and immunoblotted with anti-human PCNA antibodies, which cross-react well with *Xenopus* PCNA. As anticipated, anti-human p21 antibodies immunoprecipitated PCNA. In contrast, PCNA was not readily detected in anti-p28 immunoprecipitates (Figure II-4E), suggesting that either p28 does not bind to PCNA or it binds more weakly than human p21. To explore this issue further, approximately 40-fold more recombinant p28 was added to the *Xenopus* extracts, and was later recovered with nickel-IDA beads. We observed that p28 could associate with PCNA under these conditions, but the amount of PCNA bound to 5 μg of p28 was less than that bound to 0.7 μg of p21 (Figure II-4E). Thus, $p28^{Kix1}$, like the recently described Xic1 protein (Su *et al.*, 1995), can associate with PCNA, but not nearly as efficiently as human p21.

p28 Inhibits Chromosomal Replication and Mitosis in a Dose-Dependent Manner

To explore further the functional properties of p28, we added recombinant p28 to cell cycle extracts from *Xenopus* eggs (Murray, 1991). Upon activation with Ca^{2+}, cytostatic factor (CSF)-arrested mitotic egg extracts enter interphase, undergo a complete round of semi-conservative DNA replication, and enter mitosis shortly thereafter. Tracer

radiolabeled p28 was found to be stable in extracts throughout the duration of such experiments.

We first asked whether p28 would affect chromosomal DNA replication, which is known to require Cdk2/cyclin E activity (Jackson *et al.*, 1995). Using [α-^{32}P] dCTP as a tracer, the extent of DNA replication was assessed at various time points after Ca^{2+} activation. In control extracts treated with buffer only, replication commenced between 30 and 45 min after Ca^{2+} addition, and was essentially complete by 120 min (Figure II-5A). However, in extracts containing added p28, there was a strong inhibition of DNA replication (Figure II-5A). At the highest concentration of p28 tested (1.6 μM), there was essentially no replication within the first 90 min. At later times, even though a small amount of replication took place, it clearly occurred at a substantially reduced rate relative to the control extracts. A similar phenomenon was observed in extracts supplemented with the same amount of human p21 (Figure II-5A). At lower concentrations of p28, the onset of replication was delayed in a dose-dependent fashion (Figures II-5A and B). In particular, replication commenced at 90 min and 60 min at p28 concentrations of 800 nM and 320 nM, respectively. Interestingly, once replication began, it proceeded at a similar rate to that in the control extracts. This observation might suggest that at lower concentrations ($\leq$ 800 nM), p28 has a preferential effect on initiation versus elongation, whereas at higher concentrations, both processes are compromised. Finally, since chromosomal replication in egg extracts requires that the DNA be properly assembled into a nuclear structure, we verified by phase and

fluorescence microscopy that the control and inhibitor-treated extracts were equally competent for nuclear assembly (our unpublished results).

We also examined whether recombinant p28 could affect the entry into mitosis in extracts containing a very low concentration of sperm chromatin (25 demembranated sperm nuclei per μl of extract). It has been shown previously that this concentration of sperm nuclei is below the threshold necessary to trigger the replication checkpoint (Dasso and Newport, 1990). These extracts allow a direct assessment of the effect of p28 on mitosis independent of its effect on replication. Intriguingly, we observed that p28 elicited a dose-dependent delay of mitosis relative to control extracts (Figure II-6A). At a concentration of 800 nM, p28 delayed mitosis by approximately 60 min. In parallel, we examined the effect of p28 (800 nM) on total H1 kinase activity during the cell cycle in egg extracts (Figure II-6B). As expected, p28 suppressed the rise in H1 kinase activity that occurred in the control extracts at 90 min. Significantly, exogenously added p28 also depressed the level of H1 kinase activity at early times in the cell cycle (i.e., 30 min) when relatively little active Cdc2/cyclin B would be expected to be present. This effect could be due to inhibition of the Cdk2/cyclin E complex, which shows significant activity throughout the early embryonic cell cycles (Rempel *et al.*, 1995), or, alternatively, another unidentified Cdk. Taken together, our results indicate that at sufficiently high levels, not only does p28 abolish DNA replication, it also strongly inhibits entry into mitosis.

The Abundance of p28 Varies during Development

The abundance of p28 in *Xenopus* eggs is approximately 2 nM, whereas the concentration of recombinant p28 required to either inhibit recombinant Cdks *in vitro* or affect cell cycle progression in egg extracts is approximately 100-fold higher. To evaluate this paradox, we asked whether p28 might be expressed at higher levels during later stages of development when dividing cells acquire an extended G1 phase or withdraw from the cell cycle. For this purpose, extracts from oocytes, eggs, stage 26 embryos, and somatic *Xenopus* tissue culture (XTC) cells were immunoblotted with antibodies directed toward a C-terminal peptide of *Xenopus* p28. Although the level of p28 was similarly low in oocytes and mature eggs (~2 nM), it was approximately 100-fold higher in stage 26 embryos and XTC cells where the "somatic" cell cycle has replaced the "embryonic" one (Figure II-7A). To pinpoint more precisely at what stage during development p28 begins to be up-regulated, embryonic lysates were prepared at finer time points. The level of p28 remained low throughout the blastula and early gastrula stages. However, it increased dramatically between stages 12 and 13, and by stage 14, it had peaked to a level that remained relatively constant until at least stage 26 (Figure II-7B, and our unpublished results). The up-regulation of p28 occurs at ~5 hours after the commencement of gastrulation, a time corresponding most closely to the small yolk plug stage and the slit-blastopore stage when the neural plate first becomes discernible.

To verify that the protein detected in these experiments is *Xenopus* p28, a peptide-competition experiment was carried out (Figures II-7C). Immunoblots containing recombinant p28 and stage 26 embryonic lysates were treated with anti-p28 antibodies in the presence or absence of the immunizing peptide. The staining of both recombinant

and embryonic p28 was abolished by the peptide, whereas that of a background band was unaffected. Taken together, these experiments indicate that the expression of p28 increases as cells acquire a somatic type of cell cycle.

Discussion

To study the potential regulation of the cell cycle by Cdk inhibitors in *Xenopus* egg extracts, we have isolated *Xenopus* p28, a new member of the $p21^{CIP1}/p27^{KIP1}/p57^{KIP2}$ family of Cdk inhibitors. The Cdk inhibition domain of p28 shows significant sequence homology to those of p21, p27, and p57. Indeed, p28 effectively inhibits pre-activated G1/S Cdks, such as Cdk2/cyclin E and Cdk2/cyclin A, while exhibiting little inhibitory activity toward the mitotic Cdc2/cyclin B complex *in vitro*, like some other members of the family (Harper *et al.*, 1995; Lee *et al.*, 1995). Consistent with this observation, Cdk2, cyclin A, and cyclin E in egg extracts can be co-immunoprecipitated with p28, whereas the Cdc2/cyclin B complex appears not to be stably associated with p28.

It has been shown previously that Cdk inhibitors in the p21/p27/p57 class are also able to block the phosphorylation and activation of Cdks by CAK without directly binding to CAK or inhibiting CAK activity (Harper *et al.*, 1993; Polyak *et al.*, 1994b; Aprelikova *et al.*, 1995; Harper *et al.*, 1995; Matsuoka *et al.*, 1995). p28 has similar properties. In particular, p28 does not bind to recombinant human CAK (our unpublished results), nor does it inhibit the kinase activity of CAK toward the C-terminal peptide of RNA polymerase II (our unpublished results). However, p28 prevents Cdc2/cyclin B activation by CAK, suggesting that despite the apparent preference for G1/S Cdks, p28

could down-regulate mitotic Cdk activities through prevention of CAK-mediated activation. It seems paradoxical that p28 has little affinity for Cdc2/cyclin B or CAK, yet it is able to prevent the latter from activating the former. One possible explanation is based on the observation that multiple molecules of p21 are required to inhibit Cdks and that complexes containing a single p21 molecule is active (Zhang *et al.*, 1994). Thus, it is possible that a single molecule of p28 could bind the Cdc2/cyclin B complex to block CAK-mediated activation, whereas multiple molecules of p28 could not efficiently associate with and inhibit the pre-activated complex. Alternatively, the off-rate of p28 from Cdc2/cyclin B and/or CAK might be fast so that the kinase-inhibitor complexes do not survive successive washing steps in our binding assays. p28 would presumably also inhibit the CAK-mediated activation of Cdk2/cyclin E and Cdk2/cyclin A, since it has a higher affinity for these Cdks.

We also analyzed the biochemical functions of p28 by adding recombinant p28 to *Xenopus* egg extracts. Cdk2/cyclin E activity is required for the initiation of chromosomal DNA replication in this system (Jackson *et al.*, 1995). In egg extracts, the concentration of cyclin E1 is ~60 nM (Rempel *et al.*, 1995). At a 5-fold molar excess above cyclin E1, p28 elicited a readily observable delay in the onset of replication, consistent with the observed inhibitory effects of p28 on recombinant Cdk2/cyclin E complex. Intriguingly, although there was a delay in the onset of DNA synthesis, once replication began, it proceeded at a rate comparable to that in control extracts. At higher levels of p28, both the rate and the overall extent of DNA replication were severely inhibited. These findings could argue that although p28 preferentially inhibits initiation

as opposed to elongation, at higher concentrations, p28 could inhibit elongation as well. An alternative possibility would be that when the level of p28 is high, some replication origins could fire late, giving rise to an extended S phase reminiscent of the somatic cell cycle (for review, see Fangman and Brewer, 1992). Finally, p28 could block initiation of some replication origins, possibly by preventing the transition from pre-replicative foci to initiation complex, a phenomenon previously observed when high levels (1-2 μM) of human p21 were added to extracts (Yan and Newport, 1995; Jackson *et al.*, 1995). Further mechanistic studies will be required to evaluate these possibilities.

We have observed that p28 also elicits a dose-dependent delay of mitosis. In principle, this mitotic delay could result from the replication checkpoint responding to p28-dependent inhibition of DNA synthesis. However, we feel that this explanation is not likely because p28 elicits a mitotic delay even in the presence of a concentration of sperm chromatin (25 sperm/μl of extract) well below the threshold required to trigger the replication checkpoint in this system (Dasso and Newport, 1990). One explanation is that p28 delays mitosis by inhibiting the CAK-mediated activation of Cdc2/cyclin B, which would be consistent with the ability of p28 to block the activation of Cdc2/cyclin B in insect cell lysates. Alternatively, it is conceivable that p28 could be a more potent inhibitor of the endogenous Cdc2/cyclin B in egg extracts than the purified recombinant Cdc2/cyclin B. Finally, it could be that cyclin E1- and/or cyclin A-associated kinase activities play an additional essential role in mitosis, and that by inhibiting the kinase activities associated with these cyclins, p28 impedes the entry into mitosis.

An important characteristic of human p21 is that it can form a stable complex with the replication factor PCNA. The PCNA-interacting domain of p21 has been mapped to the peptide QTSMTDFY (residues 144 - 151) (Warbrick *et al.*, 1995). The three residues that contribute the most to PCNA binding in p21 (Q144, M147, and F150) are not conserved in *Xenopus* $p28^{Kix1}$ or Xic1(Su *et al.*, 1995), which could account for the observation that PCNA binds *Xenopus* p28 much less well than it binds human p21. Human and mouse p27 apparently do not interact with PCNA (Luo *et al.*, 1995), raising the possibility that *Xenopus* p28 may belong to the mammalian p21 subfamily. However, the C-terminal domain of p28 does contain a QT motif (LEQTPRK, residues 200-206) that is found in mammalian p27 and p57 (see Matsuoka *et al.*, 1995). Thus, further characterization of p28 will be required to classify this Cdk inhibitor definitively.

p28 is present at low levels in oocytes, mature eggs, and embryos up to stage 11. During this period, its concentration is ~2 nM, well below the concentration of 60 nM at which its preferred target, cyclin E1, is present (Rempel *et al.*, 1995). The next best candidate, namely cyclin A1, is also more abundant (18 nM-60 nM) than p28 in *Xenopus* eggs (Rempel *et al.*, 1995). Although it is conceivable that p28 might regulate a Cdk distinct from cyclin E1 and cyclin A1, a more plausible scenario is that p28 does not play a rate-limiting role in controlling the onset of replication or mitosis during early embryogenesis. This notion would be consistent with the fact that the early embryonic cleavages occur very rapidly (i.e., approximately every 35 minutes) without any discernible gaps between S-phase and M-phase. The midblastula transition (MBT, stage $8^1/_2$) defines the first developmental event where the cell cycles in certain embryonic

cells begin to slow down and become asynchronous with respect to one another (Newport and Kirschner, 1982a). This transition also coincides with the commencement of zygotic transcription (Newport and Kirschner, 1982b). Later, at stage 10, another major transition occurs during early gastrulation. This early gastrulation transition (EGT) is marked by the elimination of maternal mRNAs for cyclins A1 and A2 (Howe *et al.*, 1995). In parallel, the amount of cyclin A1 protein drops precipitously to undetectable levels, whereas the level of cyclin A2 protein translated from zygotic cyclin A2 mRNA increases dramatically (Howe *et al.*, 1995; see also Rempel *et al.*, 1995). The level of *Xenopus* p28 protein remains low at both the MBT and EGT, but it does increase dramatically at a significantly later time, namely during stages 12 and 13. In principle, the up-regulation of p28 at stages 12 and 13 could mark another developmental transition at late gastrulation in the *Xenopus* embryo. Alternatively, the increase in the levels of p28 could represent a more specialized regulatory mechanism that selectively targets certain cell types. The period encompassing stages 12 and 13 coincides with numerous significant events in development. In the case of neuronal differentiation, primary neuronal precursors undergo their final round of DNA replication (stage 12); the transcript for neuronal signaling molecule X-Delta-1 becomes expressed in prospective neurons (stage 12); and the gene for neuron-specific type-II β-tubulin is turned on in scattered cells in the neural plate (stage 12.5-13) (Hartenstein, 1989; Chitnis *et al.*, 1995). Clearly, it will be highly important to localize the p28 mRNA and protein by *in situ* methods in order to delineate precisely the developmental events which might be related to the up-regulation of p28. In any case, it appears likely that p28, like p21, p27, and

p57, may play a role in cellular differentiation. The target of p28 in later embryos has not been established, but cyclin D, the presumed somatic form of cyclin E, or the recently described somatic cyclin A2 are potential candidates (Howe *et al.*, 1995; Rempel *et al.*, 1995).

In summary, we have identified *Xenopus* p28, a new member of the p21/p27 class of Cdk inhibitors. *In vitro*, p28 inhibits pre-activated Cdk2/cyclin E and Cdk2/cyclin A, and prevents CAK-mediated activation of Cdc2/cyclin B. In *Xenopus* egg extracts, exogenously added p28 inhibits both DNA replication and mitosis. Finally, the level of p28 protein is up-regulated dramatically during stages 12 and 13, which temporally correlates with the earliest events in neural differentiation. In concert with other transitions such as the replacement of embryonic Cdks with somatic Cdks, p28 could play an important role in regulating the somatic cell cycle. Further study of p28 will help us to gain more insight into cell cycle regulation and its connection with developmental regulation.

Acknowledgements

We thank T.R. Coleman, A. Kumagai, P.R. Mueller, D. Patra, P.B. Carpenter, B.J. Wold, R.J. Deshaies, G.P. Moore, M.P. Running, and the anonymous reviewers for comments on the manuscript. W.S. is especially indebted to A. Kumagai, P.R. Mueller, R.J. Deshaies, B.J. Wold, and Z. Shou for being excellent mentors. We thank P.R. Mueller for the oocyte cDNA, oocyte cDNA library, and XTC lysates; A. Kumagai for antibodies to *Xenopus* Cdc2, cyclin A1, and cyclin B2, and for purified human cyclin B1 protein; J.

Maller (University of Colorado, Denver) for antibodies to *Xenopus* Cdk2 and cyclin E1; D. Morgan (UCSF) for recombinant baculoviruses encoding human Cdk2, cyclin A, cyclin E, Cdk7, and cyclin H; and D. Beach (Cold Spring Harbor Laboratory) for human p21 bacterial expression plasmid. W.S. is a predoctoral fellow and W.G.D. is an investigator of the Howard Hughes Medical Institute.

References

Aprelikova, O., Xiong,Y., and Liu, E.T. (1995). Both p16 and p21 families of cyclin dependent kinase (Cdk) inhibitors block the phosphorylation of cyclin-dependent kinases by the Cdk-activating kinase. *J.* Biol. Chem. *270*, 18195–18197.

Chan, F.K.M., Zhang, J., Cheng, L., Shapiro, D.N., and Winoto, A. (1995). Identification of human and mouse p19, a novel Cdk4 and Cdk6 inhibitor with homology to $p16^{Ink4}$. Mol. Cell. Biol. *15*, 2682–2688.

Chen, J., Jackson, P.K., Kirschner, M.W., and Dutta, A. (1995). Separate domains of p21 involved in the inhibition of Cdk kinase and PCNA. Nature *374*, 386–388.

Chitnis, A., Henrique, D., Lewis, J., Ish-Horowicz, D., and Kintner, C. (1995). Primary neurogenesis in *Xenopus* embryos regulated by a homologue of the *Drosophila* neurogenic gene *Delta*. Nature *375*, 761-766.

Coleman, T.R., Tang, Z., and Dunphy, W.G. (1993). Negative regulation of the wee1 protein kinase by direct action of the nim1/cdr1 mitotic inducer. Cell *72*, 919–929.

Cyert, M.S., and Kirschner, M.W. (1988). Regulation of MPF activity in vitro. Cell *53*, 185–195.

Dasso, M., and Newport, J.W. (1990). Completion of DNA replication is monitored by a feedback system that controls the initiation of mitosis *in vitro*: studies in *Xenopus*. Cell *61*, 811–823.

Deng, C., Zhang, P., Harper, J.W., Elledge, S.J., and Leder, P. (1995). Mice lacking $P21^{CIP1/WAF1}$ undergo normal development, but are defective in G1 checkpoint control. Cell *82*, 675–684.

Desai, D., Gu, Y., and Morgan, D.O. (1992). Activation of human cyclin-dependent kinases in vitro. Mol. Biol. Cell *3*, 571–582.

Dingwall, C., and Laskey, R.A. (1991). Nuclear targeting sequences - a consensus? Trends Biochem. Sci. *16*, 478–481.

Draetta, G., (1993). Cdc2 activation: the interplay of cyclin binding and Thr161 phosphorylation. Trends Cell Biol. *3*, 287–289.

Dunphy, W.G., and Newport, J.W. (1989). Fission yeast p13 blocks mitotic activation and tyrosine dephosphorylation of the *Xenopus* cdc2 protein kinase. Cell *58*, 181–191.

El-Deiry, W.S., Tokino, T., Velculescu, V.E., Levy, D.B., Parsons, R., Trent, J.M., Lin, D., Mercer, W.E., Kinzler, K.W., and Vogelstein, B. (1993). WAF1, a potential mediator of p53 tumor suppression. Cell *75*, 817–825.

Elledge, S.J., and Harper, J.W. (1994). Cdk inhibitors: on the threshold of checkpoints and development. Curr. Opin. Cell Biol. *6*, 847–852.

Fangman, W.L., and Brewer, B.J. (1992). A question of time: replication origins of eukaryotic chromosomes. Cell *71*, 363–366.

Gu, Y., Turck, C.W., and Morgan, D.O. (1993). Inhibition of Cdk2 activity *in vivo* by an associated 20K regulatory subunit. Nature *366*, 707–710.

Guan, K.-L., Jenkins, C.W., Li, Y., Nichols, M.A., Wu, X., O'Keefe, C.L., Matera, A.G., and Xiong, Y. (1994). Growth suppression by p18, a $p16^{INK4/MTS1}$ and $p14^{INK4B/MTS2}$-related CDK6 inhibitor, correlates with wild-type pRb function. Genes & Develop. *8*, 2939–2952.

Halevy, O., Novitch, B.G., Spicer, D.B., Skapek, S.X., Rhee, J., Hannon, G.J., Beach, D., and Lassar, A.B. (1995). Correlation of terminal cell-cycle arrest of skeletal-muscle with induction of p21 by MyoD. Science *267*, 1018–1021.

Hannon, G.J., and Beach, D. (1994). $p15^{INK4B}$ is a potential effector of TGFβ-induced cell cycle arrest. Nature *371*, 257–261.

Harper, J.W., Adami, G., Wei, N., Keyomarsi, K., and Elledge, S.J. (1993). The p21 Cdk-interacting protein Cip1 is a potent inhibitor of G1 cyclin-dependent kinases. Cell *75*, 805–816.

Harper, J.W., Elledge, S.J., Keyomarsi, K., Dynlacht, B., Tsai, L.-H., Zhang, P., Dobrowolski, S., Bai, C., Connell-Crowley, L., Swindell, E., Fox, M.P., and Wei, N. (1995). Inhibition of cyclin-dependent kinases by p21. Mol. Biol. Cell *6*, 387-400.

Hartenstein, V. (1989). Early neurogenesis in *Xenopus*: the spatio-temporal pattern of proliferation and cell lineages in the embryonic spinal cord. Neuron *3*, 399-411.

Howe, J.A., Howell, M., Hunt, T., and Newport, J.W. (1995). Identification of a developmental timer regulating the stability of embryonic cyclin A and a new somatic A-type cyclin at gastrulation. Genes & Devel. *9*, 1164–1176.

Jackson, P.K., Chevalier, S., Philippe, M., and Kirschner, M.W. (1995). Early events in DNA replication require cyclin E and are blocked by $p21^{CIP1}$. J. Cell Biol. *130*, 755–769.

Kato, J.-Y., Matsuoka, M., Polyak, K., Massagué, J., and Sherr, C.J. (1994). Cyclic AMP-induced G1 phase arrest mediated by an inhibitor ($p27^{KIP1}$) of cyclin-dependent kinase-4 activation. Cell *79*, 487–496.

Koff, A., Giordano, A., Desai, D., Yamashita, K., Harper, J.W., Elledge, S., Nishimoto, T., Morgan, D.O., Franza, B.R., and Roberts, J.M. (1992). Formation and activation of a cyclin E-Cdk2 complex during the G1 phase of the human cell cycle. Science *257*, 1689–1694.

Kumagai, A., and Dunphy, W.G. (1991). The cdc25 protein controls tyrosine dephosphorylation of the cdc2 protein in a cell-free system. Cell *64*, 903–914.

Kumagai, A., and Dunphy, W.G. (1995). Control of the cdc2/cyclin B complex in *Xenopus* egg extracts arrested at a G2/M checkpoint with DNA synthesis inhibitors. Mol. Biol. Cell *6*, 199–213.

Lee, M.-H., Reynisdottir, I., and Massagué, J. (1995). Cloning of $p57^{KIP2}$, a cyclin-dependent kinase inhibitor with unique domain structure and tissue distribution. Genes & Develop. *9*, 639–649.

Leno, G.H., and Laskey, R.A. (1991). DNA replication in cell-free extracts from *Xenopus laevis*. Methods Cell Biol. *36*, 561–579.

Li, R., Waga, S., Hannon, G.J., Beach, D., and Stillman, B. (1994). Differential effects by the p21 Cdk inhibitor on PCNA-dependent DNA replication and repair. Nature *371*, 534–537.

Luo, Y., Hurwitz, J., and Massagué, J. (1995). Cell-cycle inhibition by independent Cdk and PCNA binding domains in $p21^{CIP1}$. Nature *375*, 159–161.

Massagué, J., and Polyak, K. (1995). Mammalian antiproliferative signals and their targets. Curr. Opin. Genet. & Devel. *5*, 91–96.

Matsuoka, S., Edwards, M.C., Bai, C., Parker, S., Zhang, P., Baldini, A., Harper, J.W., and Elledge, S.J. (1995). $p57^{KIP2}$, a structurally distinct member of the $p21^{CIP1}$ Cdk inhibitor family, is a candidate tumor-suppressor gene. Genes & Develop. *9*, 650–662.

Minshull, J., Sun, H., Tonks, N.K., and Murray, A.W. (1994). A MAP kinase-dependent spindle assembly checkpoint in *Xenopus* egg extracts. Cell *79*, 475–486.

Mueller, P.R., Coleman, T.R., and Dunphy, W.G. (1995). Cell cycle regulation of a *Xenopus* Wee1-like kinase. Mol. Biol. Cell *6*, 119–134.

Murray, A.W. (1991). Cell cycle extracts. Methods Cell Biol. *36*, 581–605.

Newport, J., and Kirschner, M. (1982a). A major developmental transition in early *Xenopus* embryos: I. Characterization and timing of cellular changes at the midblastula stage. Cell *30*, 675–686.

Newport, J., and Kirschner, M. (1982b). A major developmental transition in early *Xenopus* embryos: II. Control of the onset of transcription. Cell *30*, 687–696.

Nieuwkoop, P., and Faber, J. (1967). Normal table of *Xenopus laevis* (Daudin). North Holland Publishing Co., Amsterdam.

Noda, A., Ning, Y., Venable, S.F., Pereira-Smith, O.M., and Smith, J.R. (1994). Cloning of senescent cell-derived inhibitors of DNA synthesis using an expression screen. Exp. Cell Res. *211*, 90–98.

Nourse, J., Firpo, E., Flanagan, W.M., Coats, S., Polyak, K., Lee, M.-H., Massagué, J., Crabtree, G.R., and Roberts, J.M. (1994). Interleukin-2-mediated elimination of the $p27^{KIP1}$ cyclin-dependent kinase inhibitor prevented by rapamycin. Nature *372*, 570–573.

Pagano, M., Tam, S.W., Theodoras, A.M., Beer-Romero, P., Del Sal, G., Chau, V., Yew, P.R., Draetta, G.F., and Rolfe, M. (1995). Role of the ubiquitin-proteasome pathway in regulating abundance of the cyclin-dependent kinase inhibitor p27. Science *269*, 682–685.

Parker, S.B., Eichele, G., Zhang, P., Rawls, A., Sands, A.T., Bradley, A., Olson, E.N., Harper, J.W., and Elledge, S.J. (1995). p53-independent expression of $p21^{CIP1}$ in muscle and other terminally differentiating cells. Science *267*, 1024–1027.

Polyak, K., Kato, J.-Y., Solomon, M.J., Sherr, C.J., Massagué, J., Roberts, J.M., and Koff, A. (1994a). $p27^{KIP1}$, a cyclin-cdk inhibitor, links transforming growth factor-β and contact inhibition to cell cycle arrest. Genes Dev. *8*, 9–22.

Polyak, K., Lee, M.-H., Erdjument-Bromage, H., Koff, A., Roberts, J.M., Tempst, P., and Massagué, J. (1994b). Cloning of $p27^{KIP1}$, a cyclin-dependent kinase inhibitor and a potential mediator of extracellular antimitogenic signals. Cell *78*, 59–66.

Rempel, R.E., Sleight, S.B., and Maller, J.L. (1995). Maternal *Xenopus* Cdk2-cyclin E complexes function during meiotic and early embryonic cell cycles that lack a G1 phase. *J.* Biol. Chem. *270*, 6843–6855.

Sambrook, J., Fritsch, E.F., and Maniatis, T. (1989). Molecular Cloning: A Laboratory Manual. Cold Spring Harbor: Cold Spring Harbor Laboratory Press.

Serrano, M., Hannon, G.J., and Beach, D. (1993). A new regulatory motif in cell-cycle control causing specific inhibition of cyclin D/Cdk4. Nature *366*, 704–707.

Sherr, C.J. (1993). Mammalian G1 cyclins. *Cell* **73**:1059-1065.

Smith, J.C., and Tata, J.R. (1991). *Xenopus* cell lines. Methods Cell Biol. *36*, 635–654.

Su, J.-Y., Rempel, R.E., Erikson, E., and Maller, J.L. (1995). Cloning and characterization of the *Xenopus* cyclin-dependent kinase inhibitor $p27^{XIC1}$. Proc. Natl. Acad. Sci. USA *92*, 10187-10191.

Tang, Z., Coleman, T.R., and Dunphy, W.G. (1993). Two distinct mechanisms for negative regulation of the wee1 protein kinase. EMBO J. *12*, 3427–3436.

Toyoshima, H., and Hunter, T. (1994). p27, a novel inhibitor of G1 cyclin-Cdk protein kinase activity, is related to p21. Cell *78*, 67–74.

Waga, S., Hannon, G.J., Beach, D., and Stillman, B. (1994). The p21 inhibitor of cyclin-dependent kinases controls DNA replication by interaction with PCNA. Nature *369*, 574–578.

Warbrick, E., Lane, D.P., Glover, D.M., and Cox, L.S. (1995). A small peptide inhibitor of DNA replication defines the site of interaction between the cyclin-dependent kinase inhibitor $p21^{WAF1}$ and proliferating cell nuclear antigen. Curr. Biol. *5*, 275-282.

Xiong, Y., Hannon, G.J., Zhang, H., Casso, D., Kobayashi, R., and Beach, D. (1993). p21 is a universal inhibitor of cyclin kinases. Nature *366*, 701–704.

Yan, H., and Newport, J. (1995). An analysis of the regulation of DNA synthesis by cdk2, Cip1, and licensing factor. J. Cell Biol. *129*, 1–15.

Zhang, H., Hannon, G.J., and Beach, D. (1994). p21-containing cyclin kinases exist in both active and inactive states. Genes & Develop. *8*, 1750-1758.

Xenopus Cdk Inhibitor (p28)

```
Xe-P28  MAAFHIALQEEMISAPAVLPRLSAGTGR----GACRNLFGPIDHDEMRSELKRQLKE   53
Hu-P27  -----MSNVRVSNGSPSLE-RMDARQAEHPKPSACRNLFGPVDHEELTRDLEKHCRD   51
Hu-P21  ----------MSEPAGDVRQNPCGSK-----ACRRLFGPVDSEQLSRDCDALMAG   40

Xe-P28  IQASDCQRWNFDFETGTPLKGIFCWEPVESKDMPSFYSQNRSIAANTTPSPRQQQPL  110
Hu-P27  MEEASQRKWNFDFQNHKPLEGKYEWQEVEKGSLPEFYYRPPRPPKGACKVPAQESQD  108
Hu-P21  CIQEARERWNFDFVTETPLEGDFAWERVRGLGLPKLYL--PTGPR------RGRDEL   89

Xe-P28  LVSRQP-EPREEAPVDTVRNVPNPPCA--KENAEKTVKRCQGVRGPAKASANT----  160
Hu-P27  VSGSRPAAPLIGAPANSEDTHLVDPKTDPSDSQTGLAEQCAGIRKRPATDDSS----  161
Hu-P21  GGGRRPGT----SPALLQGTA---------EEDHVDLSLSCTLVPRSGEQAEGSPGGP  134

Xe-P28  STQRRKREITTPITDYFPKRKKILSAKPDATKGAHLLCPLEQTPRKKIR-----  209
Hu-P27  TQNKRANRTEENVSDGSPNAGS----------------VEQTPKKPGLRRRQT  198
Hu-P21  GDSQGRKRRQTSMTDFYHSKRRLIF----------------SKRKP-------  164
```

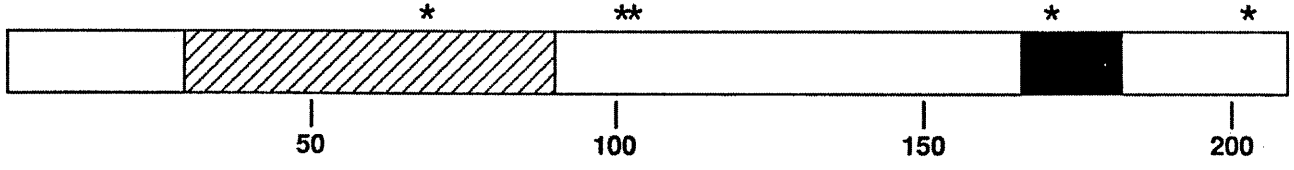

cdk inhibition domain

putative nuclear localization signal

* putative kinase phosphorylation site

Figure II-1

Figure II-1. *Xenopus* p28 belongs to the $p21^{CIP1}/p27^{KIP1}$ Cdk inhibitor family. (A) Sequence alignment of *Xenopus* p28, human $p27^{KIP1}$, and human $p21^{CIP1}$. Boxes indicate identical residues shared by two or more sequences. Arrows mark sequences that were used to design degenerate PCR primers. (B) Schematic diagram of the domain structure of *Xenopus* p28. The CDK inhibition domain (hatched box) is conserved among *Xenopus* p28, human and mouse $p21^{CIP1}$, $p27^{KIP1}$, and $p57^{KIP2}$. A putative bipartite nuclear localization signal (black box) and several potential kinase phosphorylation sites (stars) are indicated. Numbers indicate amino acid residues.

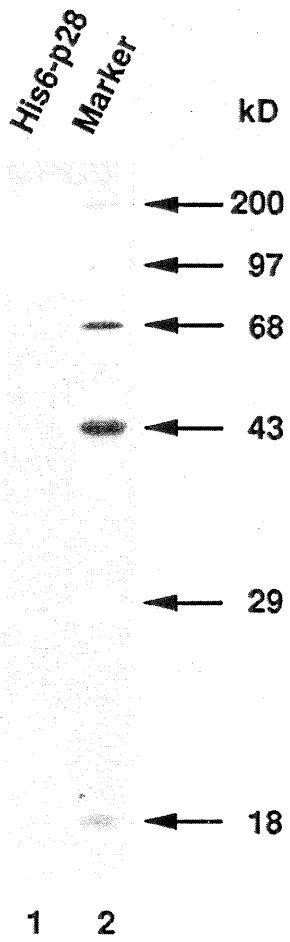

Figure II-2

Figure II-2. Purification of recombinant *Xenopus* p28. Recombinant His6-p28 was expressed in Sf9 insect cells and purified using nickel-IDA chromatography. Purified His6-p28 (lane 1) and molecular markers (lane 2) were run on a 12.5% SDS gel, and stained with Commassie Brilliant Blue.

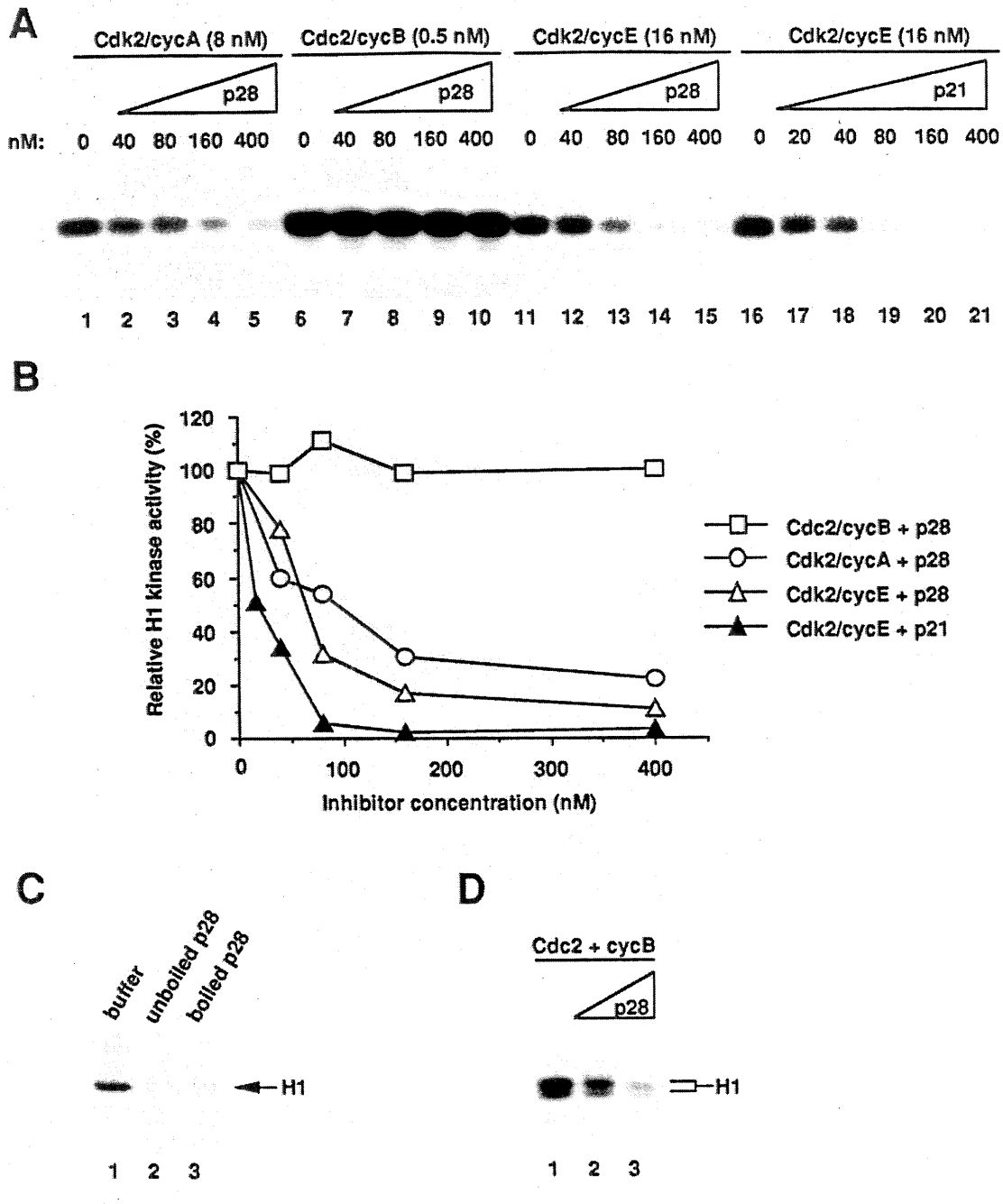
A
Cdk2/cycA (8 nM)
Cdc2/cycB (0.5 nM)
Cdk2/cycE (16 nM)
Cdk2/cycE (16 nM)
p28
p28
p28
p21
nM: 0 40 80 160 400 0 40 80 160 400 0 40 80 160 400 0 20 40 80 160 400
1 2 3 4 5 6 7 8 9 10 11 12 13 14 15 16 17 18 19 20 21
B
Relative H1 kinase activity (%)
120
100
80
60
40
20
0
0 100 200 300 400
Inhibitor concentration (nM)
Cdc2/cycB + p28
Cdk2/cycA + p28
Cdk2/cycE + p28
Cdk2/cycE + p21
C
buffer
unboiled p28
boiled p28
H1
1 2 3
D
Cdc2 + cycB
p28
H1
1 2 3

Figure II-3

Figure II-3. *Xenopus* p28 exhibits differential inhibitory activities toward various Cdk complexes. (A) Pre-activated Cdk2/cyclin A (lanes 1-5), Cdc2/cyclin B (lanes 6-10), and Cdk2/cyclin E (lanes 11-15) were incubated with the indicated amounts of p28. As a control, pre-activated Cdk2/cyclin E was also incubated with the indicated amounts of human $p21^{CIP1}$ under identical conditions (lanes 16-21). The H1 kinase activities of the Cdks were then measured. (B) H1 kinase activities in (A) were quantitated, and are plotted as the percentage of kinase activity in the absence of inhibitors. (C) p28 is heat stable. H1 kinase activities of Cdk2/cyclin E complex (16 nM) in the presence of control buffer (lane 1), native p28 (80 nM, lane 2), or p28 which had been boiled at 100°C for 5 minutes (80 nM, lane 3) were assayed. (D) p28 inhibits Cdc2/cyclin B activation. Cdc2-containing insect cell lysates were incubated at room temperature with purified cyclin B in the presence of either control buffer (lane 1) or p28 (40 nM, lane 2; 160 nM, lane 3). The mixtures were then subjected to H1 kinase assays.

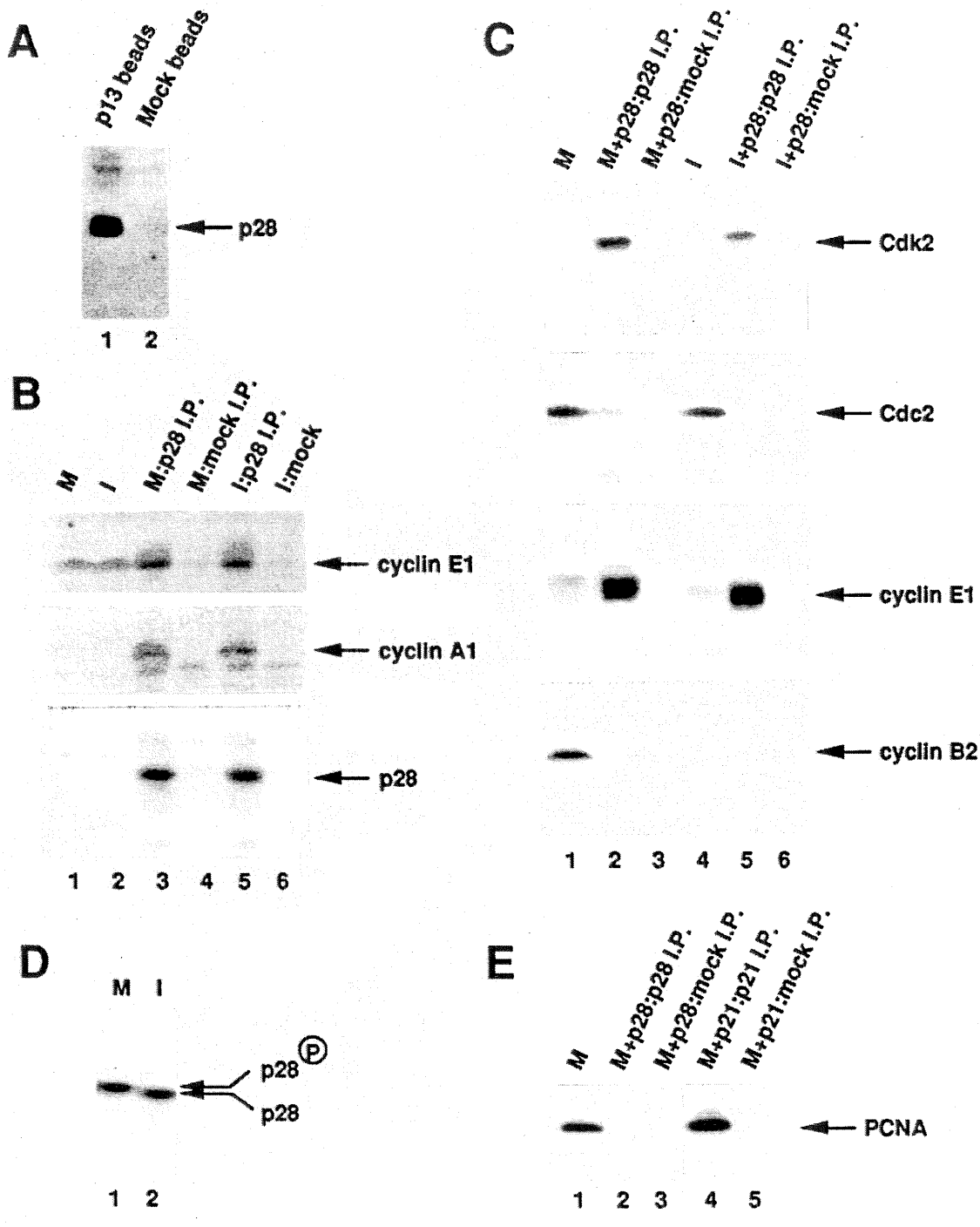
A
p13 beads
Mock beads
p28
1 2
B
M
I
M:p28 I.P.
M:mock I.P.
I:p28 I.P.
I:mock
cyclin E1
cyclin A1
p28
1 2 3 4 5 6
C
M
M+p28:p28 I.P.
M+p28:mock I.P.
I
I+p28:p28 I.P.
I+p28:mock I.P.
Cdk2
Cdc2
cyclin E1
cyclin B2
1 2 3 4 5 6
D
M I
p28 P
p28
1 2
E
M
M+p28:p28 I.P.
M+p28:mock I.P.
M+p21:p21 I.P.
M+p21:mock I.P.
PCNA
1 2 3 4 5

Figure II-4

Figure II-4. p28 associates with Cdks in *Xenopus* egg extracts. (A) M-phase extracts (160 μl) were rotated with p13 (lane 1) or control (lane 2) agarose beads. The beads were then washed and immunoblotted with anti-p28 peptide antibodies. (B) Mitotic (M-phase) extracts (300 μl, lanes 3 and 4) and interphase (I-phase) extracts (300 μl, lanes 5 and 6) were immunoprecipitated with anti-*Xenopus* p28 whole protein antibodies (lanes 3 and 5) or with control rabbit anti-mouse IgG antibodies (lanes 4 and 6). The total immunoprecipitates or M-phase and I-phase extracts (2 μl, lanes 1 and 2, respectively) were probed with antibodies against *Xenopus* cyclin E1, cyclin A1, and p28 as indicated. (C) Recombinant p28 (10 ng) was added to 100 μl of M-phase (lanes 2 and 3) or I-phase (lanes 5 and 6) extract. The total anti-p28 immunoprecipitates (lanes 2 and 5) and mock immunoprecipitates (lanes 3 and 6) from these extracts or 2 μl of M-phase and I-phase extract (lanes 1 and 4, respectively) were subsequently probed with antibodies against *Xenopus* Cdk2, Cdc2, cyclin E1, and cyclin B2 as indicated. (D) ^{35}S-Labeled p28 was added to M-phase (lane 1) and I-phase (lane 2) extracts. The slower-migrating form in lane 1 corresponds to the phosphorylated p28. (E) Lanes 2-5: the indicated amounts (in μg) of His6-p28 or His6-p21 were added to M-phase extracts (50 μl), and immunoprecipitated with anti-*Xenopus* p28 (lane 2), or anti-human p21 (lane 4) antibodies, or mock-precipitated (m) with control rabbit anti-mouse IgG antibodies (lanes 3 and 5). Lanes 6-8: nickel-IDA beads and the indicated amounts (in μg) of His6-p28 or His6-p21 were incubated in 200 μl of 2 -fold diluted M-phase extract, and the beads were then recovered. The immunoprecipitates, the nickel-IDA beads, or M-phase extracts (E) (0.5 μl, lane 1; 1 μl, lane 9) were probed with anti-human PCNA antibodies.

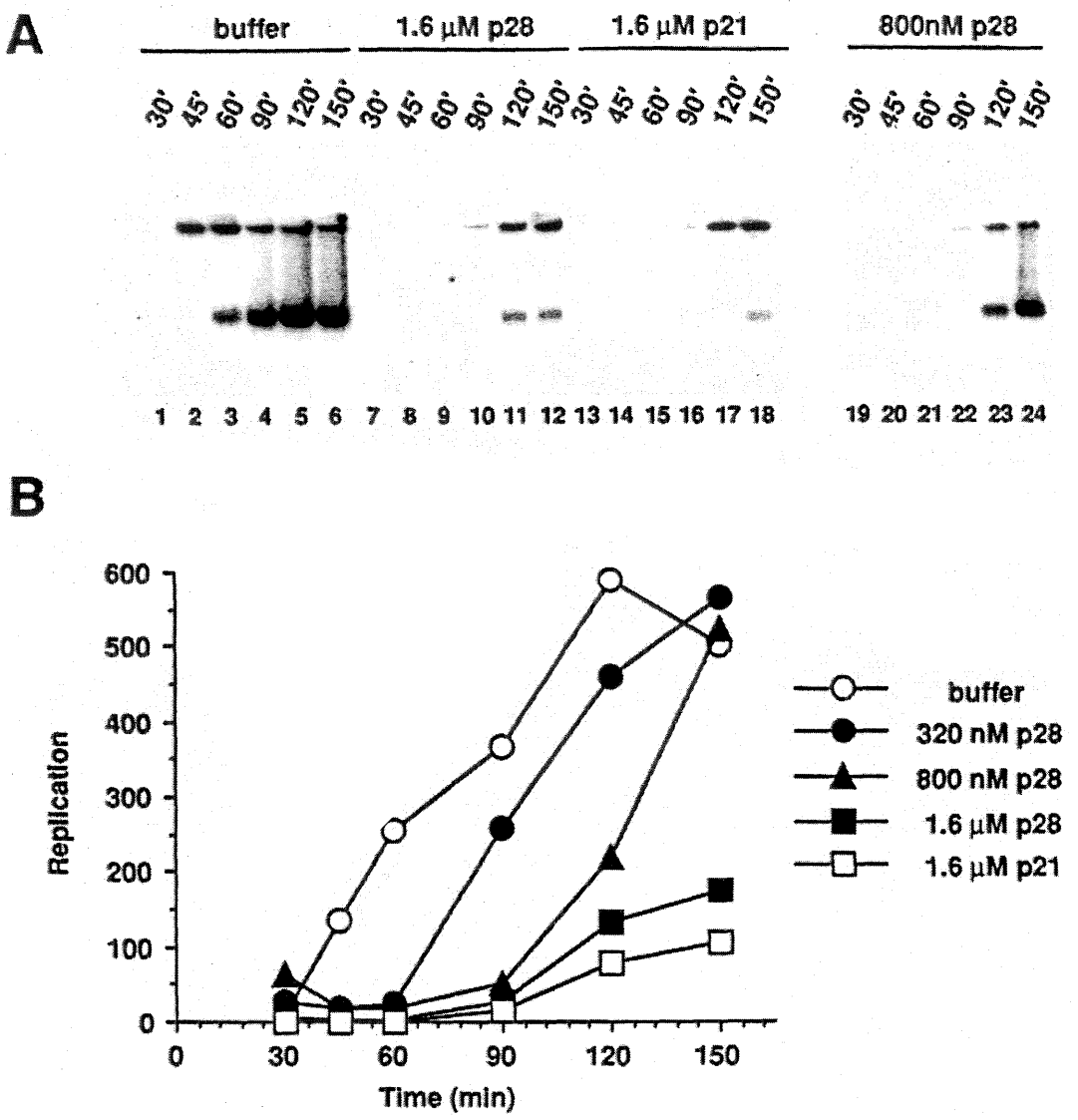
A
buffer
1.6 µM p28
1.6 µM p21
800nM p28
30' 45' 60' 90' 120' 150'
1 2 3 4 5 6 7 8 9 10 11 12 13 14 15 16 17 18 19 20 21 22 23 24
B
Replication
600
500
400
300
200
100
0
0 30 60 90 120 150
Time (min)
buffer
320 nM p28
800 nM p28
1.6 µM p28
1.6 µM p21

Figure II-5

Figure II-5. *Xenopus* p28 inhibits chromosomal replication in a dose-dependent manner. (A) Cytostatic factor (CSF) arrested extracts (500 sperm nuclei/μl, 0.2 μCi [α-^{32}P]-dCTP/μl) were incubated with buffer (lanes 1-6), *Xenopus* p28 (1.6 μM, lanes 7-12; 0.8 μM, lanes 19-24), or human $p21^{CIP1}$ (1.6 μM, lanes 13-18). The extracts were then activated by $CaCl_2$, and at the indicated time points, samples were taken to assay the extent of replication by monitoring the total incorporation of ^{32}P-dCTP into DNA. (B) Quantitation of various replication assays in arbitrary units (including those presented in part A).

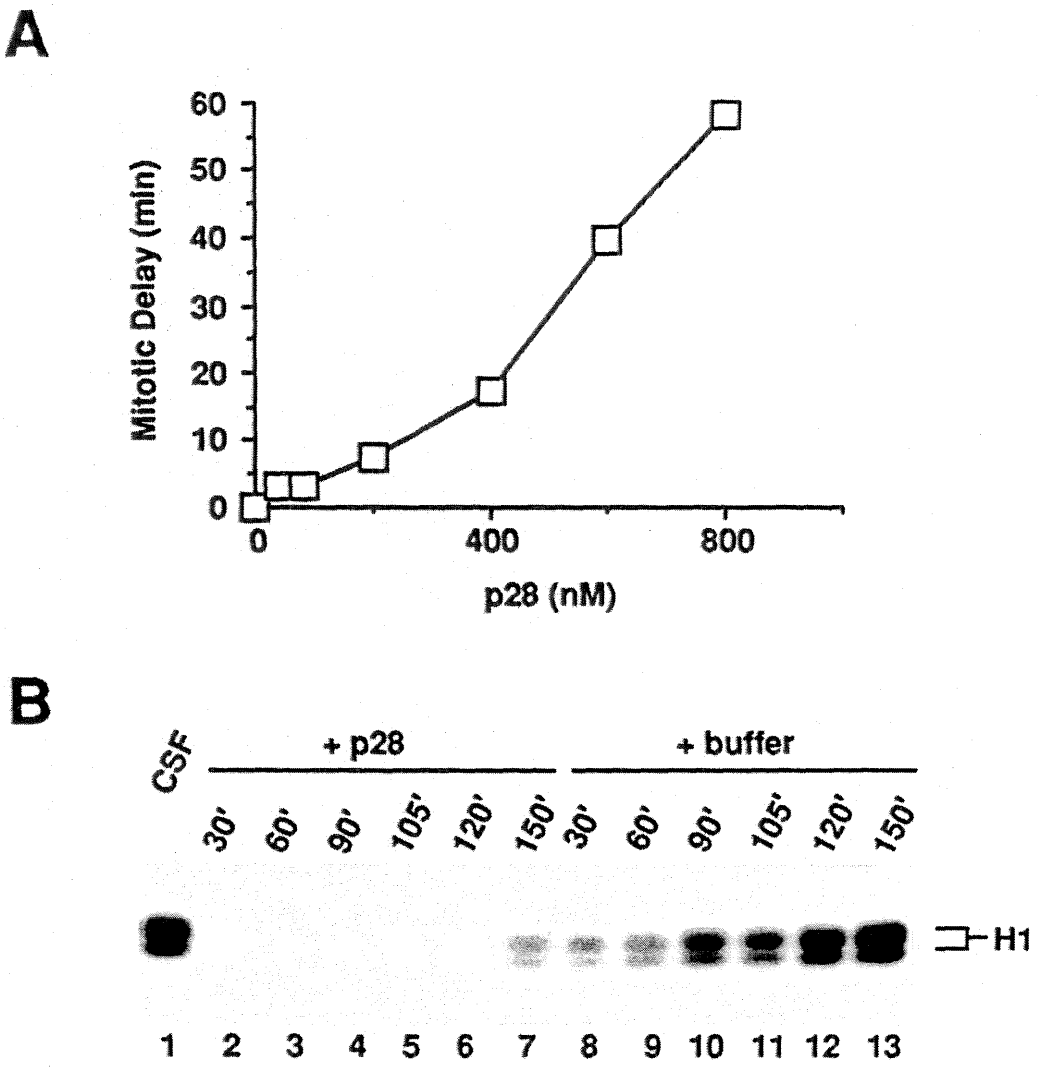
A
Mitotic Delay (min)
60
50
40
30
20
10
0
0
400
800
p28 (nM)
B
CSF
+ p28
+ buffer
30'
60'
90'
105'
120'
150'
30'
60'
90'
105'
120'
150'
H1
1 2 3 4 5 6 7 8 9 10 11 12 13

Figure II-6

Figure II-6. *Xenopus* p28 inhibits mitosis in a dose-dependent manner. (A) CSF extracts (containing 25 sperm nuclei/μl extract) were mixed with various amounts of *Xenopus* p28 protein and then activated. Entry into mitosis was scored visually and was defined as the time point where 50% of the nuclear envelopes had broken down relative to buffer-treated extracts. (B) H1 kinase activities of a CSF extract (lane 1) or activated extracts containing either p28 (800 nM, lanes 2-7) or control buffer (lanes 8-13) were measured at the indicated times after Ca^{2+} addition. The p28-treated and the control extracts entered mitosis at 150 min and 90 min, respectively.

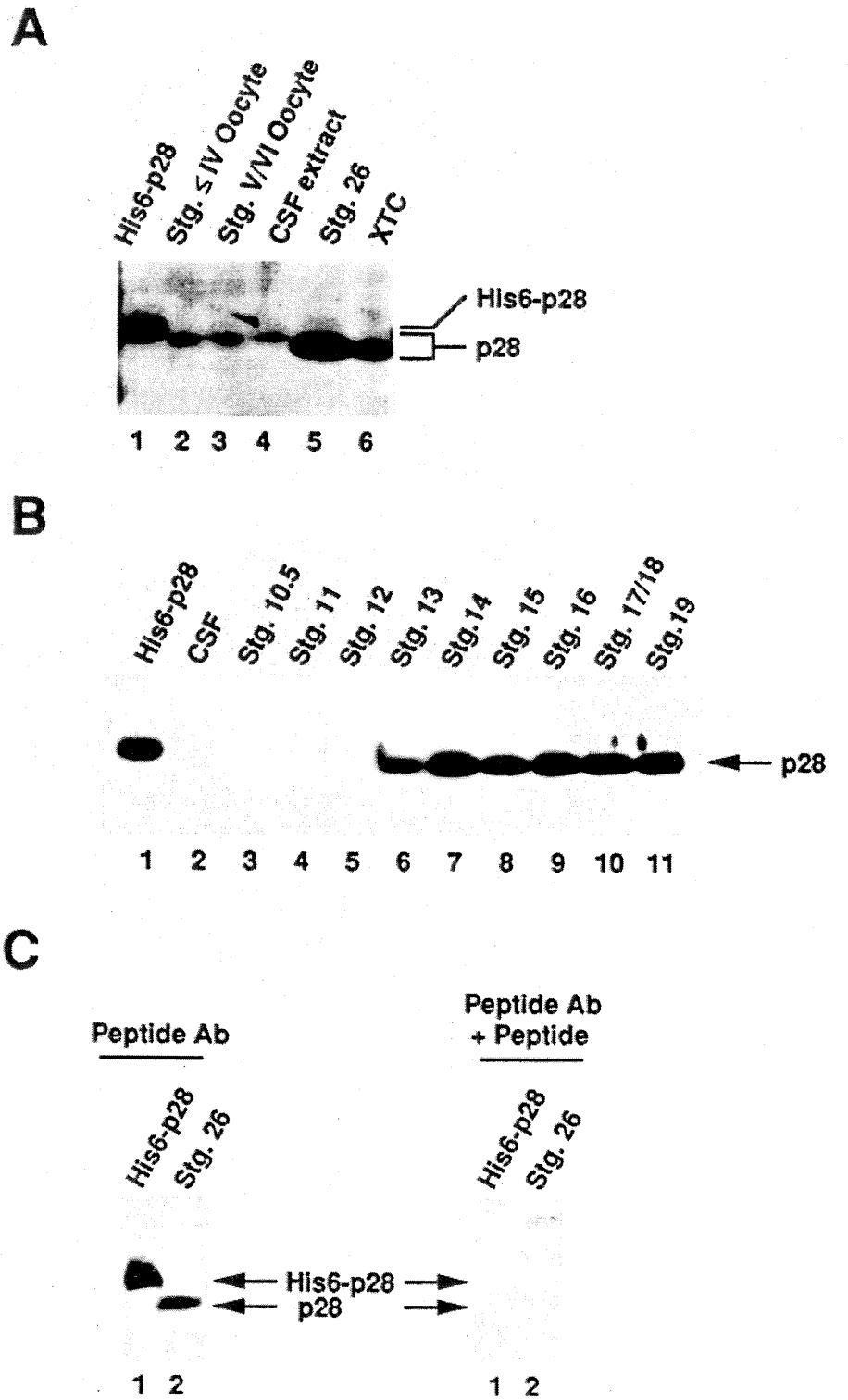
A
His6-p28
Stg. ≤ IV Oocyte
Stg. V/VI Oocyte
CSF extract
Stg. 26
XTC
His6-p28
p28
1 2 3 4 5 6
B
His6-p28
CSF
Stg. 10.5
Stg. 11
Stg. 12
Stg. 13
Stg.14
Stg. 15
Stg. 16
Stg. 17/18
Stg.19
p28
1 2 3 4 5 6 7 8 9 10 11
C
Peptide Ab
Peptide Ab
+ Peptide
His6-p28
Stg. 26
His6-p28
Stg. 26
His6-p28
p28
1 2
1 2

Figure II-7

Figure II-7. *Xenopus* p28 is developmentally regulated. (A) A comparison of p28 protein levels during *Xenopus* development. His6-p28 (10 ng, lane 1) and extracts made from stage ≤ IV oocytes (100 μg, lane 2), stage V/VI oocytes (100 μg, lane 3), CSF-arrested eggs (100 μg, lane 4), stage 26 embryos (60 μg, lane 5), and *Xenopus* tissue culture (XTC) cells (60 μg, lane 6) were immunoblotted with anti-p28 peptide antibodies. (B) The p28 protein level is elevated during stages 12 and 13. 1 ng of His6-p28 (lane 1), 100 μg of CSF extract (lane 2), and 60 μg of extract made from embryos at the indicated stages (lanes 3-11) were immunoblotted with anti-p28 peptide antibodies. (C) Peptide-blocking assay. Identical strips containing His6-p28 and stage 26 embryo extracts were immunoblotted with anti-p28 peptide antibodies (400 ng/ml) in the absence (left panel) or presence (right panel) of the p28 C-terminal peptide (200 ng/ml). All blots were visualized using ECL.

Chapter III - Multiple *telophase arrest bypassed (tab)* Mutants Alleviate the Essential Requirement for Cdc15 in Exit from Mitosis in *S. cerevisiae*

(Wenying Shou and Raymond J. Deshaies, manuscript in preparation)

Abstract

The Mitotic Exit Network (MEN) proteins- including the GTP-binding protein Tem1, protein kinases Cdc15, Dbf2, and Cdc5, and the protein phosphatase Cdc14- are essential for cell cycle progression from late anaphase/telophase to G1 in *Saccharomyces cerevisiae*. To identify regulators of this transition in general and downstream targets of the MEN in particular, we sought mutations that bypassed the essential requirement for *CDC15*. Fifteen such *telophase arrest bypassed* (*tab*) mutants were isolated, and they mapped to at least three recessive (*tab1*, *tab2*, *tab3*) and three dominant (*TAB5*, *TAB6*, *TAB7*) linkage groups. Both *tab2-1* and *tab3-1* enabled *TEM1*-independent degradation of Clb2 and accumulation of Sic1.

The *tab2-1* mutation expanded the permissive temperature range for *cdc5-1*, *cdc14-1*, and *cdc15-2* mutants, and allowed efficient bypass of *tem1Δ* and *cdc15Δ*, suggesting that *TAB2* negatively regulates the exit from mitosis, and that *TAB2* acts after *TEM1* and *CDC15*-dependent steps, or on a parallel pathway. Molecular cloning revealed that *TAB1* and *TAB2* were *MTR10* (*YOR160W*) and *NET1* (*YJL076W*), respectively. The existence of multiple dominant *TAB* and recessive *tab* mutants suggests that exit from mitosis is likely to be regulated by a signal transduction pathway that is subject to positive and negative controls.

Introduction

In *S. cerevisiae*, a key event accompanying exit from mitosis is the inactivation of Clb/Cdc28 kinase achieved through degradation of Clb and accumulation of the Clb/Cdc28 inhibitor Sic1 (reviewed in Deshaies, 1997). Anaphase-Promoting Complex/Cyclosome (APC/C) ubiquitin ligase and its substrate specific activator Hct1/Cdh1 are required for degradation of Clb2, the major mitotic cyclin in the budding yeast (reviewed in Peters, 1998). Whereas *hct1Δ* and *sic1Δ* cells appear relatively normal, *hct1Δ sic1Δ* cells are inviable, presumably due to their inability to extinguish Cdc28 activity in telophase (Schwab et al., 1997).

The complexity in the regulation of the exit from mitosis is underscored by the existence of a set of genes essential for this process. They encode the GTP-binding protein Tem1, the putative guanine nucleotide releasing factor Lte1, the dual specificity protein phosphatase Cdc14, protein kinases Cdc5, Cdc15, and Dbf2/Dbf20, and the Dbf2-binding protein Mob1 (reviewed in Deshaies, 1997; Luca and Winey, 1998). Since most of these proteins resemble components of signaling pathways and display a variety of genetic interactions with each other which are suggestive of functional interaction between the encoded proteins (Parkes and Johnston, 1992; Kitada et al., 1993; Shirayama et al., 1994; Shirayama et al., 1996; Jaspersen et al., 1998; Komarnitsky et al., 1998; Luca and Winey, 1998), we will refer to this group of proteins as the Mitotic Exit Network (MEN).

When cells harboring conditional-lethal temperature sensitive (ts) mutations in any of the MEN genes are shifted to the restrictive temperature, they uniformly arrest in late anaphase as large-budded cells with segregated chromosomes, elongated spindles, and elevated Cdc28 activity. Inactivation of Cdc28 by overexpression of Sic1 suppresses multiple MEN mutants and hyperactivation of Cdc28 by overexpression of Clb2 exacerbates their phenotypes, suggesting that an important function of MEN proteins is to eradicate Cdc28 activity during the transition from anaphase/telophase to G1 (Donovan et al., 1994; Toyn et al., 1997; Charles et al., 1998; Jaspersen et al., 1998).

To address how the Mitotic Exit Network is organized and regulated, we sought *tab* (*telophase arrest bypassed*) mutants that can alleviate the essential requirement for *CDC15*. In theory, *tab* mutants could act downstream of or parallel to *CDC15*, and could be either loss-of-function mutations in genes that inhibit exit from mitosis or gain-of-function mutations in genes that promote exit from mitosis. To our surprise, mutations in at least six linkage groups were uncovered, with three groups being recessive (*tab1-tab3*) and three groups being dominant (*TAB5-7*). Here, we report on the characterization of recessive *tab* mutants. Molecular cloning revealed that *TAB1* is identical to *MTR10* (*YOR160W*) and *TAB2* is *YJL076W* (also known as *NET1*, Shou et al., 1999; Straight et al., 1999). Mtr10 is involved in nuclear transport (Kadowaki et al., 1994; Pemberton et al., 1997; Senger et al., 1998), and Net1 is a novel protein that serves as a negative regulator of Cdc14 (Shou et al., 1999).

Materials and Methods

Strains and plasmids: All yeast strains used in this study (listed in Table III-1) are isogenic to W303. Standard methods were employed for the culturing and manipulation of yeast (Sherman, 1991). All plasmid constructions were based on the pRS vector series (Sikorski and Hieter, 1989). To replace *CDC15* and *TEM1* with *TRP1*, polymerase chain reaction (PCR) products containing *TRP1* flanked by 200-base pair (bp) homology to the 5' and 3' untranslated regions of the targeted gene were used to transform diploid strain RJD 381. To construct *[pMET3-CDC15, URA3]* (pWS100) and *[pMET3-cdc15-2, URA3]* (pWS109), the corresponding genes (from start codon to 300 bps downstream of the stop codon) were amplified by PCR from genomic DNA of wild type (RJD381) or *cdc15-2* (RJD619) cells, and cloned into the SpeI and SacII sites of RDB620 (a derivative of pRS316 containing the *MET3* promoter inserted between the HindIII and EcoRI sites). The construction of *[pGAL1-TEM1, URA3]* and *tem1Δ::GAL1-UPL-TEM1/TRP1* was described elsewhere (Shou et al., 1999).

Isolation of *tab* mutants: The scheme is outlined in Figure 2. Ninety independent cultures of *cdc15Δ [pMET3-cdc15-2, URA3]* (WY221) were grown at 25^{o}C in synthetic minimal medium + 2% glucose (SD) in the absence of methionine. For each culture, ~8x10^{6} cells were plated on SD+ methionine (2 mM) at 30^{o}C (to repress expression of *cdc15-2*, and to partially inactivate the *cdc15-2*^{ts} allele). One to two colonies were picked from each plate and tested for viability on SD+ 5-fluoroorotic acid (5-FOA) plates (Sikorski and Boeke, 1991). When more than one colony was picked from a single plate,

care was taken to pick colonies of different size or morphology. Out of ~90 colonies tested, 25 survived on 5-FOA medium (Tab$^+$). PCR analysis confirmed that all twenty five colonies had lost the *[pMET3-cdc15-2, URA3]* plasmid, indicating that they were true bypassers of *cdc15Δ*.

Mutant characterization: To determine if Tab$^+$ phenotypes were due to single mutations, *cdc15Δ tab* strains were crossed to *cdc15Δ [pMET3-cdc15-2, URA3]* and the resulting diploids were sporulated and dissected. Approximately 50% of the viable spores should bypass *cdc15Δ* (as indicated by 5-FOA resistance) if the Tab$^+$ phenotype was due to a single mutation. Out of twenty five mutants, fifteen satisfied this criterion, and the other ten were discarded since they either failed to sporulate, yielded few viable spores after dissection, or did not segregate as single mutations. The same crosses were also used to determine if Tab$^+$ was recessive or dominant: for every *tab* mutant, haploid *cdc15Δ tab [pMET3-cdc15-2, URA3]* and diploid *cdc15Δ/cdc15Δ tab/+ [pMET3-cdc15-2, URA3]* cells were pre-grown on YPD (1% yeast extract/2% peptone+2% glucose) at 25^{o}C for 2-3 days, spotted in 5 -fold serial dilutions onto SD+5-FOA plates, and the number of 5-FOA resistant colonies from the diploid was divided by that from the haploid to obtain ratio P. The mutant was defined to be dominant if P= 0.1-1, semi-dominant if P= 0.01-0.1, and recessive if P< 0.01.

To introduce *tab* mutations into the wild type background, *cdc15Δ tab* strains were crossed to *CDC15 TAB*, and *tab* spores were verified by crossing to *cdc15Δ [pMET3-CDC15, URA3]*, and demonstrating that half of the resulting *cdc15Δ* segregants

were 5-FOA resistant. All *cdc15Δ tab* mutants were also crossed to strains harboring either *[pMET3-CDC15, URA3] [pRS313, HIS3]* or *[pMET3-CDC15, URA3] [pRS315, LEU2]* to introduce these plasmids. The resulting strains grew better than the original *cdc15Δ tab* strains, and harbored selectable markers that facilitated subsequent crosses.

To test temperature sensitivity (ts) of *tab* mutants, cells were spotted or streaked onto YPD plates, and incubated at 37^{o}C. Their growth was scored after one to two days.

Linkage analysis: To assign *tab* mutants to linkage groups, *cdc15Δ tab [pMET3-CDC15, URA3]* strains were crossed against each other, and the diploids were sporulated and dissected. If two *tab* mutations belonged to the same linkage group, then all spores were expected to survive on 5-FOA. Otherwise, approximately one quarter of the spores would fail to bypass *cdc15Δ*. The alleles of *TAB2*, *TAB3*, *TAB5*, *TAB6*, and *TAB7* (see Table 2) were assigned this way. The recessive *tab* mutants exhibited a ts growth phenotype that co-segregated with the Tab^{+} phenotype. Complementation tests were used to assign two of the ts mutations as alleles of *tab1*. After *TAB1* was shown to be *MTR10*, other *tab1* alleles were ascertained by their linkage to the *MTR10* locus.

Molecular cloning of *TAB1* and *TAB2*: To clone *TAB1* and *TAB2*, *tab1-1* and *tab2-1* mutant strains were transformed with plasmid libraries harboring yeast genomic DNA fragments, and incubated at 25^{o}C for one day before being shifted to 37^{o}C (Rose and Broach, 1991). Libraries constructed by the laboratories of P. Heiter (ATCC#77164) and R. Young (Thompson et al., 1993) rescued *tab1-1*, and a 2μ library(ATCC#37323, Nasmyth and Reed, 1980) rescued *tab2-1*. Transformants (enough to cover multiple

genome equivalents) were screened, and plasmids retrieved from colonies that grew at 37°C were re-transformed into the original mutant strain to verify their complementation activity. Candidate plasmids were sequenced, and the genomic regions containing the complementing activity were identified. *TAB1* resided on Chromosome XV, 631,500-637,950, and *TAB2*, on Chromosome X, 291,900-299,466. To confirm that these genomic fragments indeed carried the *TAB* genes, complementing fragments were cloned into the integrating vector [pRS305, LEU2] and linearized to target integration into the *tab* locus in a *cdc15Δ::TRP1 tab [pMET3-CDC15, URA3]* strain. The transformants lost their Tab$^+$ phenotype, and when crossed to *cdc15Δ::TRP1 [pMET3-CDC15, URA3]*, the diploid yielded no spores that could bypass *cdc15Δ* (n=40-50). Since both genomic fragments contained multiple open reading frames (ORFs), each ORF was amplified by PCR from yeast genomic DNA and cloned into the integrating plasmid pRS305. The resulting plasmids were transformed into *cdc15Δ::TRP1 tab [pMET3-CDC15, URA3]* to identify the ORF that reversed the Tab$^+$ phenotype. This analysis revealed *TAB1* to be *MTR10*, and *TAB2* to be *YJL076W*.

Gene replacement: For gene replacement, the *S.pombe his5*$^+$ PCR amplification/ transformation method was used (Wach et al., 1997). Correct integrants were verified by PCR using primers that amplified a DNA fragment that spanned the recombination junction. *TAB1* and *TAB2* were replaced in diploid strains to generate *tab1Δ::his5*$^+$/+ (WY65) and *tab2Δ::his5*$^+$/+ (WY66), which were subsequently sporulated and dissected. To assay if *SIC1* or *HCT1* were required for the Tab$^+$ phenotype of *tab*

mutants, *SIC1* or *HCT1* was replaced by *his5*$^{+}$ in *cdc15Δ::TRP1 tab [pMET3-CDC15, URA3]* strains. Each transformant was assayed for the occurrence of correct integration and its ability to survive on 5-FOA.

Cell cycle synchronization: Cells were grown in 1% yeast extract/ 2% peptone (YP) with 2% glucose (YPD), 2% galactose (YPG), or 2% raffinose medium (YPR). For the experiment described in Figure III-1, *cdc15-2* (RJD 619) cells were grown to exponential phase in YPD at 25^{o}C, and shifted to 37^{o}C for three hours so that >95% cells were arrested as large-budded cells. Cycloheximide (CHX) was supplemented to a final concentration of 0, 10, or 100 μg/ml to inhibit translation, and α factor (10 μg/ml) was added to trap cells in the subsequent G1 phase. After five minutes, the cultures were released to 25^{o}C at time 0. Samples were taken at various time points after release. For the experiment described in Figure III-3, cells grown in YPG to exponential phase were arrested with α factor, and released into YPD. In some cases, α factor was added back following release to trap cells in the subsequent G1. To visualize cell morphology, cells were fixed, sonicated, and stained with DAPI as previously described (Pringle, 1991). Images were captured on a Zeiss Axioskop microscope using Fujichrome Provia 400 slide film.

Cell extract preparation and protein detection: Detection of proteins from crude yeast extracts was as described (Shou et al., 1999). Western transfer and immunoblotting were carried out as described (Harlow and Lane, 1988). The following primary antibodies were used: anti-Sic1 (1:8000), anti-Clb2 (1:2500), anti-Cdc28 (1:3000), and 12CA5

(directed against the haemagglutinin (HA) epitope; 1:1000, with 0.5M NaCl). The first three antibodies were raised in rabbits and affinity purified, and the last one was from mouse.

Results

Cdc15 promotes activation of Clb proteolysis by a post-translational mechanism

Transcription has been postulated to play an important role in triggering exit from mitosis. For example, Dbf2, a protein kinase that promotes exit from mitosis, is associated with the CCR4 transcription regulatory complex (Liu et al., 1997). In addition, the Swi5 transcription factor activates *SIC1* expression during late anaphase, and both *sic1Δ* and *swi5Δ* are synthetically lethal with *dbf2Δ* (Knapp et al., 1996; Toyn et al., 1997). To address if production of new proteins is essential for exit from mitosis, we examined the effects of the protein synthesis inhibitor cycloheximide on Clb2 degradation, a key aspect of this process. Mutant *cdc15-2* cells were uniformly arrested in late anaphase/telophase by incubation at the restrictive temperature 37^{o}C. The cultures were then supplemented with 0, 10, or 100 μg/ml cycloheximide before being returned to 25^{o}C to reverse the *cdc15-2* arrest. In the absence of cycloheximide, Sic1 accumulated and Clb2 disappeared as cells exited mitosis (Figure III-1, lanes 1-4). In the presence of cycloheximide, Sic1 accumulation was abolished, but Clb2 degradation still occurred with apparently normal kinetics (Figure III-1, lanes 5-8 and 9-12). Although this result does not exclude the likely possibility that synthesis of new proteins (eg Sic1)

normally facilitates the exit from mitosis, it reveals that a key aspect of mitotic exit – inactivation of Cdc28 protein kinase via degradation of the mitotic cyclin Clb2 – can proceed beyond the Cdc15-dependent step without synthesis of new proteins.

A screen for *telophase arrest bypassed (tab)* mutants

The ability of *CDC15* to regulate Clb degradation post-translationally prompted questions about the nature and regulation of the mitotic exit network. To identify downstream targets of Cdc15 that mediate Clb proteolysis and the exit from mitosis, we designed a genetic screen to isolate mutations that can bypass the late anaphase/telophase arrest phenotype of *cdc15Δ* (Figure III-2). Since the essential requirement for Clns 1,2, and 3 in entry into S phase can be bypassed by deletion of a gene (*SIC1*) that inhibits entry into S phase (Schneider et al., 1996), we reasoned by analogy that our screen might reveal key negative regulator(s) of the anaphase/telophase –> G1 transition.

Ninety independent cultures of *cdc15Δ [pMET3-cdc15-2, URA3]* were first grown in inducing medium (- methionine) at permissive temperature (25^{o}C) to allow occurrence of spontaneous mutations. The cultures were subsequently plated on repressing medium (+ methionine) at a temperature semi-restrictive for the *cdc15-2* allele (30^{o}C) to enrich for mutations that supported the growth of *CDC15*-deficient cells. To identify mutations that allowed complete bypass of *cdc15Δ*, representative colonies from each plate were tested for their ability to grow on 5-FOA-containing medium (5-FOA selectively blocks the growth of plasmid-bearing *URA3*+ cells). The parental strain failed to grow due to its

inability to proliferate without the *[MET3-cdc15-2, URA3]* plasmid (Figure III-3 and data not shown). In contrast, 25 mutants survived on 5-FOA. Furthermore, all of them had lost the plasmid as determined by PCR analysis (data not shown). Fifteen of these mutants were amenable to genetic manipulation and harbored single mutations. Fourteen mutants were assigned to three recessive and three semi-dominant/dominant linkage groups (TABLE III-2). We referred to these mutants as *tab* mutants for their telophase-arrest-bypass (Tab^+) phenotype.

Does bypass of *cdc15Δ* require Sic1 accumulation and Clb2 degradation?

Since the combination of Sic1 accumulation and Clb2 degradation is proposed to be essential for mitotic exit (Schwab et al., 1997), and *cdc15-2* mutants are defective in both processes, we asked if bypass by *tab* mutants required *SIC1* or *HCT1*. Whereas all *tab* mutants tested were able to bypass *cdc15Δ* in the absence of *HCT1*, four *tab* mutants (*tab1-1*, *tab3-1*, *TAB5-1*, and *TAB7-1*) failed to bypass in the absence of *SIC1* (TABLE III-3). These results imply that a significant fraction of *tab* mutations target Sic1 accumulation.

***tab3* bypasses *tem1Δ* by inducing ectopic Sic1 accumulation and Clb2 degradation:**

The recessive *tab* mutants were characterized further by monitoring the bypass of cell cycle arrest in synchronized cultures. We first constructed a *tem1Δ::GAL1-UPL-TEM1* strain that allowed for conditional depletion of Tem1 (Shou et al, 1999). UPL (ubiquitin-Proline-LacI extension) acts as a destabilizing module that promotes rapid depletion of a

protein upon transcriptional repression (Johnson et al., 1992). The *tem1Δ::GAL1-UPL-TEM1* strain grew normally in galactose-containing medium (*TEM1* expressed), but exhibited first cycle arrest in late anaphase/telophase upon transfer to glucose-containing medium (*TEM1* repressed). We also tried the same scheme for *CDC15*, but were unable to achieve first cycle arrest. We reasoned that since *tab* mutants bypassed *cdc15Δ* and since Cdc15 most likely acts downstream of Tem1 (Shirayama et al., 1994), *tab* mutants should bypass *tem1Δ* as well. This is indeed the case for *tab2-1* (Figure III-3). We therefore used *tem1Δ::GAL1-UPL-TEM1* to impose a conditional late mitotic block.

The *tab2-1* and *tab3-1* mutations were introduced into the *tem1Δ::GAL1-UPL-TEM1* background. This experiment was not attempted with *tab1* mutants, since by comparison they grew poorly. Wild type or *tab3-1* derivatives of *tem1Δ::GAL1-UPL-TEM1* were grown in galactose medium, arrested in G1 with α factor, and released into glucose-containing medium to repress *TEM1* expression. As expected, the majority (~80%) of *TAB*$^+$ cells arrested with large buds. In the *tab3-1* strain, however, a significant fraction (~35%) of cells had ≥3 cell bodies at 12 hours after release, indicating that they had undergone at least one extra round of bud emergence (Figure III-4A). In addition, about half of these cell clusters developed extensive chains of cells with multiple nuclei, a phenomenon also observed in *tab2-1* but not *TAB* cultures (Figure III-4B and data not shown). Thirty-five percent represents a minimum estimate of *TEM1* bypass efficiency in *tab3-1* cultures, since cells with 1-2 cell bodies could have arisen from bypass events followed by successful cell separation.

Having established that *tab3-1* indeed bypassed Tem1 deficiency at a cellular level, we tested whether Sic1 accumulation and Clb2 degradation, two hallmark events that accompany exit from mitosis, also occurred. *tem1Δ::GAL1-UPL-TEM1* cells carrying *TAB3* or *tab3-1* alleles were arrested in G1 with α factor, and released into glucose medium (*TEM1* repressed, time 0). After cells had exited G1, α factor was added back to stop cells from cycling beyond the next G1 phase. As Tem1-depleted *TAB3* cells exited G1, Clb2 accumulated and remained at high levels, whereas Sic1 was degraded and remained at low levels (Figure III-4C, left panels). In contrast, as Tem1-depleted *tab3-1* cells progressed through mitosis, Clb2 was almost completely degraded and Sic1 accumulated to high levels. Similar results were also obtained for *tab2-1* (Shou et al., 1999). These data suggest that at least some of the *tab* mutants bypassed *tem1Δ* by enabling Tem1-independent degradation of Clb2 and accumulation of Sic1.

Molecular cloning of *TAB1* and *TAB2*

We attempted to clone by complementation genes corresponding to the recessive *tab* mutations by exploiting the fact that all of the recessive *tab* mutants are ts for growth. By this approach, *TAB1* was revealed to be *MTR10*, a gene previously implicated in nuclear transport (Kadowaki et al., 1994; Pemberton et al., 1997; Senger et al., 1998), and *TAB2* was identified to be *YJL076W*, a novel gene whose sequence yielded little insight into its function. We were unable to isolate plasmids that complemented *tab3* or mutant *15D2*. *YJL076W* was previously isolated as a gene involved in the estabishment of silenced chromatin (E.D. Andrulis and R. Sternglanz, personal communication). It has also been

identified as a Sir2-binding protein involved in rDNA silencing (Straight et al., 1999). Finally, it was isolated as a Cdc14-interacting protein in a two-hybrid screen (C. Baskerville and H. Charbonneau, personal communication). We have agreed with these groups to rename *TAB2* as *NET1*. We will still retain the names *TAB1* and *TAB2* throughout this paper for consistency. Although *tab1Δ* and *tab2Δ* cells were viable in the W303 background, they exhibited severe growth defects at room temperature (small colonies in Figure III-5), and were inviable at 37^{O} (data not shown). Given that Tab2 is a novel protein that is important for cell growth, we focused our effort on characterizing further *TAB2* and its encoded product.

tab2-1 extends the permissive temperature range for a variety of mitotic exit network (MEN) mutants

Since *tab2-1* bypassed *cdc15Δ* and *tem1Δ*, we tested whether it could also bypass other deletion mutants in the mitotic exit network. *tab2-1* bypassed *dbf2Δdbf20Δ* and *mob1Δ* with high efficiency, and bypassed *cdc5Δ* with 1000-10,000 fold lower efficiency. It failed to bypass *cdc14Δ* (Figure III-3B).

We also tested if *tab2-1* could suppress other MEN mutants such as *cdc15-2*, *cdc14-1*, and *cdc5-1* (Figure III-6). MEN single mutants were spotted onto YPD plates in 5 -fold serial dilutions and incubated at 24^{O}C (left panel) or 32.5^{O}C (center panel). *tab2-1* single and *tab2-1* MEN double mutants were similarly spotted, and incubated at 32.5^{O}C (right panel). The *tab2-1* allele significantly extended the maximum permissive

temperature for *cdc15-2*, *cdc14-1*, and *cdc5-1* (compare center and right panels). Similar results were obtained for *dbf2-1* at 35.5°C (data not shown). These data suggest that *TAB2* exerts a potent repressive effect on exit from mitosis in that the recessive *tab2-1* allele reduces the requirement for all mitotic exit network genes examined.

Discussion

The transition from anaphase/telophase to the G1 phase of the cell cycle in the budding yeast *S. cerevisiae* is driven by inactivation of Clb2/Cdc28 via degradation of Clb2 and accumulation of Sic1. The regulatory mechanism that controls this step of the cell cycle program has remained elusive, although a large group of genes required for Clb degradation, Sic1 accumulation, and the exit from mitosis has been identified through genetic and physiological analyses (see references in Introduction). This group of genes, referred to here as the Mitotic Exit Network (MEN), encodes proteins implicated in signal transduction, including three protein kinases (Cdc5, Cdc15, Dbf2/Dbf20), a protein phosphatase (Cdc14), and a Ras-like GTP-binding protein (Tem1).

Isolation of *tab* mutants

To understand how the MEN controls the exit from mitosis, we conducted a genetic screen for 'telophase arrest bypassed' (*tab*) mutants that bypassed the essential requirement for *CDC15*. A deliberate search for bypass mutants was a key aspect of the screen reported here, since numerous genetic interactions have been observed among components of the MEN (consult Jaspersen et al., 1998 for a summary). Formally

speaking, it is not possible to order gene functions based on suppressive interactions involving reduction-of-function (eg ts) alleles. For example, the *tab2-1* allele suppresses a ts mutation in its downstream target *CDC14* (this paper and Shou et al., 1999), whereas mutant alleles of *SIC1* suppress the arrest phenotype of its upstream negative regulators *CLNs 1-3* (Schneider et al., 1996). Since we sought mutants that could bypass *cdc15Δ*, the *tab* genes are predicted to function either downstream of or parallel to *CDC15*, but not upstream of *CDC15*.

The tab screen yielded both dominant and recessive mutants which mapped to at least six linkage groups. The pattern of alleles (TABLE III-2) does not satisfy a Poisson distribution, suggesting that the screen has not reached saturation, or that the loci are not equally mutable. The recessive *tab* mutants are likely to represent reduction-of-function mutations in genes that inhibit exit from mitosis, and the dominant *TAB* mutants are likely to result from gain-of-function mutations in genes that promote exit from mitosis. The fact that we recovered recessive, semi-dominant, and dominant mutants suggests that components that act downstream of or parallel to Cdc15 to promote exit from mitosis are subject to dosage-sensitive positive and negative regulatory controls.

We focused on recessive *tab* mutants in this study. Both *tab2-1* and *tab3-1* appeared to bypass mitotic arrest by enabling degradation of Clb2 and accumulation of Sic1 in Tem1-depleted cells (Figure III-3, Shou et al., 1999). Although bypass of telophase arrest by *tab2-1 and tab3-1* was quite efficient (as judged from the extent of Clb2 degradation), the *tab* mutations did not restore *tem1Δ* or *cdc15Δ* cells to the wild type state: the double mutants grew very slowly, and a significant fraction of these cells

failed to undergo cell separation in a timely fashion. There are three most likely interpretations of this result. First, the MEN genes may perform multiple functions, and only the function that is most rate-limiting for growth is bypassed by the *tab* mutations. Second, constitutive derepression of the regulatory process normally controlled by the MEN genes (e.g. release of Cdc14 from the nucleolus, Shou et al., 1999) may be toxic. Third, *TAB* genes (e.g., *TAB1*) may perform multiple functions important for cell growth, and in *tab* mutants, some of these other functions may be compromised.

A genetic pathway for the anaphase/telophase -> G1 transition

The *tab2-1* mutation efficiently bypassed *tem1Δ* and *cdc15Δ* (but not *cdc14Δ*; W.S., unpublished data), and extended the permissive temperature range for *cdc15-2*, *cdc5-1*, *cdc14-1*, and *dbf2-1*. In previous work, overexpression of Tem1 was shown to bypass the essential requirement (at low temperature) for Lte1, and overexpression of Cdc15 was shown to bypass the essential requirement for Tem1 (Shirayama et al., 1994). Moreover, biochemical and cell biological experiments indicate that Tab2 acts as part of a complex named RENT that acts upstream of Cdc14 to control its phosphatase activity (Shou et al, 1999). The most parsimonious model that unifies all of these observations is as follows: the nucleotide exchange factor Lte1 activates the GTPase Tem1, which in turn activates the protein kinase Cdc15. Cdc15 subsequently activates the protein phosphatase Cdc14 by counteracting the inhibitory regulator Tab2. Our data do not address the relationship of Cdc5, Dbf2 and Mob1 to the other MEN components, but these proteins most likely

collaborate with Cdc15 to bring about the activation of Cdc14. Once Cdc14 is mobilized by release from RENT, it dephosphorylates (and thereby activates) proteins involved in Sic1 expression (Swi5) and Clb degradation (Hct1/Cdh1) (Visintin et al., 1998; Zachariae et al., 1998; Charles et al., 1999).

Both transcriptional and post-translational controls have been implicated in the operation of the Mitotic Exit Network and the regulation of the anaphase/telophase -> G1 transition (Johnston et al., 1990; Toyn et al., 1997; Visintin et al., 1998; Zachariae et al., 1998). To address whether the portion of the MEN that acts downstream of *CDC15* can trigger a key aspect of the anaphase/telophase -> G1 transition (i.e., inactivation of Clb/Cdc28 via proteolysis of Clb2) in the absence of new gene expression, we evaluated the turnover of Clb2 in cells released from a *cdc15-2* arrest in the presence of cycloheximide. Interestingly, Clb2 was rapidly and efficiently degraded upon reversal of the *cdc15-2* block regardless of whether cycloheximide was present. This observation suggests that the exit from mitosis may be controlled by fundamentally similar mechanisms in budding yeast and animal cells. Animal cells proceed through mitosis with highly condensed, transcriptionally silent chromosomes. Thus, the exit from mitosis in animal cells is likely to be orchestrated by purely post-translational mechanisms. Cdc5 has counterparts (called polo-like kinases) in higher organisms (Lee and Erikson, 1997; Descombes and Nigg, 1998), and all of the MEN genes have putative homologues in the *C.elegans* genome (http://genome-www.stanford.edu/Saccharomyces/worm/).

Molecular analysis of the *TAB1* and *TAB2* genes

We cloned both *TAB1* and *TAB2*, and established that they are *MTR10* and *YJL076W*, respectively. *MTR10* was originally identified as a gene required for export of polyadenylated mRNA from the nucleus (Kadowaki et al., 1994). Mtr10 assembles with and functions as a nuclear import receptor for the mRNA-binding protein Npl3 (Pemberton et al., 1997; Senger et al., 1998). The fact that recessive alleles of *MTR10* bypass the essential requirement for *CDC15* suggests that Mtr10 impinges on the exit from mitosis by enabling the export of factors that regulate transit through telophase. An intriguing possibility is that Mtr10 mediates export of phosphorylated Swi5 from the nucleus. Previous work has shown that Swi5 is retained in the cytoplasm during interphase, and enters the nucleus during late anaphase/telophase (Moll et al., 1991). Mutation of Cdc28 consensus phosphorylation sites in Swi5 results in its constitutive localization within the nucleus. By analogy to Pho4 (Kaffman et al, 1998), phosphorylation of Swi5 by nuclear Clb/Cdc28 complexes may promote its assembly with Mtr10 and subsequent export from the nucleus. In a *tab1* mutant, defective export of Swi5 would be predicted to result in Cdc14-independent activation of *SIC1* expression. This model accounts for the observation that bypass of *cdc15Δ* by *tab1-1* requires *SIC1*. An alternative possibility is that Mtr10 has a distinct function unrelated to its participation in nucleo-cytoplasmic transport. The *tab1-1* allele identified in our screen does not exhibit strong accumulation of polyadenylated mRNA in the nucleus (A. Tartakoff, personal communication).

TAB2/Net1 encodes an 129 kD protein with only one homologue in sequence databases: the *S.cerevisiae* topoisomerase-I interacting protein Tof2, which is 22%

homologous to Net1 over 828 amino acids. The function of Tof2 is unknown, however, and *tof2Δ* cells have no apparent phenotype (Park, H. and R. Sternglanz, cited in *Saccharomyces* Genome Database). In other work, we have found that Tab2/Net1 is the core subunit of a complex named RENT that controls the activity of Cdc14 by restraining it in the nucleolus, and by directly inhibiting its protein phosphatase activity (Shou et al., 1999). While this manuscript was being finalized for submission, Visintin et al. (1999) reported the identification of *TAB2/NET1* (which they named *CFI1*) in a two-hybrid screen for Cdc14-interacting proteins. Consistent with the data reported here and in Shou et al. (1999), Cfi1 negatively regulates exit from mitosis by tethering Cdc14 to the nucleolus. Moreover, *cfi1Δ*, like *tab2-1*, suppresses the ts phenotype of MEN mutants.

Characterization of Tab2 and the phenotype of *tab2-1* cells validate the *tab* screen and suggests that the other *TAB* genes may encode physiological regulators and effectors of the Mitotic Exit Network.

Acknowledgements

We thank M. Budd, R. Feldman, P. Sternberg, and B. Hay for discussions; H. Mountain, P. Philippsen, A. Varshavsky, and B. Futcher for *pMET3*, *S.pombe his5*$^{+}$, *UPL*, and *HA3* plasmids, respectively; C. Thompson for yeast genomic library, and D. Kellogg for anti-Clb2 antibodies. We also thank H. Charbonneau, D. Moazed, and R. Sternglanz for sharing unpublished data. W.S. is a Howard Hughes Medical Institute predoctoral fellow.

References

Charles, J.F., Jaspersen, S.L., Tinker-Kulberg, R.L., Hwang, L., Szidon, A. and Morgan, D.O. (1998). The Polo-related kinase Cdc5 activates and is destroyed by the mitotic cyclin destruction machinery in S. cerevisiae. Curr Biol *8*, 497-507.

Descombes, P. and Nigg, E.A. (1998). The polo-like kinase Plx1 is required for M phase exit and destruction of mitotic regulators in Xenopus egg extracts. Embo J *17*, 1328-35.

Deshaies, R.J. (1997). Phosphorylation and proteolysis: partners in the regulation of cell division in budding yeast. Curr Opin Genet Dev *7*, 7-16.

Donovan, J.D., Toyn, J.H., Johnson, A.L. and Johnston, L.H. (1994). $p40^{SDB25}$, a putative CDK inhibitor, has a role in the M/G1 transition in *Saccharomyces cerevisiae*. Genes & Development *8*, 1640-1653.

Jaspersen, S.L., Charles, J.F., Tinker-Kulberg, R.L. and Morgan, D.O. (1998). A late mitotic regulatory network controlling cyclin destruction in *Saccharomyces cerevisiae*. Mol Biol Cell *9*, 2803-17.

Jimenez, J., Cid, V. J., Cenamor, R., Yuste, M., Molero, G., Nombela, C. and Sanchez, M. (1998). Morphogenesis beyond cytokinetic arrest in *Saccharomyces Cerevisiae*. J Cell Biol *143,* 1617-34.

Johnson, E.S., Bartel, B., Seufert, W., and Varshavsky, A. (1992). Ubiquitin as a degradation signal. Embo J *11*, 497-505.

Johnston, L.H., Eberly, S.L., Chapman, J.W., Araki, H., and Sugino, A. (1990). The product of the *Saccharomyces cerevisiae* cell cycle gene DBF2 has homology with protein kinases and is periodically expressed in the cell cycle. Mol Cell Biol *10*, 1358-66.

Kadowaki, T., Hitomi, M., Chen, S., and Tartakoff, A. M. (1994). Nuclear mRNA accumulation causes nucleolar fragmentation in yeast mtr2 mutant. Mol Biol Cell 5, 1253-63.

Kaffman, A., Rank, N.M., O'Neill, E.M., Huang, L.S., and O'Shea, E. K. (1998). The receptor Msn5 exports the phosphorylated transcription factor Pho4 out of the nucleus. Nature 396, 482-486

Kitada, K., Johnson, A.L., Johnston, L.H. and Sugino, A. (1993). A multicopy suppressor gene of *Saccharomyces cerevisiae* G1 cell cycle mutant gene dbf4 encodes a protein kinase and is identified as CDC5. Molecular and Cellular Biology *13*, 4445-4457.

Knapp, D., Bhoite, L., Stillman, D.J. and Nasmyth, K. (1996). The transcription factor SWI5 regulates expression of the cyclin kinase inhibitor p40SIC1. Molecular and Cellular Biology *16*, 5701-5707.

Komarnitsky, S.I., Chiang, Y.C., Luca, F.C., Chen, J., Toyn, J.H., Winey, M., Johnston, L.H. and Denis, C.L. (1998). DBF2 protein kinase binds to and acts through the cell cycle-regulated MOB1 protein. Mol Cell Biol *18*, 2100-7.

Lee, K.S. and Erikson, R.L. (1997). Plk is a functional homolog of *Saccharomyces cerevisiae* Cdc5, and elevated Plk activity induces multiple septation structures. Mol Cell Biol *17*, 3408-17.

Liu, H.Y., Toyn, J.H., Chiang, Y.C., Draper, M.P., Johnston, L.H. and Denis, C.L. (1997). DBF2, a cell cycle-regulated protein kinase, is physically and functionally associated with the CCR4 transcriptional regulatory complex. Embo J *16*, 5289-98.

Luca, F.C. and Winey, M. (1998). MOB1, an essential yeast gene required for completion of mitosis and maintenance of ploidy. Mol Biol Cell *9*, 29-46.

Moll, T., Tebb, G., Surana, U., Robitsch, H., and Nasmyth, K. (1991). The Role of phosphorylation and the CDC28 protein kinase in cell cycle-regulated nuclear import of the S. cerevisiae transcription factor SWI5. Cell 66, 743-758.

Nasmyth, K. A., and Reed, S. I. (1980). Isolation of genes by complementation in yeast: molecular cloning of a cell-cycle gene. Proc Natl Acad Sci USA *77*, 2119-23.

Parkes, V., and Johnston, L.H. (1992). SPO12 and SIT4 suppress mutations in DBF2, which encodes a cell cycle protein kinase that is periodically expressed. Nucleic Acids Res *20*, 5617-23.

Pemberton, L. F., Rosenblum, J. S., and Blobel, G. (1997). A distinct and parallel pathway for the nuclear import of an mRNA- binding protein. J Cell Biol *139*, 1645-53.

Peters, J.-M., King, R.W., and Deshaies, R.J. (1998). Cell cycle control by ubiquitin-dependent proteolysis. Ubiquitin and the Biology of the Cell, Plenum Press, New York. Chapter 12, 345-387.

Rose, M. D., and Broach, J. R. (1991). Cloning genes by complementation in yeast. Methods Enzymol *194*, 195-230.

Schmidt, S., Sohrmann, M., Hofmann, K., Woollard, A. and Simanis, V. (1997). The Spg1p GTPase is an essential, dosage-dependent inducer of septum formation in *Schizosaccharomyces pombe*. Genes Dev *11*, 1519-34.

Schneider, B.L., Steiner, B., Seufert, W. and Futcher, A.B. (1996). pMPY-ZAP: a reusable polymerase chain reaction-directed gene disruption cassette for *Saccharomyces cerevisiae*. Yeast *12*, 129-34.

Schneider, B.L., Yang, Q.H. and Futcher, A.B. (1996). Linkage of replication to START by the CDK inhibitor Sic1. Science *272*, 560-562.

Schwab, M., Lutum, A.S. and Seufert, W. (1997). Yeast Hct1 is a regulator of Clb2 cyclin proteolysis. Cell *90*, 683-93.

Senger, B., Simos, G., Bischoff, F. R., Podtelejnikov, A., Mann, M., and Hurt, E. (1998). Mtr10p functions as a nuclear import receptor for the mRNA-binding protein Npl3p. Embo J 17, 2196-207.

Sherman, F. (1991). Getting started with yeast. Methods Enzymol 194, 3-21.

Shirayama, M., Matsui, Y., and Toh-E, A. (1994). The yeast TEM1 gene, which encodes a GTP-binding protein, is involved in termination of M phase. Mol Cell Biol *14*, 7476-82.

Shirayama, M., Matsui, Y., and Toh-E, A. (1996). Dominant mutant alleles of yeast protein kinase gene CDC15 suppress the lte1 defect in termination of M phase and genetically interact with CDC14. Mol Gen Genet *251*, 176-85.

Shirayama, M., Zachariae, W., Ciosk, R., and Nasmyth, K. (1998). The Polo-like kinase Cdc5p and the WD-repeat protein Cdc20p/fizzy are regulators and substrates of the anaphase promoting complex in *Saccharomyces cerevisiae*. Embo J *17*, 1336-49.

Shou, W., Seol, J.H., Shevchenko, A., Baskerville, C., Moazed, D., Chen, Z.W.S., Jang, J., Shevchenko, A., Charbonneau, H., and Deshaies, R.J. (1999). Exit from mitosis is triggered by Tem1-dependent release of the protein phosphatase Cdc14 from nucleloar RENT complex. Cell *97*: 233-244.

Sikorski, R.S. and Boeke, J.D. (1991). In vitro mutagenesis and plasmid shuffling: from cloned gene to mutant yeast. Methods Enzymol *194*, 302-18.

Sikorski, R.S. and Hieter, P. (1989). A system of shuttle vectors and yeast host strains designed for efficient manipulation of DNA in *Saccharomyces cerevisiae*. Genetics *122*, 19-27.

Straight, A.F., Shou, W., Dowd, G.J., Turck, C.W., Deshaies, R.J., Johnson, A.D., and Moazed, D. (1999). Net1, a Sir2-associated nucleolar protein required for rDNA silencing and nucleolar integrity. Cell *97*: 245-256.

Taylor, G.S., Liu, Y., Baskerville, C., and Charbonneau, H. (1997). The activity of Cdc14p, an oligomeric dual specificity protein phosphatase from *Saccharomyces cerevisiae*, is required for cell cycle progression. J Biol Chem *272*, 24054-63.

Thompson, C. M., Koleske, A. J., Chao, D. M., and Young, R. A. (1993). A multisubunit complex associated with the RNA polymerase II CTD and TATA-binding protein in yeast. Cell *73*, 1361-75.

Toyn, J.H., Johnson, A.L., Donovan, J.D., Toone, W.M., and Johnston, L.H. (1997). The Swi5 transcription factor of *Saccharomyces cerevisiae* has a role in exit from mitosis through induction of the cdk-inhibitor Sic1 in telophase. Genetics *145*, 85-96.

Visintin, R., Craig, K., Hwang, E.S., Prinz, S., Tyers, M. and Amon, A. (1998). The phosphatase Cdc14 triggers mitotic exit by reversal of Cdk-dependent phosphorylation. Molecular Cell *2*, 709-718.

Visintin, R., Hwang, E.S., and Amon, A. (1999). Cfi prevents premature exit from mitosis by anchoring Cdc14 phosphatase in the nucleolus. Nature *398*, 818-823.

Wach, A., Brachat, A., Alberti-Segui, C., Rebischung, C., and Philippsen, P. (1997). Heterologous HIS3 marker and GFP reporter modules for PCR-targeting in *Saccharomyces cerevisiae*. Yeast *13*, 1065-75.

Zachariae, W., Schwab, M., Nasmyth, K., and Seufert, W. (1998). Control of cyclin ubiquitination by CDK-regulated binding of Hct1 to the anaphase promoting complex. Science *282*, 1721-4.

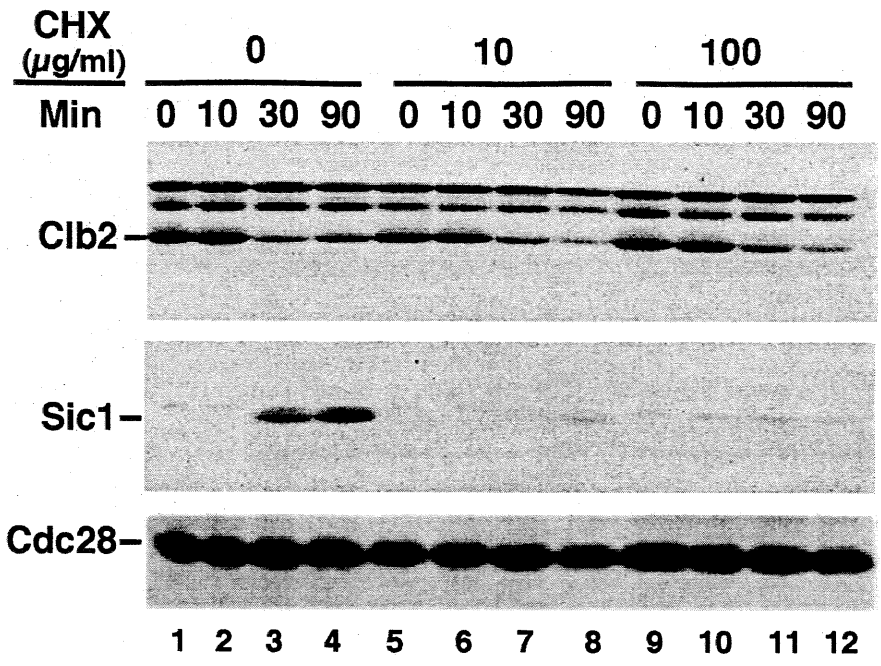
CHX
(μg/ml)
0
10
100
Min
0 10 30 90 0 10 30 90 0 10 30 90
Clb2
Sic1
Cdc28
1 2 3 4 5 6 7 8 9 10 11 12

Figure III-1

Figure III-1. Post-translational control of Clb2 proteolysis by *CDC15*. Exponentially growing *cdc15-2* (RJD619) cells were arrested in late anaphase/telophase by shifting the culture to 37^{o}C for three hours. The culture was split in three and either mock-treated (lanes 1-4) or supplemented with the protein synthesis inhibitor cycloheximide (CHX) at 10 μg/ml (lanes 5-8) or100 μg/ml (lanes 9-12). After five minutes (time = 0), the cultures were released from cell cycle arrest by downshift to 25^{o}C. At indicated time points, samples were withdrawn, and the levels of Clb2, Sic1 and Cdc28 proteins were assayed by immonoblotting.

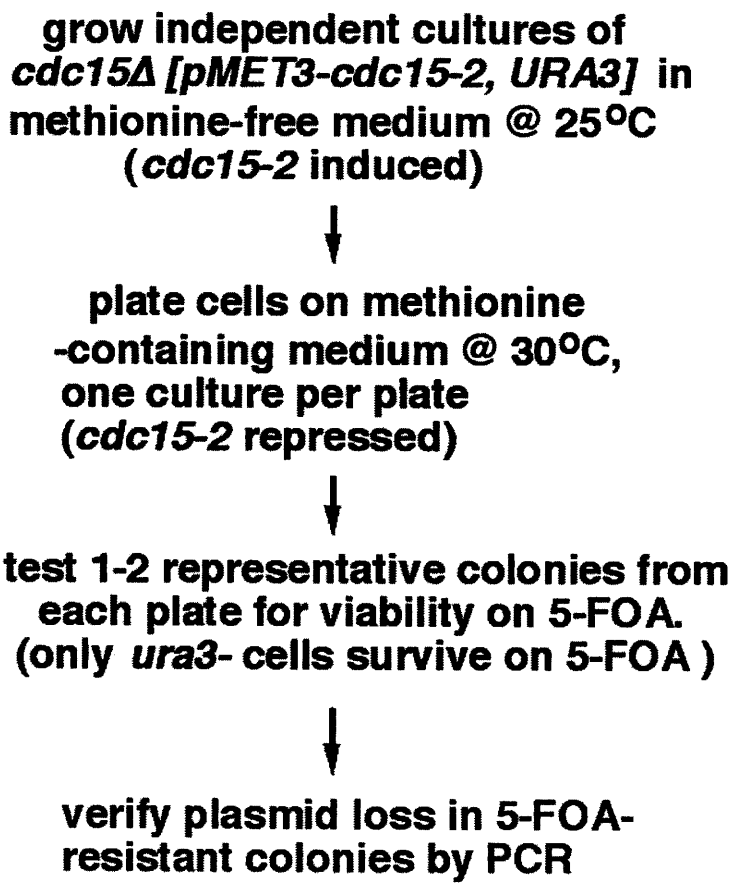
grow independent cultures of
cdc15Δ [pMET3-cdc15-2, URA3] in
methionine-free medium @ 25°C
(cdc15-2 induced)
plate cells on methionine
-containing medium @ 30°C,
one culture per plate
(cdc15-2 repressed)
test 1-2 representative colonies from
each plate for viability on 5-FOA.
(only ura3- cells survive on 5-FOA)
verify plasmid loss in 5-FOA-
resistant colonies by PCR

Figure III-2

Figure III-2. Scheme for isolating *telophase arrest bypassed* (*tab*) mutants. See text for details.

A

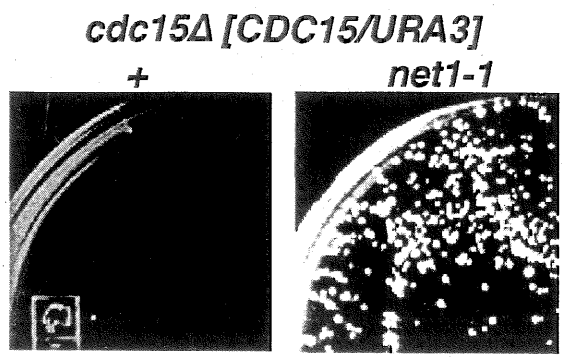

B

	net1-1 bypass?
cdc15Δ	Yes
tem1Δ	Yes
dbf2Δdbf20Δ	Yes
mob1Δ	Yes
cdc14Δ	No
cdc5Δ	negligible

Figure III-3

Figure III-3.

(A) *tab2-1* bypasses *cdc15Δ*. Strains with the indicated genotypes were pre-grown in non-selective medium, and $2x10^6$ (*TAB2*) or $2x10^4$ (*tab2-1*) cells were plated on 5-FOA plates. The plates were incubated at $25^{O}C$ for 8 days before being photographed. A representative quadrant from each plate is shown. Plasmid loss was evaluated by performing PCR analysis of 5-FOA-resistant colonies using primers complementary to sequences internal to *TEM1* or *CDC15*. In each case, all four colonies examined by PCR were confirmed to have lost the plasmid-borne allele.

(B) tab2-1 can bypass some but not all deletion mutants of MEN. Bypassing *cdc5Δ* by *tab2-1* occurs at three-four orders of magnitude lower frequency than bypassing *cdc15Δ*.

A

	hrs	1	2	3	4	multibranched
tab3-1	0	96.9	2.1	1.0	0	0
	2	39.4	12.1	44.7	0	3.8
	4	14.4	4.4	53.0	4.4	23.8
	12	17.4	0.8	45.4	0	36.4
+	0	95.0	0	5.0	0	0
	2	49.6	40.2	6.0	1.7	2.6
	4	10.2	0.9	69.8	3.6	15.6
	12	3.0	0.8	81.2	2.2	12.8

B

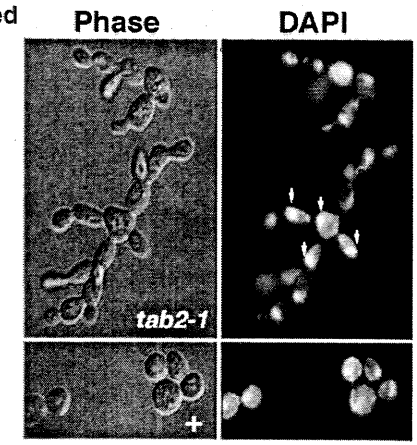

C

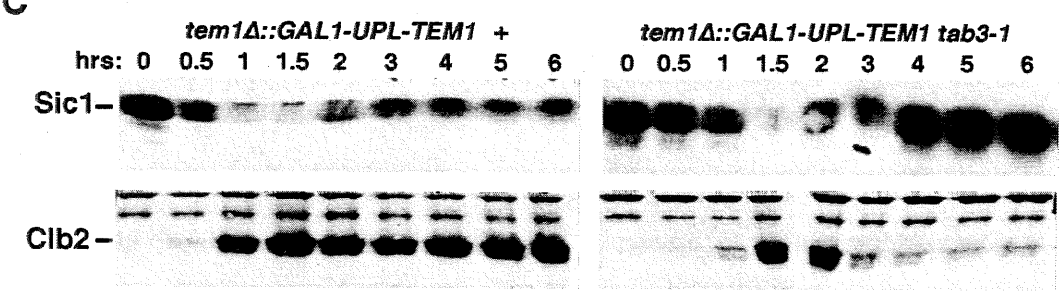

Figure III-4

Figure III-4. *tab3-1* enables *TEM1*-independent degradation of Clb2 and accumulation of Sic1. *tem1Δ::GAL1-UPL-TEM1 tab3-1* and *tem1Δ::GAL1-UPL-TEM1* cells grown in galactose medium (*TEM1* expressed) at 25°C were arrested in G1 with α factor, and released into glucose medium (*TEM1* repressed) at time = 0. (A) At indicated time points after release, budding index was monitored. (B) The same experiment was performed in parallel for *tab2-1*. At 12 hours after release, cells were fixed, sonicated, and stained with the DNA-binding dye DAPI (Phase: left panels; DAPI: right panels). The "multi-branched" phenotype of *tab3-1* is very similar to that of *tab2-1* (not shown). Although not all of the nuclei are in the plane of focus, it is apparent that in a cluster near the center of the photograph (see arrowheads), four attached buds each contain a single nucleus. (C) The experiment in (A) was repeated, except that at either 2 h (*TAB3*) or 3 h (*tab3-1*) following release from α factor arrest, α factor was added back to prevent cells from proceeding through a second cell cycle. At indicated time points, samples were withdrawn to measure Sic1 and Clb2 levels by immunoblotting.

tab1(mtr10)Δ::his5+/+

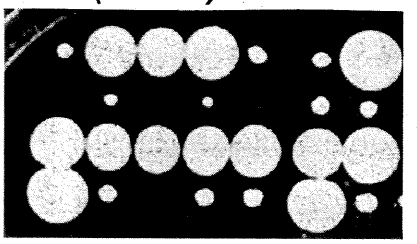

tab2(net1)Δ::his5+/+

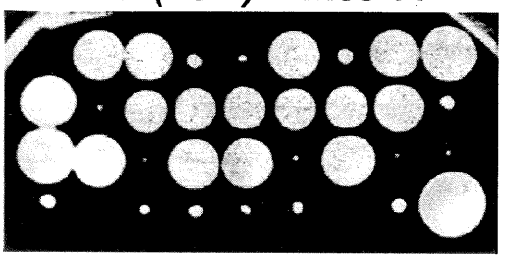

Figure III-5

Figure III-5. *tab1Δ* and *tab2Δ* cells exhibit severe growth defects. Diploids of indicated genotype (in W303 background) were sporulated, and tetrads were dissected on YPD plates. The plates were incubated at 25^{O}C for eight days before being photographed. All slow growing colonies were His^{+} (*tabΔ*), whereas all fast growing colonies were His^{-} (*TAB*$^{+}$).

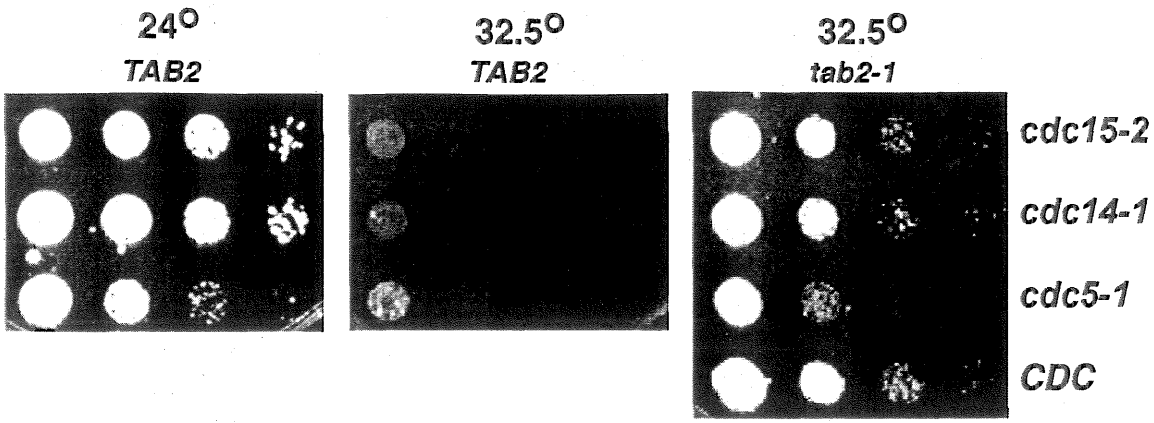

Figure III-6

Figure III-6. *tab2-1* extends the permissive temperature range for *cdc15-2*, *cdc14-1*, and *cdc5-1*. Cells with specified combinations of *TAB* alleles (indicated at the top) and *CDC* alleles (indicated on the side) were spotted onto YPD plates in 5 -fold serial dilutions. Plates were incubated at 24^{o} (left panel) or 32.5^{o} (center and right panels) for 2-4 days before being photographed. *tab2-1* was observed to suppress the ts phenotype of *dbf2-1* at 35.5°C (not shown).

TABLE 1

S.cerevisiae strains

Strain	Genotype[a]
RJD381	*MATa/MATα*
RJD619	*cdc15-2 pep4Δ::TRP1 MATa*
WY4	*TAB7-2 MATa*
WY9	*cdc15Δ::TRP1 TAB5-1 [pMET3-CDC15, URA3] [pRS315, LEU2] MATα*
WY10	*TAB5-1 [pRS315, LEU2] MATα*
WY11	*cdc15Δ::TRP1 tab2-1 [pMET3-CDC15, URA3] MATα*
WY14	*tab3-1 MATa*
WY17	*cdc15Δ::TRP1 TAB6-1 [pMET3-CDC15, URA3] [pRS315, LEU2] MATa*
WY18	*TAB6-1MATα*
WY21	*cdc15Δ::TRP1 tab1-1 [pMET3-CDC15, URA3] [pRS315, LEU2] MATα*
WY23	*cdc15Δ::TRP1 15D2 [pMET3-CDC15, URA3] [pRS315, LEU2] MATa*
WY24	*15D2 [pRS315, LEU2] MATa*
WY34	*cdc15Δ::TRP1 TAB7-1 [pMET3-CDC15, URA3] [pRS315, LEU2] MATa*
WY38	*tab1-1 MATa*
WY39	*tab2-1 MATa*
WY41	*cdc15Δ::TRP1 tab3-1 [pMET3-CDC15, URA3] MATa*
WY46	*tem1::GAL1-UPL-TEM1/TRP1 bar1::hisG MATa*

WY95	*tab2-1 tem1::GAL1-UPL-TEM1/TRP1 bar1::LEU2 MATa*
WY97	*tab3-1 tem1::GAL1-UPL-TEM1/TRP1 bar1::LEU2 MATa*
WY167	*tem1Δ::TRP1 [GAL1-TEM1, URA3] tab2-1 MATa*
WY217	*cdc15Δ::TRP1 [pMET3-CDC15, URA3] MATα*
WY218	*tem1Δ::TRP1 [GAL1-TEM1, URA3] MATα*
WY221	*cdc15Δ::TRP1 [pMET3-cdc15-2, URA3] MATα*

[a]All strains are in the W303 background (*ade2-1 can1-100 his3-11-15 leu2-3-112 trp1-1 ura3-1*), which was provided by B. Fuller. *[ ]* indicates CEN/ARS plasmid.

TABLE 2

Linkage groups of *tab* mutants

Name	# of alleles	recessive/dominant[b]	growth at 37°[c]	gene
tab1	5	recessive	inviable	*MTR10*
tab2	2	recessive	slow	*NET1*
tab3[a]	1	recessive	slow	
TAB5	2	semi-dominant	normal	
TAB6	1	dominant	slow	*CDC14*
TAB7	3	semi-dominant (*-1*)	normal	
		dominant (*-2*)		
15D2[a]	1	recessive	inviable	

[a]We have not determined if *15D2* is allelic to *tab3* or *TAB5, 6, 7.*

[b]All alleles were tested except for *TAB7*, where *TAB7-1* and *-2* were tested.

[c]All alleles of a single linkage group displayed similar ts growth phenotype.

TABLE 3

Does bypass require *SIC1* or *HCT1*?

Strain	*sic1Δ*[a]	*hct1Δ*[b]	+[c]
tab1-1	-	+	+
tab2-1	+/-	+	+
tab3-1	-	+	+
TAB5-1	-	+	+
TAB6-1	+/-	+	+
TAB7-1	-	+	+
15D2	+/-	N.D.	+

[a]To assay if bypass required *SIC1*, *cdc15Δ::TRP1 tab [pMET3-CDC15/URA3]* cells were transformed with *S. pombe his5*$^+$ DNA fragment whose termini were engineered to be homologous to SIC1 5' and 3' untranslated regions. All transformants were tested for their ability to bypass *cdc15Δ* using the 5-FOA growth assay. They were also screened for the absence of *SIC1* as the result of homologous integration. In the case of *tab2, 4*, and *6*, about half of *sic1Δ* transformants could bypass. Sample size n = 4 - 17.

[b]Similar assay was conducted for *HCT1*. N.D. = not determined. Sample size n= 1 - 7.

[c]Transformants from a and b that resulted from non-homologous integration (and hence no deletion of *SIC1* or *HCT1*) were used as a control. Sample size n=12 - 86.

Chapter IV - Exit from mitosis is triggered by Tem1-dependent release of the protein phosphatase Cdc14 from nucleolar RENT complex

(Wenying Shou, Jae Hong Seol, Anna Shevchenko, Christopher Baskerville, Danesh Moazed, Z.W. Susan Chen, Joanne Jang, Andrej Shevchenko, Harry Charbonneau, and Raymond J. Deshaies. Published in Cell 97:233-244, 1999; Appendix II.

Contributions from collaborators: JHS: Fig. IV-2A; AS& AS: Fig. IV-2B; CB, HC & DM: intellectual contributions; SC & JJ: helped to develop Cdc14 phosphatase assay and to construct the Tem1-depletable strain, respectively.)

Summary

Exit from mitosis in budding yeast requires a group of essential proteins – including the GTPase Tem1 and the protein phosphatase Cdc14 – that are thought to mobilize factors that down-regulate cyclin-dependent kinase (Cdk) activity. We identified a mutation, *net1-1*, that bypasses the essential requirement for *TEM1*. *NET1* encodes a novel protein with no obvious motifs. Mass spectrometric identification of Net1-interacting proteins reveals that it is a key component of a multifunctional complex, denoted RENT (for REgulator of Nucleolar silencing and Telophase), that also contains Cdc14 and the silencing regulator Sir2. From G1 through anaphase, RENT localizes to the nucleolus, and Cdc14 activity is inhibited by Net1. In late anaphase, Cdc14 dissociates from RENT and disperses throughout the cell in a Tem1-dependent manner. We propose that Tem1 activates the discharge of Cdc14 from RENT in anaphase, resulting in a wave of Cdc14

activity that triggers Cdk inactivation and exit from mitosis. Nucleolar sequestration may be a general mechanism for the regulation of diverse biological processes.

Introduction

Activation and inactivation of cyclin- dependent kinases (Cdks) govern cell cycle transitions. In the budding yeast *Saccharomyces cerevisiae*, a single Cdk, Cdc28, orchestrates various stages of the cell cycle by taking on different cyclin partners: Cln 1-3 for G1 phase, Clb 5-6 for S phase, and Clb 1-4 for M phase (reviewed by Deshaies, 1997). There are at least three key cell cycle transitions in this organism: G1 -> S, metaphase -> anaphase, and the exit from mitosis (reviewed by King et al., 1996; Deshaies, 1997). Cdc28 inactivation mediated by proteolysis of Clb2 and/or accumulation of the Cdc28/Clb inhibitor Sic1 seems to lie at the heart of the latter transition (Schwab et al., 1997; Visintin et al., 1998). Anaphase-Promoting Complex/Cyclosome ubiquitin ligase (APC/C) and its substrate-specific activator Hct1/Cdh1 are required for Clb2 degradation. Clb degradation was originally thought to be required for exit from mitosis (Surana et al., 1993). However, cells devoid of Hct1/Cdh1 fail to degrade Clb2 and are viable (Schwab et al., 1997; Visintin et al., 1997), probably because Sic1 accumulates and turns off Cdc28 activity. Whereas cells devoid of Sic1 can degrade Clb2 and exit mitosis, cells devoid of both Hct1 and Sic1 are inviable, presumably due to their inability to extinguish Cdc28 activity during telophase (Schwab et al., 1997).

In addition to APC/C, another set of genes plays a pivotal role in exit from mitosis. They include *TEM1*, *LTE1*, *CDC15*, *DBF2/DBF20*, *CDC5*, *MOB1*, and *CDC14* (reviewed in Deshaies, 1997; Luca and Winey, 1998). When cells that harbor conditional-lethal temperature-sensitive (ts) mutations in any of these genes are shifted to the restrictive temperature, they uniformly arrest in late anaphase/telophase as large-budded cells with segregated chromosomes, fully elongated microtubule spindles, and elevated Cdc28/Clb2 protein kinase activity. Clb2 proteolysis is not completed, and *SIC1* transcripts and protein fail to accumulate to high levels (Surana et al., 1993; Shirayama et al., 1994b; Toyn and Johnston, 1994; Irniger et al., 1995; Charles et al., 1998; Jaspersen et al., 1998; Visintin et al., 1998). Furthermore, manipulation of Sic1 and Clb2 levels has dramatic effects on these mutants (Donovan et al., 1994; Shirayama et al., 1994b; Toyn et al., 1997; Charles et al., 1998; Jaspersen et al., 1998): overexpression of Clb2 or deletion of Sic1 typically exacerbates their phenotype, whereas overexpression of Sic1 has the opposite effect.

Most of these proteins required for exit from mitosis resemble components of signaling pathways: Tem1 is a GTP-binding protein (Shirayama et al., 1994b), *LTE1* encodes a putative guanine nucleotide exchange factor (Shirayama et al., 1994a), Dbf2/Dbf20, Cdc15, and Cdc5 are protein kinases (Toyn and Johnston, 1994; Jaspersen et al., 1998; Hardy and Pautz, 1996), Mob1 is a novel protein that associates with Dbf2 (Komarnitsky et al., 1998; Luca and Winey, 1998) and Cdc14 is a dual specificity protein phosphatase (Taylor et al., 1997). Consistent with the notion that these proteins constitute elements of a signaling pathway, the corresponding genes display a variety of

genetic interactions with each other (Parkes and Johnston, 1992; Kitada et al., 1993; Shirayama et al., 1994b; Shirayama et al., 1996; Jaspersen et al., 1998; Komarnitsky et al., 1998; Luca and Winey, 1998; Visintin et al., 1998). Thus, for simplicity, we will refer to this group of genes as the mitotic exit network.

Although the functional organization of the mitotic exit network is poorly understood, recent work suggests that the protein phosphatase Cdc14 might act directly on cell cycle regulators to promote mitotic exit. First, overexpression of Cdc14 can activate ectopic degradation of Clb2 and accumulation of Sic1 (Visintin et al., 1998; W.S. and R.J.D., unpublished). Second, mutation of Cdk consensus phosphorylation sites in Swi5 and Hct1 activates their ability to promote *SIC1* transcription and Clb2 degradation, respectively (Moll et al., 1991; Zachariae et al., 1998), and Cdc14 antagonizes the phosphorylation of both proteins (Visintin et al., 1998; Jaspersen et al., 1999). Although these data suggest that Cdc14 is required to dephosphorylate Swi5 and Hct1 as cells exit mitosis, they fail to address the key question of whether Cdc14 is a regulated component of the biochemical switch that flips the cell from mitosis to G1.

We report here the identification of a protein complex, named RENT, that tethers Cdc14 to the nucleolus throughout most of the cell cycle. As cells progress through mitosis, Cdc14 is released from the nucleolus in a Tem1-dependent manner. We propose that the Tem1-dependent discharge of Cdc14 from the nucleolar RENT complex lies at the heart of the biochemical engine that drives cells from mitosis to G1.

Results

net1-1 enables _TEM1_-independent Clb2 degradation and Sic1 accumulation

To delineate how *CDC15* promotes exit from telophase, we conducted a genetic screen to isolate *tab* (for *Telophase Arrest Bypassed*) mutants that allow *cdc15Δ* cells containing a complementing [*CDC15, URA3*] plasmid to survive without the plasmid (W.S. and R.J.D., manuscript in preparation). The gene corresponding to one of these mutants, *TAB2*, was cloned by complementation of the ts growth defect of *tab2-1* cells, and was identified as *YJL076W*. It encodes an 129 kD protein with only one obvious homologue in sequence databases: the *S.cerevisiae* topoisomerase-I interacting protein Tof2 encoded by *YKR010C*, which is 22% homologous to Net1 over 828 amino acids. *TAB2* and the *tab2-1* allele were subsequently renamed *NET1* (for Nucleolar silencing Establishing factor and Telophase regulator) and *net1-1*, respectively. The name *NET1* also reflects its independent identification as *NUS1* (Nucleolar Specific Silencing protein, Straight et al., 1999), *ESC5* (Establishes Silencing, Andrulis and Sternglanz, personal communication), and *TAB2* (this report; W.S. and R.J.D., manuscript in preparation). *NET1* was also identified in a two-hybrid screen for Cdc14-interacting proteins (Traverso et al., 2001). Disruption of *NET1* was not lethal, although *net1Δ* cells grew very slowly (Moazed et al., submitted; W.S. and R.J.D., unpublished data).

Double mutant *cdc15Δ net1-1* cells were able to form colonies (W.S. and R.J.D., manuscript in preparation), as were *tem1Δ net1-1* and *cdc15Δ net1Δ* cells (Figure IV-3; data not shown). These genetic data formally suggest that Net1 is an inhibitor of mitotic exit that acts either downstream of, or parallel to, Tem1 and Cdc15. To address whether *net1-1* can efficiently bypass the requirement for Tem1 in Clb2 degradation and Sic1

accumulation, we constructed a *tem1Δ::GAL1-UPL-TEM1* strain that allowed for the rapid, conditional depletion of Tem1. UPL, which stands for Ubiquitin-Proline-LacI, acts as a destabilizing module that permits rapid degradation of appended proteins (Johnson et al., 1992). *tem1Δ::GAL1-UPL-TEM1* cells grew at a normal rate in YP-galactose medium (YPG, *TEM1* expressed), but exhibited first cycle arrest in telophase upon transfer to YP-glucose medium (YPD, *TEM1* repressed). We also tried to construct a similar conditional allele for *CDC15*, but first cycle arrest was not achieved.

tem1Δ::GAL1-UPL-TEM1 cells in the wild type or *net1-1* background were arrested in G1 phase with the mating pheromone α factor, and synchronously released into YPD to extinguish expression of *UPL-TEM1*. As expected, the majority (~ 80%) of *NET1 tem1Δ::GAL1-UPL-TEM* cells arrested with large buds. At 12 hours after release, however, ~ 60% of *net1-1 tem1Δ::GAL1-UPL-TEM1* cells exhibited ≥3 cells bodies (Figure IV-1A), indicating a further round of division without cell separation. Those cells with 1-2 cell bodies could have resulted from bypass events followed by successful cell separation. Extensive chains of cells with multiple nuclei were commonly observed in the *net1-1* culture, but rarely observed with *NET1* cells (data not shown). These data suggest that *net1-1* efficiently bypasses the cell division arrest caused by depletion of Tem1, although *net1-1 tem1Δ::GAL1-UPL-TEM1* cells still appear to exhibit a cytokinesis or cell separation defect.

Since Clb2 degradation and Sic1 accumulation normally accompany exit from mitosis, we tested if *net1-1* influenced the levels of these two proteins in Tem1-deficient cells. *tem1Δ::GAL1-UPL-TEM1* cells in the wild type or *net1-1* background were

arrested in G1 phase with α factor, and released into YPD (Tem1 synthesis repressed; time 0). After cells had exited G1, α factor was added back to trap any cycling cells in the next G1 phase. Cells were harvested at various time points after α factor release and assayed for Clb2, Sic1, and Cdc28 by immunoblotting. In Tem1-deficient *NET1* cells, Clb2 accumulated and remained at high levels, whereas Sic1 was degraded as cells exited G1 and remained at low levels (Figure IV-1B, left panels). In Tem1-deficient *net1-1* cells, Clb2 accumulation and Sic1 degradation were delayed, presumably due to the reduced growth rate of *net1-1* (data not shown). Nevertheless, eventually Clb2 was completely degraded and Sic1 accumulated to high levels (Figure IV-1B, right panels). These data suggest that *net1-1* bypassed *tem1Δ* by enabling both Clb2 degradation and Sic1 accumulation.

Net1 physically associates with Cdc14 and Sir2

To delineate the mechanism by which *NET1* influences mitotic exit, we sought to identify proteins that interact with Net1. The chromosomal copy of *NET1* was modified to encode a protein with 9 copies of the Myc epitope at its N-terminus, and Myc9-Net1 was affinity purified from cell extracts on a 9E10 monoclonal antibody matrix. Besides Myc9-Net1, three proteins were specifically detected in silver-stained SDS-polyacrylamide gels of Myc9-Net1 immunoprecipitates, but not in control immunoprecipitates (Figure IV-2A). Protein bands were identified by high mass accuracy matrix-assisted laser desorption/ionization (MALDI) peptide mapping and nanoelectrospray tandem mass spectrometric sequencing combined in a layered approach

(Shevchenko et al., 1996). One Net1-interacting protein (Cdc14) was identified by MALDI (Figure IV-2B). The identity of the other two proteins (Sir2 and Ypl126w) was revealed by subsequent tandem mass spectrometric sequencing.

To verify the interactions between Net1, Sir2, and Cdc14, we carried out co-immunoprecipitation experiments. Myc9-Net1 was specifically detected in anti-HA immunoprecipitates prepared from a strain containing chromosomal *CDC14* modified to encode a protein with 3 copies of the haemagglutinin epitope at its C-terminus (Cdc14-HA3), but not from a strain that expressed untagged Cdc14 (Figure IV-2C, compare lanes 4 and 5). Conversely, Cdc14-HA3 was selectively recovered in anti-Myc immunoprecipitates prepared from strains that express Myc9-Net1 (Figure IV-2C, compare lanes 6 and 7). By a similar analysis, it was confirmed that Myc9-Net1 bound specifically to Sir2 (Straight et al., 1999). Cdc14-HA3 was also detected in anti-Sir2 immunoprecipitates prepared from wild type cells (Figure IV-2D lane 6), but not those prepared from *sir2Δ* (lane 5), *net1-1* (lane 7) or *net1Δ* (lane 8) mutants, suggesting that Net1 bridges the interaction between Cdc14 and Sir2. We refer to the Cdc14-Net1-Sir2 complex as 'RENT', for REgulator of Nucleolar silencing and Telophase (see discussion and Straight et al., 1999).

We have only performed a cursory analysis of the third Net1-associated protein, Ypl126w. *YPL126W* was determined to be an essential gene, and Myc9-tagged Ypl126w was localized to the nucleolus by indirect immunofluorescence, consistent with it being an authentic Net1-binding partner (W.S., unpublished data). To reflect its known properties, we suggest *YPL126W* be renamed *NAN1* (Net1-associated nucleolar protein).

Although *net1-1* is defective in rDNA silencing, loss of silencing does not bypass *tem1Δ*

Sir2 regulates transcriptional silencing at telomeres and the silent mating type loci (reviewed by Lustig, 1998). Sir2 also mediates silencing of some RNA polymerase II-transcribed genes integrated within the rDNA, a phenomenon referred to as 'rDNA silencing' (Bryk et al., 1997; Fritze et al., 1997; Smith and Boeke, 1997). Net1 was independently discovered as a Sir2-binding protein (Straight et al., 1999), and both *net1Δ* and *net1-1* were shown to be defective in rDNA silencing. This raised the possibility that loss of silencing accounted for the *tem1Δ* bypass activity of *net1-1*. To test this hypothesis, we compared the bypass activity of *net1-1*, *sir2Δ*, *sir3Δ*, and *sir4Δ* in *tem1Δ* cells kept alive by a *URA3*-plasmid harboring *GAL1-TEM1*. The parental *tem1Δ [GAL1-TEM1, URA3]* strain failed to grow on 5-fluoroorotic acid (5-FOA) -containing medium (5-FOA selectively prevents the growth of Ura+ cells) due to its inability to survive without the *[GAL1-TEM1, URA3]* plasmid. The *net1-1* allele, but not *sir2Δ, sir3Δ, or sir4Δ* allowed *tem1Δ [GAL1-TEM1, URA3]* cells to survive on 5-FOA (Figure IV-3). PCR analysis confirmed that the viable colonies indeed lacked the *TEM1*-containing plasmid (data not shown). Thus, the effects of *net1-1* on *tem1Δ* bypass and 'rDNA silencing' can be uncoupled.

Net1 is an inhibitor of and a candidate substrate for Cdc14

Cdc14 is a dual specificity protein phosphatase essential for mitotic exit (Culotti and Hartwell, 1971; Taylor et al., 1997). Net1 bound to Cdc14, and behaved genetically as a negative regulator of mitotic exit (Figure IV-2; W.S. and R.J.D., manuscript in preparation). Therefore, we postulated that Net1 might either be an inhibitor of Cdc14, or a mitotic exit inhibitor whose activity was counteracted by Cdc14. To test if Net1 is an inhibitor of Cdc14, we measured Cdc14 activity in wild type, *net1-1*, and *net1Δ* cell extracts. Cdc14-HA3 was immunoprecipitated from asynchronous cultures of *net1-1*, *net1Δ*, and wild type strains, and incubated with [^{32}P]-labeled-Sic1. It is not clear if phospho-Sic1 is a physiological substrate for Cdc14, but it provides a convenient assay to measure the phosphatase activity of Cdc14. The specific activity of Cdc14-HA3 isolated from *net1-1* and *net1Δ* cells was on average 3.6 and 3.8 times as much as that from wild type cells, respectively (Figure IV-4A). This elevation in Cdc14-HA3 specific activity was not due to altered cell cycle kinetics, since the specific activity of Cdc14-HA3 purified from G1-synchronized *net1-1* cells was still 3.8-4.5 fold as high as that obtained from G1-synchronized wild type cells (Figure IV-4B).

To address whether the effect of *net1* mutations on Cdc14 protein phosphatase activity was direct, we tested if immunopurified Myc9-Net1 could inhibit recombinant GST-Cdc14 purified from *E. coli*. Wild type or catalytically inactive GST-Cdc14 (Taylor et al., 1997) was recruited to matrices that contained either immobilized Myc9-Net1, or immobilized anti-GST antibodies. To prepare Net1 beads lacking endogenous Cdc14 activity, Myc9-Net1 was immunopurified from extracts treated with phosphatase inhibitor sodium orthovanadate, which reduced the amount of endogenous Cdc14 protein

bound to Net1 beads (data not shown); to prepare anti-GST beads, rabbit α-GST antibodies were absorbed to protein A matrix. Following the recruitment step, bead-bound GST-Cdc14 was assayed for its phosphatase activity toward [^{32}P]-Sic1. GST-Cdc14 recovered on the Myc9-Net1 matrix had 50-fold lower specific activity than GST-Cdc14 bound to the anti-GST matrix (Figure IV-4C). Taken together, these experiments suggest that Net1 directly inhibits the protein phosphatase activity of Cdc14.

Having established that Net1 is associated with potent Cdc14 inhibitory activity, we tested if Net1 might also be a substrate for Cdc14. First, Net1 was a phosphoprotein in vivo, since a radioactive band with the expected molecular weight of Myc9-Net1 was apparent in immunoprecipitates prepared from [^{32}P]-labeled *Myc9-NET1* cells, but not from untagged cells (Figure IV-4D). Second, immunoblotting of anti-myc immunoprecipitates revealed that Myc9-Net1 isolated from a 37°C *cdc14-1* culture (nonpermissive temperature) migrated slower in SDS-PAGE than that from a 25°C culture (permissive temperature; Figure IV-4E, lane 3 vs. lane 4). In contrast, no effect of temperature was observed for Myc9-Net1 isolated from wild type cells (Figure IV-4E, lanes 1 and 2). The slower migrating form of Myc9-Net1 from the 37°C *cdc14-1* culture was collapsed down to a faster migrating form upon treatment with wild type (A) but not mutant (I) GST-Cdc14 purified from *E. coli.* (Figure IV-4E, lanes 5 and 6). Since Cdc14 modulates the phosphorylation state of Net1 *in vivo* and *in vitro*, we conclude that Net1 is most likely one of its physiological substrates. In the Discussion, we consider the

possibility that Net1 and Cdc14 reciprocally control each others' activities via a negative feedback loop.

Net1 resides in the nucleolus, and is required for Cdc14 localization to the nucleolus

Both Net1 (Straight et al., 1999) and a portion of Sir2 (Gotta et al., 1997) localize to the nucleolus. These data suggest that the entire RENT complex, including Cdc14, might be tethered to the nucleolus. To test this possibility, we compared the localization of *Myc9-Net1* and *Cdc14-HA3* by indirect immunofluorescence. Myc9-Net1 displayed a crescent-shaped staining pattern characteristic of nucleolar localization (Figure IV-5A, middle row). A similar pattern was observed for Cdc14-HA3 (Figure IV-5A, bottom row). To confirm that both proteins do in fact localize to the nucleolus, we probed cells with antibodies directed against the relevant epitope tag and antibodies directed against the RNA polymerase 1 A190 subunit (RPA190), a nucleolar marker (Oakes et al., 1998). A striking overlap in the antibody staining patterns was observed (Figure IV-5A), indicating that both Net1 and Cdc14 localize to the nucleolus.

Net1 was required for localization of Sir2 to the nucleolus (Straight et al., 1999), which prompted us to examine if Net1 was also required for the nucleolar localization of Cdc14. Cdc14 localization was visualized in wild type, *net1-1* and *net1Δ* cells. In wild type and *net1-1* cells, Cdc14 assumed a sharp nucleolar staining pattern (Figure IV-5B, center rows). However, in *net1Δ* cells, Cdc14 was diffused throughout the entire cell (Figures IV-5B and 5C, bottom row). Although there was four-fold less Cdc14 protein in *net1Δ* cells (Figure IV-5D), the level of delocalized Cdc14 staining was clearly greater

than that seen in *CDC14-HA3 NET1* cells, or in cells that lacked tagged *CDC14*. These data suggest that Net1 anchors the RENT complex to the nucleolus. The significance of the nucleolar localization of Cdc14 in *net1-1* is considered in the Discussion.

Cdc14 is released from the nucleolus during progression through mitosis

If Net1 sequesters the bulk of Cdc14 in the nucleolus in a presumably inactive form, how does Cdc14 fulfill its essential role in promoting mitotic exit? To resolve this puzzle, we looked more carefully at the localization of Net1 and Cdc14 during the cell cycle. Asynchronous populations of cells expressing Myc9-Net1 and Cdc14-HA3 were probed with antibodies directed against the relevant epitope tags and with anti-tubulin antibodies to visualize the mitotic spindle. Cells in late anaphase and telophase contain elongated spindles, whereas cells in other stages exhibit either focal tubulin staining (G1 and early S phase cells), or a short spindle (S phase and pre-anaphase cells). Like the well-characterized nucleolar protein Nop1 (Aris and Blobel, 1988), Net1 exhibited a characteristic nucleolar staining pattern throughout the cell cycle (Figure IV-6A, upper and middle rows; Straight et al., 1999). Intriguingly, the localization of Cdc14 varied as a function of the cell cycle (Figures IV-6A bottom row and 6B): in cells with short spindles, Cdc14 was localized to the nucleolus (Figure IV-6B bottom row). However, in late anaphase/telophase cells with long spindles, Cdc14 was diffused throughout the nucleus (Figure IV-6B middle row) or the entire cell (Figure IV-6B top row, note the diffuse cytoplasmic staining that extends beyond the nucleus).

To evaluate more rigorously the relationship between long spindles and delocalized Cdc14, we carried out a cell cycle block-release experiment. *Myc9-NET1 CDC14-HA3* cells were synchronized in G1 with α factor, and at various time points after release, samples were processed for indirect immunofluorescence. The percentage of cells with long mitotic spindles, delocalized Cdc14-HA3, and delocalized Myc9-Net1 were plotted as a function of time. Although Myc9-Net1 remained localized to the nucleolus throughout the cell cycle, release of Cdc14-HA3 from the nucleolus mirrored the appearance of long spindles (Figure IV-6C).

The release of Cdc14 from nucleolus requires Tem1

An intriguing possibility is that *tem1* cells fail to exit mitosis due to a failure to dislodge Cdc14 from its Net1 tether in the nucleolus. To test this hypothesis, we examined whether the release of Cdc14 from the nucleolus requires Tem1. *CDC14-HA3 tem1Δ::GAL1-UPL-TEM1* cells were either maintained in YPG (*TEM1* expressed) as an exponentially growing culture, or were released from α-factor-induced G1 arrest into YPD (*TEM1* repressed) to yield a synchronous population of cells arrested in late anaphase/telophase due to a deficit of Tem1 activity. In cells grown in YPG, Cdc14 was largely delocalized in 92% of cells containing a long mitotic spindle (Figure IV-7B), whereas the nucleolar antigen RPA190 retained a distinctive nucleolar staining pattern (Figure IV-7A, top row). In contrast, in cells that were arrested in late anaphase/telophase by depletion of Tem1, Cdc14 (Figure IV-7A, bottom row) and the

nucleolar marker RPA190 (data not shown) displayed overlapping focal staining patterns in the vast majority (93%) of cells with long spindles (Figure IV-7B).

A simple view would argue that *net1-1* bypasses *tem1Δ* by causing ectopic release of Cdc14 from the nucleolus. Surprisingly, Cdc14-HA3 appears correctly localized in *net1-1* cells (Figure IV-5B). However, it is important to note that the bypass activity of *net1-1* would not necessarily require constitutive delocalization of Cdc14. To test whether Tem1-independent release of Cdc14 from the nucleolus occurred in mitotic cells, we compared Cdc14-HA3 localization in Tem1-depeleted *net1-1* and *NET1* cells. Whereas Cdc14-HA3 was localized to the nucleolus in >90% of Tem1-deficient *NET1* cells that contained a long spindle, it was delocalized in ~40% of the equivalently staged Tem1-depleted *net1-1* cells (Figure IV-7B). These results argue that Tem1 is normally required for release of Cdc14 from the nucleolus during anaphase/telophase, and that *net1-1* allows ectopic release of Cdc14 (from at least a fraction of cells) during late mitosis even in the absence of *TEM1* function.

Discussion

RENT control: A model for the control of mitotic exit in budding yeast

Tem1, Cdc15, and Cdc14 are required for mitotic exit. These proteins have been implicated in ensuring a rapid and irreversible drop in mitotic cyclin/Cdk activity at the end of mitosis by promoting the proteolysis of the mitotic cyclin Clb2 and the accumulation of the cyclin/Cdk inhibitor Sic1. Despite the appeal of this scenario, it has remained unclear how the activities of these proteins are mobilized at the end of mitosis.

Based on the data presented here, we propose the following model (Figure IV-8). Throughout G1, S, and early M phase, a pool of Cdc14 is confined to the nucleolus as a subunit of the RENT complex (which also contains Net1 and Sir2). As cells proceed through anaphase, Tem1-dependent signaling impinges on the RENT complex, enabling the release of Cdc14 (and a portion of Sir2, Moazed et al., submitted) from Net1. Unfettered Cdc14 diffuses into the nucleus and cytoplasm, where it modulates the phosphorylation state of proteins involved in the proteolysis of Clb2 (Hct1) and transcription of *SIC1* (Swi5) (Visintin et al., 1998; Jaspersen et al., 1999). The RENT complex then reassembles once Clb/Cdk activity is quenched and Tem1-dependent signaling has been terminated, possibly via a negative feedback loop that involves Cdc14-dependent dephosphorylation of Net1.

We present five major lines of evidence in support of this model. First, Net1 and Cdc14 assemble into a complex, and Net1 is required to anchor Cdc14 to the nucleolus throughout interphase. Second, binding of Net1 to Cdc14 inhibits the protein phosphatase activity of Cdc14 *in vitro*, and *net1* mutants display elevated Cdc14 protein phosphatase activity. Third, Cdc14 is released from its inhibitory nucleolar tether as wild type cells proceed through mitosis. Fourth, Cdc14 is not released from the nucleolus in cells arrested in late mitosis due to deficiency of *TEM1* function. Fifth, recessive mutations in *NET1* bypass the essential requirement of Tem1 for: (i) release of Cdc14 from the nucleolus during late mitosis, (ii) destruction of Clb2 and accumulation of Sic1 during late mitosis, and (iii) growth.

The 'RENT control' model opens up several key questions regarding the function and regulation of RENT. What is the nature of the stimulus that initiates Tem1-dependent signaling? What are the proximal biochemical events that trigger the release of Cdc14 from RENT? How is the RENT complex re-established as cells return to G1 phase? What functions does the RENT complex play in the regulation of nucleolar processes? Identification of the dynamic RENT complex provides a focus for exploring the molecular events that culminate in the release of active Cdc14 during anaphase/telophase.

Net1 is a multifunctional protein

Affinity purification of Net1 revealed at least two binding partners – Sir2 and Cdc14 – which possess disparate cellular functions. Net1 also appears to associate with the essential nucleolar protein Ypl126w (Nan1), but we do not know whether Nan1 is a component of the RENT complex, or part of a distinct Net1-containing complex. Sir2 mediates the silencing of RNA polymerase II-dependent transcription in specific regions of the genome (the rDNA locus, the mating type loci, and telomeres) (Bryk et al., 1997; Fritze et al., 1997; Smith and Boeke, 1997; and reviewed by Lustig, 1998). Consistent with the company it keeps, Net1 also participates in the silencing of RNA polymerase II-dependent transcription in the nucleolus (but not at the telomeres or silent mating loci) by tethering Sir2 to rDNA (Straight et al., 1999). In addition, *net1* mutations cause partial delocalization of the nucleolar protein Nop1, and alter the structure of the nucleolus (Straight et al., 1999; W.S. and R.J.D., unpublished data). The nucleolar and cell cycle

functions of Net1 are at least partially separable: unlike *net1-1*, *sir2Δ* was not able to bypass *cdc15Δ*, does not cause growth defects, and has no obvious effect on the ultrastructure of the nucleolus (Ivy et al., 1986). Taken together, these observations suggest that the nucleolar functions of Net1 extend beyond its ability to recruit Sir2. Point mutations that specifically disrupt one function at a time will be of great value in dissecting the activities of this multifaceted protein.

On the relationship between Net1 and Cdc14

Net1 inhibits Cdc14 by two independent mechanisms. First, it physically assembles with Cdc14 and inhibits its protein phosphatase activity, as evidenced by the fact that the specific activity of Cdc14 is elevated in *net1* mutants, and Cdc14 recruited to Net1-containing beads is inactive. Multiple protein kinase inhibitors (e.g., p16, p21, p27; reviewed in Xiong, 1996) and serine/threonine protein phosphatase inhibitors (reviewed in Shenolikar, 1995) have been reported. To our knowledge, Net1 is the first known protein inhibitor of a member of the protein tyrosine phosphatase family that does not work by a dominant-negative mechanism. It will be interesting to determine whether human Cdc14 homologs (Li et al., 1997; H.C. unpublished data) and other members of the dual-specificity protein phosphatase family are regulated by Net1-like molecules.

As described in the previous section, Net1 also tethers Cdc14 to the nucleolus from G1 until late mitosis. Whereas Cdc14 is completely delocalized in *net1Δ* cells at all stages of the cell cycle, a nucleolar pool of Cdc14 persists in *net1-1* mutants during interphase. However, Cdc14 is released from the nucleolus in ~40% of Tem1-deficient

net1-1 cells in late anaphase/telophase, but is released in only 8% of the equivalent Tem1-deficient *NET1* cells. These observations are consistent with the notion that release of Cdc14 from its nucleolar bonds requires the action of two independent signals: an unknown signal and the Tem1-dependent signal, both of which are active only during mitosis (Figure IV-8). We suggest that *net1-1* relieves the requirement for the latter but not the former such that Cdc14 is still localized to the nucleolus in Tem1-depleted *net1-1* cells during interphase, but is delocalized once they proceed through mitosis.

The specific activity of Cdc14 is elevated in *net1-1* to about the same extent as in *net1Δ* although the majority of Cdc14 is associated with the nucleolus in *net1-1* but not in *net1Δ* cells. One explanation for this discrepancy is that the enfeebled Net1-1/Cdc14 protein complex is not stable under our immunoprecipitation conditions such that *net1-1* behaves like a null allele in this assay. Alternatively, the Net1-1 protein could have lost its inhibitory activity, but not its binding affinity, toward Cdc14. It is interesting to note that the level of Cdc14 is reduced in *net1-1*, and further reduced in *net1Δ*, suggesting that Cdc14 bound to Net1 is more stable than the released protein. Degradation of free Cdc14 may contribute to the extinction of Cdc14 activity once the exit from mitosis is completed.

Intriguingly, we found that Net1 is a phosphoprotein and can be dephosphorylated by Cdc14. This raises the possibility that there is a negative feedback loop connecting Net1 and Cdc14. We suggest the following scenario: from G1 to anaphase, hypophosphorylated Net1 binds to and sequesters Cdc14 in the nucleolus. In anaphase/telophase, Tem1-dependent signaling activates a Net1 kinase, which in turn

hyperphosphorylates Net1, thereby stimulating Cdc14 release. As cells enter G1, Tem1 signaling ceases, the Net1 kinase becomes inactive, and Cdc14 dephosphorylates Net1. The dephosphorylated Net1 subsequently binds Cdc14, thereby resetting Cdc14 activity to the ground state (Figure IV-8).

Although Net1 influences cell cycle progression by sequestering Cdc14 in the nucleolus, it is not yet clear whether Cdc14 contributes to the assembly or function of this organelle. *cdc14*^{ts}, but not *cdc15*^{ts} mutants fail to completely segregate the nucleolar antigen Nop1 (Granot and Snyder, 1991) and the rDNA-bound proteins Net1 and Sir2 (Straight et al., 1999), suggesting that Cdc14 might contribute to the organization or segregation of nucleolar chromatin.

Net1 provides a missing link between Tem1/Cdc15 and Cdc14

Exit from mitosis in *S. cerevisiae* involves an elaborate signaling network consisting of at least seven essential genes: *CDC5, CDC14, CDC15, DBF2/DBF20, LTE1, MOB1*, and *TEM1*. Since overexpression of the GTP-binding protein Tem1 bypasses the essential requirement (at low temperature) for the nucleotide exchange factor Lte1, and overexpression of the protein kinase Cdc15 bypasses the essential requirement for Tem1 (Shirayama et al., 1994b), it is likely that Lte1 activates Tem1, which in turn activates Cdc15. In support of this model, the *S. pombe* Cdc15 homologue Cdc7 binds to and is genetically downstream of *S. pombe* Tem1 homologue Spg1 (Schmidt et al., 1997). Since the recessive *net1-1* mutation bypasses *cdc15Δ* and *tem1Δ*, *NET1* formally behaves as a mitotic exit inhibitor acting downstream of or parallel to *TEM1* and *CDC15* (W.S.

and R.J.D., manuscript in preparation). Based on our observations that Net1 binds to and inhibits Cdc14, the most parsimonious model is as follows: during progression through mitosis, an unknown signal activates Lte1, which in turn activates Tem1. Tem1 then activates Cdc15, which in turn relieves the inhibition of Cdc14 by Net1. Although we have yet to test this directly, we suggest that Cdc5, Dbf2/Dbf20, and Mob1 are also required for the release of Cdc14 from RENT. Active Cdc14 then promotes Clb2 degradation and Sic1 accumulation (Visintin et al., 1998; Jaspersen et al., 1999; W. Reynolds,W.S., and R.J.D., unpublished data), which shuts off Cdc28 activity.

Nucleolus as a sequestration center?

The nucleolus is a discrete sub-nuclear area for ribosomal RNA synthesis and pre-ribosome assembly (reviewed in Shaw and Jordan, 1995). Some nucleolar proteins- including nucleolin, B23, and Nopp140- were initially shown to localize to the nucleolus by immunofluorescence, and later shown to shuttle between the nucleolus and the cytoplasm (reviewed in Shaw and Jordan, 1995). Therefore, it is possible that Net1 also shuttles between the nucleolus and the cytoplasm to ferry cytoplasmic and nuclear Cdc14 to the nucleolus.

Cdc14 is localized to the nucleolus at times during the cell cycle when it is not needed, and is released from the nucleolus when its activity is required for cell cycle progression. Might the nucleolus serve an unappreciated role as a "sequestration center" for proteins that are to be kept inactive? Interestingly, a $p34^{cdc2}$ homologue has been shown to localize to the nucleoli of neurons and glia in the mitotically quiescent murine

central and peripheral nervous systems (Ino et al., 1993). This notion raises the possibility that some of the many proteins that have been localized to the nucleolus may not act solely (or even primarily) in the nucleolus, but may be stockpiled there in anticipation of their eventual release. It is not clear how many other proteins might be regulated by nucleolar sequestration; only future research can reveal the generality of this mode of regulation.

Experimental Procedures

Yeast Strain Constructions

All yeast strains used in this study are in the W303 background (*can1-100, leu2-3,-112, his3-11,-15, trp1-1 ,ura3-1, ade2-1*). The pRS vector series was described previously (Sikorski and Hieter, 1989). The details of plasmid and strain construction are available upon request. To obtain *tem1Δ::TRP1 [GAL1-TEM1, URA3]* (RJD1017), the diploid strain RJD1005 (*tem1Δ::TRP1/TEM1, MATa/α*) was transformed with pWS102 *[pRS316: GAL1-TEM1, URA3]*, and dissected. To construct *GAL1-UPL-TEM1*, the UPL degron of the UFD pathway (Johnson et al., 1992) was amplified by PCR and inserted upstream of *TEM1* in pWS102. The *GAL1-UPL-TEM1* cassette was then excised and cloned into pRS304 (TRP1), which was subsequently digested with both BglII and KpnI, blunt-ended with Klenow, and self-ligated to generate pWS103 (*[GAL1-UPL-tem1ΔC /TRP1]*). pWS103 was linearized with EcoRI to direct integration at the *TEM1* locus, yielding WY46 (*tem1Δ::GAL1-UPL-TEM1, bar1::hisG, MATa*). To construct *net1::Myc9-NET1/LEU2* (WY53), pWS104 (containing nucleotides (Nts) -293 –> +3 and

Nts +4 –> +844 of *NET1* flanking Myc9) was linearized with Bsg1, and integrated into a wild type strain. To construct *cdc14::CDC14-Flag-His6-HA3/HIS3* strain (RJD 1191), pGJR (pRS315 containing Nts 1336-1653 of the *CDC14* ORF, followed by Flag-His6-HA3, followed by Nts 1654-2095 of *CDC14* 3' untranslated region) was linearized with EcoRV and transformed into a wild type strain. To delete *SIR* genes, strains were transformed with *sirΔ::LEU2* plasmids (Ivy et al., 1986), and correct transformants were identified based on their sterility. The *NET1* locus was replaced by *S.pombe his5+* using the PCR amplification/transformation method described previously (Wach et al., 1997). Correct integrants were verified by PCR, sporulated, and dissected (WY 69 and 70).

Cell Growth, Synchronization Procedures, and In vivo Labeling

Cells were grown on 1% yeast extract/2% peptone (YP) + 2% glucose (YPD) or YP+ 2% galactose (YPG) medium. 5-FOA plates were prepared as described (Sikorski and Boeke, 1991). To perform *GAL1-UPL-TEM1* shut-off experiments, exponential phase cells grown in YPG were arrested with α factor (10 μg/ml for *BAR1* and 0.1 μg/ml for *bar1Δ* strains), and released into YPD. In some cases, α factor was added back a few hours after release to trap cells in the subsequent G1 phase. To label cells with ^{32}P-phosphate, 5 x 10^8 exponential phase cells grown in phosphate-free YPD (Warner, 1991) were resuspended in 2.5 ml of phosphate-free YPD and labeled with 0.3 mCi ^{32}P-phosphate (ICN) for 45 min at room temperature. Cells were washed with ice-cold water and harvested. To arrest cells at *cdc* blocks, cells were shifted to 37°C for 2.5-3.5 hours until ≥90% cells were arrested.

Cell Extract Preparation, Immunoprecipitation and Western Blot

To detect proteins by immunoblotting, 200 μl of SDS-sample buffer were added to 8 x 10^7 cells, vortexed for 2", and boiled for 3'. 100 μl of acid-washed glass beads (0.5 mm) were added and the mixture was vortexed for 2'. The samples were boiled again for 2', and 8 μl of samples were loaded on SDS-polyacrylamide gels. To prepare extracts for immunoprecipitation (IP), 4-6 x 10^8 cells were pelleted, washed once with HBS (20 mM Hepes pH 7.2, 150 mM NaCl), and resuspended in 200 μl of Lysis Buffer (HBS + 2 mM dithiothreitol (DTT), 0.2% Triton, and protease inhibitors) (Shou and Dunphy, 1996). Glass beads (200 μl) were added, and cells were lysed by twelve cycles of vortexing for 30" followed by a 1'- incubation on ice. Extracts were clarified by two consecutive centrifugations (14,000 g for 5 min). Protein concentration of extracts was typically 5-10 mg/ml. Extracts (80-150 μl) were incubated with 1 μl of 12CA5 (for HA-tagged protein) or 9E10 (for Myc-tagged protein) monoclonal antibodies on ice (1 hour), supplemented with 15-20 μl of either protein A (12CA5 antibodies) or anti-mouse IgG beads (9E10 antibodies), and incubated on a rotator at 4^oC for 1 hour. Beads were then washed extensively with lysis buffer lacking protease inhibitors. 1/3 - 1/4 of the washed immunoprecipitates were subjected to SDS-PAGE and immunoblotting as described (Harlow and Lane, 1988). In the experiment described in Figure 4C, 2 mM Na_3VO_4 was included in the Myc9-Net1 IP reaction (but not the wash buffers) to inhibit the endogenous Cdc14 from binding to Net1 in the extracts. To prepare anti-GST beads, 20 μl of Protein A beads were incubated with 1 μl of anti-GST antibodies, and washed after

1 hr-incubation. Western blot detection relied upon either ^{125}I-labeled secondary antibodies (ICN) or HRP- conjugated secondary antibodies followed by ECL+ (Amersham). The blots were scanned and quantitated using Molecular Dynamics STORM system.

Protein Identification by Mass Spectrometry

Protein bands were excised from a single silver stained SDS-polyacrylamide gel, reduced with dithiothreitol, alkylated with iodoacetamide and *in-gel* digested with trypsin (37°C, overnight) as described previously (Shevchenko et al., 1996). An aliquot (0.3 - 0.5 μL) of the digest was withdrawn and analyzed by high mass accuracy MALDI peptide mapping on a modified REFLEX mass spectrometer (Bruker Daltonics, Bremen, Germany) essentially as described previously (Shevchenko et al., 1996). If MALDI peptide mass mapping could not provide a conclusive identification of the protein, the gel pieces were further extracted with 5% formic acid and acetonitrile. The extracts were pooled and lyophilized, and the unseparated mixture of tryptic peptides was sequenced by nanoelectrospray tandem mass spectrometry on an API III triple quadruple instrument (PE Sciex, Concord, ON, Canada) as described previously (Wilm et al., 1996). Database searches were performed against a comprehensive nonredundant protein sequence database using PeptideSearch v. 3.0 software developed in EMBL. No limitations of protein molecular weight and species of origin were imposed.

Detection of Phospho-Net1 and Treatment with Cdc14

To retrieve [^{32}P]-Net1, *Myc9-NET1* cells were labeled with [^{32}P]-phosphate and disrupted with glass beads in Lysis Buffer supplemented with phosphatase inhibitors as described (Verma et al., 1997), and clarified extracts were immunoprecipitated with 9E10 antibodies. To assay if phospho-Net1 might be a substrate for GST-Cdc14, GST-Cdc14 and catalytically inactive GST-Cdc14 (C283S) were purified from *E. coli* as described (Taylor et al., 1997). Myc9-Net1 was IP'd in the presence of phosphatase inhibitors (excluding Na_3VO_4), and washed extensively with the final wash being Cdc14 buffer (50 mM imidazole, pH 6.6, 1 mM EDTA, 1 mM DTT, 0.1 mg/ml BSA, 25 μg/ml aprotinin, 10 μg/ml PLC). Beads were incubated with 1.2 μg of GST-Cdc14 (wild type or mutant) in 50 μl of Cdc14 buffer at 30°C for 1 hour.

Cdc14 Activity Assay

MBP-Sic1-MycHis6 (10 μg) was phosphorylated by GST-Cdc28/Cln2/Cks1/Cak1 kinase in the presence of [^{32}P]-γ-ATP (Skowyra et al., 1997), retrieved from the kinase reaction on Ni-NTA resin (Qiagen), and eluted in 120 μl of 200-250 mM imidazole (pH 7.5). To assay bead-bound Cdc14 activity, the beads were incubated with 30 μl of Cdc14 buffer containing 1 μl of [^{32}P]-Sic1, and rotated at 22°C for 18'-20' (or 18°C for 15', Figure 4C). Control experiments indicated that at most 40-50% of the input substrate was dephosphorylated under these conditions. The supernatant was removed, and the beads were washed 2x with 30 μl HBS + 0.1% Triton X-100. The washes were pooled with the supernatant, adjusted to 10% trichloroacetic acid, incubated for 30 min on ice, and

centrifuged for 10 min at 14,000 g. Soluble radioactivity was measured by scintillation counting.

Immunofluorescence

Immunofluorescence was carried out essentially as described previously (Pringle et al., 1991). Cells were fixed with 4.5% formaldehyde at room temperature for 0.5 hour for anti-RPA190, and 1 hour for all other antibodies. Primary antibodies included: 1:1000 mouse monoclonal antibodies HA.11 and 9E10 (Babco), 1:1000 rabbit anti-RPA190, 1:2000 rabbit-anti-tubulin antibodies, and 1:12,000 mouse-anti-Nop1. Secondary antibodies included 1:1000 rhodamine-conjugated-donkey-anti-rabbit antibodies (Jackson Lab) and 1:1000 fluorescein-conjugated-goat-anti-mouse antibodies (Cappel). Images were captured on a Zeiss Axioskop microscope using Fujichrome Provia 400 slide film.

Acknowledgements

W.S. dedicates this paper to her parents who have supported her unconditionally. We thank D. Kellogg, M. Nomura, F. Solomon, and J. Aris for anti-Clb2, anti-RPA190, anti-tubulin, and anti-Nop1 antibodies, respectively; A. Varshavsky, K. Nasmyth, P. Philippsen, and J. Hicks for the UPL, Myc9, *S.pombe his5*$^{+}$, and *sirΔ::LEU2* plasmids, respectively; R. Feldman and R. Verma for MBP-Sic1 and Sic1 kinase. We thank G. Reynard for constructing CDC14-HA3; J. Archer for sharing immunofluorescence expertise, and R.Verma, R. Feldman, W. Dunphy, and H. Rao for critically reading the manuscript. W.S. thanks B. Hay for insight and encouragement, and D. Harrington for

assistance with graphics. W.S. is a Howard Hughes Medical Institute predoctoral fellow. H.C. was supported by NIH grant CA59935, and R.J.D. was supported by Junior Investigator Awards from the Searle/Chicago Community Trust and the Beckman Foundation.

References

Aris, J.P. and Blobel, G. (1988). Identification and characterization of a yeast nucleolar protein that is similar to a rat liver nucleolar protein. J Cell Biol *107*, 17-31.

Bryk, M., Banerjee, M., Murphy, M., Knudsen, K. E., Garfinkel, D. J., and Curcio, M. J. (1997). Transcriptional silencing of Ty1 elements in the RDN1 locus of yeast. Genes Dev 11, 255-69.

Charles, J.F., Jaspersen, S.L., Tinker-Kulberg, R.L., Hwang, L., Szidon, A., and Morgan, D.O. (1998). The Polo-related kinase Cdc5 activates and is destroyed by the mitotic cyclin destruction machinery in *S. cerevisiae*. Curr Biol *8*, 497-507.

Culotti, J. and Hartwell, L.H. (1971). Genetic control of the cell division cycle in yeast. 3. Seven genes controlling nuclear division. Exp Cell Res *67*, 389-401.

Deshaies, R.J. (1997). Phosphorylation and proteolysis: partners in the regulation of cell division in budding yeast. Curr Opin Genet Dev *7*, 7-16.

Donovan, J.D., Toyn, J.H., Johnson, A.L., and Johnston, L.H. (1994). $p40^{SDB25}$, a putative CDK inhibitor, has a role in the M/G1 transition in *Saccharomyces cerevisiae*. Genes & Development *8*, 1640-1653.

Fritze, C. E., Verschueren, K., Strich, R., and Easton Esposito, R. (1997). Direct evidence for SIR2 modulation of chromatin structure in yeast rDNA. Embo J *16*, 6495-509.

Gotta, M., Strahl-Bolsinger, S., Renauld, H., Laroche, T., Kennedy, B.K., Grunstein, M., and Gasser, S.M. (1997). Localization of Sir2p: the nucleolus as a compartment for silent information regulators. Embo J *16*, 3243-55.

Granot, D. and Snyder, M. (1991). Segregation of the nucleolus during mitosis in budding and fission yeast. Cell Motil Cytoskeleton *20*, 47-54.

Hardy, C. F., and Pautz, A. (1996). A novel role for Cdc5p in DNA replication. Mol Cell Biol *16*, 6775-82.

Ino, H., Mochizuki, T., Yanaihara, N. and Chiba, T. (1993). p34cdc2 homologue is located in nucleoli of the nervous and endocrine systems. Brain Res *614*, 131-6.

Irniger, S., Piatti, S., Michaelis, C. and Nasmyth, K. (1995). Genes involved in sister chromatid separation are needed for B-type cyclin proteolysis in budding yeast. Cell *81*, 269-277.

Ivy, J.M., Klar, A.J. and Hicks, J.B. (1986). Cloning and characterization of four SIR genes of *Saccharomyces cerevisiae*. Mol Cell Biol *6*, 688-702.

Jaspersen, S.L., Charles, J.F., Tinker-Kulberg, R.L., and Morgan, D.O. (1998). A late mitotic regulatory network controlling cyclin destruction in *Saccharomyces cerevisiae*. Mol Biol Cell *9*, 2803-17.

Jaspersen, S.L., Charles, J.F., and Morgan, D.O. (1999). Inhibitory phosphorylation of the APC regulator Hct1 is controlled by the kinase Cdc28 and the phosphatase Cdc14. Curr Biol *9*, 227-236.

Johnson, E.S., Bartel, B., Seufert, W., and Varshavsky, A. (1992). Ubiquitin as a degradation signal. Embo J *11*, 497-505.

King, R.W., Deshaies, R.J., Peter, J.M. and Kirschner, M. (1996). How proteolysis controls cell division. Science *274*, 1652-1659.

Kitada, K., Johnson, A.L., Johnston, L.H. and Sugino, A. (1993). A multicopy suppressor gene of the *Saccharomyces cerevisiae* G1 cell cycle mutant gene dbf4 encodes a protein kinase and is identified as CDC5. Mol Cell Biol *13*, 4445-57.

Komarnitsky, S.I., Chiang, Y.C., Luca, F.C., Chen, J., Toyn, J.H., Winey, M., Johnston, L.H., and Denis, C.L. (1998). DBF2 protein kinase binds to and acts through the cell cycle-regulated MOB1 protein. Mol Cell Biol *18*, 2100-7.

Li, L., Ernsting, B. R., Wishart, M. J., Lohse, D. L., and Dixon, J. E. (1997). A family of putative tumor suppressors is structurally and functionally conserved in humans and yeast. J Biol Chem *272*, 29403-6.

Luca, F.C. and Winey, M. (1998). MOB1, an essential yeast gene required for completion of mitosis and maintenance of ploidy. Mol Biol Cell *9*, 29-46.

Lustig, A. J. (1998). Mechanisms of silencing in *Saccharomyces cerevisiae*. Curr Opin Genet Dev 8, 233-9.

Moll, T., Tebb, G., Surana, U., Robitsch, H. and Nasmyth, K. (1991). The role of phosphorylation and the CDC28 protein kinase in cell cycle-regulated nuclear import of the *S. cerevisiae* transcription factor SWI5. Cell *66*, 743-58.

Oakes, M., Aris, J.P., Brockenbrough, J.S., Wai, H., Vu, L. and Nomura, M. (1998). Mutational analysis of the structure and localization of the nucleolus in the yeast *Saccharomyces cerevisiae*. J Cell Biol *143*, 23-34.

Parkes, V. and Johnston, L.H. (1992). SPO12 and SIT4 suppress mutations in DBF2, which encodes a cell cycle protein kinase that is periodically expressed. Nucleic Acids Res *20*, 5617-23.

Pringle, J.R., Adams, A.E., Drubin, D.G., and Haarer, B.K. (1991). Immunofluorescence methods for yeast. Methods Enzymol *194*, 565-602.

Schmidt, S., Sohrmann, M., Hofmann, K., Woollard, A., and Simanis, V. (1997). The Spg1p GTPase is an essential, dosage-dependent inducer of septum formation in *Schizosaccharomyces pombe*. Genes Dev *11*, 1519-34.

Schwab, M., Lutum, A.S., and Seufert, W. (1997). Yeast Hct1 is a regulator of Clb2 cyclin proteolysis. Cell *90*, 683-93.

Shaw, P.J. and Jordan, E.G. (1995). The nucleolus. Annu Rev Cell Dev Biol *11*, 93-121.

Shenolikar, S. (1995). Protein phosphatase regulation by endogenous inhibitors. Semin Cancer Biol *6*, 219-27.

Shevchenko, A., Jensen, O. N., Podtelejnikov, A. V., Sagliocco, F., Wilm, M., Vorm, O., Mortensen, P., Shevchenko, A., Boucherie, H., and Mann, M. (1996). Linking Genome and Proteome by Mass Spectrometry: Large Scale Identification of Yeast Proteins From Two-Dimensional Gels. Proc. Natl. Acad. Sci. USA *93*, 14440-14445.

Shevchenko, A., Wilm, M., Vorm, O., and Mann, M. (1996). Mass Spectrometric Sequencing of Proteins from Silver Stained Polyacrylamide Gels. Anal. Chem. *68*, 850 - 858.

Shirayama, M., Matsui, Y., Tanaka, K., and Toh-e, A. (1994a). Isolation of a CDC25 family gene, MSI2/LTE1, as a multicopy suppressor of ira1. Yeast *10*, 451-61.

Shirayama, M., Matsui, Y., and Toh-e, A. (1994b). The yeast TEM1 gene, which encodes a GTP-binding protein, is involved in termination of M phase. Molecular and Cellular Biology *14*, 7476-7482.

Shirayama, M., Matsui, Y., and Toh-e, A. (1996). Dominant mutant alleles of yeast protein kinase gene CDC15 suppress the lte1 defect in termination of M phase and genetically interact with CDC14. Mol Gen Genet *251*, 176-85.

Shirayama, M., Zachariae, W., Ciosk, R., and Nasmyth, K. (1998). The Polo-like kinase Cdc5p and the WD-repeat protein Cdc20p/fizzy are regulators and substrates of the anaphase promoting complex in *Saccharomyces cerevisiae*. Embo J *17*, 1336-49.

Shou, W. and Dunphy, W.G. (1996). Cell cycle control by Xenopus p28Kix1, a developmentally regulated inhibitor of cyclin-dependent kinases. Mol Biol Cell *7*, 457-69.

Sikorski, R.S. and Boeke, J.D. (1991). In vitro mutagenesis and plasmid shuffling: from cloned gene to mutant yeast. Methods Enzymol *194*, 302-18.

Sikorski, R.S. and Hieter, P. (1989). A system of shuttle vectors and yeast host strains designed for efficient manipulation of DNA in *Saccharomyces cerevisiae*. Genetics *122*, 19-27.

Skowyra, D., Craig, K., Tyers, M., Elledge, S., and Harper, J. (1997). F-box proteins are receptors that recruit phosphorylated substrates to the SCF ubiquitin-ligase complex. Cell *91*, 209-219.

Smith, J. S., and Boeke, J. D. (1997). An unusual form of transcriptional silencing in yeast ribosomal DNA. Genes Dev *11*, 241-54.

Straight, A.F., Shou, W., Dowd, G.J., Turck, C.W., Deshaies, R.J., Johnson, A.D., and Moazed, D. (1999) Net1, a Sir2-associated nucleolar protein required for rDNA silencing and nucleolar integrity. Cell *97*: 245-56.

Surana, U., Amon, A., Dowzer, C., McGrew, J., Byers, B., and Nasmyth, K. (1993). Destruction of the CDC28/CLB mitotic kinase is not required for the metaphase to anaphase transition in budding yeast. Embo J *12*, 1969-1978.

Taylor, G.S., Liu, Y., Baskerville, C. and Charbonneau, H. (1997). The activity of Cdc14p, an oligomeric dual specificity protein phosphatase from *Saccharomyces cerevisiae*, is required for cell cycle progression. J Biol Chem *272*, 24054-63.

Toyn, J.H., Johnson, A.L., Donovan, J.D., Toone, W.M. and Johnston, L.H. (1997). The Swi5 transcription factor of *Saccharomyces cerevisiae* has a role in exit from mitosis through induction of the cdk-inhibitor Sic1 in telophase. Genetics *145*, 85-96.

Toyn, J.H. and Johnston, L.H. (1994). The Dbf2 and Dbf20 protein kinases of budding yeast are activated after the metaphase to anaphase cell cycle transition. Embo J *13*, 1103-1113.

Traverso, E.E., Baskerville, C., Liu, Y., Shou, W., James, P., Deshaies, R.J., and Charbonneau, H. (2001). Characterization of the net1 cell cycle-dependent regulator of the Cdc14 phosphatase from budding yeast. J Biol Chem, in press.

Verma, R., Annan, R.S., Huddleston, M.J., Carr, S.A., Reynard, G., and Deshaies, R.J. (1997). Phosphorylation of Sic1p by G1 Cdk required for its degradation and entry into S phase. Science *278*, 455-60.

Visintin, R., Craig, K., Hwang, E.S., Prinz, S., Tyers, M. and Amon, A. (1998). The phosphatase Cdc14 triggers mitotic exit by reversal of Cdk-dependent phosphorylation. Molecular Cell *2*, 709-718.

Visintin, R., Prinz, S. and Amon, A. (1997). CDC20 and CDH1: a family of substrate-specific activators of APC-dependent proteolysis. Science *278*, 460-3.

Wach, A., Brachat, A., Alberti-Segui, C., Rebischung, C., and Philippsen, P. (1997). Heterologous HIS3 marker and GFP reporter modules for PCR-targeting in *Saccharomyces cerevisiae*. Yeast *13*, 1065-75.

Warner, J.R. (1991). Labeling of RNA and phosphoproteins in *Saccharomyces cerevisiae*. Methods Enzymol *194*, 423-8.

Wilm, M., Shevchenko, A., Houthaeve, T., Breit, S., Schweigerer, L., Fotsis, T., and Mann, M. (1996). Femtomole Sequencing of Proteins from Polyacrylamide Gels by NanoElectrospray Mass Spectrometry. Nature *379*, 466 - 469.

Xiong, Y. (1996). Why are there so many CDK inhibitors? Biochim Biophys Acta *1288*, 01-5.

Zachariae, W., Schwab, M., Nasmyth, K. and Seufert, W. (1998). Control of cyclin ubiquitination by CDK-regulated binding of Hct1 to the anaphase promoting complex. Science *282*, 1721-4.

A

	hrs				+	+ + multibranched
net1-1	0	93.4	0	5.7	0	0.9
	2	66.5	16.5	11.7	2.9	2.4
	4	19.1	6.4	61.8	3.4	9.3
	12	15.8	3.7	19.5	8.9	52.1
NET1	0	95.0	0	5.0	0	0
	1	49.6	40.2	6.0	1.7	2.6
	4	10.2	0.9	69.8	3.6	15.6
	12	3.0	0.8	81.2	2.2	12.8

B

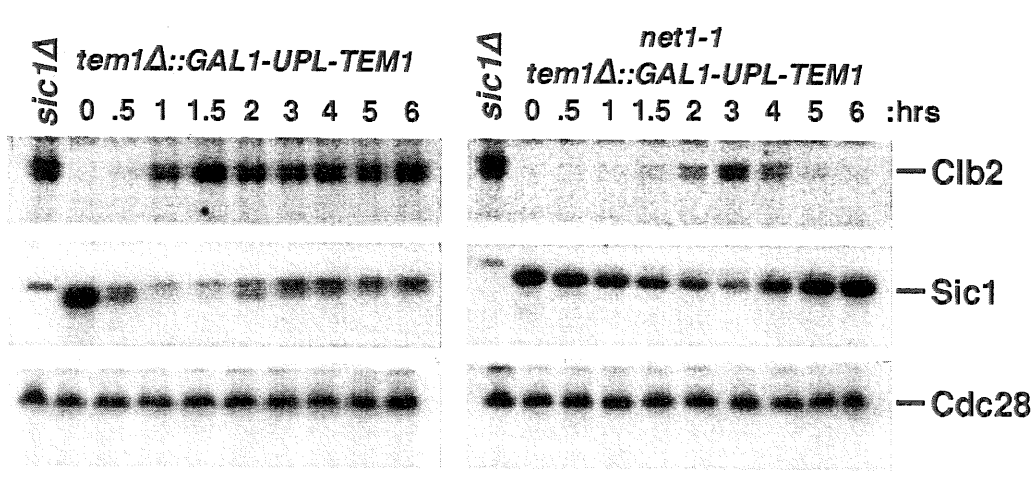

Figure IV-1

Figure IV-1: *net1-1* bypasses *tem1Δ* by inducing ectopic Clb2 degradation and Sic1 accumulation.

*tem1Δ::GAL1-UPL-TEM1 net1-1*and *tem1Δ::GAL1-UPL-TEM1* cells grown in YPG (*TEM1* expressed) at 25°C were arrested in G1 phase with α factor, and released into YPD (*TEM1* repressed) at time = 0.

(C) At 0, 1, 2, 4, and 12 h, samples were taken to measure budding index.

(D) Same as (A), except that at either 2 h (*NET1*) or 3 h (*net1-1*) following release from α factor arrest, α factor was added back to prevent cells from proceeding through a second cell cycle. At the indicated time points (hrs), samples were taken to measure Clb2, Sic1, and Cdc28 protein levels by immunoblotting.

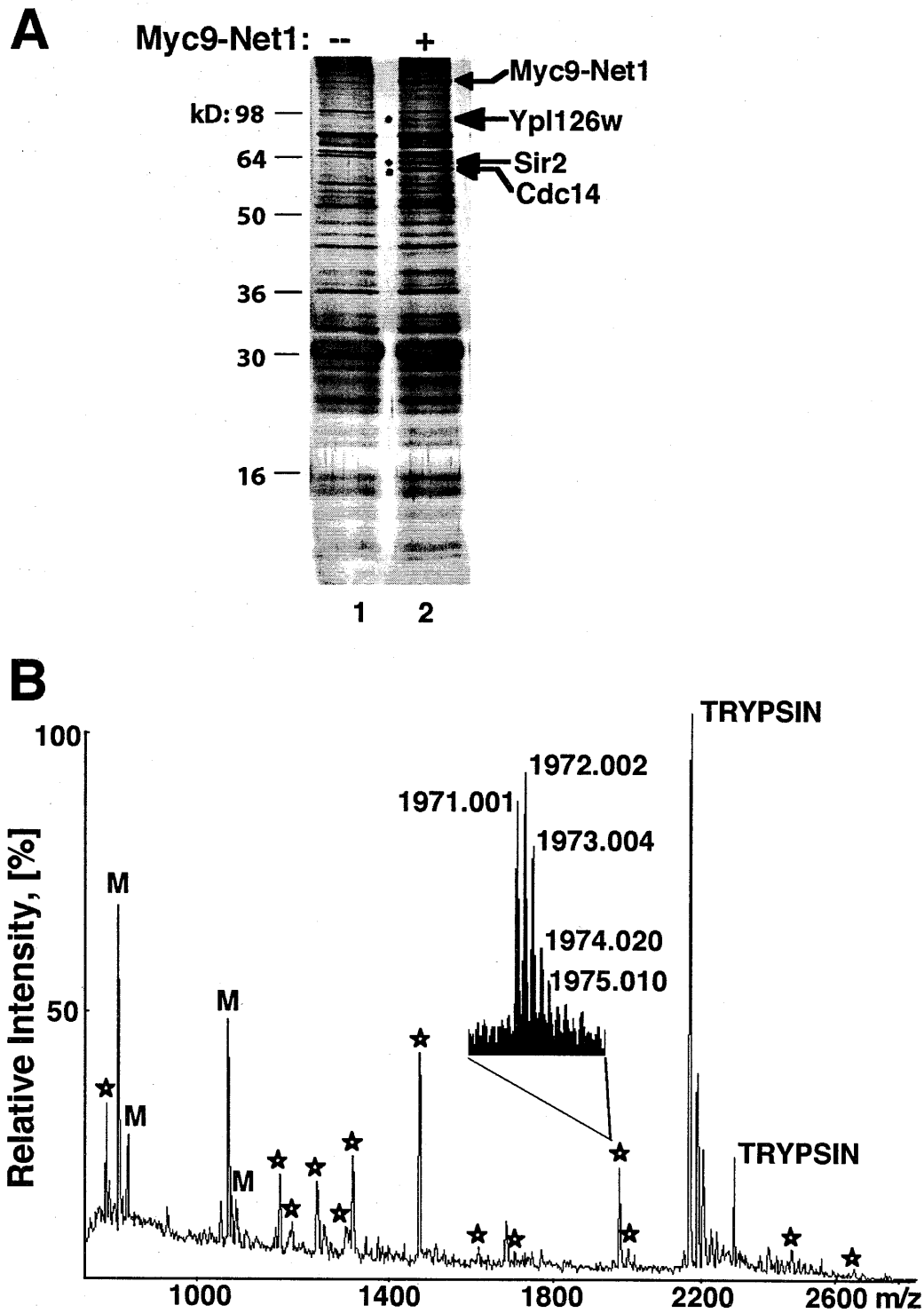

Figure IV-2. A and B

Figure IV-2: Identification of the RENT complex.

(A) Purification of Net1. Extracts (35 mg) of *Myc9-NET1* (lane 2) and untagged control (lane 1) strains were fractionated on beads containing covalently-linked anti-Myc monoclonal antibody 9E10. Eluted proteins were separated on a 10% - 15% SDS-polyacrylamide gradient gel and visualized by silver staining. Protein bands specifically detected in the immunoprecipitates from *Myc9-NET1* but not untagged control strain were excised and identified by mass spectrometry.

(B) Protein identification by high mass accuracy MALDI peptide mass mapping. Mass spectrum acquired from an 0.5 μL aliquot of *in-gel* digest of the 62 kDa band revealed 13 peptide ions that matched the calculated masses of protonated tryptic peptides from Cdc14 with accuracy better than 50 ppm (designated with asterisks). These peptides covered more than 26% of the protein sequence. Ions originating from the matrix are designated by "M." Peptide ions of known trypsin autolysis products are also marked. The inset shows isotopically resolved peptide ion having the monoisotopic weight 1971.001. Mass resolution was better than 7000 (FWHM) despite the very low amount of protein present in the gel.

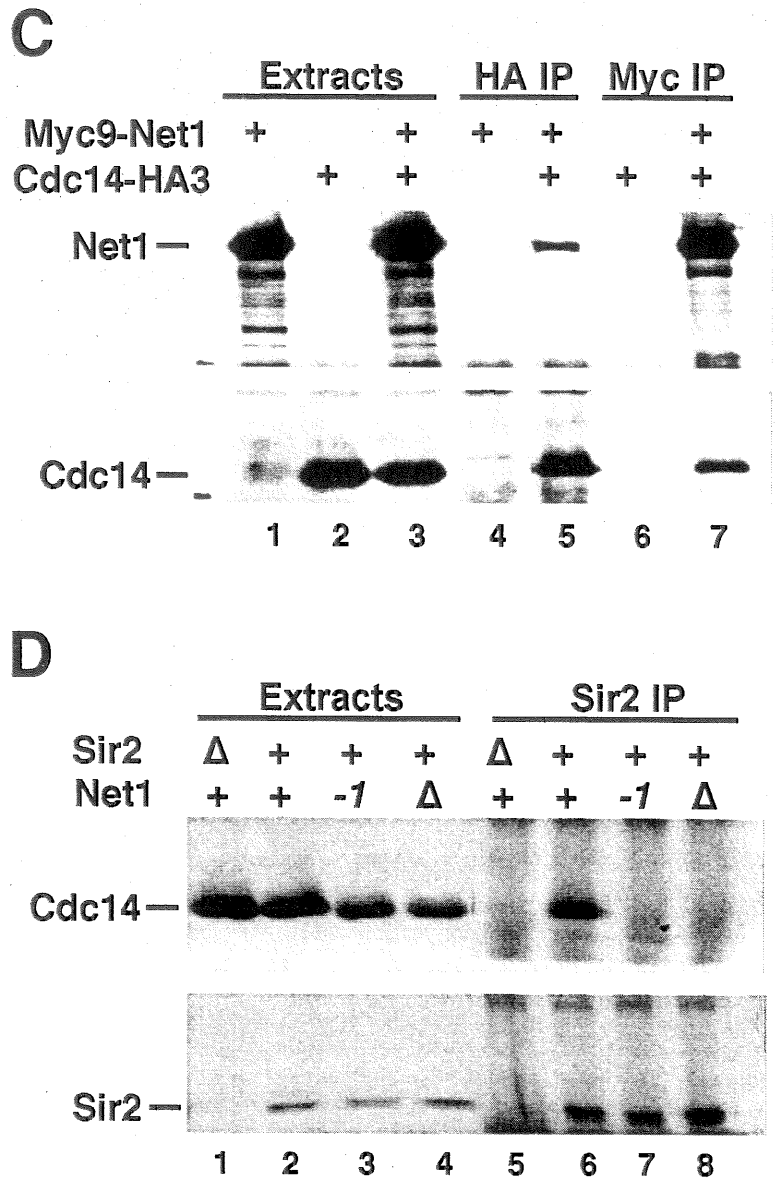

Figure IV-2. C and D

Figure IV-2: Identification of the RENT complex.

(C) Net1 associates with Cdc14. Extracts from strains with the indicated genotypes were immunoprecipitated with either 9E10 antibodies or anti-haemagglutinin (HA) monoclonal antibodies 12CA5. The immunoprecipitates (IP) and the input extracts were immunoblotted with 9E10 (top panel) and 12CA5 (bottom panel) to detect Net1 and Cdc14 proteins, respectively.

(D) Net1-dependent association between Sir2 and Cdc14. Extracts of *CDC14-HA3* cells with the indicated genotypes were immunoprecipitated with anti-Sir2 antibodies. Δ refers to strains deleted for *SIR2* or *NET1*, and *-1* refers to the *net1-1* allele. The immunoprecipitates (IP) and the input extracts were immunoblotted with 12CA5 (top panel) and anti-Sir2 antibodies (bottom panel) to detect the Cdc14 and Sir2 proteins, respectively.

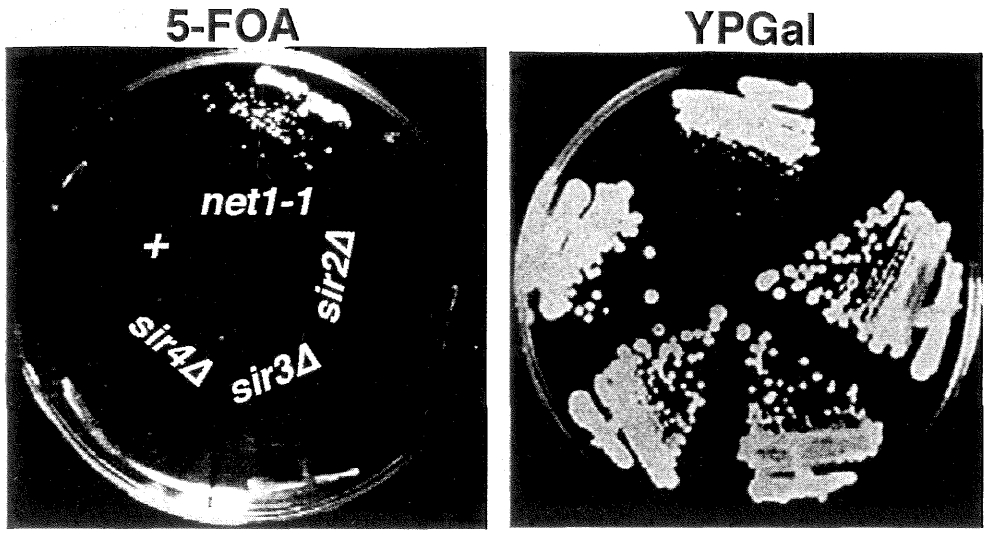

Figure IV-3

Figure IV-3: Loss of silencing fails to bypass the essential requirement for *TEM1*. Wild type (+), *net1-1*, *sir2Δ*, *sir3Δ*, or *sir4Δ* cells that carried *tem1Δ* and were sustained by a [*GAL1-TEM1, URA3*] plasmid were grown on YPG (*TEM1* expressed), and then plated onto either YPG (right panel) or synthetic glucose medium supplemented with 5-FOA (left panel) to select for colonies that were able to grow in the absence of the [*GAL1-TEM1, URA3*] plasmid. The plates were incubated at 25°C and photographed after one week (YPGal plate) or two weeks (5-FOA plate).

A

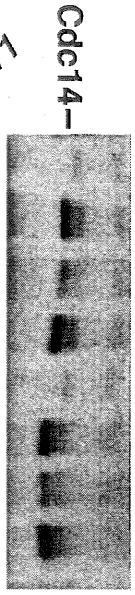

		Corrected cpm	Corrected protein	Specific Activity
-	+	0	0	---
+	+	635	635	1.0
+	*-1*	1007	261	3.9
+	*Δ*	3137	728	4.3
-	+	0	0	---
+	+	710	710	1.0
+	*-1*	944	279	3.4
+	*Δ*	2700	795	3.4

B

Strain	Specific 14 Activity
+	1
net1-1	3.8
net1-1	4.5

C

Beads	Specific 14 Activity
α-GST	50
Net1	1
Net1	1

D

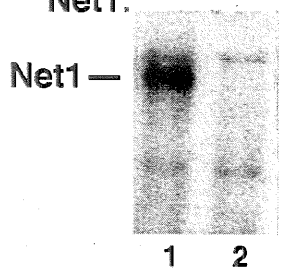

E

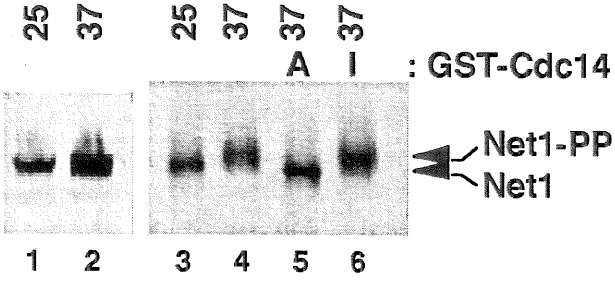

Figure IV-4

Figure IV-4: Net1 is an inhibitor of and a candidate substrate for Cdc14.

(A, B) Cdc14 activity is elevated in *net1* mutants. Cdc14-HA3 was retrieved from lysates of the indicated strains (in the "14-HA3" column: -, untagged; +, *CDC14-HA3*; in the "*NET1*" column: +, *NET1*; *-1*, *net1-1*; *Δ*, *net1Δ*) by immunoprecipitation with 12CA5 antibodies, and was incubated with [^{32}P]-Sic1 for 20 min at 22°C. The specific activity of Cdc14-HA3 in each reaction was determined by measuring trichloroacetic acid-soluble counts released during the incubation, and dividing by the relative amount of Cdc14-HA3 as determined by immunoblotting. All values were corrected by subtracting out background signals obtained with untagged control sample; relative amounts of proteins were normalized such that the specific activity of Cdc14 was 1.0 in wild type cells. The background signals were ~350 and ~27 in the ^{32}P release and immunoblot assays, respectively. The results of duplicate reactions are presented. In panel (A), asynchronous cells were used, whereas in panel (B), cells were synchronized in G1 phase with α factor prior to analysis.

(C) Net1 inhibits Cdc14 phosphatase activity *in vitro*. Extracts of *Myc9-NET1* cells were immunoprecipitated with 9E10 antibodies, and protein A beads were coated with anti-GST antibodies to prepare Net1 and α-GST beads, respectively. Both matrices were washed extensively and incubated with wild type or mutant GST-Cdc14 purified from *E. coli* (20 ng for GST beads and 60 ng for Net1 beads). The specific activity of bead-bound GST-Cdc14 was evaluated as described above using [^{32}P]-Sic1 as the substrate.

Levels of GST-Cdc14 recruited to the Net1 and α-GST beads were assessed by immunoblotting with α-GST antibodies. The activity of mutant Cdc14 bound to the α-GST beads was used for background correction. For simplicity, in panels (B) and (C) only the final values ([^{32}P]-Sic1 dephoshorylation divided by relative amount of Cdc14 antigen) are shown.

(D-E) Net1 is a candidate substrate for Cdc14. (D) Net1 is a phosphoprotein *in vivo*. *Myc9-NET1* (lane 1) and untagged (lane 2) strains were labeled with [^{32}P]-inorganic phosphate. Extracts of labeled cells were immunoprecipitated with 9E10 antibodies, and recovered proteins were fractionated by SDS-PAGE and detected by autoradiography. (E) Net1 can be dephosphorylated by Cdc14 in vitro. *CDC14 Myc9-NET1* (+, lanes 1-2) and *cdc14-1 Myc9-NET1* (*cdc14-1*, lanes 3-6) cells were grown at 25^{o}C or shifted to 37^{o}C for 3 hours, as indicated. Myc9-Net1 was immunoprecipitated from cell extracts with 9E10 antibodies, and portions of the Net1 immunoprecipitate from the 37^{o}C *cdc14-1* culture were either left untreated (lane 4), or incubated with wild type (A; lane 5) or C283S mutant (I; lane 6) GST-Cdc14 for 60 min at 30°C. All immunoprecipitates were fractionated by SDS-PAGE and immunoblotted with 9E10 to detect Myc9-Net1.

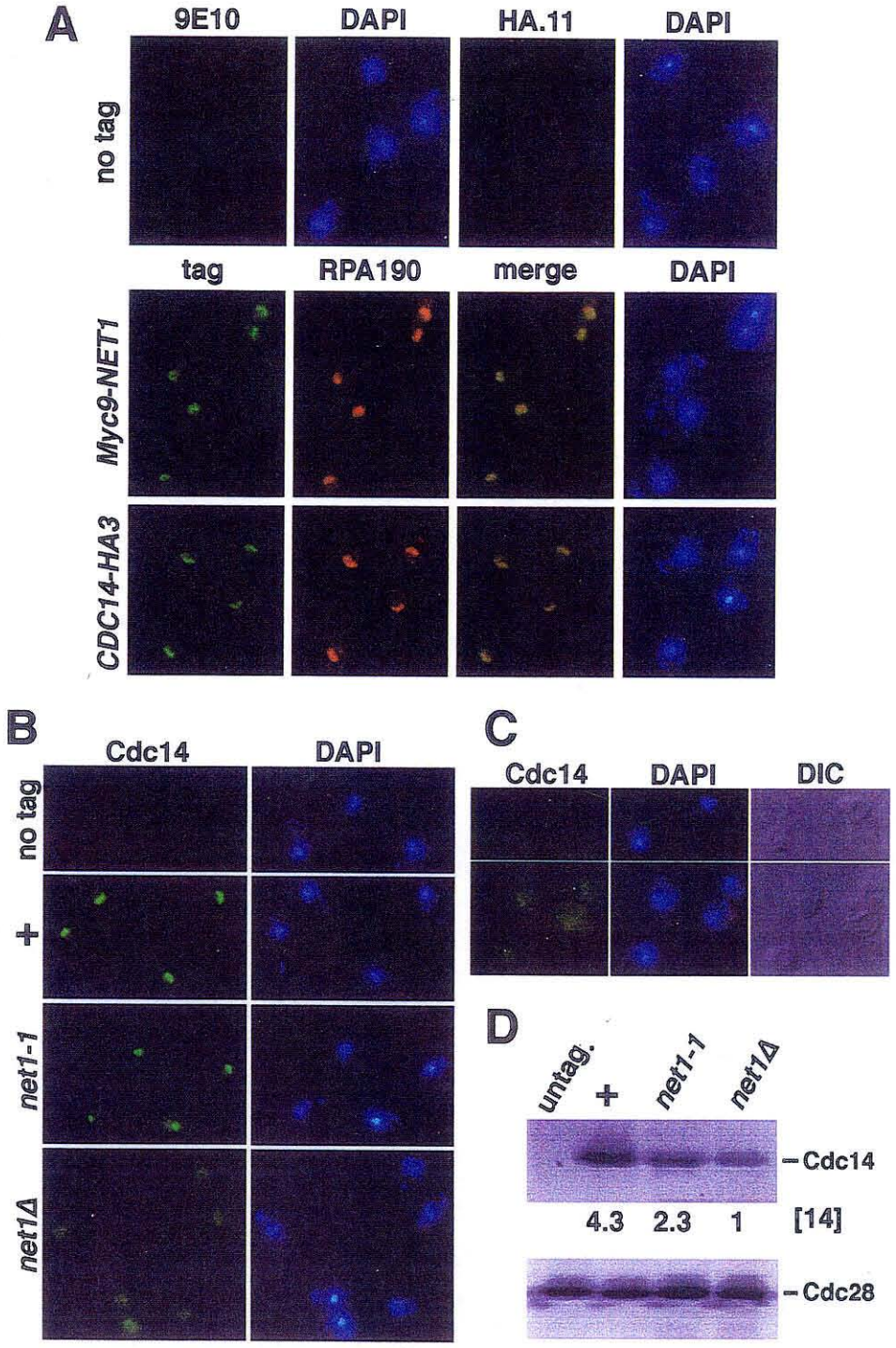
A
9E10
DAPI
HA.11
DAPI
no tag
tag
RPA190
merge
DAPI
Myc9-NET1
CDC14-HA3
B
Cdc14
DAPI
no tag
+
net1-1
net1Δ
C
Cdc14
DAPI
DIC
D
untag.
+
net1-1
net1Δ
Cdc14
4.3
2.3
1
[14]
Cdc28

Figure IV-5

Figure IV-5: Net1-dependent localization of Cdc14 to the nucleolus.

(A) Net1 and Cdc14 both localize to the nucleolus. Top row: untagged wild type cells were probed with 9E10 antibodies or anti-hemagglutinin monoclonal antibody HA.11 plus the DNA-binding dye DAPI . Center and bottom rows: cells with the indicated genotype were probed with monoclonal antibodies (9E10 or HA.11, column 1) and rabbit anti-RPA 190 antibodies (column 2). The third column shows a merge of the two antibody staining patterns in columns 1 and 2. The fourth column shows the position of nuclei, as revealed by DAPI staining.

(B) Untagged control (top row) and *CDC14-HA3* cells carrying *NET1*, *net1-1*, or *net1Δ* alleles (rows 2-4, respectively) were stained with HA.11 antibodies (column 1) and DAPI (column 2).

(C) Untagged control (top row) and *net1Δ CDC14-HA3* (bottom row) cells were stained with HA.11 antibodies (column 1) and DAPI (column 2). DIC images are shown in column 3 to reveal the outline of cells.

(D) The levels of Cdc14-HA3 and Cdc28 proteins in the indicated strains were evaluated by immunoblotting with 12CA5 antibodies. The relative levels of Cdc14-HA3 ([14]) are indicated below the top panel.

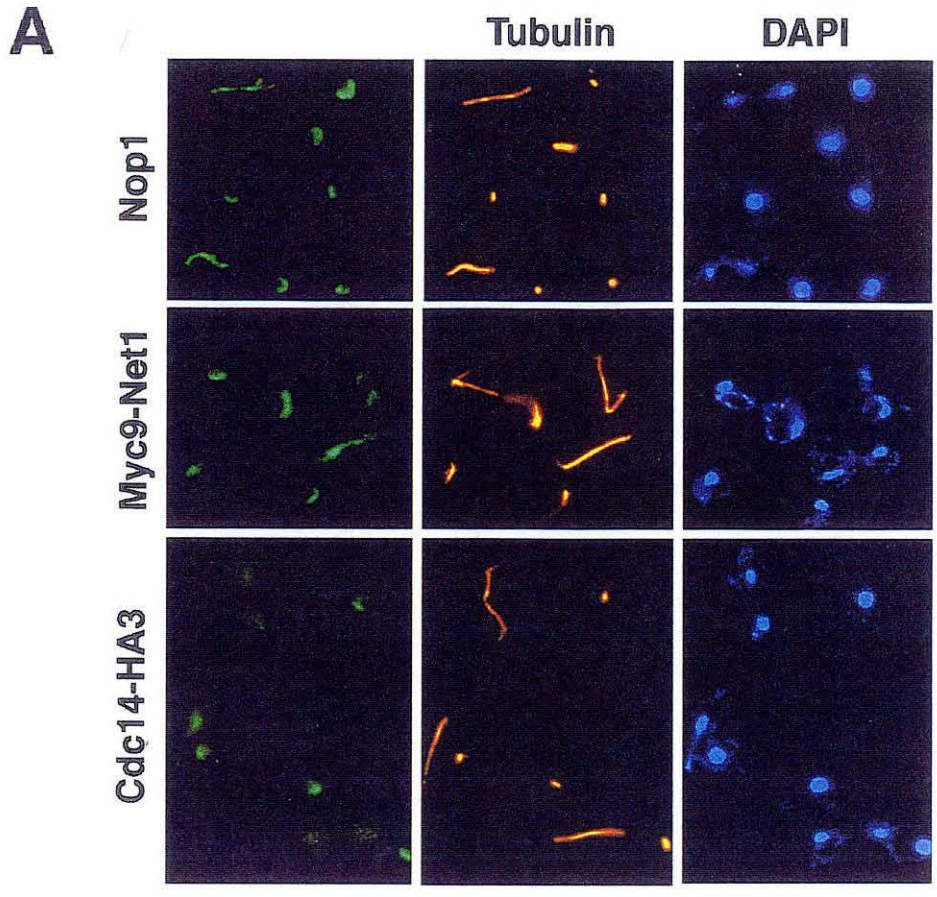

Figure IV- 6A

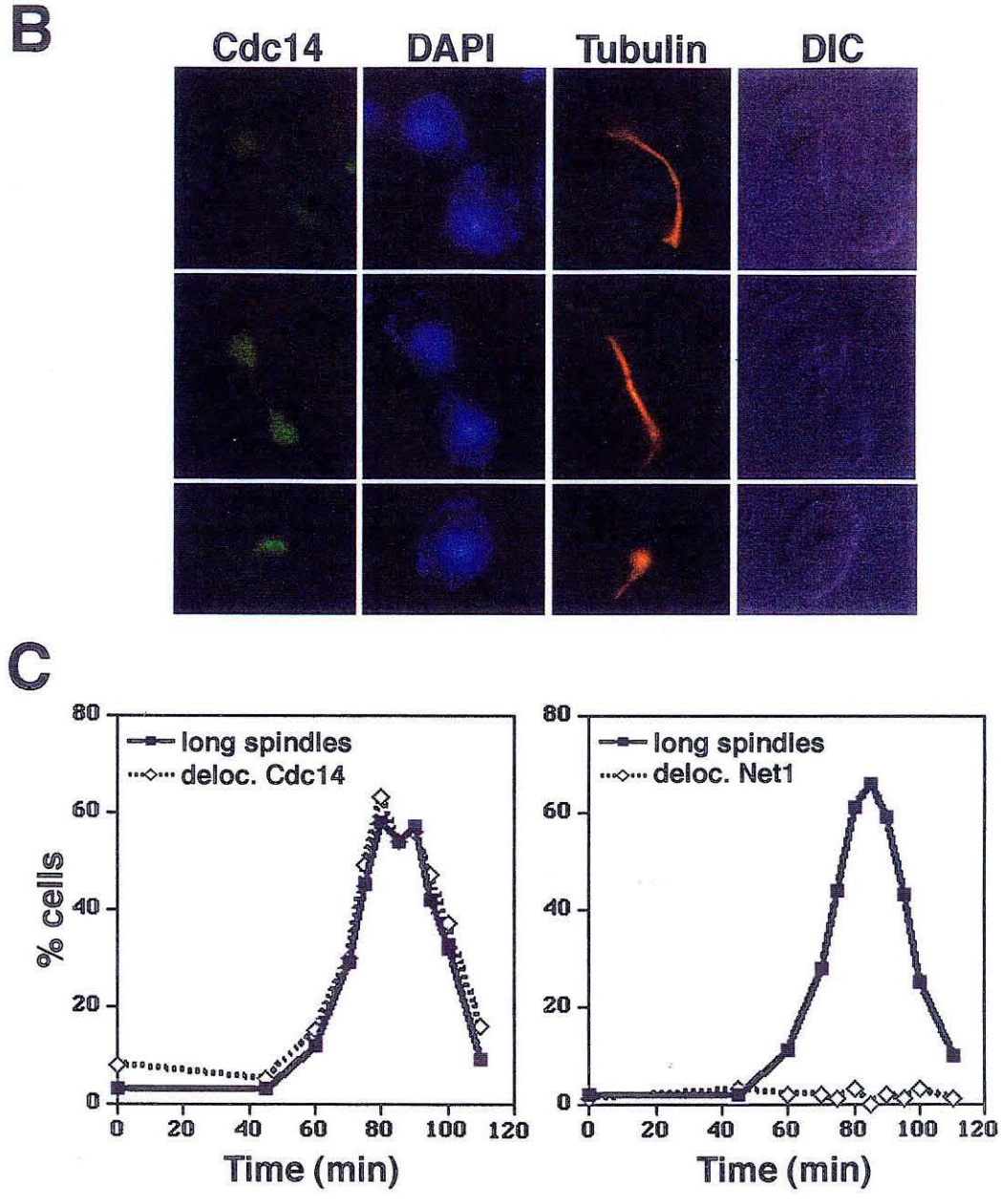

Figure IV-6. B and C

Figure IV-6: Cdc14 is released from the nucleolus during anaphase/telophase.

(A) Asynchronous *Myc9-NET1 CDC14-HA3* cells were double–labeled with rabbit anti-tubulin antibodies (column 2) and one of the following mouse antibodies (column 1): anti-Nop1 (top panel), 9E10 (center panel), or HA.11 (bottom panel). The positions of nuclei, as revealed by DAPI staining, are shown in Column 3.

(B) *CDC14-Myc9/CDC14* diploid cells were probed with 9E10, DAPI, and anti-tubulin antibodies (Columns 1-3, respectively). DIC images are shown in Column 4. Cdc14 exhibits three different types of staining patterns: delocalized over the entire nucleus (center row), or the entire cell (top row) during anaphase/telophase, or restricted to the nucleolus (bottom row) during interphase. Note the absence of extranucleolar Cdc14 in the G1 cell shown in the bottom row.

(C) *Myc9-NET1 CDC14-HA3* cells were synchronized with α factor and then released into YPD at time = 0. Samples withdrawn and fixed at the indicated time points were double labeled with anti-tubulin and either 9E10 (to detect Myc9-Net1) or HA.11 (to detect Cdc14-HA3) antibodies. For each sample, more than 200 cells were counted to calculate the percentage of cells with delocalized Cdc14 or Net1 and the percentage of cells with long spindles.

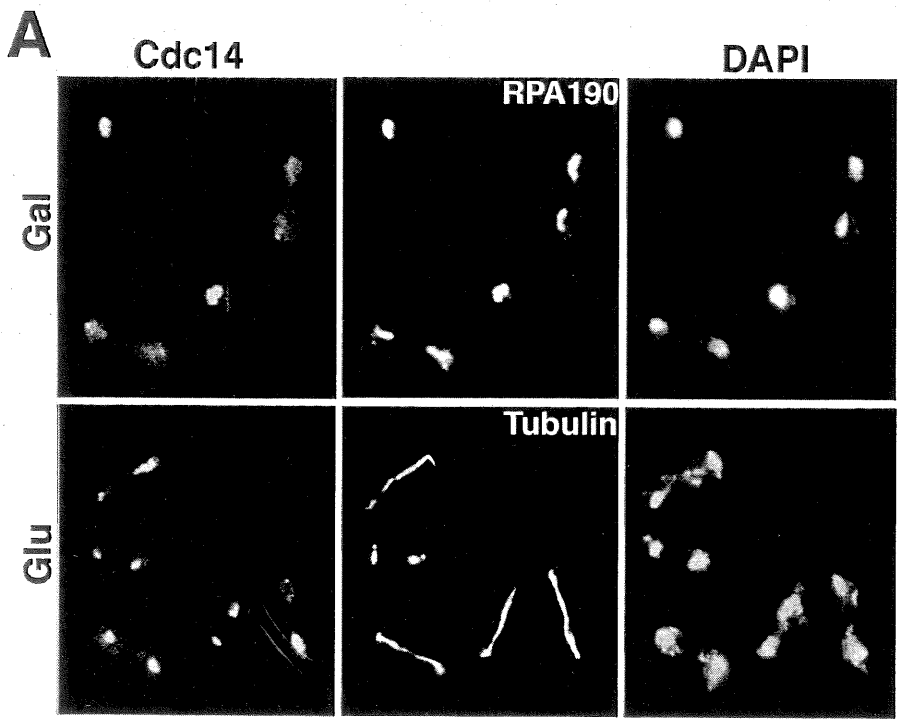

B

Strain		Growth Condition	% long spindles w/ focal Cdc14 1 focus	2 foci	Total
tem1Δ:: GAL1-UPL-TEM1	+	Gal	1.9	5.8	7.7
	+	Glu	15.1	77.4	92.5
	net1-1	Glu	5.6	55.5	61.1

Figure IV-7

Figure IV-7: Release of Cdc14 from the nucleolus requires Tem1.

(A) *tem1Δ::GAL1-UPL-TEM1 CDC14-HA3* cells grown in YPG (*TEM1* expressed) were either sampled directly (top panel) or were arrested in G1 phase with α factor, and subsequently released into YPD (*TEM1* repressed) for 3 hours (bottom panel). Cells were double–labeled with HA.11 to visualize Cdc14-HA3 (column 1) and either anti-RPA190 or anti-tubulin antibodies to visualize nucleoli or mitotic spindles, respectively (column 2).

(B) A similar block/release protocol was conducted with a *tem1Δ::GAL1-UPL-TEM1 CDC14-HA3 net1-1* strain, except that samples were processed for indirect immunofluorescence 4-6 hours after release from α-factor arrest. A longer release time was required for *net1-1* strains to progress from G1 to anaphase/telophase due to the ~2-fold longer doubling time of this mutant (W.S., data not shown). The percentages of cells with long spindles and focal Cdc14-HA3 staining were quantitated for this sample as well as the samples from panel A. More than 50 cells were counted for each sample.

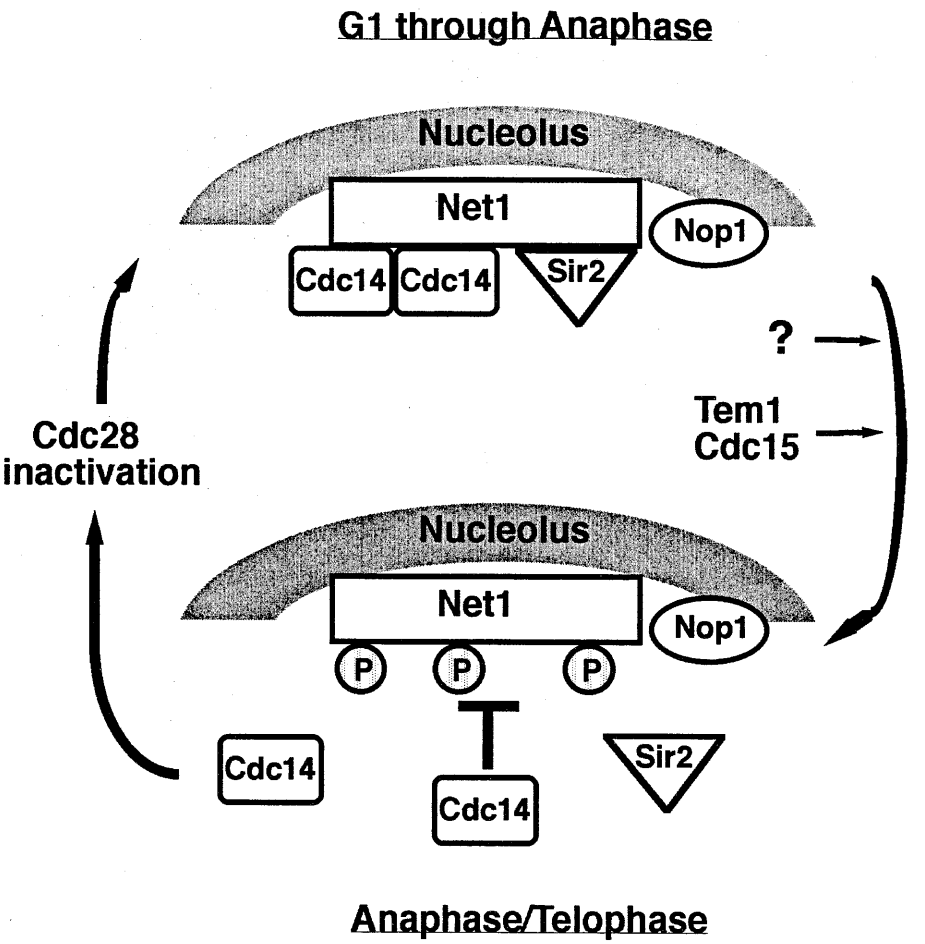
G1 through Anaphase
Nucleolus
Net1
Nop1
Cdc14
Cdc14
Sir2
?
Tem1
Cdc15
Cdc28
inactivation
Nucleolus
Net1
Nop1
P
P
P
Cdc14
Sir2
Cdc14
Anaphase/Telophase

Figure IV-8

Figure IV-8: The "RENT Control" hypothesis.

See text for details.

Chapter V. Net1 stimulates RNA Polymerase I transcription and regulates nucleolar structure independently of controlling mitotic exit

Wenying Shou, Kathleen M. Sakamoto, John Keener, Kenji W. Morimoto, Edwin E. Traverso, Ramzi Azzam, Georg J. Hoppe, R.M. Renny Feldman, John DeModena, Danesh Moazed, Harry Charbonneau, Masayasu Nomura, and Raymond J. Deshaies

(Molecular Cell, in press).

Contributions from collaborators: KS: Figs V-7D and V-6B; JK & MN: Fig V-5; KM: Figs V-3B, 6A and B; ET& HC: Fig V-7A-C, and contributed anti-Cdc14 antibodies; RA: Fig V-4B-C; GH & DM: Fig V-2A; RF: constructed Myc9-Net1 baculo-virus; JD: helped to run CHEF gels.

Summary

The RENT complex in yeast, consisting of at least three proteins (Net1, Cdc14, and Sir2), is anchored to the nucleolus by the Net1 subunit. RENT controls mitotic exit, nucleolar silencing, and proper localization of the nucleolar antigen Nop1. Here, we report two new functions of Net1. First, Net1 directly stimulates rRNA transcription. In *net1* mutants, A190, a subunit of RNA polymerase I (Pol I), is delocalized from the nucleolus, and the rate of rRNA synthesis is decreased. The temperature sensitive growth defects of *net1* mutants are suppressed by extra copies of *RRN3*, a transcriptional activator of Pol I. Furthermore, purified Net1 binds to and directly stimulates Pol I activity. Second, Net1

modulates nucleolar structure, but in a manner distinct from Sir2. In *net1* mutants, localization of multiple nucleolar antigens and morphology of rDNA are abnormal. Importantly, we show that the nucleolar and previously-described cell cycle functions of the RENT complex are distinct in that they can be uncoupled by a dominant mutant allele of *CDC14*. The independent functions of Net1 link a key event in the cell division cycle to nucleolar processes that are fundamental to cell growth.

Introduction

Unexpected links between the nucleolus and the cell cycle have been recently uncovered (reviewed by Garcia and Pillus, 1999; Cockell and Gasser, 1999). In the budding yeast *Saccharomyces cerevisiae*, the RENT protein complex regulates mitotic exit, nucleolar silencing, and Nop1 localization through its three known components: Cdc14, Sir2, and Net1 (also known as Cfi1) (Shou et al., 1999; Straight et al., 1999; Visintin et al., 1999).

The yeast nucleolus, which contains ~150 consecutive repeats of the rDNA, is the center for ribosomal RNA synthesis and ribosome assembly (reviewed in Shaw and Jordan, 1995). The chromatin structure in the nucleolus silences transcription by RNA polymerase II without interfering with highly active transcription by RNA polymerase I (Pol I) (Bryk et al., 1997; Fritze et al., 1997; Smith and Boeke, 1997). This restriction, termed "nucleolar silencing," may be the consequence of a mechanism that evolved to suppress recombination amongst rDNA repeats and thereby reduce the production of

rDNA circles which have been shown to cause cellular senescence (reviewed in Guarente, 2000). The RENT complex, tethered to the nucleolus by its core subunit Net1, influences the nucleolus in at least two ways. First, both Net1 and Sir2 are essential for nucleolar silencing, and Net1 is thought to influence rDNA chromatin in part by tethering Sir2 to the nucleolus (Straight et al., 1999). Sir2 in turn mediates silencing, suppression of recombination, and extension of longevity through its NAD-dependent histone deacetylase activity (reviewed by Gottschling, 2000; Guarente, 2000) and/or other mechanisms such as NAD breakdown and generation of O-acetyl-ADP-ribose (Tanner et al., 2000; Tanny and Moazed, 2000). Second, Net1 is required to maintain nucleolar localization of Nop1 (Straight et al., 1999), a protein implicated in pre-rRNA processing, methylation, and ribosome assembly (Tollervey et al., 1993). It is not known whether defective localization of Nop1 in *net1* cells is specific, or results from a general perturbation of nucleolar structure. Despite the key role of the nucleolus in cellular metabolism, the molecular basis for nucleolar assembly/organization and the role of Net1 in this process remain mysterious.

Besides its role in nucleolar processes, the RENT complex also controls mitotic exit. When cells exit mitosis, the mitotic exit network (MEN) triggers accumulation of the Cdk inhibitor Sic1 and degradation of B-type mitotic cyclins (Clbs), and consequently inactivation of mitotic Cdc28 (reviewed by Zachariae and Nasmyth, 1999). Members of the MEN include *TEM1*, *LTE1*, *CDC15*, *DBF2/DBF20*, *CDC5*, *CDC14*, *MOB1* (reviewed in Morgan, 1999), and *NUD1* (Gruneberg et al., 2000). Tem1 is a GTP-binding protein (Shirayama et al., 1994a); *LTE1* encodes a putative guanine nucleotide

releasing factor (Shirayama et al., 1994b); Cdc15, Dbf2/Dbf20, and Cdc5 are protein kinases (Toyn and Johnston, 1994; Hardy and Pautz, 1996; Jaspersen et al., 1998); Mob1 is a novel protein that associates with Dbf2 (Komarnitsky et al., 1998; Luca and Winey, 1998); Cdc14 is a dual specificity protein phosphatase (Taylor et al., 1997); and Nud1 binds to Bfa1 and Bub2, the two-component GAP (GTPase activating protein) for Tem1 (Gruneberg et al., 2000). When cells harboring conditional-lethal temperature sensitive (ts) mutations in any of the MEN genes are shifted to the restrictive temperature, they uniformly arrest in late anaphase as large-budded cells with segregated chromosomes, elongated spindles, and in all tested cases, elevated Cdc28 activity.

To address how the Mitotic Exit Network is organized and regulated, we previously sought *tab* (*telophase arrest bypassed*) mutants that can alleviate the essential requirement for *CDC15* and *TEM1*. One of these mutants, *tab2-1* (*net1-1*), enabled Clb2 degradation and Sic1 accumulation even in the absence of Tem1 (Shou et al., 1999). Further characterization of Net1 led us to propose the "RENT control" hypothesis: throughout most of the cell cycle, Net1 sequesters Cdc14 in the nucleolus and inhibits its phosphatase activity. As cells exit mitosis, a *TEM1/CDC15*-dependent signal leads to disassembly of the RENT complex, causing Cdc14 and Sir2 to vacate the nucleolus (Shou et al., 1999; Straight et al., 1999; Visintin et al., 1999). The evicted Cdc14 subsequently catalyzes Cdc28 inactivation (Visintin et al., 1998; Jaspersen, 1999). However, it is unknown whether release of Cdc14 from the nucleolus is sufficient to bypass *cdc15Δ* and *tem1Δ*.

In this study, we describe new functions of Net1 in the nucleolus: it directly activates synthesis of rRNA by RNA Pol I, and in addition, plays a general role in regulating nucleolar structure. The perturbed nucleolar structure in *net1-1* cells raises the possibility that mislocalized nucleolar proteins other than Cdc14 could cause or contribute to the *cdc15Δ* bypass phenotype. Characterization of a second *tab* locus, *TAB6-1,* proves this possibility unlikely and provides key support to the RENT control hypothesis. *TAB6-1* is a dominant allele of *CDC14* that bypasses *cdc15Δ* and *tem1Δ* without perturbing nucleolar structure or Pol I function. Thus, the release of Cdc14 from the nucleolus is sufficient to trigger mitotic exit in the absence of MEN proteins, and the role of RENT in cell cycle control can be uncoupled from its roles in maintenance of nucleolar integrity and Pol I transcription.

Results

RRN3 suppresses temperature sensitivity of net1 mutants

NET1 has been implicated in three potentially distinct cellular processes: mitotic exit, nucleolar silencing, and proper localization of the nucleolar antigen Nop1 (Shou et al., 1999; Straight et al., 1999; Visintin et al., 1999). *net1-1* cells grow slowly and *net1Δ* cells fail to grow at 37^{0}C, which could result from improper mitosis, an abnormal nucleolus, or defects in some other unknown functions of *NET1*. To distinguish between these possibilities, we screened a CEN/ARS based yeast genomic library to identify genes that rescued the temperature sensitive (ts) growth defect of *net1-1*. In addition to

NET1, this effort yielded *RRN3* (Fig. 1A; see Experimental Procedures), a transcription activator for RNA polymerase I (Pol I) (Yamamoto et al., 1996). Strikingly, centromeric plasmids containing *NET1* (*[NET1]*) or *RRN3* (*[RRN3]*) driven by their respective native promoters rescued the temperature sensitivity of *net1Δ* to similar extents (Fig. V-1B). The level of Rrn3 protein in *net1* mutants was not diminished at 25°C or 37°C (Fig. V-1C), suggesting that the ts growth defects of *net1* mutants did not result from reduced amounts of Rrn3.

It is unlikely that *RRN3* suppressed the growth defect of *net1* mutants by restoring nucleolar silencing, because lack of silencing in *sir2Δ* does not affect growth. It is also unlikely that suppression involved mitotic exit, since in the presence of *[RRN3]*, *net1-1* still bypassed *cdc15Δ* (WS, data not shown). Nop1, a protein involved in pre-rRNA processing and ribosome assembly, is delocaized from the nucleolus in *net1Δ* cells (Straight et al., 1999). Although it is not known whether delocalization of Nop1 impedes cell growth, we tested whether the *RRN3* plasmid affected Nop1 localization in *net1* mutants. Whereas Nop1 assumed a characteristic nucleolar localization pattern (a crescent-shaped structure abutting the nucleus) in 98% of wild type cells, only 17% of *net1-1* cells showed significant or complete Nop1 localization to the nucleolus at 37°C (Fig. V-1D). However, this fraction was increased to 64% by the *RRN3* plasmid (Fig. V-1D). Similarly, the fraction of cells with significant or complete localization of Nop1 to the nucleolus was increased from 9% in *net1Δ* to 46% in *net1Δ [RRN3]* at 25°C (Fig. V-1D). Thus, *RRN3* on a centromeric plasmid partially restored correct Nop1 localization

in *net1* mutants, suggesting that the growth defect of these mutants arose from a disruption of nucleolar structure and function.

rRNA synthesis is reduced in net1-1

Given that extra Rrn3, a transcription factor for Pol I, suppressed the ts growth defect of *net1* mutants, a key function of Net1 might be to sustain Pol I activity. To test this hypothesis, we evaluated rRNA and actin mRNA accumulation in *net1-1* mutants by ethidium bromide staining and Northern blotting, respectively. The level of rRNA in *net1-1* cells at 37^{0}C, normalized to actin mRNA, was reduced by ~40% compared to that in wild type cells (Fig. V-2A). In contrast, both *sir2Δ* and *cdc14-1* mutants displayed normal levels of rRNA (Fig. V-2A).

The reduced level of rRNA in *net 1-1* could result from a reduced rate of transcription, defective processing of pre-rRNA, or increased rate of degradation. To distinguish between these possibilities, we performed pulse-chase experiments using [^{3}H]-methionine which has the advantage of being rapidly incorporated into rRNA through methylation and even more rapidly chased (Warner, 1991). *net1* mutants did not exhibit a major defect in 35S, 27S and 20S pre-rRNA processing (Fig. V-2B, lower panel), even though known rRNA processing factors (e.g., Nop1) are partially mislocalized. However, the *net1* mutants incorporated much less [^{3}H]-methionine (Fig. V-2B, lower panel; note the 7 -fold longer exposure time for *net1Δ*), which could result from reduced rRNA methylation or transcription. We therefore repeated the pulse-chase experiment using [^{3}H]-uracil, and adjusted exposure time such that the labeling of tRNA

(synthesized by Pol III) was approximately equivalent. In *net1* mutants, 25S and 18S rRNA transcripts were produced at a slower rate (Fig. V-2C, lower panel; quantitation in Fig. V-2D). The slow-growth phenotype of *net1Δ* cells is not uniform and is unstable: the two *net1Δ* spores from a single tetrad frequently display unequal growth rates; upon subculturing, *net1Δ* cells always display less aberrant cell morphology and acquire an improved growth rate. Thus, it is possible that *net1Δ* cells accumulate second site mutations more effeciently than *net1-1*, or acquire more rDNA repeats to compensate for the severe reduction in rRNA synthesis. This may explain the less severe phenotype of *net1Δ* compared with *net1-1* (Fig. V-2C, D). Nevertheless, *net1* mutants suffer from a significantly reduced rate of rRNA synthesis compared with wild type cells.

Net1 retains the A190 subunit of Pol I in the nucleolus

Reduced transcription of rRNA is indicative of diminished activity of the Pol I transcriptional machinery in *net1* mutants, which could result from reduced protein levels, mislocalization, or inactivity of Pol I itself. To compare the levels of Pol I, wild type and *net1* cell extracts were immunoblotted with antibodies against the A190 catalytic subunit. Whereas the level of A190 was slightly reduced in *net1Δ*, it was normal in *net1-1* cells (Fig. V-3E, top panel), suggesting that although Net1 helps to sustain normal levels of Pol I, Pol I levels alone can not account for the reduced rRNA transcription in *net1-1*. To test whether Pol I failed to localize properly to the nucleolus in *net1* mutants, we probed for the localization of A190 by indirect immunofluorescence.

Whereas A190 displayed a characteristic nucleolar staining pattern in wild type cells, it was partially delocalized in *net1-1* and *net1Δ* mutants (Fig. V-3A).

Because Net1 was required for the proper localization of both A190 and Nop1, we asked if Net1 physically associates with them. Extract prepared from *MYC9-NET1* cells was purified on 9E10 antibody resins, and bound proteins were detected by immunoblotting. Besides Sir2 (not shown; Straight et al., 1999), A190 but not Nop1 was specifically recovered in association with Myc9-Net1 (Fig. V-4A, lanes 3 and 4). Mass spectrometry-based sequencing of Net1-associated proteins confirmed that other subunits of Pol I co-immunoprecipitated with Net1, suggesting that Net1 binds the intact Pol I holoenzyme (RA and A. Shevchenko, unpublished data).

To determine whether Net1 binds directly to Pol I, we attempted to reconstitute the association of these proteins *in vitro*. His6-Myc9-Net1 was expressed in insect cells, and purified on a nickel affinity column. The purified protein was functional because it bound GST-Sir2 (Fig. V-4B) and GST-Cdc14 (RA and WS, data now shown). HA epitope-tagged, purified Pol I complexes also efficiently captured His6-Myc9-Net1 (Fig. V-4C. Lanes 3 and 4). This observation indicates that Pol I bound directly to the Net1 subunit of RENT.

Net1 stimulates Pol I activity in vitro

To test if Net1 could directly activate Pol I, we further purified His6-Myc9-Net1 on SP- and Q-sepharose columns, resulting in a preparation with >90% purity (Fig. V-5A). Highly purified Net1 was added to a standard transcription reaction that contained

linearized rDNA template, 10-15 nM Pol I, Rrn3, TBP (TATA-binding protein), UAF (upstream activating factor), and CF (core factor) at much lower concentrations (Keener et al., 1998). The amount of [^{32}P]-labeled runoff transcripts (arrow in Fig. V-5B) increased as a function of input Net1 (Fig. V-5B and C), with the maximum stimulation being slightly more than four-fold. Furthermore, maximum stimulation occurred at a concentration of Net1 that was approximately equimolar with Pol I (and much greater than UAF or CF). Taken together, our data indicate that Net1 is required for optimal activity of RNA Pol I, both *in vivo* and *in vitro*.

Nucleolar structure is perturbed in net1 mutants

The failure of Cdc14, Sir2, and Pol I to localize properly to the nucleolus in *net1Δ* (Shou et al., 1999; Straight et al., 1999; Visintin et al., 1999; Fig. V-3A) could be explained by the fact that they all directly bound Net1 (Traverso et al., 2001; Fig. V-4B and C). In contrast, delocalization of Nop1 in *net1* mutants (Fig. V-3B) is harder to explain given that Nop1 did not stably associate with Net1 (Fig. V-4A). The simplest model predicts that Net1 directly or indirectly influenced nucleolar structure which in turn dictated the localization pattern of Nop1 and possibly other nucleolar proteins.

To test this model, we examined the localization patterns of two additional nucleolar proteins in various mutants using indirect immunofluorescence. Nop2 (de Beus et al., 1994) exhibited a nucleolar staining pattern in wild type and *net1-1* but not *net1Δ* cells (Fig. V-3C, top three rows). Mislocalization of Nop2 in *net1Δ* was not due to increased levels of this protein (Fig. V-3E, bottom panel). In contrast, the localization

pattern of Fpr3 (Benton et al., 1994) was altered in a different way in both *net1* mutants: despite near equivalent levels of Fpr3 in all strains examined (Fig. V-3E, bottom panel), the staining area of Fpr3 appeared to be smaller in *net1* mutants than in wild type cells (Fig. V-3D, compare Rows 2 and 3 with Row 1).

The abnormal localization patterns of most nucleolar proteins examined so far in *net1* mutants led us to examine whether the organization of rDNA itself was perturbed in these cells. Cells were arrested in mitosis with nocodazole, and subjected to fluorescence in situ hybridization (FISH) (Guacci et al., 1994). Whereas wild type cells displayed line-shaped rDNA that appeared to be spooled away from the focus of DAPI staining, the majority (93%) of *net1-1* cells possessed more condensed rDNA semicircles that abutted directly against the DAPI-stained material (Fig. V-3F, compare Rows 1 and 3). *net1Δ* cells did not arrest well in nocodazole, but they showed similar rDNA morphology as *net1-1* (data not shown), suggesting that Net1 is not an essential determinant of the unusual chromatin structure observed in rDNA. Thus, in *net1* mutants, localization patterns of multiple nucleolar antigens as well as rDNA morphology are altered, although rDNA still congregates to a structure distinct from the bulk DNA.

net1 and sir2 mutations have distinct effects on the nucleolus

Sir2 plays an important role in the nucleolus by suppressing intrachromosomal recombination within the rDNA repeats (Gottlieb and Espostito, 1989) and silencing transcription by Pol II (Bryk et al., 1997; Fritze et al., 1997; Smith and Boeke, 1997). Because Net1 tethers Sir2 to rDNA (Straight et al., 1999), all the phenotypes observed for

net1 could, in theory, have been caused by loss of Sir2 function within the nucleolus. However, this is clearly not the case, because *net1* cells had either distinct or more severe phenotypes than *sir2Δ* in all assays that were conducted. First, unlike in *net1* mutants, accumulation of rRNA was normal in *sir2Δ* (Fig. V-2A). Second, A190, Nop1, Nop2, and Fpr3 displayed normal (or nearly normal) nucleolar localization patterns in *sir2Δ* (Fig. V-3A-D). Third, rDNA in *sir2Δ* cells, as revealed by FISH, displayed considerable heterogeneity, and seemed to be less compact than that in wild type or *net1-1* cells (Fig. V-3F). Thus, Net1 and Sir2 regulated nucleolar structure and function in distinct ways.

The TAB6-1 allele of CDC14 bypasses tem1Δ and *cdc15Δ*

The pleiotropic defects of the nucleolus in *net1* mutants add a confounding twist to the RENT control hypothesis. We originally proposed that Tem1-dependent disassembly of the RENT complex and the subsequent release of Cdc14 from the nucleolus drive cells from mitosis to interphase. *tem1Δ* and *cdc15Δ* cells arrest in late mitosis, but the *net1-1* mutation (also known as *tab2-1* for *telophase arrest bypassed*) enables these cells to exit mitosis, presumably by allowing Cdc14 to escape the nucleolus (Shou et al., 1999). However, given the profound disruption of nucleolar structure in *net1-1* cells, it is also possible that displaced nucleolar proteins other than Cdc14 caused or contributed to the *tem1Δ* and *cdc15Δ* bypass phenotype.

To test the RENT control hypothesis rigorously, we sort to identify a mutant form of Cdc14 with reduced binding affinity for Net1. If our hypothesis is correct, two predictions can be made for this mutant: 1. like *net1-1*, it should be a *tab* mutant, because

both mutations should allow ectopic release of Cdc14 from the nucleolus; 2. the *tem1Δ* and *cdc15Δ* bypass phenotype should be dominant. Based on this reasoning, we tested dominant mutants recovered in our earlier *tab* screen, and found that the dominant *TAB6-1* mutation demonstrated tight linkage to *CDC14* (zero recombinants in 30 spores tested). Importantly, cloned *CDC14* sequence amplified from *TAB6-1*, but not wild type cells, allowed bypass of *tem1Δ* (Fig. V-6A), confirming that *TAB6-1* is allelic to *CDC14*. The *TAB6-1* allele contained a Pro (116) -> Leu mutation in *CDC14* (Fig. V-6B). Pro116 is conserved in Cdc14 homologs in *Drosophila* and *S.pombe* (CG7134 and SPAC1782.09c, respectively) (Fig. V-6B), but not in *C.elegans*, *M. musculus*, or *H. sapiens*.

$Cdc14^{TAB6}$ has reduced affinity for Net1, which renders Clb5 essential for cell viability

To properly interpret the phenotype of *TAB6-1* cells, it is important to understand the molecular mechanism by which *TAB6-1* bypassed *tem1Δ* and *cdc15Δ*. In *net1-1* mutants, bypass of the anaphase arrest that normally occurs upon depletion of Tem1 is accompanied by ectopic Clb2 degradation and Sic1 accumulation (Shou et al., 1999). *TAB6-1* cells behaved similarly to *net1-1* cells upon depletion of Tem1 (Fig. V-6C, compare Lanes 8-14 (*TAB6-1*) with Lanes 1-7 (+)). Moreover, like *net1-1*, *TAB6-1* bypassed anaphase arrest in almost all cells, since Clb2 degradation proceeded to near completion in Tem1-depleted cells (Fig. V-6C). Based on the similarity of their *tab* phenotypes, we conclude that *net1-1* and *TAB6-1* most likely bypassed *cdc15Δ* by related mechanisms. To address whether *TAB6-1*, like *net1-1*, compromised the stability of RENT, we evaluated the Net1-binding and enzymatic activity of Cdc14 and $Cdc14^{TAB6}$.

Whereas purified Cdc14^{TAB6} had nearly wild type levels of phosphatase activity towards p-nitrophenyl phosphate and tyrosine-phosphorylated myelin basic protein (Fig. V-7A), it was bound less efficiently (Fig. V-7C) and was ~14-fold less sensitive to inhibition (Fig. V-7B) by a purified N-terminal fragment (amino acids 1-600) of Net1 which has been shown to bind and inhibit Cdc14 (Traverso et al., 2001). Similarly, Cdc14^{TAB6}, but not Sir2, was less efficiently recovered in association with Myc9-Net1 upon immunoprecipitation of the RENT complex from yeast cell extracts (Fig. V-7D). These data imply that the P116L substitution allowed bypass of *cdc15Δ* and *tem1Δ* by reducing the affinity of Cdc14^{TAB6} for Net1.

Unexpectedly, *TAB6-1* cells grew robustly at 25°C (Fig. V-7E), even though loss of temporal control over Cdc14 activity would be expected to perturb cell division and growth. Interestingly, whereas *TAB6-1 clb2Δ* cells were viable, *TAB6-1 clb5Δ* was lethal (Fig. V-7F), suggesting that in the absence of the opposing activity of Clb5/Cdc28 (Shirayama et al., 1999), proper control of Cdc14 becomes essential for cell viability.

Cell cycle control and nucleolar functions of RENT complex can be uncoupled by the TAB6-1 allele of CDC14

Whereas both the *net1-1* and *TAB6-1* mutations destabilized the RENT complex and efficiently bypassed *tem1Δ*, *TAB6-1* cells grow much better than *net1-1* cells (Fig. V-7E). *CDC14^{TAB6}* cells appeared to have a normal nucleolus by three distinct criteria: the localization patterns of A190, Nop1, Nop2, and Fpr3 (Fig. V-3A - D), the morphology of rDNA (Fig. V-3F), and the levels of rRNA accumulation (Fig. V-2A) were all

indistinguishable in *TAB6-1* and wild type cells. These observations imply that regulation of the nucleolar processes by Net1 was significant to cell growth, that bypass of *cdc15Δ* and *tem1Δ* by *TAB6-1* was not sustained by a general perturbation of nucleolar structure, and that ectopic release of Cdc14 from the nucleolus was sufficient for bypass. These data further imply that the nucleolar defects of *net1* mutants were not caused by weakened interaction between Net1 and Cdc14. Thus, $CDC14^{TAB6\text{-}1}$ uncoupled the cell cycle and nucleolar functions of the RENT complex by affecting the former without interfering with the latter.

Discussion

The Net1 subunit of RENT complex directly stimulates transcription by Pol I

The RENT complex, consisting of at least three proteins (Net1, Cdc14, and Sir2), controls mitotic exit, mediates nucleolar silencing, and sustains proper localization of Nop1 (Shou et al., 1999; Straight et al., 1999; Visintin et al., 1999). The first two functions of RENT are well-documented, and derive from the ability of Net1 to tether both Cdc14 and Sir2 to the nucleolus, respectively. Besides these phenotypes, we show here that *net1* mutants also exhibit delocalization of the A190 subunit of RNA Pol I, a decreased rate of rRNA synthesis, and a reduced level of rRNA accumulation. The role of Net1 in RNA Pol I-dependent rDNA expression is likely to be distinct from the nucleolar silencing and cell cycle control functions of RENT, because $cdc14^{ts}$ and *sir2Δ* mutants do not exhibit defects in accumulation of rRNA. A simple model accommodating our data is that Net1 promotes expression of rDNA by helping to tether

Pol I within the nucleolus. This hypothesis is supported by three lines of evidence. First, a Pol I subunit co-immunoprecipitates with Net1 from cell extracts. Second, purified Net1 binds purified Pol I *in vitro* and stimulates its activity at near equimolar ratio. Third, an additional copy of *RRN3*, which encodes an RNA Pol I promoter recruitment factor, is sufficient to suppress the temperature sensitive growth of both *net1-1* and *net1Δ* mutants. A more detailed mechanistic understanding of how Net1 promotes Pol I action awaits further biochemical studies.

Role of Net1 in global nucleolar structure

Two proteins (Sir2 and Cdc14) and one protein complex (Pol I) that bind directly to Net1 are delocalized in *net1* mutants. However, Nop1, which does not bind stably to Net1, is also delocalized in *net1* mutant cells. Thus, in addition to serving as a direct nucleolar tether, Net1 appears to regulate indirectly the sequestration of other nucleolar proteins. Both Nop1 and Nop2 are involved in pre-mRNA processing (Tollervey et al., 1993; Hong et al., 1997). The exclusive localization of rRNA processing factors Nop1 and Gar1 to the nucleolus depends upon continuous transcription of rDNA (Trumtel et al., 2000). Hence, we propose that Nop1 and Nop2 become delocalized in *net1Δ* mutants in part due to decreased synthesis of rRNA (note that Nop2 localization is normal in *net1-1*, but diffused in *net1Δ*, suggesting that the *net1-1* allele retains partial function). Supporting this proposal, *RRN3* suppression of *net1*, presumably involving stimulation of Pol I transcription (Yamamoto et al., 1996; Keener et al., 1998), correlates with partial restoration of Nop1 nucleolar localization (Fig. V-1D). Intriguingly, in *net1* cells, the

nucleolar protein Fpr3 retains a focal, albeit more compact localization, resembling the morphology of *net1-1* rDNA. A similar compaction has been reported for the 'nucleolar remnant' visualized by electron microscopy upon thermal inactivation of RNA Pol I (Trumtel et al., 2000). Thus, we suggest that Fpr3 is recruited to the nucleolus by a Net1- and transcription- independent pathway.

Although the nucleolar defects of *net1* cells are likely to arise in part due to diminished Pol I activity and dispersion of Sir2, it seems probable that Net1 serves additional functions within the nucleolus. This prediction is based on four observations. First, the overall growth defect and thermosensitive phenotypes of *net1* mutants are partially corrected by *RRN3*, but are not alleviated by ectopic expression of rDNA by Pol II at a level sufficient to support growth of cells lacking a subunit of Pol I (J. Claypool and WS, data not shown). Second, chromatin IP experiments indicate that Net1 decorates the entire rDNA sequence and is not restricted to the promoter region (Straight et al., 1999). Indeed, Net1 still localized to the altered nucleolus in a *rrn5Δ PSW* (polymerase switched) strain in which Pol II instead of Pol I transcribes rDNA (I. Siddiqi, M. Oakes, and MN, unpublished data; for PSW strains, see Oakes et al., 1999). These observations suggest that Net1 "coats" rDNA and regulates its structure in the presence or absence of the Pol I transcriptional machinery. Third, *rrn5Δ PSW* cells are viable when Pol I is inactivated, but are inviable in combination with *net1Δ* (I. Siddiqi and MN, unpublished results). Fourth, the morphologies of rDNA in *net1-1* and *sir2Δ*, as judged by FISH analysis, are clearly distinct, suggesting that *SIR2* alone can not account for *NET1* functions. On the other hand, loss of Sir2 function may account for the perturbation of

rDNA copy number control that we observed in *net1* mutants. Chromosome XII ran as a smear in *net1Δ* cells (WS, JD, and M. Oakes, unpublished results), possibly due to increased recombination among rDNA repeats upon delocalization of Sir2 (Gottlieb and Esposito, 1989).

TAB6-1 uncouples nucleolar and cell cycle functions of RENT complex

net1-1 was originally isolated as a bypass suppressor of *cdc15Δ*, and was subsequently shown to also bypass *tem1Δ*, presumably because the *net1-1* mutation allows Cdc14 to be released from the nucleolus during anaphase in a Tem1/Cdc15-independent manner (Shou et al., 1999). However, the exact mechanism of bypass is obscured by the pleiotropic nucleolar defects of the *net1-1* mutant. The possibility that the release of some nucleolar protein other than Cdc14 is responsible for *tem1Δ* bypass was instigated further by the observation that two other recessive *tab* mutants (*tab1*, *tab4*) exhibited defects in nucleolar integrity (KS and WS, unpublished data). Furthermore, it is unclear if the severe growth defect of *net1Δ* and *net1-1* (Shou et al., 1999; Straight et al., 1999) arises from loss of the cell cycle or nucleolar functions of Net1.

The identification of the *TAB6-1* allele of *CDC14* allowed us to begin to address how the cell cycle and nucleolar functions of RENT are related (Fig. V-8). Like *net1-1*, *TAB6-1* destabilizes the interaction between Net1 and Cdc14. Both *TAB6-1* and *net1-1* efficiently bypass cell cycle arrest in Tem1-depleted cells, presumably because free Cdc14 enables ectopic degradation of Clb2 and accumulation of Sic1. Unlike *net1-1* mutants, there are no obvious general defects in nucleolar organization or function in

TAB6-1 mutants, as judged by the localization patterns of Nop1, Nop2, Fpr3, and A190, the morphology of rDNA, the number of rDNA repeats (WS and JD, data not shown), and the level of rRNA accumulation. Thus, the more severe growth phenotype observed in *net1* mutants is likely due to defective nucleolar functions rather than cell cycle functions. Furthermore, by affecting cell cycle functions without perturbing nucleolar functions of the RENT complex, *TAB6-1* confirms that release of Cdc14 from RENT is sufficient to trigger mitotic exit in *cdc15Δ* cells.

Acknowledgements

We thank R. Verma, T. Powers, M. Oakes, J. Claypool, and B. Hay for discussions; D. Chan, W. Dunphy, B. Hay, H. Rao, R. Lipford, R. Verma, D. Mohl, and S. Schwarz for critical reading of the manuscript; H. Mountain and P. Philippsen for *pMET3* and *S.pombe his5*$^{+}$ plasmids; F. Cross and M. Shirayama for *clb5Δ::URA3* strains; D. Koshland and V. Guacci for DIG-labeled FISH probes and detailed FISH protocols; C. Thompson for yeast genomic library; and J. Aris, J. Thorner, and D. Kellogg for antibodies against Nop1, Nop2, Fpr3, and Clb2. W.S. was a Howard Hughes Medical Institute predoctoral fellow. This work was supported by a Beckman Foundation Young Investigator Award (to RJD), NIH grants GM59940 (to RJD), GM35949 (to MN), CA59935 (to HC), and an Ellison Medical Foundation grant (to DM).

Experimental Procedures

Isolation of RRN3 as a low-copy suppressor of net1-1

The *net1-1* mutant strain was transformed with plasmid libraries harboring yeast genomic DNA fragments, and incubated at 25°C for one day before being shifted to 37°C. Low copy CEN/ARS - based libraries constructed by the laboratories of P. Heiter (ATCC#77164), and R. Young (Thompson et al., 1993) yielded a *net1-1* complementing activity from Chromosome XI, 206,300 – 210, 665. Each open reading frame in this genomic region was amplified by PCR from yeast genomic DNA and tested for its ability to complement the temperature sensitivity of *net1-1*. The complementing activity resided in *RRN3*.

RNA isolation and Northern blot

Cells grown in 12 ml YPD at 23°C, to an OD_{600} of about 0.8, were shifted to 37°C for 3 hrs. Cell pellets were resuspended in 1 ml buffer (50 mM sodium acetate, 10 mM EDTA, 0.1% SDS), and RNA was extracted with 1ml of phenol, followed by 1ml of phenol/chloroform (1:1) by incubation at 65°C for 4 min, followed by 4 min on ice. Extracted RNA was precipitated with ethanol, and 5 μg RNA per lane was fractionated on a 1.5% agarose gel containing formaldehyde. Quantification of ethidium bromide stained bands was done using the Alpha Image 2000 system. Northern blotting was performed using 10X SSC buffer (1.5 M NaCl, 150 mM sodium citrate) onto a Duralon-UV membrane (Stratagene). After UV-crosslinking with a Stratalinker (Stratagene), the

membrane was incubated in hybridization buffer (1% BSA, 1 mM EDTA, 0.5 M NaHPO4, pH 7.2, 7% SDS) at 65°C overnight (Church and Gilbert, 1984). The actin probe was generated by PCR using primers CCAATTGCTCGAGAGATTTCT and AGTGATGACTTGACCATC. Random priming was performed with the Megaprime DNA labeling system (Amersham) following the manufacturer's protocol. The membrane was washed ten times with hybridization buffer and once with 2X SSC/0.1% SDS before exposure to a BioRad Phosphorimager screen. Quantification was done on a Quantity One Phosphorimager (BioRad).

Pulse-chase labeling of rRNA

Pulse-chase labeling and analysis of rRNA was carried out essentially as described (Udem and Warner, 1972; Warner, 1991; Powers and Walter, 1999). For [C-$^3H_3$]-methionine labeling experiments, cultures were grown in SD -methionine at 25°C to OD_{600} = 0.2-0.3, and incubated at 37°C for 3 hours. Cultures were adjusted to 8 ml of OD_{600} = 0.4, supplemented with 320 μl of [C-$^3H_3$]-methionine (1 mCi/ ml, New England Nuclear Life Sciences), and incubated at 37°C for 5 min. At the end of incubation, 1.56 ml of the culture was transferred to an Eppendorf tube (chase time = 0). 200 μl of unlabeled methionine (100 mM) was added to the rest of culture, and after 3, 6, 15, and 30 min of chase time, samples (1.6 ml) were retrieved. All samples were immediately centrifuged (Eppendorf), and cell pellets drop-frozen in liquid N_2. Uracil labeling was performed identically except that cells were grown in SD-uracil, and that 7.5 ml of

culture was labeled with 165 μl of [^{3}H] uracil (1 mCi/ml) and chased with 1/10 volume of unlabeled uracil (3 mg/ml). RNA was extracted with hot phenol method, isopropanol precipitated, and resuspended in 6 μl of H_2O, of which 0.5 μl was analyzed in a scintillation counter and the rest was fractionated on a 6.7% formaldehyde and 1.5% agarose gel. The gel was soaked in Enhance (Dupont) overnight, dried under medium heat and vacuum, and exposed to film with an enhancer screen at –80°C for 1 – 4 days.

Purification of full length Net1 and in vitro transcription assay

His6-Myc9-Net1 was expressed in Hi5 insect cells, and purified using a nickel affinity column as described (Shou and Dunphy, 1996). Eluted protein was dialyzed in 20 mM Tris-Cl pH 7.9, 20% glycerol, 0.05% Tween-20, 1 mM DTT, 50 mM KCl. It was then applied to a 1 ml SP-sepharose cartridge (Pharmacia), and eluted with a 48 ml salt gradient from 50 mM to 1 M KCl in the above buffer at 0.25 ml/min. Net1 eluted around 200 mM KCl. Peak fractions were applied to a 1 ml Q-sepharose cartridge (Pharmacia) and eluted with a 9 ml salt gradient from 50 mM to 1 M KCl in the above buffer at 0.25 ml/min. Net1 eluted at 300 mM KCl. Peak fractions were concentrated about four-fold using a Microcon 30 concentrator (Amicon) according to the manufacturer's instructions, and assayed for activity. *In vitro* transcription was carried out essentially as described previously (Keener et al., 1998). Present in all the reactions were: 0.2-0.4 nM wild type linear template (extending 210 bp upstream of the +1 start site), Rrn3 (2-6 nM) -Pol I (10-15 nM) complex, and much smaller amounts of UAF, TBP, and CF (Keener et al., 1998).

Purification and analysis of Net1(1-600), Cdc14 and Cdc14^{TAB6}

GST-Cdc14 and GST-Cdc14^{TAB6} were purified from *E. coli* using glutathione-Sepharose beads (Traverso et al., submitted). Net1(1-600)-His$_6$ was purified from *E. coli* on His-bind resin (Novagen) (Traverso et al., submitted). Phosphatase assays were performed in buffer P (50 mM imidazole pH 6.6, 1 mM EDTA, 1 mM DTT, 0.5 mg/ml bovine serum albumin) at 30°C using 20 mM *p*-nitrophenyl phosphate or 4 μM myelin basic protein phosphorylated on tyrosines (Tyr-P-MBP) (Taylor et al., 1997). The ability of purified Net1(1-600)-His$_6$ to inhibit GST-Cdc14 and GST-Cdc14^{TAB6} was assessed in phosphatase assays performed at 30°C with 10 nM enzyme and 4 μM Tyr-P-MBP in buffer P containing 120 mM KCl.

Affinity matrices containing 0.25 nmol of GST-Cdc14 or GST-Cdc14^{TAB6} were prepared by immobilizing each fusion protein on glutathione-Sepharose beads (Traverso et al., submitted). One nmol of Net1(1-600)-His$_6$ was added to each affinity matrix in one ml of binding buffer B (25 mM Tris pH 7.4, 137 mM NaCl, 2.6 mM KCl, 0.1% 2-mercaptoethanol). The mixture was mixed by inversion for 30 min at 4°C, centrifuged, and washed four times with 1 ml buffer B containing 0.01% (v/v) Triton X-100. Aliquots (20 μl) of washed matrices were separated on a 12% SDS-polyacrylamide gel and stained with Coomassie Blue.

Other methods

Extract preparation, immunoprecipitation, immunofluorescence, cell synchronization and release procedures were described previously (Shou et al., 1999). For Western blots, primary antibodies were: 1:2,000 anti-A190, 1:2,500 anti-Sir2, 1:5,000 anti-Nop1, 1:2,000 9E10, 1:2,500 anti-Clb2, 1:8,000 anti-Sic1, 1:6,000 anti-Cdc28, and 1:1,000 anti-Cdc14. For immunofluorescence, cells were fixed with 4.5% formaldehyde at room temperature for 0.5 hour for all primary antibodies, which included 1:1,000 rabbit anti-A190, 1:12,000 mouse anti-Nop1, 1;1,000 9E10 (Babco), and 1:200 rabbit anti-Cdc14. FISH analysis was carried out as previously described (Guacci et al., 1994).

References

Benton, B. M., Zang, J. H., and Thorner, J. (1994). A novel FK506- and rapamycin-binding protein (FPR3 gene product) in the yeast Saccharomyces cerevisiae is a proline rotamase localized to the nucleolus. J Cell Biol *127*, 623-39.

Bryk, M., Banerjee, M., Murphy, M., Knudsen, K. E., Garfinkel, D. J., and Curcio, M. J. (1997). Transcriptional silencing of Ty1 elements in the RDN1 locus of yeast. Genes Dev *11*, 255-69.

Church, G. M., and Gilbert, W. (1984). Genomic sequencing. Proc. Natl. Acad. Sci. USA *81*, 1991-5.

Cockell, M. M., and Gasser, S. M. (1999). The nucleolus: nucleolar space for RENT. Curr Biol *9*, R575-6.

de Beus, E., Brockenbrough, J. S., Hong, B., and Aris, J. P. (1994). Yeast NOP2 encodes an essential nucleolar protein with homology to a human proliferation marker. J Cell Biol. *127*, 1799-813.

Fritze, C. E., Verschueren, K., Strich, R., and Easton, E. R. (1997). Direct evidence for SIR2 modulation of chromatin structure in yeast rDNA. Embo J *16*, 6495-509.

Garcia, S. N., and Pillus, L. (1999). Net results of nucleolar dynamics. Cell *97*, 825-8.

Gottlieb, S., and Esposito, R. E. (1989). A new role for a yeast transcriptional silencer gene, SIR2, in regulation of recombination in ribosomal DNA. Cell *56*, 771-6.

Gottschling, D. E. (2000). Gene silencing: two faces of SIR2. Curr Biol *10*, R708-11.

Gruneberg, U., Campbell, K., Simpson, C., Grindlay, J., and Schiebel, E. (2000). Nud1p links astral microtubule organization and the control of exit from mitosis. Embo J *19*, 6475-88.

Guacci, V., Hogan, E., and Koshland, D. (1994). Chromosome condensation and sister chromatid pairing in budding yeast. J Cell Biol *125*, 517-30.

Guarente, L. (2000). Sir2 links chromatin silencing, metabolism, and aging. Genes Dev *14*, 1021-6.

Hardy, C. F., and Pautz, A. (1996). A novel role for Cdc5p in DNA replication. Mol Cell Biol *16*, 6775-82.

Hong, B., Brockenbrough, J. S., Wu, P., and Aris, J. P. (1997). Nop2p is required for pre-rRNA processing and 60S ribosome subunit synthesis in yeast. Mol Cell Biol *17*, 378-88.

Jaspersen, S. L., Charles, J. F., Tinker, K. R., and Morgan, D. O. (1998). A late mitotic regulatory network controlling cyclin destruction in Saccharomyces cerevisiae. Mol Biol Cell *9*, 2803-17.

Jaspersen, S. L., Charles, J. F., and Morgan, D. O. (1999). Inhibitory phosphorylation of the APC regulator Hct1 is controlled by the kinase Cdc28 and the phosphatase Cdc14. Curr Biol *9*, 227-36.

Keener, J., Josaitis, C. A., Dodd, J. A., and Nomura, M. (1998). Reconstitution of yeast RNA polymerase I transcription in vitro from purified components. TATA-binding protein is not required for basal transcription. J Biol Chem *273*, 33795-802.

Komarnitsky, S. I., Chiang, Y. C., Luca, F. C., Chen, J., Toyn, J. H., Winey, M., Johnston, L. H., and Denis, C. L. (1998). DBF2 protein kinase binds to and acts through the cell cycle-regulated MOB1 protein. Mol Cell Biol *18*, 2100-7.

Luca, F. C., and Winey, M. (1998). MOB1, an essential yeast gene required for completion of mitosis and maintenance of ploidy. Mol Biol Cell *9*, 29-46.

Morgan, D. O. (1999). Regulation of the APC and the exit from mitosis. Nat Cell Biol *1*, E47-53.

Oakes, M., Siddiqi, I., Vu, L., Aris, J., and Nomura, M. (1999). Transcription factor UAF, expansion and contraction of ribosomal DNA (rDNA) repeats, and RNA polymerase switch in transcription of yeast rDNA. Mol Cell Biol *19*, 8559-69.

Powers, T., and Walter, P. (1999). Regulation of ribosome biogenesis by the rapamycin-sensitive TOR-signaling pathway in Saccharomyces cerevisiae. Mol Biol Cell *10*, 987-1000.

Shaw, P. J., and Jordan, E. G. (1995). The nucleolus. Annu Rev Cell Dev Biol *11*, 93-121.

Shirayama, M., Matsui, Y., Tanaka, K., and Toh-E. A. (1994). Isolation of a CDC25 family gene, MSI2/LTE1, as a multicopy suppressor of ira1. Yeast *10*, 451-61.

Shirayama, M., Matsui, Y., and Toh-E. A. (1994). The yeast TEM1 gene, which encodes a GTP-binding protein, is involved in termination of M phase. Mol Cell Biol *14*, 7476-82.

Shirayama, M., Toth, A., Galova, M., and Nasmyth, K. (1999). APC(Cdc20) promotes exit from mitosis by destroying the anaphase inhibitor Pds1 and cyclin Clb5. Nature *402*, 203-7.

Shou, W., and Dunphy, W. G. (1996). Cell cycle control by Xenopus p28Kix1, a developmentally regulated inhibitor of cyclin-dependent kinases. Mol Biol Cell *7*, 457-69.

Shou, W., Seol, J. H., Shevchenko, A., Baskerville, C., Moazed, D., Chen, Z. W., Jang, J., Shevchenko, A., Charbonneau, H., and Deshaies, R. J. (1999). Exit from mitosis is triggered by Tem1-dependent release of the protein phosphatase Cdc14 from nucleolar RENT complex. Cell *97*, 233-44.

Smith, J. S., and Boeke, J. D. (1997). An unusual form of transcriptional silencing in yeast ribosomal DNA. Genes Dev *11*, 241-54.

Straight, A. F., Shou, W., Dowd, G. J., Turck, C. W., Deshaies, R. J., Johnson, A. D., and Moazed, D. (1999). Net1, a Sir2-associated nucleolar protein required for rDNA silencing and nucleolar integrity. Cell *97*, 245-56.

Tanner, K. G., Landry, J., Sternglanz, R., and Denu, J. M. (2000). Silent information regulator 2 family of NAD- dependent histone/protein deacetylases generates a unique product, 1-O-acetyl-ADP-ribose. Proc. Natl. Acad. Sci. USA. *97*, 14178-82.

Tanny, J. C., and Moazed, D. (2000). Coupling of histone deacetylation to NAD breakdown by the yeast silencing protein Sir2: Evidence for acetyl transfer from substrate to an NAD breakdown product. Proc. Natl. Acad. Sci. USA. *98*, 415-420

Taylor, G. S., Liu, Y., Baskerville, C., and Charbonneau, H. (1997). The activity of Cdc14p, an oligomeric dual specificity protein phosphatase from Saccharomyces cerevisiae, is required for cell cycle progression. J Biol Chem *272*, 24054-63.

Thompson, C. M., Koleske, A. J., Chao, D. M., and Young, R. A. (1993). A multisubunit complex associated with the RNA polymerase II CTD and TATA-binding protein in yeast. Cell *73*, 1361-75.

Tollervey, D., Lehtonen, H., Jansen, R., Kern, H., and Hurt, E. C. (1993). Temperature-sensitive mutations demonstrate roles for yeast fibrillarin in pre-rRNA processing, pre-rRNA methylation, and ribosome assembly. Cell *72*, 443-57.

Toyn, J. H., and Johnston, L. H. (1994). The Dbf2 and Dbf20 protein kinases of budding yeast are activated after the metaphase to anaphase cell cycle transition. Embo J *13*, 1103-13.

Traverso, E.E., Baskerville, C., Liu, Y., Shou, W., James, P., Deshaies, R.J., and Charbonneau, H. (2001). Characterization of the net1 cell cycle-dependent regulator of the Cdc14 phosphatase from buddingyeast. J Biol Chem, in press.

Trumtel, S., Leger, S. I., Gleizes, P. E., Teulieres, F., and Gas, N. (2000). Assembly and functional organization of the nucleolus: ultrastructural analysis of Saccharomyces cerevisiae mutants. Mol Biol Cell *11*, 2175-89.

Udem, S. A., and Warner, J. R. (1972). Ribosomal RNA synthesis in Saccharomyces cerevisiae. J Mol Biol *65*, 227-42.

Visintin, R., Craig, K., Hwang, E. S., Prinz, S., Tyers, M., and Amon, A. (1998). The phosphatase Cdc14 triggers mitotic exit by reversal of Cdk-dependent phosphorylation. Mol Cell *2*, 709-18.

Visintin, R., Hwang, E. S., and Amon, A. (1999). Cfi1 prevents premature exit from mitosis by anchoring Cdc14 phosphatase in the nucleolus. Nature *398*, 818-23.

Warner, J. R. (1991). Labeling of RNA and phosphoproteins in Saccharomyces cerevisiae. Methods Enzymol *194*, 423-8.

Yamamoto, R. T., Nogi, Y., Dodd, J. A., and Nomura, M. (1996). RRN3 gene of Saccharomyces cerevisiae encodes an essential RNA polymerase I transcription factor which interacts with the polymerase independently of DNA template. Embo J *15*, 3964-73.

Zachariae, W., and Nasmyth, K. (1999). Whose end is destruction: cell division and the anaphase-promoting complex. Genes Dev *13*, 2039-58.

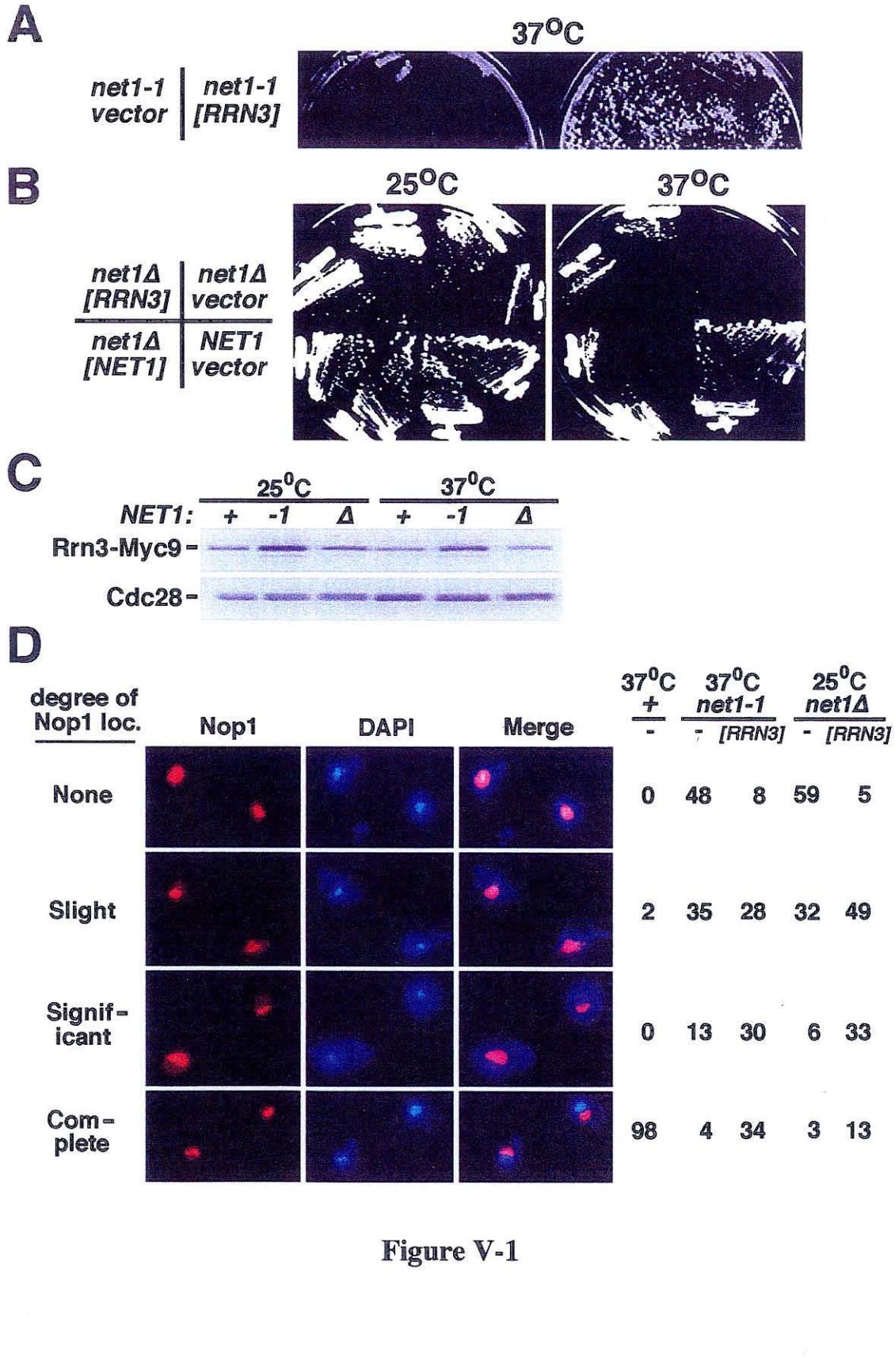
A
37°C
net1-1 vector
net1-1 [RRN3]
B
25°C
37°C
net1Δ [RRN3]
net1Δ vector
net1Δ [NET1]
NET1 vector
C
25°C
37°C
NET1: + -1 Δ + -1 Δ
Rrn3-Myc9
Cdc28
D
degree of Nop1 loc.
Nop1
DAPI
Merge
37°C + -
37°C net1-1 - [RRN3]
25°C net1Δ - [RRN3]
None 0 48 8 59 5
Slight 2 35 28 32 49
Signif-icant 0 13 30 6 33
Com-plete 98 4 34 3 13

Figure V-1

Figure V-1. A CEN/ARS plasmid containing *RRN3 ([RRN3])* suppresses the temperature sensitive (ts) growth defect and Nop1 mislocalization phenotype of *net1* mutants.

(A, B) *[RRN3]* suppresses *net1* ts growth defect. (A) *net1-1* cells transformed with a *CEN/ARS/LEU2* plasmid harboring either no insert (vector) or *RRN3* under its natural promoter were plated onto synthetic dextrose medium lacking leucine. After 25°C for one day, both plates were shifted to 37°C for two more days, and then photographed. (B) *NET1* and *net1Δ* cells transformed with a *CEN/ARS/LEU2* plasmid harboring either no insert (vector), *RRN3* or *NET1* (driven by their natural promoters) were streaked onto synthetic dextrose medium lacking leucine. Two independent colonies were analyzed in each case. The plates were photographed after four days at 25°C, or five days at 37°C. (C) Wild type and *net1* mutants were pre-grown at 25°C to exponential phase and shifted to 25°C or 37°C for three more hours. Extracts were fractionated by SDS-PAGE and immunoblotted with 9E10 antibodies (against the Myc epitope) to measure the level of Rrn3-Myc9. Cdc28 served as a loading control. (D) *[RRN3]* partially restores Nop1 nucleolar localization in *net1* mutants. Wild type and *net1* mutants with or without *[RRN3]* plasmid were grown at 25°C to exponential phase. Some cultures were further incubated at 37°C for 3 hours as indicated. Cells were subjected to indirect immunofluorescence with anti-Nop1, and the extent of Nop1 delocalization in *net1*

mutants was categorized into four classes: None: complete delocalization such that Nop1 staining is uniform across the entire nucleus; Slight: strong nuclear staining with stronger nucleolar staining; Significant: intense nucleolar staining and subdued nuclear staining; and Complete: nucleolar localization with no detectable nuclear staining. Fractions of cells that fell in the four different classes were quantitated.

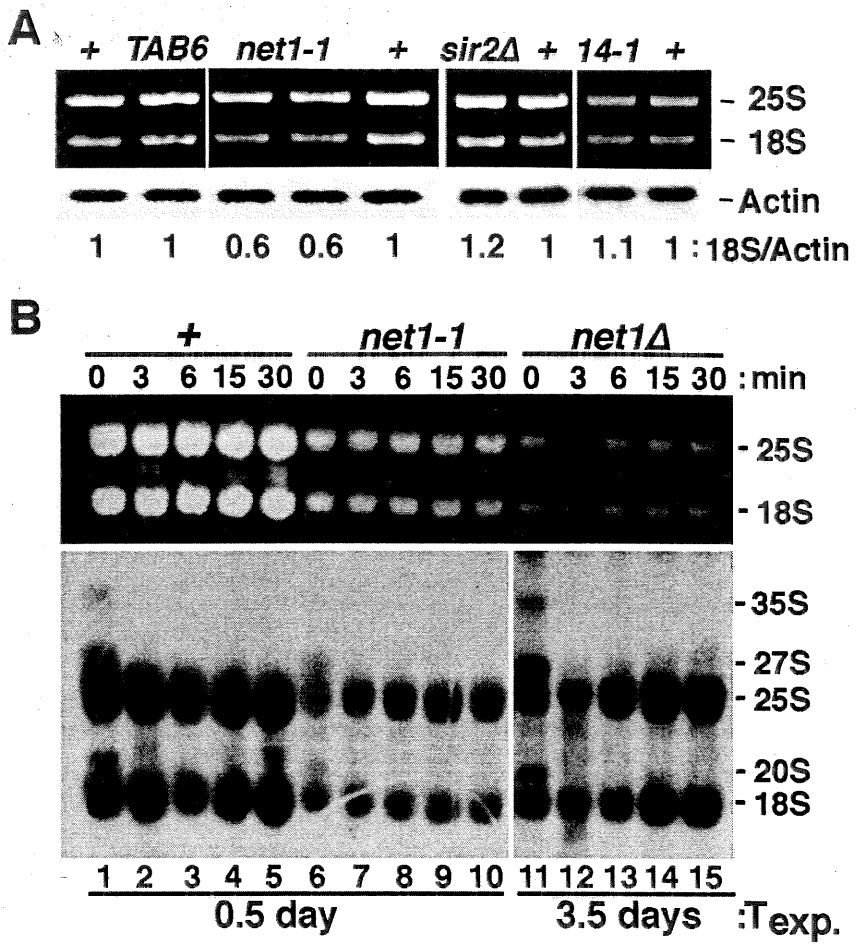

Figure V-2. A and B

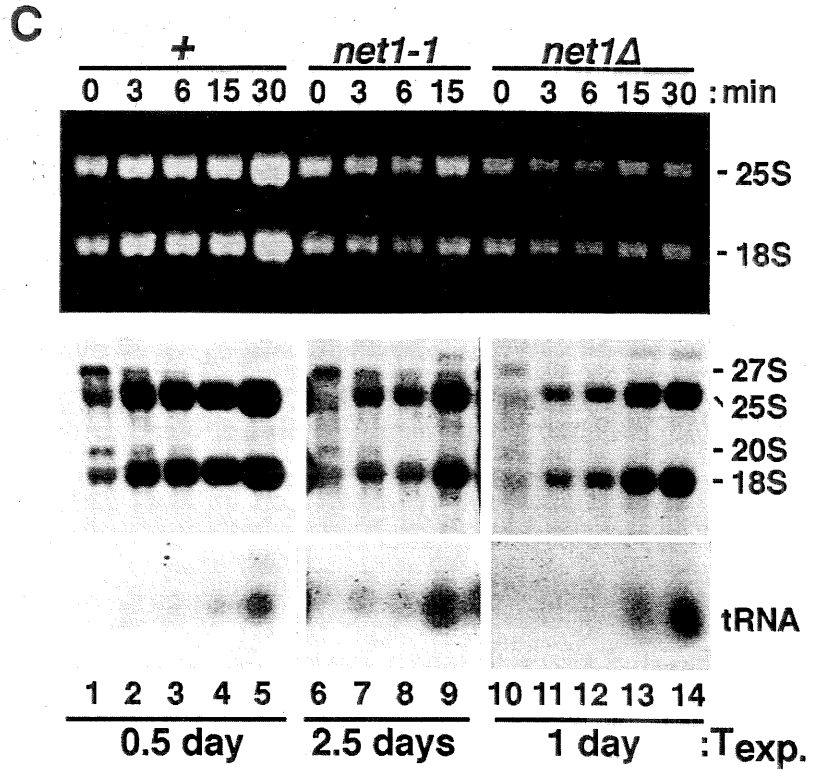

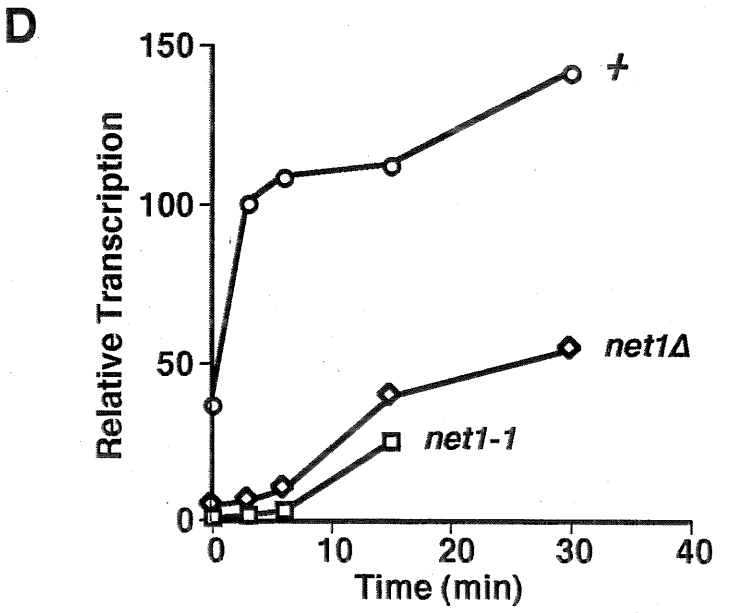

Figure V-2. C and D

Figure V-2. *net1* mutants have a reduced rate of rRNA synthesis.

(A) The steady state level of rRNA is reduced in *net1-1*. Total RNA was extracted from cells grown at 23°C and shifted to 37°C for three hours. Equal amounts of total RNA were separated by agarose gel electrophoresis, first stained with ethidium bromide to show the levels of 25S and 18S rRNA (upper panel), and then probed for actin mRNA in a Northern blot (lower panel). The ratio of 18S rRNA to actin mRNA is shown below each lane. (B, C, D) *net1* mutants have normal rRNA processing but reduced rRNA transcription. Cells were grown at 25°C, shifted to 37°C for three hours, and kept at 37°C thereafter. They were pulse-labeled with [^{3}H]-methionine (B) or [^{3}H]-uracil (C) for 5 min, and chased with unlabeled methionine (B) or uracil (C) for 0, 3, 6, 15, or 30 min, as indicated. Total RNA was separated by agarose gel electrophoresis, stained with ethidium bromide (upper panel), and subjected to autoradiography for the indicated amounts of time (T_{exp}) (lower panel). The intensity of the 27S and 25S rRNA bands in (C) was quantitated using NIH imaging, with difference in exposure time taken into consideration.

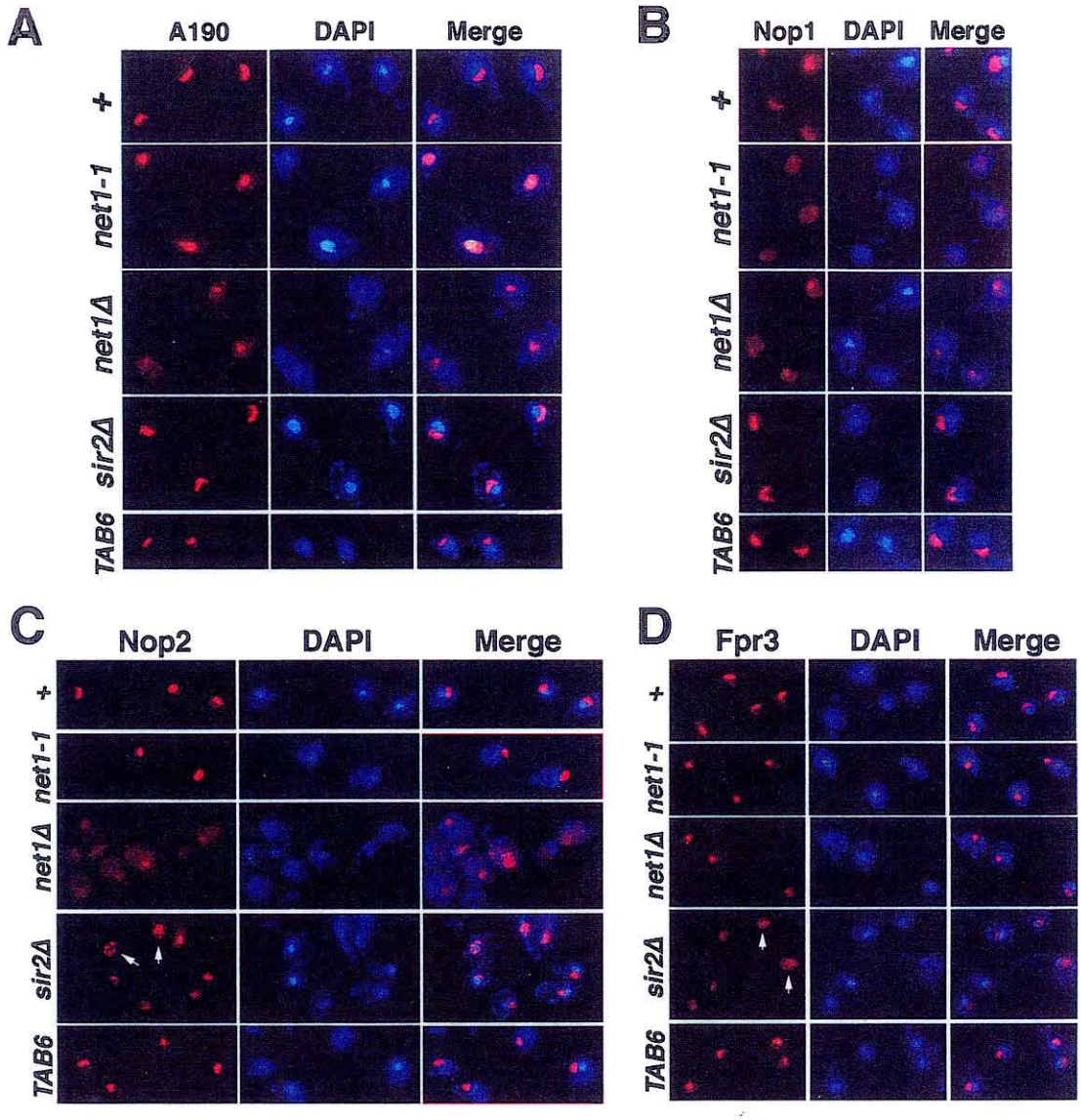
A
A190
DAPI
Merge
+
net1-1
net1Δ
sir2Δ
TAB6
B
Nop1
DAPI
Merge
+
net1-1
net1Δ
sir2Δ
TAB6
C
Nop2
DAPI
Merge
+
net1-1
net1Δ
sir2Δ
TAB6
D
Fpr3
DAPI
Merge
+
net1-1
net1Δ
sir2Δ
TAB6

Figure V-3. A-D

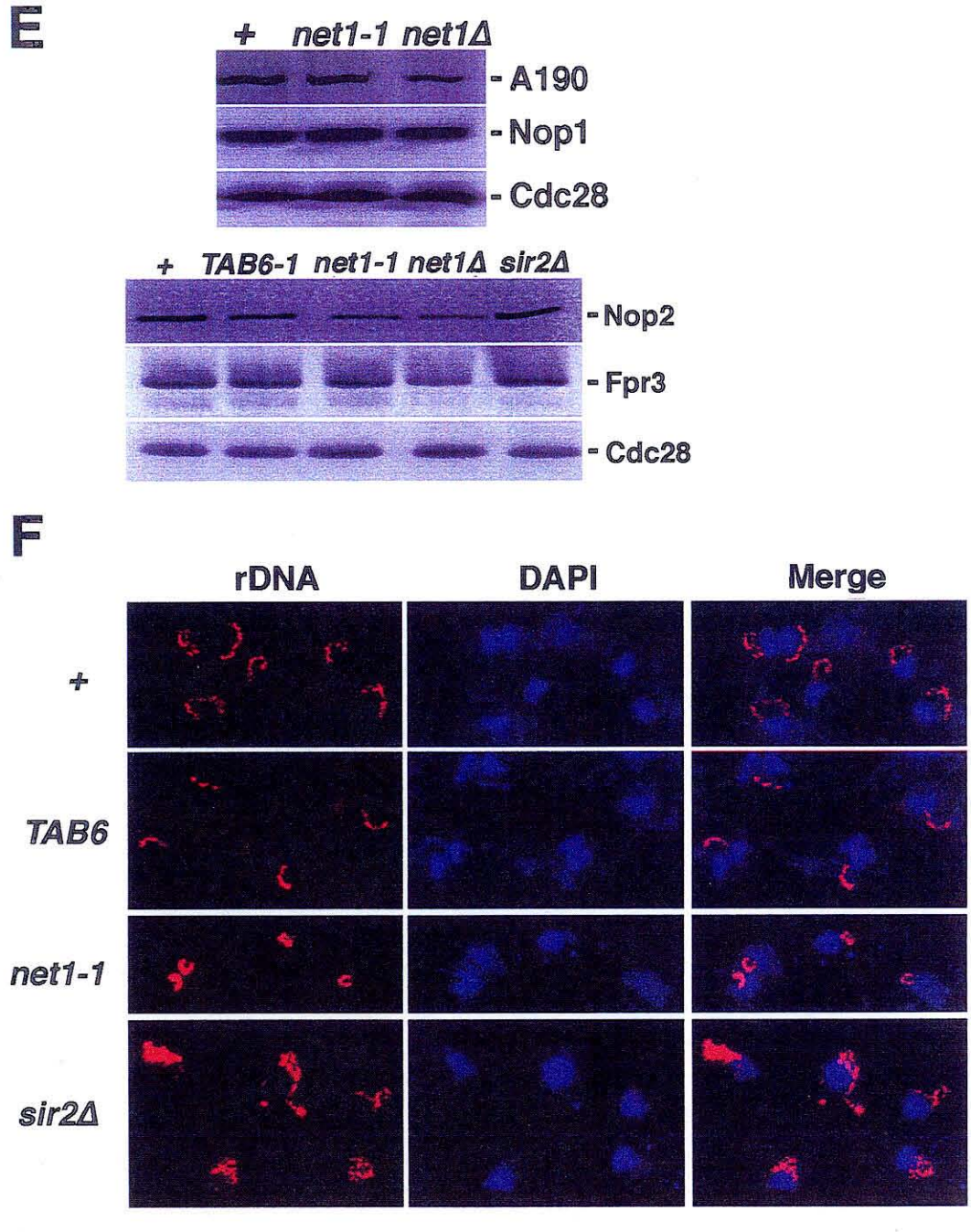

Figure V-3. E and F

Figure V-3. Net1 is required for the proper localization of multiple nucleolar proteins. (A – D) Cells with indicated genotypes were grown at 25^{O}C, and subjected to indirect immunofluorescence with anti-A190 (A), anti-Nop1 (B), anti-Nop2 (C), or anti-Fpr3 (D) antibodies (Column 1). They were also stained with DAPI to show the position of nuclei (Column 2). The images in Columns 1 and 2 were merged in Column 3. In 40-50% of *sir2Δ* and 20% of wild type cells, Nop2 and Fpr3 assumed diffused staining patterns that covered the majority of the nucleus or even exceeded the boundary of the nucleus (white arrows in panels C and D). (E) Protein levels of the four nucleolar antigens in wild type and mutant cells were compared in Western blots, with Cdc28 serving as the loading control. (F) rDNA morphology is altered in *net1* and *sir2* but not *TAB6-1* mutants. Cells were arrested in nocodazole, and subjected to Fluorescence In Situ Hybridization (FISH) using DIG-labeled probes against rDNA followed by rhodamine-anti-DIG (Column 1). DNA was visualized by DAPI staining (Column 2). The merged image is shown in Column 3.

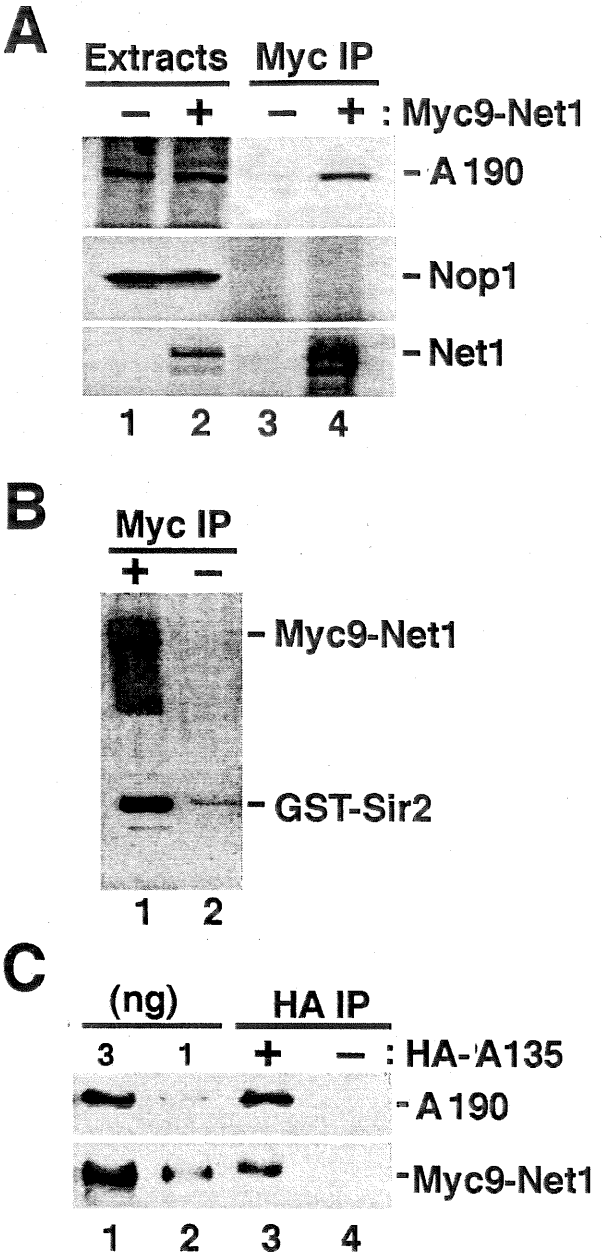
A
Extracts
Myc IP
– + – + : Myc9-Net1
- A190
- Nop1
- Net1
1 2 3 4
B
Myc IP
+ –
- Myc9-Net1
- GST-Sir2
1 2
C
(ng)
HA IP
3 1 + – : HA-A135
- A190
- Myc9-Net1
1 2 3 4

Figure V-4

Figure V-4: Pol I but not Nop1 binds stably to Net1.

(A) A190 but not Nop1 binds stably to Net1. Extracts from strains with the indicated genotypes were immunoprecipitated with 9E10 antibodies ("–" refers to a strain with a natural (ie untagged) *NET1* allele). The immunoprecipitates (Myc IP) and the input extracts were fractionated by SDS-PAGE and immunoblotted with antibodies against A190 (first row), Nop1 (second row), and Myc9-Net1 (third row). (B) His6-Myc9-Net1 and GST-Sir2 interact *in vitro*. His6-Myc9-Net1 and GST-Sir2 were expressed and purified from insect cells and bacteria, respectively. 9E10 antibody beads were incubated with GST-Sir2 in the presence (+) or absence (-) of Myc9-Net1. Proteins captured by the beads were immunoblotted with 9E10 and α-GST antibodies. (C) Purified Pol I and Myc9-Net1 interact *in vitro*. Purified Pol I (150 ng/ 0.26 pmol, Keener et al., 1998) with its A135 subunit tagged with HA (+) or untagged (-) was immunoprecipitated with 12CA5 antibodies (against the HA epitope). The antibody beads were subsequently incubated with Myc9-Net (150ng/0.83 pmol) purified from insect cells, and proteins bound to the beads (Lanes 3 and 4) were immunoblotted with antibodies against A190 and Myc9-Net1. To estimate the relative amount of Net1 complexed to Pol I, 3 ng (Lane 1) and 1 ng (Lane 2) of Pol I (top panel) and Myc9-Net1 (bottom panel) were immunoblotted with anti-A190 and 9E10 antibodies, respectively. We estimate that almost all Pol I molecules bound Net1 in this assay.

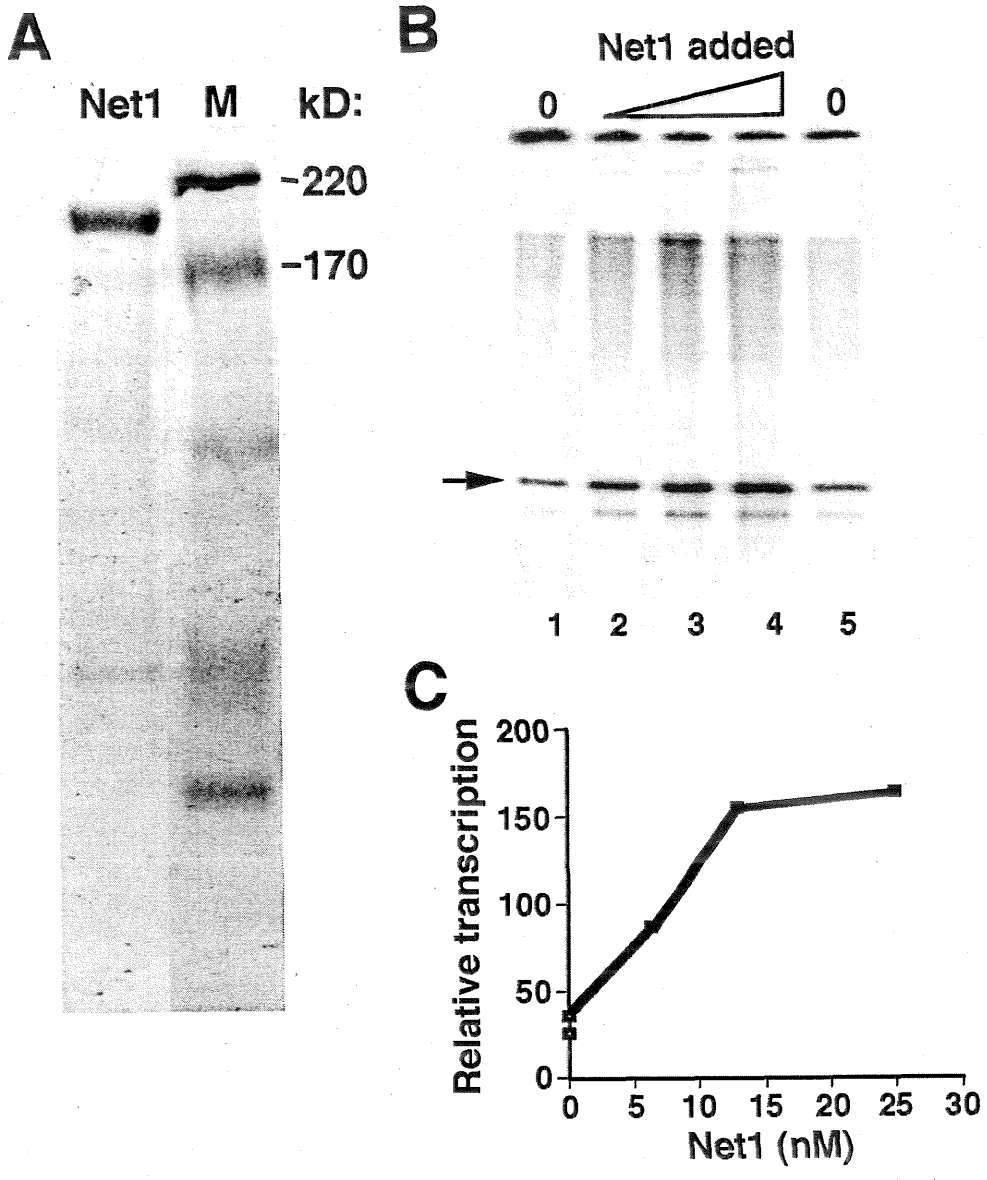
A
Net1
M
kD:
-220
-170
B
Net1 added
0
0
1
2
3
4
5
C
Relative transcription
200
150
100
50
0
0
5
10
15
20
25
30
Net1 (nM)

Figure V-5

Figure V-5: Net1 stimulates Pol I activity.

(A) Net1 enriched to > 90% purity (Experimental Procedures) was fractionated by SDS-PAGE and stained with Coomassie Blue. M refers to molecular weight markers. (B, C) Net1 stimulates Pol I activity. Dilution buffer (Lanes 1 and 5) or increasing amounts of Net1 (Lanes 2 to 4) were added to a standard transcription reaction which employed a linearized plasmid template that contained rDNA linked to its full promoter (extending to –210) as the template and 10 – 15 nM Pol I (Keener et al., 1998). An arrow indicates the position of [^{32}P]- labeled runoff transcripts. Quantitation of the amount of transcripts as a function of Net1 concentration is plotted in (C).

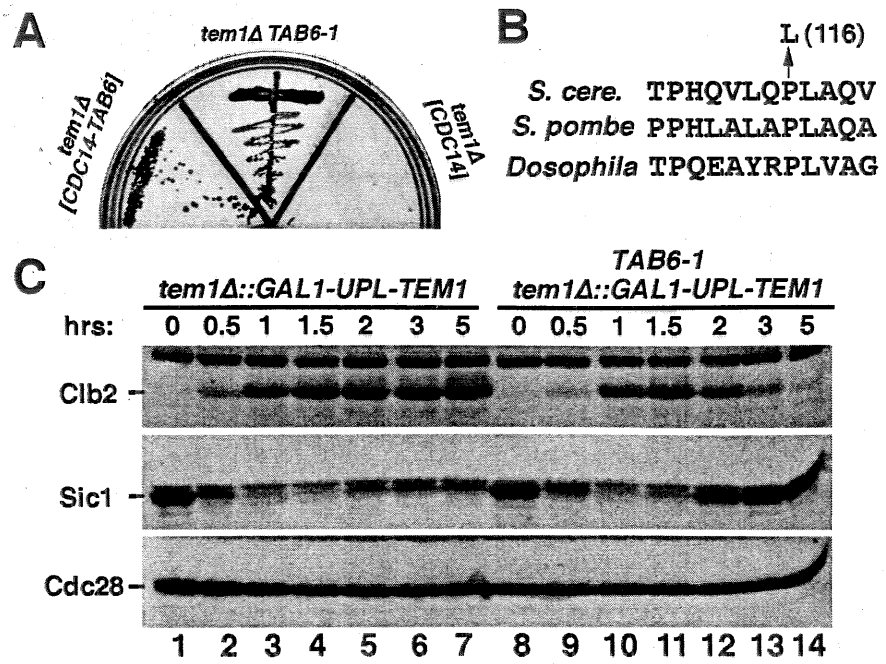
A
tem1Δ TAB6-1
tem1Δ [CDC14-TAB6]
tem1Δ [CDC14]
B
L (116)
S. cere. TPHQVLQPLAQV
S. pombe PPHLALAPLAQA
Dosophila TPQEAYRPLVAG
C
tem1Δ::GAL1-UPL-TEM1
TAB6-1 tem1Δ::GAL1-UPL-TEM1
hrs: 0 0.5 1 1.5 2 3 5 0 0.5 1 1.5 2 3 5
Clb2
Sic1
Cdc28
1 2 3 4 5 6 7 8 9 10 11 12 13 14

Figure V-6

Figure V-6: *TAB6-1* is an allele of *CDC14* that bypasses *tem1Δ*.

(A) *TAB6-1* is an allele of *CDC14*. *tem1Δ::TRP1 [GAL-TEM1/URA3] TAB6-1* cells (center), or *tem1Δ::TRP1 [GAL-TEM1/URA3]* cells transformed with a *HIS3*-marked plasmid harboring *CDC14* derived from either wild type cells (right), or *TAB6* cells (left) were grown on YP galactose (YPG, *TEM1* expressed), and then plated on synthetic glucose medium containing 5-FOA to select for colonies that had lost the *[GAL-TEM1/URA3]* plasmid. After ten days at room temperature, the plate was photographed. (B) *TAB6-1* has a single point mutation P116 -> L. Cdc14 sequences flanking this amino acid from *S.cerevisiae*, *S. pombe*, and *Drosophila* are aligned. (C) *TAB6-1* bypass of *tem1Δ* is accompanied by Clb2 degradation and Sic1 accumulation. Cells of the indicated genotypes grown in YPG (*TEM1* expressed) at 25°C were arrested in G1 phase with α factor, and released into YP glucose (*TEM1* repressed) at time = 0. One and a half hours later, α factor was added back to prevent cells from proceeding through a second cell cycle. At the indicated times, samples were taken to measure Clb2, Sic1, and Cdc28 protein levels by immunoblotting.

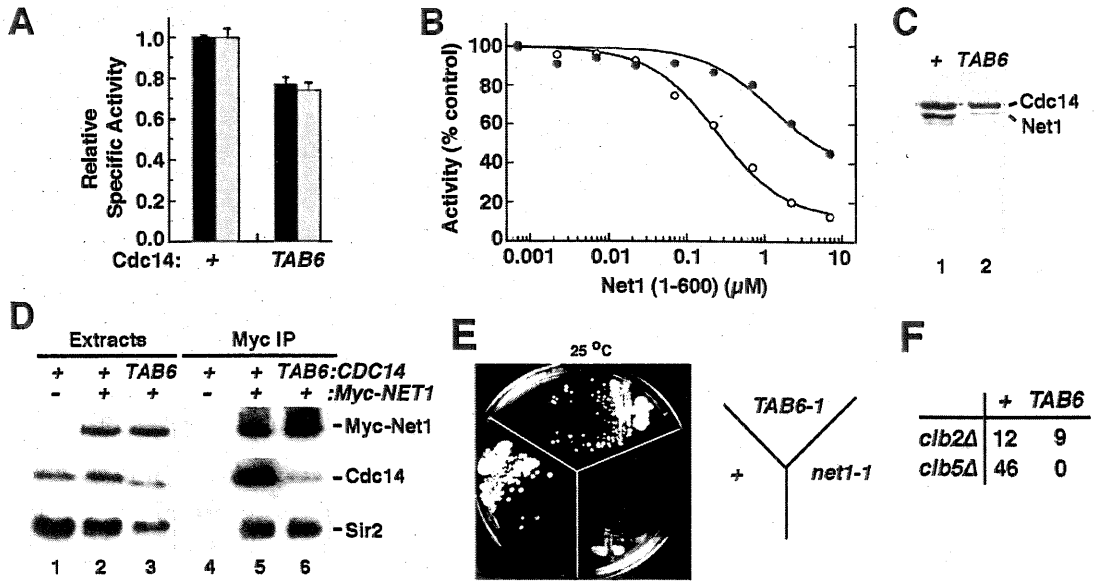
A
Relative Specific Activity
1.0
0.8
0.6
0.4
0.2
0.0
Cdc14: + TAB6
B
Activity (% control)
100
80
60
40
20
0
0.001
0.01
0.1
1
10
Net1 (1-600) (μM)
C
+ TAB6
Cdc14
Net1
1 2
D
Extracts
Myc IP
+ + TAB6 + + TAB6:CDC14
- + + - + + :Myc-NET1
Myc-Net1
Cdc14
Sir2
1 2 3 4 5 6
E
25 °C
TAB6-1
+
net1-1
F
+ TAB6
clb2Δ 12 9
clb5Δ 46 0

Figure V-7

Figure V-7: Cdc14^{TAB6} has reduced affinity for Net1, which renders Clb5 essential for cell viability.

(A) Cdc14^{TAB6} is nearly as active as Cdc14. The relative specific activities (± standard deviation, n=3) of purified GST-Cdc14 and GST-Cdc14^{TAB6} were determined using the artificial substrates *p*-nitrophenyl phosphate (black bars) and tyrosine-phosphorylated myelin basic protein (Tyr-P-MBP) (gray bars). (B) GST-Cdc14^{TAB6} is less sensitive to inhibition by Net1(1-600). The activity of GST-Cdc14 (open circles) and GST-Cdc14^{TAB6} (closed circles) was measured with 4 μM Tyr-P-MBP in the presence of the indicated concentrations of purified Net1(1-600)-His$_6$. The IC_{50} values for Cdc14 and Cdc14^{TAB6} are ~0.35 μM and 5 μM, respectively. (C) The affinity of Cdc14^{TAB6} for Net1 is greatly reduced *in vitro*. Affinity matrices containing GST-Cdc14 (lane 1) and GST-Cdc14^{TAB6} (lane 2) were mixed with a four-fold molar excess of Net1(1-600)-His$_6$. Proteins bound to the matrices were resolved by SDS-PAGE and stained with Coomassie Blue. (D) *TAB6-1* selectively disengages Cdc14^{TAB6} from the RENT complex. Extracts prepared from *NET1* (Lanes 1 and 4), *MYC9-NET1* (Lanes 2 and 5), and *MYC9-NET1 TAB6-1* (Lanes 3 and 6) strains were immunoprecipitated with 9E10 antibodies. The input extracts (Lanes 1 – 3) and immunoprecipitates (Lanes 4 – 6) were immunoblotted with 9E10, α- Cdc14, and α- Sir2 antibodies as indicated. (E) *TAB6-1* cells grow much better than *net1-1* cells at 25°C. Wild type, *TAB6-1*, and *net1-1* cells were struck out on a YPD plate and allowed to grow at 25°C for 2.5 days before the photograph was taken.

(F) *TAB6-1* is synthetic lethal with *clb5Δ* but not *clb2Δ*. *clb2Δ::LEU2 CDC14/HIS3* and *clb5Δ::URA3 CDC14/HIS3* strains were mated with *TAB6-1*, and the diploid strains were dissected. The number of viable spores of the indicated genotypes were tabulated. Although *CLB5* (Chromosome XVI) and *TAB6-1* (Chromosome VI) are unlinked, *clb5Δ TAB6-1* recombinants were not recovered.

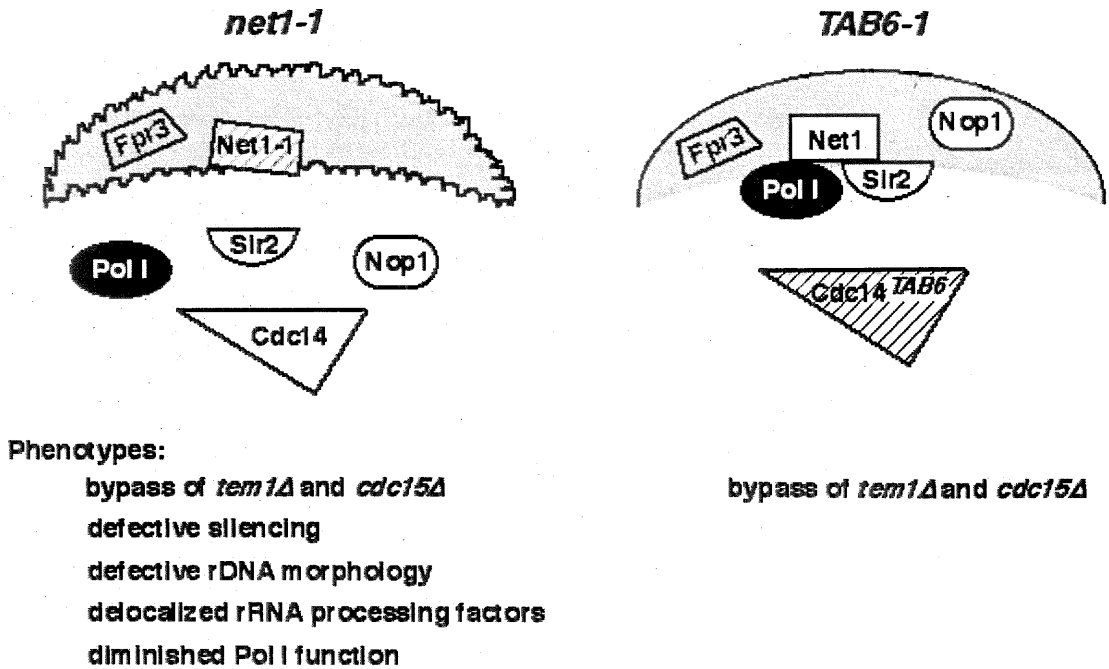

Phenotypes:

bypass of *tem1Δ* and *cdc15Δ*
defective silencing
defective rDNA morphology
delocalized rRNA processing factors
diminished Pol I function

bypass of *tem1Δ* and *cdc15Δ*

Figure V-8

TAB6-1 **uncouples the nucleolar and cell cycle functions of RENT.**

Chapter VI. Future Directions

There are still many unresolved questions, and I list some of them here:

0. Is the release of Cdc14 from the nucleolus essential for mitotic exit?

1. What are the two signals that catalyze the disruption of the RENT complex and the subsequent release of Cdc14?

2. After Cdc14 is released, how does it bring about mitotic exit?

3. Mutations in Mtr10 and Srp1, two proteins involved in nuclear transport, bypass *cdc15Δ*. What are the mechanisms of their bypass and how does nuclear transport link to mitotic exit?

4. What are the unidentified *tab* mutants and how do they bypass *cdc15Δ*?

5. How is MEN organized?

6. The guanine nucleotide exchange factor Lte1 is only essential at cold temperature. How is Tem1 activated in *lte1Δ* cells grown at normal room temperature?

7. APC^{Cdc20} initiates Clb2 degradation without completing it. What mechanisms prevent APC^{Cdc20} from degrading all Clb2?

8. What signals regulate cAMP/PKA which inhibits mitotic exit?

9. How do proteins in MEN regulate cytokinesis?

10. It is not yet clear whether nucleolar sequstration and inhibition of Cdc14 by Net1 can be uncoupled. It would be interesting to identify domains in Net1 that are responsible for nucleloar localization and Cdc14 inhibition, and ask whether they are distinct.

11. How does the DNA damage checkpoint adaptation pathway feed into MEN?

APPENDIX I

Molecular Biology of the Cell
Vol. 7, 457–469, March 1996

Cell Cycle Control by *Xenopus* p28^{Kix1}, a Developmentally Regulated Inhibitor of Cyclin-dependent Kinases

Wenying Shou and William G. Dunphy*

Division of Biology 216–76, Howard Hughes Medical Institute, California Institute of Technology, Pasadena, California 91125

Submitted October 19, 1995; Accepted December 15, 1995
Monitoring Editor: Tim Hunt

We have isolated *Xenopus* p28^{Kix1}, a member of the p21^{CIP1}/p27^{KIP1}/p57^{KIP2} family of cyclin-dependent kinase (Cdk) inhibitors. Members of this family negatively regulate cell cycle progression in mammalian cells by inhibiting the activities of Cdks. p28 shows significant sequence homology with p21, p27, and p57 in its N-terminal region, where the Cdk inhibition domain is known to reside. In contrast, the C-terminal domain of p28 is distinct from that of p21, p27, and p57. In co-immunoprecipitation experiments, p28 was found to be associated with Cdk2, cyclin E, and cyclin A, but not the Cdc2/cyclin B complex in *Xenopus* egg extracts. *Xenopus* p28 associates with the proliferating cell nuclear antigen, but with a substantially lower affinity than human p21. In kinase assays with recombinant Cdks, p28 inhibits pre-activated Cdk2/cyclin E and Cdk2/cyclin A, but not Cdc2/cyclin B. However, at high concentrations, p28 does prevent the activation of Cdc2/cyclin B by the Cdk-activating kinase. Consistent with the role of p28 as a Cdk inhibitor, recombinant p28 elicits an inhibition of both DNA replication and mitosis upon addition to egg extracts, indicating that it can regulate multiple cell cycle transitions. The level of p28 protein shows a dramatic developmental profile: it is low in *Xenopus* oocytes, eggs, and embryos up to stage 11, but increases ~100-fold between stages 12 and 13, and remains high thereafter. The induction of p28 expression temporally coincides with late gastrulation. Thus, although p28 may play only a limited role during the early embryonic cleavages, it may function later in development to establish a somatic type of cell cycle. Taken together, our results indicate that *Xenopus* p28 is a new member of the p21/p27/p57 class of Cdk inhibitors, and that it may play a role in developmental processes.

INTRODUCTION

Progression through the cell cycle is controlled by the cyclin-dependent kinases (Cdks), which comprise a family containing various catalytic subunits and regulatory partners called cyclins. In mammalian cells, Cdk4/cyclin D, Cdk2/cyclin E, Cdk2/cyclin A, and Cdc2/cyclin B act sequentially at different points in the cell cycle (for review, see Draetta, 1993; Sherr, 1993). Although particular details vary, the central mechanisms of cell cycle regulation by Cdks are conserved from yeast to vertebrates.

Cdk activities are strictly controlled to ensure that a cell undergoes cell division cycles only under the appropriate circumstances. The Cdks are regulated by at least three distinct mechanisms: cyclin binding, subunit phosphorylation, and association with Cdk inhibitors. To date, two classes of Cdk inhibitors have been identified in mammalian cells (for review, see Elledge and Harper, 1994; Massagué and Polyak, 1995). The p15/p16 class includes p15^{INK4B} (Hannon and Beach, 1994), p16^{INK4} (Serrano *et al.*, 1993), p18 (Guan *et al.*, 1994), and p19 (Chan *et al.*, 1995). Proteins in this class share considerable sequence homology with each other. They exclusively associate with and inhibit D-type Cdks, and appear to play a role in cellular differ-

* Corresponding author.

entiation and tumor suppression (reviewed in Elledge and Harper, 1994). A second class of Cdk inhibitors includes p21 (also known as CIP1, WAF1, CAP20, and SDI1) (El-Deiry *et al.*, 1993; Gu *et al.*, 1993; Harper *et al.*, 1993; Xiong *et al.*, 1993; Noda *et al.*, 1994), $p27^{KIP1}$ (Polyak *et al.*, 1994b; Toyoshima and Hunter, 1994), and $p57^{KIP2}$ (Lee *et al.*, 1995; Matsuoka *et al.*, 1995). The N-terminal regions of these three proteins share significant homology; this domain can bind to and inhibit Cdk2/cyclin E, Cdk2/cyclin A, Cdk4/cyclin D, and to a lesser extent, Cdc2/cyclin B. Although p21 and p27 do not directly inhibit Cdk-activating kinase (CAK), they can associate with Cdks and prevent them from being phosphorylated and activated by CAK (Polyak *et al.*, 1994b; Aprelikova *et al.*, 1995). Except for a bipartite nuclear localization signal, the C-terminal domains of these proteins are not strongly conserved: $p21^{CIP1}$ binds proliferating cell nuclear antigen (PCNA; a DNA polymerase δ-subunit), while $p27^{KIP1}$ and $p57^{KIP2}$ do not (Waga *et al.*, 1994; Chen *et al.*, 1995; Luo *et al.*, 1995). Moreover, in the central regions, human $p57^{KIP2}$ has PAPA repeats while mouse $p57^{KIP2}$ has a proline-rich domain followed by acidic repeats (Lee *et al.*, 1995; Matsuoka *et al.*, 1995). The structural diversity among $p21^{CIP1}$, $p27^{KIP1}$, and $p57^{KIP2}$ suggests that these proteins may play distinct roles in cell cycle regulation.

p21 and p27 participate in diverse regulatory responses. Following radiation-induced DNA damage, the tumor suppressor protein p53 up-regulates p21 mRNA levels (El-Deiry *et al.*, 1993). p21 inhibits Cdk2/cyclin E activity, and thereby prevents DNA replication (Jackson *et al.*, 1995). Although the C-terminal domain of p21 associates with PCNA and blocks PCNA-dependent DNA replication, it does not inhibit PCNA-dependent DNA repair (Li *et al.*, 1994), giving irradiated cells the opportunity to remain in G1 and repair their DNA. Consistent with these observations, embryonic fibroblasts derived from $p21^{-/-}$ mice are significantly deficient in their ability to arrest in G1 in response to DNA damage (Deng *et al.*, 1995). Besides playing a role in the G1 checkpoint, p21 may also be involved in cellular differentiation under normal circumstances. For example, p21 mRNA levels increase in senescent cells (Noda *et al.*, 1994). Also, MyoD, a skeletal-muscle–specific transcriptional regulator, activates the expression of p21 during differentiation in a p53-independent fashion (Halevy *et al.*, 1995). The expression pattern of p21 in the mouse correlates with terminal differentiation and cell cycle withdrawal, suggesting roles in development (Parker *et al.*, 1995). However, $p21^{-/-}$ mice undergo normal development, and do not develop spontaneous tumors (Deng *et al.*, 1995), implying the existence of redundant pathways that ensure proper development and tumor prevention in this organism.

Although the functions of p27 and p57 are less well understood, they appear to play a role in differentiation-mediated cell cycle arrest and possibly in tumor prevention. In the mouse, most of the p57-expressing cells are terminally differentiated (Matsuoka *et al.*, 1995). The human p57 gene is located at a chromosomal region implicated in both sporadic cancers and a familial cancer syndrome, suggesting that p57 is a candidate tumor suppressor (Matsuoka *et al.*, 1995). The regulation of p27 appears to be cell-type dependent. In transforming growth factor β–arrested or contact-inhibited mink epithelial cells, p27 dissociates from Cdk4/cyclin D, and binds to and prevents the CAK-mediated activation of Cdk2/cyclin E (Polyak *et al.*, 1994a,b). In macrophages, cAMP exerts its antimitogenic effects by raising the level of p27, which then associates with Cdk4/cyclin D and prevents its activation by CAK (Kato *et al.*, 1994). During T cell mitogenesis, interleukin 2 signaling activates Cdk2/cyclin E complexes by eliminating the p27 protein, whereas p27 levels fail to drop when the immunosuppressant rapamycin is present (Nourse *et al.*, 1994). In at least some human cell lines, proliferating cells have a lower level of p27 due to an elevated p27-ubiquitinating activity that targets p27 to the ubiquitin-dependent proteasome degradation pathway (Pagano *et al.*, 1995).

Although considerable information about Cdk inhibitors has emerged recently, much remains to be learned about the evolution of these families and the diversity of their functions. Two Cdk inhibitors from *Saccharomyces cerevisiae* (the Cdc28/Cln inhibitor Far1 and the Cdc28/Clb2,5,6 inhibitor $p40^{SIC1}$) and one from *Schizosaccharomyces pombe* (the Cdc2/Cdc13 inhibitor Rum1) have been identified, but these show little homology with p15/p16 or p21/p27 Cdk inhibitors (for review, see Elledge and Harper, 1994). Since cell-free extracts from *Xenopus* eggs faithfully recapitulate many cell cycle events including DNA replication, mitosis, and various checkpoint mechanisms (Dasso and Newport, 1990; Leno and Laskey, 1991; Murray, 1991; Minshull *et al.*, 1994; Kumagai and Dunphy, 1995), it will be valuable to ascertain the extent to which Cdk inhibitors contribute to the regulation of the various Cdks present in this system. Because *Xenopus* embryos are readily available and easy to manipulate, *Xenopus* is also an attractive organism for the study of developmental regulatory mechanisms. Isolation of Cdk inhibitors from *Xenopus* and characterization of their upstream regulators, downstream targets, and expression during embryogenesis will contribute to our understanding of cell cycle regulation and its dynamic changes during development. With these goals in mind, we have searched for Cdk inhibitors in *Xenopus laevis* using a polymerase chain reaction (PCR)-based approach. Here, we report the

isolation and initial characterization of *Xenopus* $p28^{Kix1}$, a p21/p27-class Cdk inhibitor.

MATERIALS AND METHODS

Cloning of Xenopus p28

An internal fragment of *Xenopus* p28 was isolated by PCR using degenerate primers specific to conserved regions among human $p21^{CIP1}$, mouse $p21^{CIP1}$, and human $p27^{KIP1}$ (see Figure 1A). The 5′ primer was (5′) CGCGGATCCTG(C/T)(A/C)G(I/C)(I/C)(G/A)(I/C)(T/C)T(I/C)TT(C/T)GG(I/C)CC(I/C)GT (3′), and the 3′ primer was (5′) CGGGGTACCT(G/C)(I/C)IT(I/C)I(G/C)IAA(G/A)TC-(G/A)AA(A/G)TTCCA (3′). The 5′ end of each primer contains nine extra nucleotides (underlined) to provide restriction sites for *Bam*HI or *Kpn*I, respectively. PCR reactions (50 μl) contained 15 ng of *Xenopus* oocyte cDNA as template (Mueller *et al.*, 1995) and 50 pmol of each primer. PCR reactions were carried out as described (Mueller *et al.*, 1995), except that the first five cycles were 94°C for 1 min, 54°C for 2 min, and 72°C for 1 min, and the remaining 30 cycles were 94°C for 1 min, 57°C for 2 min, and 72°C for 1 min. An ~130-bp DNA fragment was isolated and cloned into the TA cloning vector (Invitrogen, San Diego, CA). After the fragment was sequenced to confirm its identity, it was radiolabeled by PCR and used to screen a *Xenopus* oocyte cDNA library by colony hybridization (Sambrook *et al.*, 1989; Mueller *et al.*, 1995). Approximately 1.2 million colonies were screened. Four positives were identified, two of which encoded the full-length *Xenopus* p28 gene. The entire cDNA was sequenced on both strands by primer walking using Sequenase (United States Biochemical, Cleveland, OH) with the dideoxy chain termination method. The GenBank accession number is U38844.

Subcloning of Xenopus p28 into Protein Expression Vectors

The pAX-NMT plasmid (Mueller *et al.*, 1995) harboring the full-length *Xenopus* p28 cDNA was mutagenized by PCR to create an *Nde*I site at the initiation codon. Briefly, the 5′ primer (5′) GGAAGTCCATATGGCTGCTTTCCACATCGC (3′) containing an *Nde*I site (underlined) and the 3′ primer (5′) CTAGATTCGATTG-GTGCCATGG (3′) containing an *Nco*I site (underlined) were used to amplify 10 ng of the pAX-NMT-p28 plasmid in the presence of 2.5 U of Pfu DNA polymerase and dNTPs in the buffer supplied by the manufacturer (Stratagene, La Jolla, CA). The reactions were heated to 94°C for 2.5 min and 95°C for 0.5 min followed by 20 cycles at 94°C for 1 min, 56°C for 2 min, and 75°C for 5 min. In addition, an extra 5 min at 75°C was added to the last cycle. After verification by sequencing, the PCR product was digested with *Nde*I and *Nco*I, generating fragment A (~650 bp), which included the entire coding region of *Xenopus* p28. Fragment B (~1 kb) containing the 3′-untranslated region of *Xenopus* p28 was obtained by digesting *Xenopus* p28 in the pBlueScript vector (Stratagene) with *Nco*I and *Eco*RI. Finally, the bacterial expression vector pET9-His6 (Kumagai and Dunphy, 1995) and the insect cell expression vector pVL1393-His6 (Tang *et al.*, 1993) were digested with *Nde*I and *Eco*RI, and were ligated with fragments A and B through a three-piece ligation. The resulting plasmids pET9-His6-p28 and pVL1393-His6-p28 were used for production of recombinant proteins. Sequence alignments were performed using the PILEUP program.

Antibody Production

Rabbits were immunized either with a C-terminal peptide from *Xenopus* p28 (CPLEQTPRKKIR) coupled to keyhole limpet hemocyanin or with purified *Xenopus* p28 protein expressed in bacteria (see below). Anti-peptide antibodies were affinity-purified on Affi-Gel 10 columns (Bio-Rad, Hercules, CA) containing covalently attached peptides. Anti-p28 protein antibodies were affinity purified on purified p28 protein coupled to CNBr-activated Sepharose 4B columns (Pharmacia Biotech, Uppsala, Sweden). Affinity-purified anti-*Xenopus* cyclin E1 antibodies and anti-*Xenopus* Cdk2 antibodies were a generous gift from J. Maller (University of Colorado, Denver, CO). Purified monoclonal anti-human PCNA antibodies and polyclonal rabbit anti-human p21 antibodies were purchased from PharMingen (San Diego, CA). Affinity-purified rabbit anti-mouse IgG antibodies were purchased from Cappel (West Chester, PA). Antibodies to *Xenopus* Cdc2, cyclin A1, and cyclin B2 were generously provided by A. Kumagai (Kumagai and Dunphy, 1995; our unpublished results).

Production and Purification of Proteins from Insect Cells and Bacteria

The pET9-His6-p28 and pET3d-His6-human p21 (Xiong *et al.*, 1993) plasmids were transformed into BL21(DE3)pLysS bacteria. The bacteria were grown to mid-log phase and then induced, harvested, and lysed as described (Kumagai and Dunphy, 1991). The lysates were clarified and the p28 protein was purified by nickel-IDA Sepharose chromatography (Kumagai and Dunphy, 1995). In the case of *Xenopus* p28, the protein was further purified using SDS-PAGE followed by electro-eluting in an Elutrap (Schleicher & Schuell, Keene, NH). The pure protein was used to produce rabbit anti-*Xenopus* p28 protein antibodies.

Histidine-tagged *Xenopus* p28, histidine-tagged human cyclin B1 (Kumagai and Dunphy, 1995), and histidine-tagged human cyclin A and cyclin E (Desai *et al.*, 1992; Koff *et al.*, 1992) were purified from insect cell lysates using established protocols (Desai *et al.*, 1992). *Xenopus* Cdc2- or human Cdk2-containing lysates were aliquoted, drop frozen in liquid nitrogen, and stored at −80°C. ^{35}S-labeled His6-p28 was purified from metabolically labeled insect cells using a standard protocol (Kumagai and Dunphy, 1995).

In Vitro Cdk Inhibition Assays

Active Cdk2/cyclin A, Cdk2/cyclin E, and Cdc2/cyclin B complexes were prepared essentially as described previously (Kumagai and Dunphy, 1995). Briefly, 20 μl of histidine-tagged cyclins bound to nickel-IDA beads were agitated with 100 μl of Cdk2- or Cdc2-containing insect cell lysates in the presence of 0.5 mM ATP and 10 mM $MgCl_2$ for 20 min at room temperature. The beads were then washed four times with ice-cold HBS (150 mM NaCl, 10 mM *N*-2-hydroxyethylpiperazine-*N*′-2-ethanesulfonic acid, pH 7.5), and eluted with 20 μl of 300 mM imidazole in HBS. All kinase assays were performed in the linear range. Kinase complexes were mixed with increasing amounts of *Xenopus* p28 or human p21, preincubated on ice for 5 min, and finally histone H1 assays were performed as described in Dunphy and Newport (1989). To assess the effect of *Xenopus* p28 on the activation of the Cdc2/cyclin B complex in insect cell lysates, increasing amounts of p28 were incubated with Cdc2-containing insect cell lysates (2 μl) and purified cyclin B (0.3 μl) at room temperature for 20 min, and the histone H1 kinase activity was measured. Quantitation of kinase assays was performed with a PhosphorImager (Molecular Dynamics, Sunnyvale, CA).

Preparation of Extracts from Xenopus Eggs, Embryos, Oocytes, and Tissue Culture Cells

Xenopus cytostatic factor (CSF)-arrested egg extracts were prepared as described by Murray (1991). Interphase extracts were obtained by activation of CSF extracts with 0.4 mM $CaCl_2$. Freshly squeezed eggs were fertilized in vitro to obtain synchronously developing embryos (Newport and Kirschner, 1982a). Embryos were maintained in 0.2× MMR (Murray, 1991) for the first 6 h, and in 0.1× MMR thereafter. Embryos were staged according to the method of Nieuwkoop and Faber (1967). Typically, 20 embryos were homogenized in 200 μl of ice cold EB (80 mM β-glycerol phosphate, pH 7.3, 20 mM EGTA, and 15 mM $MgCl_2$) containing 1 mM dithiothreitol,

and 10 μg/ml each of pepstatin, chymostatin, and leupeptin (PCL). The homogenate was clarified by centrifugation at 16,000 × *g* for 5 min at 4°C. The crude cytoplasmic fraction was aliquoted and drop frozen in liquid nitrogen. Oocytes were separated from ovary tissue by treatment with collagenase (Cyert and Kirschner, 1988). Oocytes at different stages were manually selected and homogenized as described above for embryos. *Xenopus* tissue culture (XTC) cells were cultured using standard methods (Smith and Tata, 1991). Proliferating cells were harvested, and cell pellets were dissolved in SDS gel sample buffer.

Immunoprecipitation and Western Blotting

Affinity-purified anti-p28 protein antibodies (2 μg) or control rabbit anti-mouse IgG antibodies (2 μg) were incubated with protein A beads (Sigma, St. Louis, MO) in HBS for 1 h at 4°C. In the case of p21 immunoprecipitation, 2 μl of rabbit anti-human p21 antibodies were used. The antibody-coated beads were then incubated with mitotic extracts or interphase extracts for 1 h at 4°C. In some cases, recombinant p28 was added to the extracts, and in these experiments, cycloheximide was also included. Following incubation with the extracts, the beads were collected by centrifugation and washed four times with EB containing 0.1% NP-40, 25 μg/ml aprotinin, 1 mM phenylmethylsulfonyl fluoride, 1 mM benzamidine, and 10 μg/ml PCL, and then three times with HBS. All washes were done at 4°C. Similar washes were carried out for nickel-IDA beads recovered from the extracts (which had been diluted two-fold in EB containing PCL). To recover p28 using p13 beads, CSF extracts were incubated with a 25% volume of p13 beads (5 mg p13/ml beads) or control beads lacking p13 for 1 h at 4°C. Beads were removed by centrifugation, and the extracts were re-incubated with fresh beads. The p13 beads or the control beads were pooled, and washed as described for protein A beads. Immunoblotting using ^{125}I-labeled protein A (ICN, Irvine, CA) or ^{125}I-labeled sheep anti-mouse IgG antibodies (Amersham, Arlington Heights, IL) was performed as described (Coleman *et al.*, 1993). Alternatively, ECL (Amersham) was performed using horseradish peroxidase-conjugated goat anti-rabbit IgG antibodies (Bio-Rad).

Replication Assays

Replication assays were performed essentially as described previously (Dasso and Newport, 1990). Briefly, 40 μl of CSF extracts containing 100 μg/ml cycloheximide, 10 μCi [α-^{32}P]dCTP (ICN), and demembranated sperm nuclei (500 per μl) were incubated with 10 μl of Cdk inhibitors for 5 min at room temperature before activation with $CaCl_2$. At various time points, 3-μl aliquots were taken, mixed with replication sample buffer, and frozen at −20°C. The samples were digested with proteinase K (Boehringer Mannheim, Mannheim, Germany) and separated on a 0.8% agarose gel. Quantitation was performed using a PhosphorImager (Molecular Dynamics).

RESULTS

Isolation of Xenopus p28

To search for Cdk inhibitors from *Xenopus laevis*, we designed degenerate PCR primers based upon conserved residues in the Cdk inhibition domain of human and mouse p21^{CIP1} as well as human p27^{KIP1} (Figure 1A). PCR amplification of *Xenopus* oocyte cDNA yielded a ~130-bp fragment, which was used to isolate the corresponding full-length cDNA from an oocyte library. Several positive clones were identified; the longest (~1.7 kb) encodes a protein of 209 amino acids with a predicted molecular weight of 23,460 Da (Figure 1A). Since the endogenous protein in *Xenopus* extracts migrated at 28 kDa during SDS gel electrophoresis (see below), we have designated this protein as p28^{Kix1} (for cyclin-dependent kinase inhibitor from *Xenopus*).

The N-terminal region of p28 is 35% identical to p21/p27-class Cdk inhibitors (Figure 1A). The most noticeable conservation is within the Cdk inhibition domain (the hatched box in Figure 1B; residues 30–90 in p28), which in the cases of p21, p27, and p57, is sufficient to bind and inhibit Cdks (Polyak *et al.*, 1994b; Luo *et al.*, 1995). The C-terminal regions of p28, p21, and p27/p57 are less well conserved (21–25% identical), but they all have a putative nuclear localization signal. In the case of p28, residues 166–182 (KREITTPITDYFPKRKK; the black box in Figure 1B) fit the consensus for the bipartite nuclear localization signal first found in nucleoplasmin (Dingwall and Laskey, 1991). Moreover, p28 has several Ser/Thr-Pro motifs (stars in Figure 1B) that are potential sites for phosphorylation by various mitotic kinases. Recently, Su *et al.* (1995) have cloned a distinct *Xenopus* Cdk inhibitor (Xic1) that is 90% identical to Kix1 at the amino acid level, indicating that multiple genes for Cdk inhibitors are expressed in this organism.

Recombinant p28 Can Inhibit Cdks via Two Mechanisms

To characterize its biochemical properties, p28 was expressed as a histidine-tagged fusion protein in baculovirus-infected insect cells, and purified using nickel-IDA affinity chromatography (Figure 2). His6-p28 migrated with an apparent molecular weight of 28 kDa, slightly larger than the endogenous *Xenopus* p28 (see Figure 6A).

Because p28 possesses a Cdk inhibition domain similar to that of other p21/p27 Cdk inhibitors, we examined whether p28 could inhibit various recombinant Cdk complexes. In particular, the effect of p28 upon Cdk2/cyclin E, Cdk2/cyclin A, and Cdc2/cyclin B was examined. Active Cdk complexes were prepared by mixing insect cell lysates containing the individual Cdk components under conditions that allowed formation of the complex and its activation by an endogenous insect cell CAK. After Cdk complexes were purified by nickel-IDA chromatography and mixed with either human p21 or *Xenopus* p28, their activities were measured with histone H1 as the substrate (Figure 3A). As expected, p21 inhibited Cdk2/cyclin E in a dose-dependent manner (Figure 3, A and B). In parallel experiments, p28 effectively inhibited the kinase activity of both Cdk2/cyclin E and Cdk2/cyclin A when present in only a fivefold molar excess of the Cdk (Figure 3, A and B). In contrast, p28 displayed little inhibitory activity toward Cdc2/cyclin B even at molar concentrations ~800-fold higher than the Cdk

complex. Finally, like p21 and p27, *Xenopus* p28 is heat stable: heating p28 to 100°C for 5 min had little effect upon its capacity to inhibit Cdk2/cyclin E (Figure 3C). Taken together, these data suggest that p28 is a Cdk inhibitor with a striking preference for the G1/S Cdks over the mitotic Cdk in these in vitro assays.

In addition to directly inhibiting Cdk activity, both the p21/p27 and p15/p16 classes of inhibitors have been observed to exert their effects by preventing CAK-mediated activation of Cdks (Polyak *et al.*, 1994b; Aprelikova *et al.*, 1995). To investigate the possibility that p28 might have a similar function, we added p28 during the step at which the active Cdk complex was prepared. Although p28 did not inhibit pre-activated Cdc2/cyclin B, it nevertheless blocked the formation of the activated Cdc2/cyclin B complex. At a concentration of 160 nM, p28 elicited a 90% reduction in the H1 kinase activity generated by mixing insect cell lysates containing Cdc2 and cyclin B (Figure 3D). This inhibition coincided with a reduction in the level of the threonine-161-phosphorylated (active) form of Cdc2 (our unpublished results), indicating that p28 can interfere with CAK-mediated activation of Cdc2/cyclin B.

p28 Associates with Cyclin-dependent Kinases in Xenopus Extracts

Having characterized the effect of p28 upon recombinant Cdks, we examined whether p28 might associate with any of these Cdks in *Xenopus* egg extracts. As an initial method to monitor the association of p28 with Cdks in egg extracts, we utilized p13-agarose beads, an affinity matrix that binds Cdc2, Cdk2, and associated proteins. p28 was recovered efficiently by p13 beads but not control beads (Figure 4A), suggesting that endogenous p28 is associated with Cdks in egg extracts. To identify which Cdks associate with p28, we immunoprecipitated p28 from egg extracts with anti-p28 whole protein antibodies, and subsequently subjected the immunoprecipitates to immunoblotting with various antibodies. Cyclin E1 and cyclin A1 (Figure 4B), but not cyclin B2, co-immunoprecipitated with p28. We also probed the immunoprecipitates

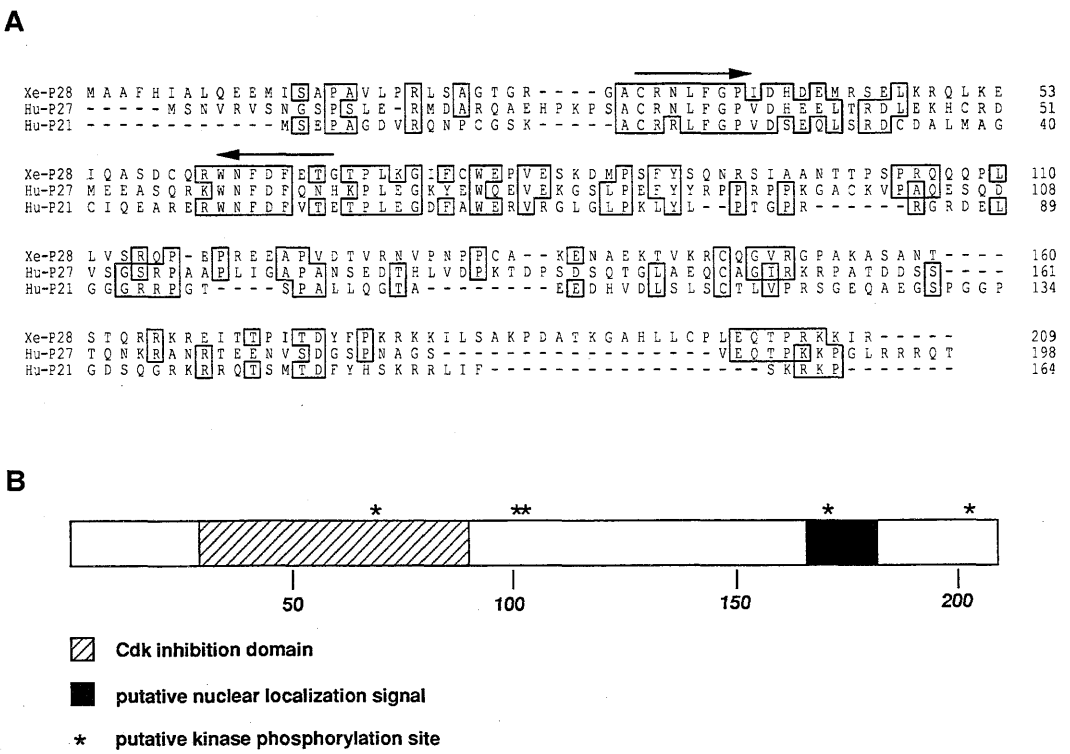

Figure 1. *Xenopus* p28 belongs to the $p21^{CIP1}/p27^{KIP1}$ Cdk inhibitor family. (A) Sequence alignment of *Xenopus* p28, human $p27^{KIP1}$, and human $p21^{CIP1}$. Boxes indicate identical residues shared by two or more sequences. Arrows mark sequences that were used to design degenerate PCR primers. (B) Schematic diagram of the domain structure of *Xenopus* p28. The CDK inhibition domain (hatched box) is conserved among *Xenopus* p28, human and mouse $p21^{CIP1}$, $p27^{KIP1}$, and $p57^{KIP2}$. A putative bipartite nuclear localization signal (black box) and several potential kinase phosphorylation sites (stars) are indicated. Numbers indicate amino acid residues.

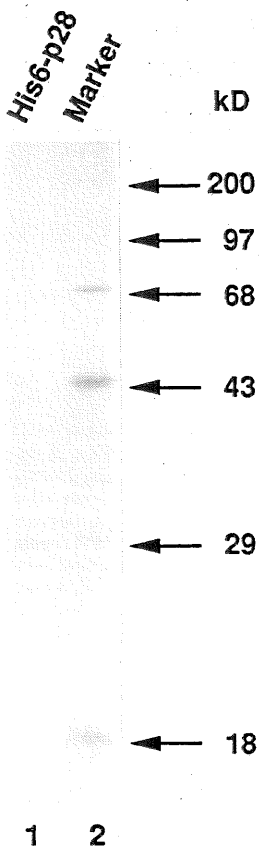

Figure 2. Purification of recombinant *Xenopus* p28. Recombinant His6-p28 was expressed in Sf9 insect cells and purified using nickel-IDA chromatography. Purified His6-p28 (lane 1) and molecular markers (lane 2) were run on a 12.5% SDS gel, and stained with Coomassie brilliant blue.

with anti-p28 antibodies to monitor the endogenous p28 protein (Figure 4B). Using recombinant p28 as a standard, we estimated that p28 was present at a rather low concentration (0.05 ng/μl, or 2 nM) in *Xenopus* egg extracts (our unpublished results). In control experiments with ^{35}S-labeled p28, we verified that the anti-p28 antibodies immunoprecipitated p28 quantitatively under these conditions. In accompanying studies, recombinant p28 was incubated with extracts, and then immunoprecipitated (Figure 4C). Immunoblotting of these immunoprecipitates revealed a significant association of p28 with cyclin E1 and Cdk2, but not cyclin B2. In addition, only small amounts of Cdc2 (perhaps complexed with cyclin A1 or A2) were detected in the anti-p28 immunoprecipitates.

Next, we tested whether p28 was modified during the cell cycle, and if so, whether this could affect its association with Cdks. Radiolabeled recombinant p28 was incubated with either mitotic or interphase extracts. The electrophoretic mobility of p28 incubated in mitotic extracts was reduced compared with p28 from interphase extracts (Figure 4D). Furthermore, the upshifted form of p28 could be shifted down by protein phosphatase 2A (our unpublished results), suggesting that certain kinase(s) in mitotic extracts can phosphorylate p28. Although p28 was differentially phosphorylated during the cell cycle, its association with Cdk complexes did not vary discernibly (Figure 4, B and C).

The C-terminal domain of human p21 associates with the replication and repair factor PCNA (Waga *et al.*, 1994; Chen *et al.*, 1995; Luo *et al.*, 1995). To determine whether p28 could bind PCNA, equivalent amounts (0.12 μg) of recombinant p28 or human p21 (as a positive control) were added to extracts, immunoprecipitated with their respective antibodies, and immunoblotted with anti-human PCNA antibodies, which cross-react well with *Xenopus* PCNA. As anticipated, anti-human p21 antibodies immunoprecipitated PCNA. In contrast, PCNA was not readily detected in anti-p28 immunoprecipitates (Figure 4E), suggesting that either p28 does not bind to PCNA or it binds more weakly than human p21. To explore this issue further, approximately 40-fold more recombinant p28 was added to the *Xenopus* extracts, and was later recovered with nickel-IDA beads. We observed that p28 could associate with PCNA under these conditions, but the amount of PCNA bound to 5 μg of p28 was less than that bound to 0.7 μg of p21 (Figure 4E). Thus, $p28^{Kix1}$, like the recently described Xic1 protein (Su *et al.*, 1995), can associate with PCNA, but not nearly as efficiently as human p21.

p28 Inhibits Chromosomal Replication and Mitosis in a Dose-dependent Manner

To explore further the functional properties of p28, we added recombinant p28 to cell cycle extracts from *Xenopus* eggs (Murray, 1991). Upon activation with Ca^{2+}, CSF-arrested mitotic egg extracts enter interphase, undergo a complete round of semi-conservative DNA replication, and enter mitosis shortly thereafter. Tracer radiolabeled p28 was found to be stable in extracts throughout the duration of such experiments.

We first asked whether p28 would affect chromosomal DNA replication, which is known to require Cdk2/cyclin E activity (Jackson *et al.*, 1995). Using [α-^{32}P]dCTP as a tracer, the extent of DNA replication was assessed at various time points after Ca^{2+} activation. In control extracts treated with buffer only, replication commenced between 30 and 45 min after Ca^{2+} addition, and was essentially complete by 120 min (Figure 5A). However, in extracts containing added p28, there was a strong inhibition of DNA replication (Figure 5A). At the highest concentration of p28 tested (1.6 μM), there was essentially no replication within the first 90 min. At later times, even though a small amount of replication took place, it clearly occurred at a substantially reduced rate relative to the control

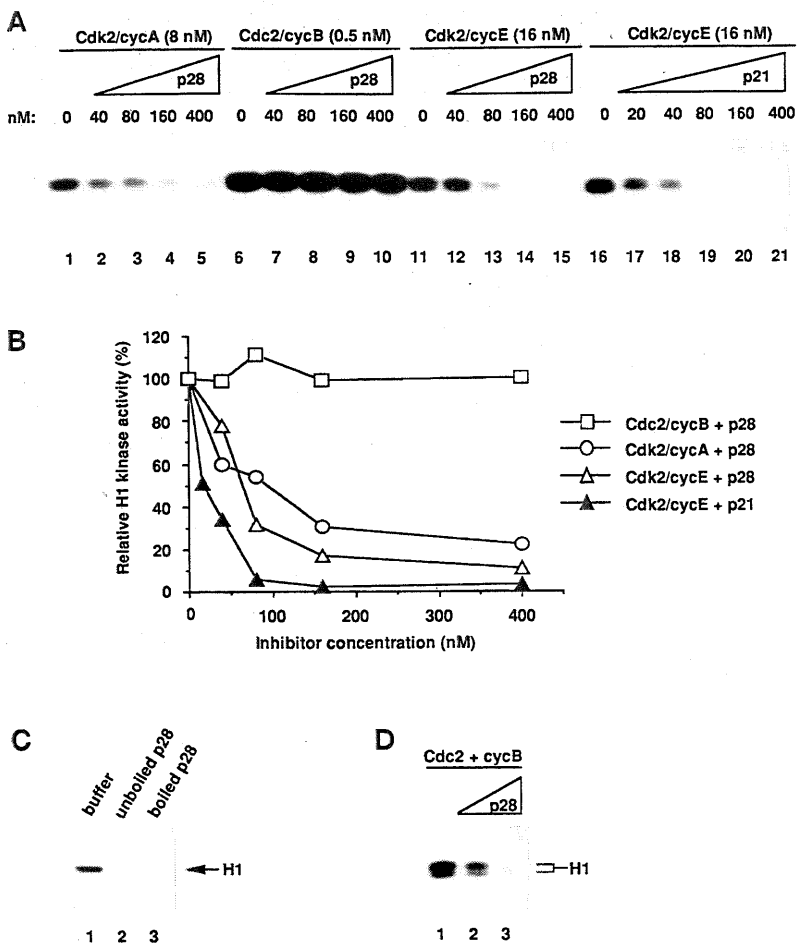

Figure 3. *Xenopus* p28 exhibits differential inhibitory activities toward various Cdk complexes. (A) Pre-activated Cdk2/cyclin A (lanes 1–5), Cdc2/cyclin B (lanes 6–10), and Cdk2/cyclin E (lanes 11–15) were incubated with the indicated amounts of p28. As a control, pre-activated Cdk2/cyclin E was also incubated with the indicated amounts of human $p21^{CIP1}$ under identical conditions (lanes 16–21). The H1 kinase activities of the Cdks were then measured. (B) H1 kinase activities in panel A were quantitated, and are plotted as the percentage of kinase activity in the absence of inhibitors. (C) p28 is heat stable. H1 kinase activities of Cdk2/cyclin E complex (16 nM) in the presence of control buffer (lane 1), native p28 (80 nM, lane 2), or p28 that had been boiled at 100°C for 5 min (80 nM, lane 3) were assayed. (D) p28 inhibits Cdc2/cyclin B activation. Cdc2-containing insect cell lysates were incubated at room temperature with purified cyclin B in the presence of either control buffer (lane 1) or p28 (40 nM, lane 2; 160 nM, lane 3). The mixtures were then subjected to H1 kinase assays.

extracts. A similar phenomenon was observed in extracts supplemented with the same amount of human p21 (Figure 5A). At lower concentrations of p28, the onset of replication was delayed in a dose-dependent fashion (Figure 5, A and B). In particular, replication commenced at 90 min and 60 min at p28 concentrations of 800 nM and 320 nM, respectively. Interestingly, once replication began, it proceeded at a similar rate to that in the control extracts. This observation might suggest that at lower concentrations (≤800 nM), p28 has a preferential effect on initiation versus elongation, whereas at higher concentrations, both processes are compromised. Finally, because chromosomal replication in egg extracts requires that the DNA be properly assembled into a nuclear structure, we verified by phase and fluorescence microscopy that the control and inhibitor-treated extracts were equally competent for nuclear assembly (our unpublished results).

We also examined whether recombinant p28 could affect the entry into mitosis in extracts containing a very low concentration of sperm chromatin (25 demembranated sperm nuclei per microliter of extract). It has been shown previously that this concentration of sperm nuclei is below the threshold necessary to trigger the replication checkpoint (Dasso and Newport, 1990). These extracts allow a direct assessment of the effect of p28 on mitosis independent of its effect on replication. Intriguingly, we observed that p28 elicited a dose-dependent delay of mitosis relative to control extracts (Figure 6A). At a concentration of 800 nM, p28 delayed mitosis by approximately 60 min. In parallel, we examined the effect of p28 (800 nM) on total H1 kinase activity during the cell cycle in egg extracts (Figure 6B). As expected, p28 suppressed the rise in H1 kinase activity that occurred in the control extracts at 90 min. Significantly, exogenously added

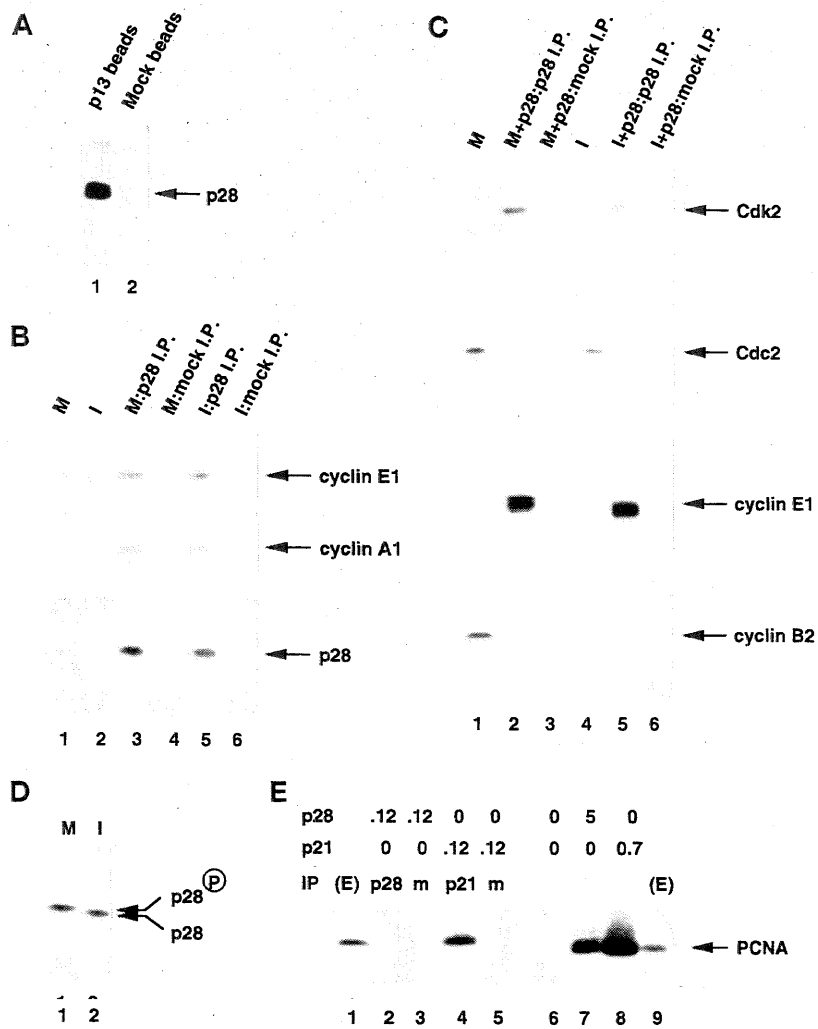

Figure 4. p28 associates with Cdks in *Xenopus* egg extracts. (A) M-phase extracts (160 μl) were rotated with p13 (lane 1) or control (lane 2) agarose beads. The beads were then washed and immunoblotted with anti-p28 peptide antibodies. (B) Mitotic (M-phase) extracts (300 μl, lanes 3 and 4) and interphase (I-phase) extracts (300 μl, lanes 5 and 6) were immunoprecipitated with anti-*Xenopus* p28 whole protein antibodies (lanes 3 and 5) or with control rabbit anti-mouse IgG antibodies (lanes 4 and 6). The total immunoprecipitates or M-phase and I-phase extracts (2 μl, lanes 1 and 2, respectively) were probed with antibodies against *Xenopus* cyclin E1, cyclin A1, and p28 as indicated. (C) Recombinant p28 (10 ng) was added to 100 μl of M-phase (lanes 2 and 3) or I-phase (lanes 5 and 6) extract. The total anti-p28 immunoprecipitates (lanes 2 and 5) and mock immunoprecipitates (lanes 3 and 6) from these extracts or 2 μl of M-phase and I-phase extract (lanes 1 and 4, respectively) were subsequently probed with antibodies against *Xenopus* Cdk2, Cdc2, cyclin E1, and cyclin B2 as indicated. (D) ^{35}S-labeled p28 was added to M-phase (lane 1) and I-phase (lane 2) extracts. The slower-migrating form in lane 1 corresponds to the phosphorylated p28. (E) Lanes 2–5: the indicated amounts (in μg) of His6-p28 or His6-p21 were added to M-phase extracts (50 μl), and immunoprecipitated with anti-*Xenopus* p28 (lane 2), or anti-human p21 (lane 4) antibodies, or mock-precipitated (m) with control rabbit anti-mouse IgG antibodies (lanes 3 and 5). Lanes 6–8: nickel-IDA beads and the indicated amounts (in μg) of His6-p28 or His6-p21 were incubated in 200 μl of two-fold diluted M-phase extract, and the beads were then recovered. The immunoprecipitates, the nickel-IDA beads, or M-phase extracts (E) (0.5 μl, lane 1; 1 μl, lane 9) were probed with anti-human PCNA antibodies.

p28 also depressed the level of H1 kinase activity at early times in the cell cycle (i.e., 30 min) when relatively little active Cdc2/cyclin B would be expected to be present. This effect could be due to inhibition of the Cdk2/cyclin E complex, which shows significant activity throughout the early embryonic cell cycles (Rempel *et al.*, 1995), or, alternatively, another unidentified Cdk. Taken together, our results indicate that at sufficiently high levels, not only does p28 abolish DNA replication, it also strongly inhibits entry into mitosis.

The Abundance of p28 Varies during Development

The abundance of p28 in *Xenopus* eggs is approximately 2 nM, whereas the concentration of recombinant p28 required to either inhibit recombinant Cdks in vitro or affect cell cycle progression in egg extracts is approximately 100-fold higher. To evaluate this paradox, we asked whether p28 might be expressed at higher levels during later stages of development when dividing cells acquire an extended G1 phase or withdraw from the cell cycle. For this purpose, extracts from oocytes, eggs, stage 26 embryos, and somatic XTC cells were immunoblotted with antibodies directed toward a C-terminal peptide of *Xenopus* p28. Although the level of p28 was similarly low in oocytes and mature eggs (~2 nM), it was approximately 100-fold higher in stage 26 embryos and XTC cells where the "somatic" cell cycle has replaced the "embryonic" one (Figure 7A). To pinpoint more precisely at what stage during development p28 begins to be up-

regulated, embryonic lysates were prepared at finer time points. The level of p28 remained low throughout the blastula and early gastrula stages. However, it increased dramatically between stages 12 and 13, and by stage 14, it had peaked to a level that remained relatively constant until at least stage 26 (Figure 7B; our unpublished results). The up-regulation of p28 occurs at ~5 h after the commencement of gastrulation, a time corresponding most closely to the small yolk plug stage and the slit-blastopore stage when the neural plate first becomes discernible.

To verify that the protein detected in these experiments is *Xenopus* p28, a peptide-competition experiment was carried out (Figures 7C). Immunoblots containing recombinant p28 and stage 26 embryonic lysates were treated with anti-p28 antibodies in the presence or absence of the immunizing peptide. The staining of both recombinant and embryonic p28 was abolished by the peptide, whereas that of a background band was unaffected. Taken together, these experiments indicate that the expression of p28 increases as cells acquire a somatic type of cell cycle.

DISCUSSION

To study the potential regulation of the cell cycle by Cdk inhibitors in *Xenopus* egg extracts, we have isolated *Xenopus* p28, a new member of the $p21^{CIP1}$/$p27^{KIP1}$/$p57^{KIP2}$ family of Cdk inhibitors. The Cdk inhibition domain of p28 shows significant sequence homology to those of p21, p27, and p57. Indeed, p28 effectively inhibits pre-activated G1/S Cdks, such as Cdk2/cyclin E and Cdk2/cyclin A, while exhibiting little inhibitory activity toward the mitotic Cdc2/cyclin B complex in vitro, like some other members of the family (Harper *et al.*, 1995; Lee *et al.*, 1995). Consistent with this observation, Cdk2, cyclin A, and cyclin E in egg extracts can be co-immunoprecipitated with p28, whereas the Cdc2/cyclin B complex appears not to be stably associated with p28.

It has been shown previously that Cdk inhibitors in the p21/p27/p57 class are also able to block the phosphorylation and activation of Cdks by CAK without directly binding to CAK or inhibiting CAK activity (Harper *et al.*, 1993, 1995; Polyak *et al.*, 1994b; Aprelikova *et al.*, 1995; Matsuoka *et al.*, 1995). p28 has

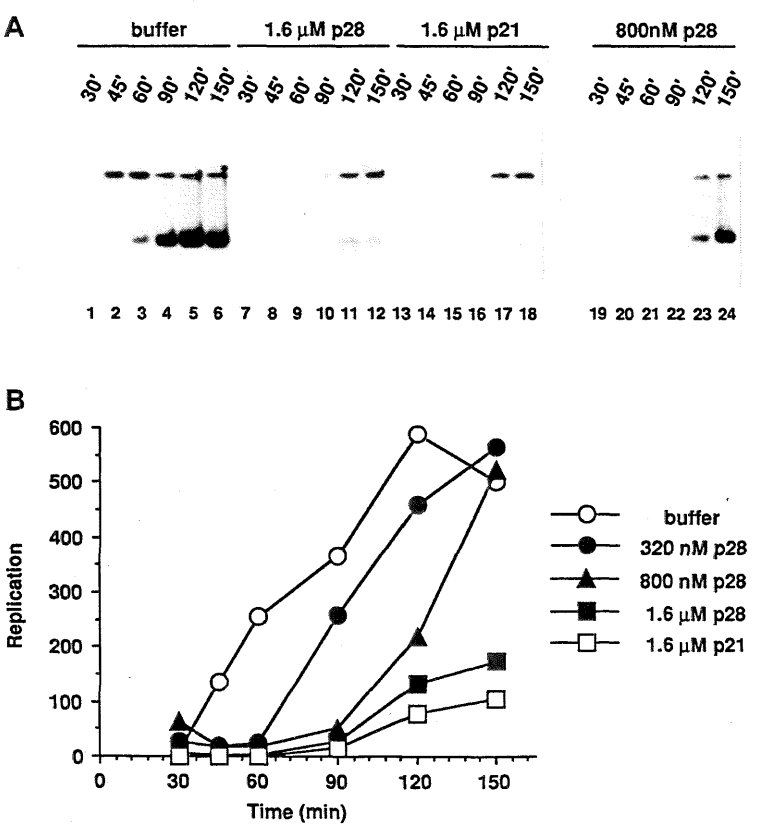

Figure 5. *Xenopus* p28 inhibits chromosomal replication in a dose-dependent manner. (A) CSF-arrested extracts (500 sperm nuclei/μl, 0.2 μCi [α-^{32}P]dCTP/μl) were incubated with buffer (lanes 1–6), *Xenopus* p28 (1.6 μM, lanes 7–12; 0.8 μM, lanes 19–24), or human $p21^{CIP1}$ (1.6 μM, lanes 13–18). The extracts were then activated by $CaCl_2$, and at the indicated time points, samples were taken to assay the extent of replication by monitoring the total incorporation of [^{32}P]dCTP into DNA. (B) Quantitation of various replication assays in arbitrary units (including those presented in part A).

similar properties. In particular, p28 does not bind to recombinant human CAK (our unpublished results), nor does it inhibit the kinase activity of CAK toward the C-terminal peptide of RNA polymerase II (our unpublished results). However, p28 prevents Cdc2/cyclin B activation by CAK, suggesting that despite the apparent preference for G1/S Cdks, p28 could down-regulate mitotic Cdk activities through prevention of CAK-mediated activation. It seems paradoxical that p28 has little affinity for Cdc2/cyclin B or CAK, yet it is able to prevent the latter from activating the former. One possible explanation is based on the observation that multiple molecules of p21 are required to inhibit Cdks and that complexes containing a single p21 molecule are active (Zhang *et al.*, 1994). Thus, it is possible that a single molecule of p28 could bind the Cdc2/cyclin B complex to block CAK-mediated activation, whereas multiple molecules of p28 could not efficiently associate with and inhibit the pre-activated complex. Alternatively, the off-rate of p28 from Cdc2/cyclin B and/or CAK might be fast so that the kinase-inhibitor complexes do not survive successive washing steps in our binding assays. p28 would presumably also inhibit the CAK-mediated activation of Cdk2/cyclin E and Cdk2/cyclin A, since it has a higher affinity for these Cdks.

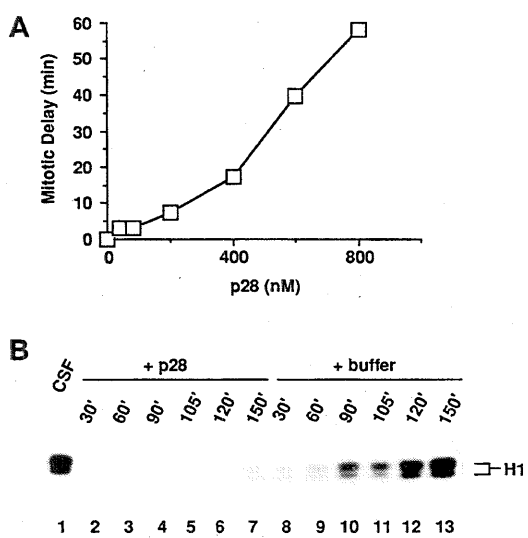

Figure 6. *Xenopus* p28 inhibits mitosis in a dose-dependent manner. (A) CSF extracts (containing 25 sperm nuclei/μl extract) were mixed with various amounts of *Xenopus* p28 protein and then activated. Entry into mitosis was scored visually and was defined as the time point where 50% of the nuclear envelopes had broken down relative to buffer-treated extracts. (B) H1 kinase activities of a CSF extract (lane 1) or activated extracts containing either p28 (800 nM, lanes 2–7) or control buffer (lanes 8–13) were measured at the indicated times after Ca^{2+} addition. The p28-treated and the control extracts entered mitosis at 150 min and 90 min, respectively.

We also analyzed the biochemical functions of p28 by adding recombinant p28 to *Xenopus* egg extracts. Cdk2/cyclin E activity is required for the initiation of chromosomal DNA replication in this system (Jackson *et al.*, 1995). In egg extracts, the concentration of cyclin E1 is ~60 nM (Rempel *et al.*, 1995). At a fivefold molar excess above cyclin E1, p28 elicited a readily observable delay in the onset of replication, consistent with the observed inhibitory effects of p28 on recombinant Cdk2/cyclin E complex. Intriguingly, although there was a delay in the onset of DNA synthesis, once replication began, it proceeded at a rate comparable to that in control extracts. At higher levels of p28, both the rate and the overall extent of DNA replication were severely inhibited. These findings could argue that although p28 preferentially inhibits initiation as opposed to elongation, at higher concentrations, p28 could inhibit elongation as well. An alternative possibility would be that when the level of p28 is high, some replication origins could fire late, giving rise to an extended S phase reminiscent of the somatic cell cycle (for review, see Fangman and Brewer, 1992). Finally, p28 could block initiation of some replication origins, possibly by preventing the transition from pre-replicative foci to initiation complex, a phenomenon previously observed when high levels (1–2 μM) of human p21 were added to extracts (Jackson *et al.*, 1995; Yan and Newport, 1995). Further mechanistic studies will be required to evaluate these possibilities.

We have observed that p28 also elicits a dose-dependent delay of mitosis. In principle, this mitotic delay could result from the replication checkpoint responding to p28-dependent inhibition of DNA synthesis. However, we feel that this explanation is not likely because p28 elicits a mitotic delay even in the presence of a concentration of sperm chromatin (25 sperm/μl of extract) well below the threshold required to trigger the replication checkpoint in this system (Dasso and Newport, 1990). One explanation is that p28 delays mitosis by inhibiting the CAK-mediated activation of Cdc2/cyclin B, which would be consistent with the ability of p28 to block the activation of Cdc2/cyclin B in insect cell lysates. Alternatively, it is conceivable that p28 could be a more potent inhibitor of the endogenous Cdc2/cyclin B in egg extracts than the purified recombinant Cdc2/cyclin B. Finally, it could be that cyclin E1- and/or cyclin A-associated kinase activities play an additional essential role in mitosis, and that by inhibiting the kinase activities associated with these cyclins, p28 impedes the entry into mitosis.

An important characteristic of human p21 is that it can form a stable complex with the replication factor PCNA. The PCNA-interacting domain of p21 has been mapped to the peptide QTSMTDFY (residues 144–151) (Warbrick *et al.*, 1995). The three residues that contribute the most to PCNA binding in p21 (Q144, M147, and F150) are not conserved in *Xenopus* $p28^{Kix1}$

or Xic1 (Su *et al.*, 1995), which could account for the observation that PCNA binds *Xenopus* p28 much less well than it binds human p21. Human and mouse p27 apparently do not interact with PCNA (Luo *et al.*, 1995), raising the possibility that *Xenopus* p28 may belong to the mammalian p21 subfamily. However, the C-terminal domain of p28 does contain a QT motif (LEQTPRK, residues 200–206) that is found in mammalian p27 and p57 (see Matsuoka *et al.*, 1995). Thus, further characterization of p28 will be required to classify this Cdk inhibitor definitively.

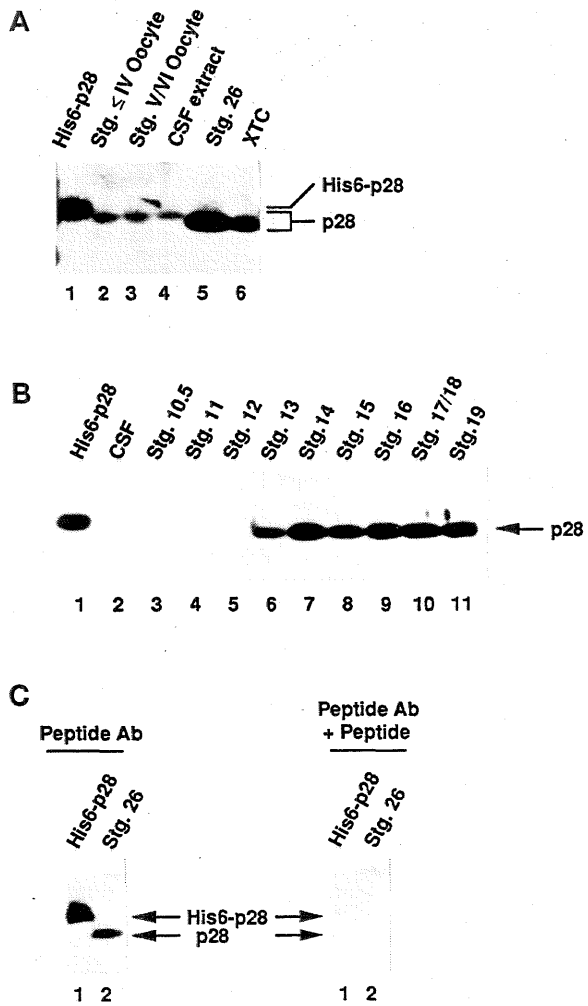

Figure 7. *Xenopus* p28 is developmentally regulated. (A) A comparison of p28 protein levels during *Xenopus* development. His6-p28 (10 ng, lane 1) and extracts made from stage IV or earlier oocytes (100 μg, lane 2), stage V/VI oocytes (100 μg, lane 3), CSF-arrested eggs (100 μg, lane 4), stage 26 embryos (60 μg, lane 5), and XTC cells (60 μg, lane 6) were immunoblotted with anti-p28 peptide antibodies. (B) The p28 protein level is elevated during stages 12 and 13. One nanogram of His6-p28 (lane 1), 100 μg of CSF extract (lane 2), and 60 μg of extract made from embryos at the indicated stages (lanes 3–11) were immunoblotted with anti-p28 peptide antibodies. (C) Peptide-blocking assay. Identical strips containing His6-p28 and stage 26 embryo extracts were immunoblotted with anti-p28 peptide antibodies (400 ng/ml) in the absence (left panel) or presence (right panel) of the p28 C-terminal peptide (200 ng/ml). All blots were visualized using ECL.

The p28 is present at low levels in oocytes, mature eggs, and embryos up to stage 11. During this period, its concentration is ~2 nM, well below the concentration of 60 nM at which its preferred target, cyclin E1, is present (Rempel *et al.*, 1995). The next best candidate, namely cyclin A1, is also more abundant (18 nM-60 nM) than p28 in *Xenopus* eggs (Rempel *et al.*, 1995). Although it is conceivable that p28 might regulate a Cdk distinct from cyclin E1 and cyclin A1, a more plausible scenario is that p28 does not play a rate-limiting role in controlling the onset of replication or mitosis during early embryogenesis. This notion would be consistent with the fact that the early embryonic cleavages occur very rapidly (i.e., approximately every 35 min) without any discernible gaps between S-phase and M-phase. The midblastula transition (stage 8½) defines the first developmental event where the cell cycles in certain embryonic cells begin to slow down and become asynchronous with respect to one another (Newport and Kirschner, 1982a). This transition also coincides with the commencement of zygotic transcription (Newport and Kirschner, 1982b). Later, at stage 10, another major transition occurs during early gastrulation. This early gastrulation transition is marked by the elimination of maternal mRNAs for cyclins A1 and A2 (Howe *et al.*, 1995). In parallel, the amount of cyclin A1 protein drops precipitously to undetectable levels, whereas the level of cyclin A2 protein translated from zygotic cyclin A2 mRNA increases dramatically (Howe *et al.*, 1995; see also Rempel *et al.*, 1995). The level of *Xenopus* p28 protein remains low at both the midblastula transition and early gastrulation transition, but it does increase dramatically at a significantly later time, namely during stages 12 and 13. In principle, the up-regulation of p28 at stages 12 and 13 could mark another developmental transition at late gastrulation in the *Xenopus* embryo. Alternatively, the increase in the levels of p28 could represent a more specialized regulatory mechanism that selectively targets certain cell types. The period encompassing stages 12 and 13 coincides with numerous significant events in development. In the case of neuronal differentiation, primary neuronal precursors undergo their final round of DNA replication (stage 12), the transcript for neuronal signaling molecule X-Delta-1 becomes expressed in prospective neurons (stage 12), and the gene for neuron-specific type-II β-tubulin is turned on in scattered cells in the neural plate (stage 12.5–13) (Hartenstein, 1989; Chitnis *et al.*, 1995). Clearly, it will be highly important to localize

the p28 mRNA and protein by in situ methods to delineate precisely the developmental events that might be related to the up-regulation of p28. In any case, it appears likely that p28, like p21, p27, and p57, may play a role in cellular differentiation. The target of p28 in later embryos has not been established, but cyclin D, the presumed somatic form of cyclin E, or the recently described somatic cyclin A2 are potential candidates (Howe *et al.*, 1995; Rempel *et al.*, 1995).

In summary, we have identified *Xenopus* p28, a new member of the p21/p27 class of Cdk inhibitors. In vitro, p28 inhibits pre-activated Cdk2/cyclin E and Cdk2/cyclin A, and prevents CAK-mediated activation of Cdc2/cyclin B. In *Xenopus* egg extracts, exogenously added p28 inhibits both DNA replication and mitosis. Finally, the level of p28 protein is up-regulated dramatically during stages 12 and 13, which temporally correlates with the earliest events in neural differentiation. In concert with other transitions such as the replacement of embryonic Cdks with somatic Cdks, p28 could play an important role in regulating the somatic cell cycle. Further study of p28 will help us to gain more insight into cell cycle regulation and its connection with developmental regulation.

ACKNOWLEDGMENTS

We thank T.R. Coleman, A. Kumagai, P.R. Mueller, D. Patra, P.B. Carpenter, B.J. Wold, R.J. Deshaies, G.P. Moore, M.P. Running, and the anonymous reviewers for comments on the manuscript. W.S. is especially indebted to A. Kumagai, P.R. Mueller, R.J. Deshaies, B.J. Wold, and Z. Shou for being excellent mentors. We thank P.R. Mueller for the oocyte cDNA, oocyte cDNA library, and XTC lysates; A. Kumagai for antibodies to *Xenopus* Cdc2, cyclin A1, and cyclin B2, and for purified human cyclin B1 protein; J. Maller (University of Colorado, Denver, CO) for antibodies to *Xenopus* Cdk2 and cyclin E1; D. Morgan (University of California, San Francisco, CA) for recombinant baculoviruses encoding human Cdk2, cyclin A, cyclin E, Cdk7, and cyclin H; and D. Beach (Cold Spring Harbor Laboratory, Cold Spring Harbor, NY) for human p21 bacterial expression plasmid. W.S. is a predoctoral fellow and W.G.D. is an investigator of the Howard Hughes Medical Institute.

REFERENCES

Aprelikova, O., Xiong, Y., and Liu, E.T. (1995). Both p16 and p21 families of cyclin-dependent kinase (Cdk) inhibitors block the phosphorylation of cyclin-dependent kinases by the Cdk-activating kinase. J. Biol. Chem. *270*, 18195–18197.

Chan, F.K.M., Zhang, J., Cheng, L., Shapiro, D.N., and Winoto, A. (1995). Identification of human and mouse p19, a novel Cdk4 and Cdk6 inhibitor with homology to $p16^{ink4}$. Mol. Cell. Biol. *15*, 2682–2688.

Chen, J., Jackson, P.K., Kirschner, M.W., and Dutta, A. (1995). Separate domains of p21 involved in the inhibition of Cdk kinase and PCNA. Nature *374*, 386–388.

Chitnis, A., Henrique, D., Lewis, J., Ish-Horowicz, D., and Kintner, C. (1995). Primary neurogenesis in *Xenopus* embryos regulated by a homologue of the *Drosophila* neurogenic gene *Delta*. Nature *375*, 761–766.

Coleman, T.R., Tang, Z., and Dunphy, W.G. (1993). Negative regulation of the wee1 protein kinase by direct action of the nim1/cdr1 mitotic inducer. Cell *72*, 919–929.

Cyert, M.S., and Kirschner, M.W. (1988). Regulation of MPF activity in vitro. Cell *53*, 185–195.

Dasso, M., and Newport, J.W. (1990). Completion of DNA replication is monitored by a feedback system that controls the initiation of mitosis in vitro: studies in *Xenopus*. Cell *61*, 811–823.

Deng, C., Zhang, P., Harper, J.W., Elledge, S.J., and Leder, P. (1995). Mice lacking $P21^{CIP1/WAF1}$ undergo normal development, but are defective in G1 checkpoint control. Cell *82*, 675–684.

Desai, D., Gu, Y., and Morgan, D.O. (1992). Activation of human cyclin-dependent kinases in vitro. Mol. Biol. Cell *3*, 571–582.

Dingwall, C., and Laskey, R.A. (1991). Nuclear targeting sequences: a consensus? Trends Biochem. Sci. *16*, 478–481.

Draetta, G., (1993). Cdc2 activation: the interplay of cyclin binding and Thr161 phosphorylation. Trends Cell Biol. *3*, 287–289.

Dunphy, W.G., and Newport, J.W. (1989). Fission yeast p13 blocks mitotic activation and tyrosine dephosphorylation of the *Xenopus* cdc2 protein kinase. Cell *58*, 181–191.

El-Deiry, W.S., Tokino, T., Velculescu, V.E., Levy, D.B., Parsons, R., Trent, J.M., Lin, D., Mercer, W.E., Kinzler, K.W., and Vogelstein, B. (1993). WAF1, a potential mediator of p53 tumor suppression. Cell *75*, 817–825.

Elledge, S.J., and Harper, J.W. (1994). Cdk inhibitors: on the threshold of checkpoints and development. Curr. Opin. Cell Biol. *6*, 847–852.

Fangman, W.L., and Brewer, B.J. (1992). A question of time: replication origins of eukaryotic chromosomes. Cell *71*, 363–366.

Gu, Y., Turck, C.W., and Morgan, D.O. (1993). Inhibition of Cdk2 activity in vivo by an associated 20K regulatory subunit. Nature *366*, 707–710.

Guan, K.-L., Jenkins, C.W., Li, Y., Nichols, M.A., Wu, X., O'Keefe, C.L., Matera, A.G., and Xiong, Y. (1994). Growth suppression by p18, a $p16^{INK4/MTS1}$ and $p14^{INK4B/MTS2}$-related CDK6 inhibitor, correlates with wild-type pRb function. Genes Dev. *8*, 2939–2952.

Halevy, O., Novitch, B.G., Spicer, D.B., Skapek, S.X., Rhee, J., Hannon, G.J., Beach, D., and Lassar, A.B. (1995). Correlation of terminal cell-cycle arrest of skeletal-muscle with induction of p21 by MyoD. Science *267*, 1018–1021.

Hannon, G.J., and Beach, D. (1994). $p15^{INK4B}$ is a potential effector of TGFβ-induced cell cycle arrest. Nature *371*, 257–261.

Harper, J.W., Adami, G., Wei, N., Keyomarsi, K., and Elledge, S.J. (1993). The p21 Cdk-interacting protein Cip1 is a potent inhibitor of G1 cyclin-dependent kinases. Cell *75*, 805–816.

Harper, J.W., *et al.* (1995). Inhibition of cyclin-dependent kinases by p21. Mol. Biol. Cell *6*, 387–400.

Hartenstein, V. (1989). Early neurogenesis in *Xenopus*: the spatiotemporal pattern of proliferation and cell lineages in the embryonic spinal cord. Neuron *3*, 399–411.

Howe, J.A., Howell, M., Hunt, T., and Newport, J.W. (1995). Identification of a developmental timer regulating the stability of embryonic cyclin A and a new somatic A-type cyclin at gastrulation. Genes Dev. *9*, 1164–1176.

Jackson, P.K., Chevalier, S., Philippe, M., and Kirschner, M.W. (1995). Early events in DNA replication require cyclin E and are blocked by $p21^{CIP1}$. J. Cell Biol. *130*, 755–769.

Kato, J.-Y., Matsuoka, M., Polyak, K., Massagué, J., and Sherr, C.J. (1994). Cyclic AMP-induced G1 phase arrest mediated by an inhib-

itor ($p27^{KIP1}$) of cyclin-dependent kinase-4 activation. Cell *79*, 487–496.

Koff, A., Giordano, A., Desai, D., Yamashita, K., Harper, J.W., Elledge, S., Nishimoto, T., Morgan, D.O., Franza, B.R., and Roberts, J.M. (1992). Formation and activation of a cyclin E-Cdk2 complex during the G1 phase of the human cell cycle. Science *257*, 1689–1694.

Kumagai, A., and Dunphy, W.G. (1991). The cdc25 protein controls tyrosine dephosphorylation of the cdc2 protein in a cell-free system. Cell *64*, 903–914.

Kumagai, A., and Dunphy, W.G. (1995). Control of the cdc2/cyclin B complex in *Xenopus* egg extracts arrested at a G2/M checkpoint with DNA synthesis inhibitors. Mol. Biol. Cell *6*, 199–213.

Lee, M.-H., Reynisdottir, I., and Massagué, J. (1995). Cloning of $p57^{KIP2}$, a cyclin-dependent kinase inhibitor with unique domain structure and tissue distribution. Genes Dev. *9*, 639–649.

Leno, G.H., and Laskey, R.A. (1991). DNA replication in cell-free extracts from *Xenopus laevis*. Methods Cell Biol. *36*, 561–579.

Li, R., Waga, S., Hannon, G.J., Beach, D., and Stillman, B. (1994). Differential effects by the p21 Cdk inhibitor on PCNA-dependent DNA replication and repair. Nature *371*, 534–537.

Luo, Y., Hurwitz, J., and Massagué, J. (1995). Cell-cycle inhibition by independent Cdk and PCNA binding domains in $p21^{CIP1}$. Nature *375*, 159–161.

Massagué, J., and Polyak, K. (1995). Mammalian antiproliferative signals and their targets. Curr. Opin. Genet. Dev. *5*, 91–96.

Matsuoka, S., Edwards, M.C., Bai, C., Parker, S., Zhang, P., Baldini, A., Harper, J.W., and Elledge, S.J. (1995). $p57^{KIP2}$, a structurally distinct member of the $p21^{CIP1}$ Cdk inhibitor family, is a candidate tumor-suppressor gene. Genes Dev. *9*, 650–662.

Minshull, J., Sun, H., Tonks, N.K., and Murray, A.W. (1994). A MAP kinase-dependent spindle assembly checkpoint in *Xenopus* egg extracts. Cell *79*, 475–486.

Mueller, P.R., Coleman, T.R., and Dunphy, W.G. (1995). Cell cycle regulation of a *Xenopus* Wee1-like kinase. Mol. Biol. Cell *6*, 119–134.

Murray, A.W. (1991). Cell cycle extracts. Methods Cell Biol. *36*, 581–605.

Newport, J., and Kirschner, M. (1982a). A major developmental transition in early *Xenopus* embryos. I. Characterization and timing of cellular changes at the midblastula stage. Cell *30*, 675–686.

Newport, J., and Kirschner, M. (1982b). A major developmental transition in early *Xenopus* embryos. II. Control of the onset of transcription. Cell *30*, 687–696.

Nieuwkoop, P., and Faber, J. (1967). Normal table of *Xenopus laevis* (Daudin), Amsterdam, The Netherlands: North Holland Publishing.

Noda, A., Ning, Y., Venable, S.F., Pereira-Smith, O.M., and Smith, J.R. (1994). Cloning of senescent cell-derived inhibitors of DNA synthesis using an expression screen. Exp. Cell Res. *211*, 90–98.

Nourse, J., Firpo, E., Flanagan, W.M., Coats, S., Polyak, K., Lee, M.-H., Massagué, J., Crabtree, G.R., and Roberts, J.M. (1994). Interleukin 2-mediated elimination of the $p27^{KIP1}$ cyclin-dependent kinase inhibitor prevented by rapamycin. Nature *372*, 570–573.

Pagano, M., Tam, S.W., Theodoras, A.M., Beer-Romero, P., Del Sal, G., Chau, V., Yew, P.R., Draetta, G.F., and Rolfe, M. (1995). Role of the ubiquitin-proteasome pathway in regulating abundance of the cyclin-dependent kinase inhibitor p27. Science *269*, 682–685.

Parker, S.B., Eichele, G., Zhang, P., Rawls, A., Sands, A.T., Bradley, A., Olson, E.N., Harper, J.W., and Elledge, S.J. (1995). p53-independent expression of $p21^{CIP1}$ in muscle and other terminally differentiating cells. Science *267*, 1024–1027.

Polyak, K., Kato, J.-Y., Solomon, M.J., Sherr, C.J., Massagué, J., Roberts, J.M., and Koff, A. (1994a). $p27^{KIP1}$, a cyclin-cdk inhibitor, links transforming growth factor-β and contact inhibition to cell cycle arrest. Genes Dev. *8*, 9–22.

Polyak, K., Lee, M.-H., Erdjument-Bromage, H., Koff, A., Roberts, J.M., Tempst, P., and Massagué, J. (1994b). Cloning of $p27^{KIP1}$, a cyclin-dependent kinase inhibitor and a potential mediator of extracellular antimitogenic signals. Cell *78*, 59–66.

Rempel, R.E., Sleight, S.B., and Maller, J.L. (1995). Maternal *Xenopus* Cdk2-cyclin E complexes function during meiotic and early embryonic cell cycles that lack a G1 phase. J. Biol. Chem. *270*, 6843–6855.

Sambrook, J., Fritsch, E.F., and Maniatis, T. (1989). Molecular Cloning: A Laboratory Manual, Cold Spring Harbor, NY: Cold Spring Harbor Laboratory Press.

Serrano, M., Hannon, G.J., and Beach, D. (1993). A new regulatory motif in cell-cycle control causing specific inhibition of cyclin D/Cdk4. Nature *366*, 704–707.

Sherr, C.J. (1993). Mammalian G1 cyclins. Cell *73*, 1059–1065.

Smith, J.C., and Tata, J.R. (1991). *Xenopus* cell lines. Methods Cell Biol. *36*, 635–654.

Su, J.-Y., Rempel, R.E., Erikson, E., and Maller, J.L. (1995). Cloning and characterization of the *Xenopus* cyclin-dependent kinase inhibitor $p27^{XIC1}$. Proc. Natl. Acad. Sci. USA *92*, 10187–10191.

Tang, Z., Coleman, T.R., and Dunphy, W.G. (1993). Two distinct mechanisms for negative regulation of the wee1 protein kinase. EMBO J. *12*, 3427–3436.

Toyoshima, H., and Hunter, T. (1994). p27, a novel inhibitor of G1 cyclin-Cdk protein kinase activity, is related to p21. Cell *78*, 67–74.

Waga, S., Hannon, G.J., Beach, D., and Stillman, B. (1994). The p21 inhibitor of cyclin-dependent kinases controls DNA replication by interaction with PCNA. Nature *369*, 574–578.

Warbrick, E., Lane, D.P., Glover, D.M., and Cox, L.S. (1995). A small peptide inhibitor of DNA replication defines the site of interaction between the cyclin-dependent kinase inhibitor $p21^{WAF1}$ and proliferating cell nuclear antigen. Curr. Biol. *5*, 275–282.

Xiong, Y., Hannon, G.J., Zhang, H., Casso, D., Kobayashi, R., and Beach, D. (1993). p21 is a universal inhibitor of cyclin kinases. Nature *366*, 701–704.

Yan, H., and Newport, J. (1995). An analysis of the regulation of DNA synthesis by cdk2, Cip1, and licensing factor. J. Cell Biol. *129*, 1–15.

Zhang, H., Hannon, G.J., and Beach, D. (1994). p21-containing cyclin kinases exist in both active and inactive states. Genes Dev. *8*, 1750–1758.

APPENDIX II

Cell, Vol. 97, 233–244, April 16, 1999, Copyright ©1999 by Cell Press

Exit from Mitosis Is Triggered by Tem1-Dependent Release of the Protein Phosphatase Cdc14 from Nucleolar RENT Complex

Wenying Shou,* Jae Hong Seol,*
Anna Shevchenko,† Christopher Baskerville,‡
Danesh Moazed,§ Z. W. Susan Chen,*
Joanne Jang,* Andrej Shevchenko,†
Harry Charbonneau,‡ and Raymond J. Deshaies*‖
*Division of Biology
California Institute of Technology
Pasadena, California 91125
†Peptide and Protein Group
European Molecular Biology Laboratory
Meyerhofstraße 1
69012 Heidelberg
Germany
‡Department of Biochemistry
Purdue University
West Lafayette, Indiana 47907-1153
§Department of Cell Biology
Harvard Medical School
Boston, Massachusetts 02115

Summary

Exit from mitosis in budding yeast requires a group of essential proteins—including the GTPase Tem1 and the protein phosphatase Cdc14—that downregulate cyclin-dependent kinase activity. We identified a mutation, *net1-1*, that bypasses the lethality of *tem1Δ*. *NET1* encodes a novel protein, and mass spectrometric analysis reveals that it is a key component of a multifunctional complex, denoted RENT (for *r*egulator of *n*ucleolar silencing and *t*elophase), that also contains Cdc14 and the silencing regulator Sir2. From G1 through anaphase, RENT localizes to the nucleolus, and Cdc14 activity is inhibited by Net1. In late anaphase, Cdc14 dissociates from RENT, disperses throughout the cell in a Tem1-dependent manner, and ultimately triggers mitotic exit. Nucleolar sequestration may be a general mechanism for the regulation of diverse biological processes.

Introduction

Activation and inactivation of cyclin-dependent kinases (Cdks) governs cell cycle transitions. In the budding yeast *Saccharomyces cerevisiae*, a single Cdk, Cdc28, orchestrates various stages of the cell cycle by taking on different cyclin partners: Cln1–3 for G1 phase, Clb5–6 for S phase, and Clb1–4 for M phase (reviewed by Deshaies, 1997). There are at least three key cell cycle transitions in this organism: G1→S, metaphase→anaphase, and the exit from mitosis (reviewed by King et al., 1996; Deshaies, 1997). Cdc28 inactivation mediated by proteolysis of Clb2 and/or accumulation of the Cdc28/Clb inhibitor Sic1 seems to lie at the heart of the latter transition (Schwab et al., 1997; Visintin et al., 1998).

‖To whom correspondence should be addressed (e-mail: deshaies@cco.caltech.edu).

Anaphase-promoting complex/cyclosome ubiquitin ligase (APC/C) and its substrate-specific activator Hct1/Cdh1 are required for Clb2 degradation. Clb degradation was originally thought to be required for exit from mitosis (Surana et al., 1993). However, cells devoid of Hct1/Cdh1 fail to degrade Clb2 and are viable (Schwab et al., 1997; Visintin et al., 1997), probably because Sic1 accumulates and turns off Cdc28 activity. Whereas cells devoid of Sic1 can degrade Clb2 and exit mitosis, cells devoid of both Hct1 and Sic1 are inviable, presumably due to their inability to extinguish Cdc28 activity during telophase (Schwab et al., 1997).

In addition to APC/C, another set of genes plays a pivotal role in exit from mitosis. They include *TEM1*, *LTE1*, *CDC15*, *DBF2/DBF20*, *CDC5*, *MOB1*, and *CDC14* (reviewed in Deshaies, 1997; Luca and Winey, 1998). When cells that harbor conditional-lethal temperature-sensitive (ts) mutations in any of these genes are shifted to the restrictive temperature, they uniformly arrest in late anaphase/telophase as large-budded cells with segregated chromosomes, fully elongated microtubule spindles, and elevated Cdc28/Clb2 protein kinase activity. Clb2 proteolysis is not completed, and *SIC1* transcripts and protein fail to accumulate to high levels (Surana et al., 1993; Shirayama et al., 1994b; Toyn and Johnston, 1994; Irniger et al., 1995; Charles et al., 1998; Jaspersen et al., 1998; Visintin et al., 1998). Furthermore, manipulation of Sic1 and Clb2 levels has dramatic effects on these mutants (Donovan et al., 1994; Shirayama et al., 1994b; Toyn et al., 1997; Charles et al., 1998; Jaspersen et al., 1998): overexpression of Clb2 or deletion of Sic1 typically exacerbates their phenotype, whereas overexpression of Sic1 has the opposite effect.

Most of these proteins required for exit from mitosis resemble components of signaling pathways: Tem1 is a GTP-binding protein (Shirayama et al., 1994b); *LTE1* encodes a putative guanine nucleotide exchange factor (Shirayama et al., 1994a); Dbf2/Dbf20, Cdc15, and Cdc5 are protein kinases (Toyn and Johnston, 1994; Hardy and Pautz, 1996; Jaspersen et al., 1998); Mob1 is a novel protein that associates with Dbf2 (Komarnitsky et al., 1998; Luca and Winey, 1998); and Cdc14 is a dual specificity protein phosphatase (Taylor et al., 1997). Consistent with the notion that these proteins constitute elements of a signaling pathway, the corresponding genes display a variety of genetic interactions with each other (Parkes and Johnston, 1992; Kitada et al., 1993; Shirayama et al., 1994b, 1996; Jaspersen et al., 1998; Komarnitsky et al., 1998; Luca and Winey, 1998; Visintin et al., 1998). Thus, for simplicity, we will refer to this group of genes as the mitotic exit network.

Although the functional organization of the mitotic exit network is poorly understood, recent work suggests that the protein phosphatase Cdc14 might act directly on cell cycle regulators to promote mitotic exit. First, overexpression of Cdc14 can activate ectopic degradation of Clb2 and accumulation of Sic1 (Visintin et al., 1998; W. S. and R. J. D., unpublished). Second, mutation of Cdk consensus phosphorylation sites in Swi5 and Hct1 activates their ability to promote *SIC1* transcription and

Clb2 degradation, respectively (Moll et al., 1991; Zachariae et al., 1998), and Cdc14 antagonizes the phosphorylation of both proteins (Visintin et al., 1998; Jaspersen et al., 1999). Although these data suggest that Cdc14 is required to dephosphorylate Swi5 and Hct1 as cells exit mitosis, they fail to address the key question of whether Cdc14 is a regulated component of the biochemical switch that flips the cell from mitosis to G1.

We report here the identification of a protein complex, named RENT, that tethers Cdc14 to the nucleolus throughout most of the cell cycle. As cells progress through mitosis, Cdc14 is released from the nucleolus in a Tem1-dependent manner. We propose that the Tem1-dependent discharge of Cdc14 from the nucleolar RENT complex lies at the heart of the biochemical engine that drives cells from mitosis to G1.

Results

net1-1 Enables *TEM1*-Independent Clb2 Degradation and Sic1 Accumulation

To delineate how *CDC15* promotes exit from telophase, we conducted a genetic screen to isolate *tab* (*telophase arrest bypassed*) mutants that allow *cdc15Δ* cells containing a complementing *[CDC15, URA3]* plasmid to survive without the plasmid (W. S. and R. J. D., in preparation). The gene corresponding to one of these mutants, *TAB2*, was cloned by complementation of the ts growth defect of *tab2-1* cells and identified as *YJL076W*. It encodes a 129 kDa protein with only one obvious homolog in sequence databases: the *S. cerevisiae* topoisomerase-I interacting protein Tof2 encoded by *YKR010C*, which is 22% homologous to Net1 over 828 amino acids. *TAB2* and the *tab2-1* allele were subsequently renamed *NET1* (for nucleolar silencing establishing factor and telophase regulator) and *net1-1*, respectively. The name *NET1* also reflects its independent identification as *NUS1* (nucleolar specific silencing protein; Straight et al., 1999 [this issue of Cell]), *ESC5* (establishes silencing; E. D. Andrulis and R. Sternglanz, personal communication), and *TAB2* (this report; W. S. and R. J. D., in preparation). *NET1* was also identified in a two-hybrid screen for Cdc14-interacting proteins (C. B. and H. C., in preparation). Disruption of *NET1* was not lethal, although *net1Δ* cells grew very slowly (Straight et al., 1999; W. S. and R. J. D., unpublished data).

Double mutant *cdc15Δ net1-1* cells were able to form colonies (W. S. and R. J. D., in preparation), as were *tem1Δ net1-1* and *cdc15Δ net1Δ* cells (Figure 3; data not shown). These genetic data formally suggest that Net1 is an inhibitor of mitotic exit that acts either downstream of, or parallel to, Tem1 and Cdc15. To address whether *net1-1* can efficiently bypass the requirement for Tem1 in Clb2 degradation and Sic1 accumulation, we constructed a *tem1Δ::GAL1-UPL-TEM1* strain that allowed for the rapid, conditional depletion of Tem1. UPL, which stands for ubiquitin-proline-LacI, acts as a destabilizing module that permits rapid degradation of appended proteins (Johnson et al., 1992). *tem1Δ::GAL1-UPL-TEM1* cells grew at a normal rate in YP-galactose medium (YPG; *TEM1* expressed) but exhibited first cycle arrest in telophase upon transfer to YP-glucose medium (YPD; *TEM1* repressed). We also tried to construct a similar conditional allele for *CDC15*, but first cycle arrest was not achieved.

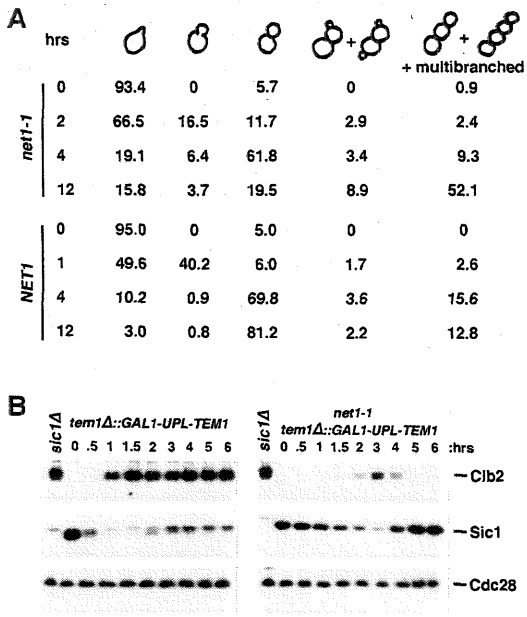

Figure 1. *net1-1* Bypasses *tem1Δ* by Inducing Ectopic Clb2 Degradation and Sic1 Accumulation

tem1Δ::GAL1-UPL-TEM1 net1-1 and *tem1Δ::GAL1-UPL-TEM1* cells grown in YPG (*TEM1* expressed) at 25°C were arrested in G1 phase with α factor and released into YPD (*TEM1* repressed) at time = 0. (A) At 0, 1, 2, 4, and 12 hr, samples were taken to measure budding index.

(B) Same as (A), except that at either 2 hr (*NET1*) or 3 hr (*net1-1*) following release from α factor arrest, α factor was added back to prevent cells from proceeding through a second cell cycle. At the indicated time points (hr), samples were taken to measure Clb2, Sic1, and Cdc28 protein levels by immunoblotting.

tem1Δ::GAL1-UPL-TEM1 cells in the wild-type or *net1-1* background were arrested in G1 phase with the mating pheromone α factor and synchronously released into YPD to extinguish expression of *UPL-TEM1*. As expected, the majority (~80%) of *NET1 tem1Δ::GAL1-UPL-TEM* cells arrested with large buds. At 12 hr after release, however, ~60% of *net1-1 tem1Δ::GAL1-UPL-TEM1* cells exhibited ≥3 cell bodies (Figure 1A), indicating a further round of division without cell separation. Those cells with one to two cell bodies could have resulted from bypass events followed by successful cell separation. Extensive chains of cells with multiple nuclei were commonly observed in the *net1-1* culture but rarely observed with *NET1* cells (data not shown). These data suggest that *net1-1* efficiently bypasses the cell division arrest caused by depletion of Tem1, although *net1-1 tem1Δ::GAL1-UPL-TEM1* cells still appear to exhibit a cytokinesis or cell separation defect.

Since Clb2 degradation and Sic1 accumulation normally accompany exit from mitosis, we tested if *net1-1* influenced the levels of these two proteins in Tem1-deficient cells. *tem1Δ::GAL1-UPL-TEM1* cells in the wild-type or *net1-1* background were arrested in G1

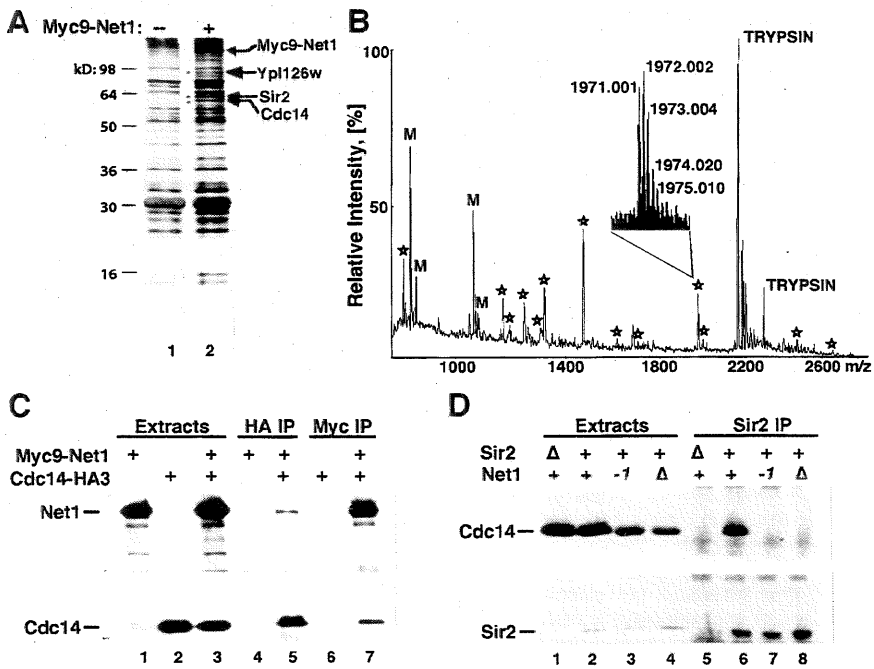

Figure 2. Identification of the RENT Complex

(A) Purification of Net1. Extracts (35 mg) of *myc9-NET1* (lane 2) and untagged control (lane 1) strains were fractionated on beads containing covalently linked anti-Myc monoclonal antibody 9E10. Eluted proteins were separated on a 10%–15% SDS-polyacrylamide gradient gel and visualized by silver staining. Protein bands specifically detected in the immunoprecipitates from *myc9-NET1* but not the untagged control strain were excised and identified by mass spectrometry.

(B) Protein identification by high mass accuracy MALDI peptide mass mapping. Mass spectrum acquired from a 0.5 μL aliquot of in-gel digest of the 62 kDa band revealed 13 peptide ions that matched the calculated masses of protonated tryptic peptides from Cdc14 with accuracy better than 50 ppm (designated with asterisks). These peptides covered more than 26% of the protein sequence. Ions originating from the matrix are designated by "M." Peptide ions of known trypsin autolysis products are also marked. The inset shows an isotopically resolved peptide ion having the monoisotopic weight 1971.001. Mass resolution was better than 7000 FWHM (full width at half maximum) despite the very low amount of protein present in the gel.

(C) Net1 associates with Cdc14. Extracts from strains with the indicated genotypes were immunoprecipitated with either 9E10 antibodies or anti-haemagglutinin (HA) monoclonal antibodies 12CA5. The immunoprecipitates (IP) and the input extracts were immunoblotted with 9E10 (top panel) and 12CA5 (bottom panel) to detect Net1 and Cdc14 proteins, respectively.

(D) Net1-dependent association between Sir2 and Cdc14. Extracts of *CDC14-HA3* cells with the indicated genotypes were immunoprecipitated with anti-Sir2 antibodies. Δ, strains deleted for *SIR2* or *NET1*; +, wild type; *−1*, the *net1-1* allele. The immunoprecipitates (IP) and the input extracts were immunoblotted with 12CA5 (top panel) and anti-Sir2 antibodies (bottom panel) to detect the Cdc14 and Sir2 proteins, respectively.

phase with α factor and released into YPD (Tem1 synthesis repressed; time 0). After cells had exited G1, α factor was added back to trap any cycling cells in the next G1 phase. Cells were harvested at various time points after α factor release and assayed for Clb2, Sic1, and Cdc28 by immunoblotting. In Tem1-deficient *NET1* cells, Clb2 accumulated and remained at high levels, whereas Sic1 was degraded as cells exited G1 and remained at low levels (Figure 1B, left panels). In Tem1-deficient *net1-1* cells, Clb2 accumulation and Sic1 degradation were delayed, presumably due to the reduced growth rate of *net1-1* (data not shown). Nevertheless, eventually Clb2 was completely degraded and Sic1 accumulated to high levels (Figure 1B, right panels). These data suggest that *net1-1* bypassed *tem1*Δ by enabling both Clb2 degradation and Sic1 accumulation.

Net1 Physically Associates with Cdc14 and Sir2

To delineate the mechanism by which *NET1* influences mitotic exit, we sought to identify proteins that interact with Net1. The chromosomal copy of *NET1* was modified to encode a protein with nine copies of the Myc epitope at its N terminus, and Myc9-Net1 was affinity purified from cell extracts on a 9E10 monoclonal antibody matrix. Besides Myc9-Net1, three proteins were specifically detected in silver-stained SDS-polyacrylamide gels of Myc9-Net1 immunoprecipitates but not in control immunoprecipitates (Figure 2A). Protein bands were identified by high mass accuracy matrix-assisted laser desorption/ionization (MALDI) peptide mapping and nanoelectrospray tandem mass spectrometric sequencing combined in a layered approach (Shevchenko et al., 1996a). One Net1-interacting protein (Cdc14) was identified by MALDI (Figure 2B). The identity of the other two proteins (Sir2 and Ypl126w) was revealed by subsequent tandem mass spectrometric sequencing.

To verify the interactions between Net1, Sir2, and Cdc14, we carried out coimmunoprecipitation experiments. Myc9-Net1 was specifically detected in anti-HA immunoprecipitates prepared from a strain containing

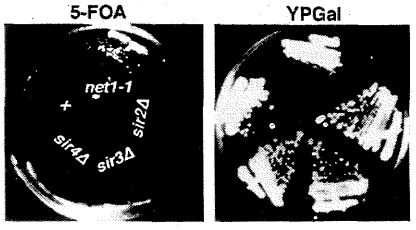

Figure 3. Loss of Silencing Fails to Bypass the Essential Requirement for *TEM1*

Wild-type (+), *net1-1*, *sir2*Δ, *sir3*Δ, or *sir4*Δ cells that carried *tem1*Δ and were sustained by a *[GAL1-TEM1, URA3]* plasmid were grown on YPG (*TEM1* expressed) and then plated onto either YPG (right panel) or synthetic glucose medium supplemented with 5-FOA (left panel) to select for colonies that were able to grow in the absence of the *[GAL1-TEM1, URA3]* plasmid. The plates were incubated at 25°C and photographed after 1 (YPGal plate) or 2 weeks (5-FOA plate).

chromosomal *CDC14* modified to encode a protein with three copies of the haemagglutinin epitope at its C terminus (Cdc14-HA3), but not from a strain that expressed untagged Cdc14 (Figure 2C, compare lanes 4 and 5). Conversely, Cdc14-HA3 was selectively recovered in anti-Myc immunoprecipitates prepared from strains that express Myc9-Net1 (Figure 2C, compare lanes 6 and 7). By a similar analysis, it was confirmed that Myc9-Net1 bound specifically to Sir2 (Straight et al., 1999). Cdc14-HA3 was also detected in anti-Sir2 immunoprecipitates prepared from wild-type cells (Figure 2D, lane 6) but not those prepared from *sir2*Δ (lane 5), *net1-1* (lane 7), or *net1*Δ (lane 8) mutants, suggesting that Net1 bridges the interaction between Cdc14 and Sir2. We refer to the Cdc14-Net1-Sir2 complex as "RENT," for *r*egulator of *n*ucleolar silencing and *t*elophase (see Discussion and Straight et al., 1999).

We have only performed a cursory analysis of the third Net1-associated protein, Ypl126w. *YPL126W* was determined to be an essential gene, and Myc9-tagged Ypl126w was localized to the nucleolus by indirect immunofluorescence, consistent with it being an authentic Net1-binding partner (W. S., unpublished data). To reflect its known properties, we suggest *YPL126W* be renamed *NAN1* (*N*et1-associated *n*ucleolar protein).

Although *net1-1* Is Defective in rDNA Silencing, Loss of Silencing Does Not Bypass *tem1*Δ

Sir2 regulates transcriptional silencing at telomeres and the silent mating type loci (reviewed by Lustig, 1998). Sir2 also mediates silencing of some RNA polymerase II–transcribed genes integrated within the rDNA, a phenomenon referred to as "rDNA silencing" (Bryk et al., 1997; Fritze et al., 1997; Smith and Boeke, 1997). Net1 was independently discovered as a Sir2-binding protein (Straight et al., 1999), and both *net1*Δ and *net1-1* were shown to be defective in rDNA silencing. This raised the possibility that loss of silencing accounted for the *tem1*Δ bypass activity of *net1-1*. To test this hypothesis, we compared the bypass activity of *net1-1*, *sir2*Δ, *sir3*Δ, and *sir4*Δ in *tem1*Δ cells kept alive by a *URA3* plasmid harboring *GAL1-TEM1*. The parental *tem1*Δ *[GAL1-TEM1, URA3]* strain failed to grow on 5-fluoroorotic acid (5-FOA)-containing medium (5-FOA selectively prevents the growth of Ura$^+$ cells) due to its inability to survive without the *[GAL1-TEM1, URA3]* plasmid. The *net1-1* allele, but not *sir2*Δ, *sir3*Δ, or *sir4*Δ, allowed *tem1*Δ *[GAL1-TEM1, URA3]* cells to survive on 5-FOA (Figure 3). PCR analysis confirmed that the viable colonies indeed lacked the *TEM1*-containing plasmid (data not shown). Thus, the effects of *net1-1* on *tem1*Δ bypass and rDNA silencing can be uncoupled.

Net1 Is an Inhibitor of and a Candidate Substrate for Cdc14

Cdc14 is a dual specificity protein phosphatase essential for mitotic exit (Culotti and Hartwell, 1971; Taylor et al., 1997). Net1 bound to Cdc14 and behaved genetically as a negative regulator of mitotic exit (Figure 2; W. S. and R. J. D., in preparation). Therefore, we postulated that Net1 might either be an inhibitor of Cdc14 or a mitotic exit inhibitor whose activity was counteracted by Cdc14. To test if Net1 is an inhibitor of Cdc14, we measured Cdc14 activity in wild-type, *net1-1*, and *net1*Δ cell extracts. Cdc14-HA3 was immunoprecipitated from asynchronous cultures of *net1-1*, *net1*Δ, and wild-type strains and incubated with ^{32}P-labeled Sic1. It is not clear if phospho-Sic1 is a physiological substrate for Cdc14, but it provides a convenient assay to measure the phosphatase activity of Cdc14. The specific activity of Cdc14-HA3 isolated from *net1-1* and *net1*Δ cells was on average 3.6 and 3.8 times as much as that from wild-type cells, respectively (Figure 4A). This elevation in Cdc14-HA3-specific activity was not due to altered cell cycle kinetics, since the specific activity of Cdc14-HA3 purified from G1-synchronized *net1-1* cells was still 3.8- to 4.5-fold as high as that obtained from G1-synchronized wild-type cells (Figure 4B).

To address whether the effect of *net1* mutations on Cdc14 protein phosphatase activity was direct, we tested if immunopurified Myc9-Net1 could inhibit recombinant GST-Cdc14 purified from *E. coli*. Wild-type or catalytically inactive GST-Cdc14 (Taylor et al., 1997) was recruited to matrices that contained either immobilized Myc9-Net1 or immobilized anti-GST antibodies. To prepare Net1 beads lacking endogenous Cdc14 activity, Myc9-Net1 was immunopurified from extracts treated with phosphatase inhibitor sodium orthovanadate, which reduced the amount of endogenous Cdc14 protein bound to Net1 beads (data not shown); to prepare anti-GST beads, rabbit α-GST antibodies were absorbed to protein A matrix. Following the recruitment step, bead-bound GST-Cdc14 was assayed for its phosphatase activity toward ^{32}P-Sic1. GST-Cdc14 recovered on the Myc9-Net1 matrix had 50-fold lower specific activity than GST-Cdc14 bound to the anti-GST matrix (Figure 4C). Taken together, these experiments suggest that Net1 directly inhibits the protein phosphatase activity of Cdc14.

Having established that Net1 is associated with potent Cdc14 inhibitory activity, we tested if Net1 might also be a substrate for Cdc14. First, Net1 was a phosphoprotein in vivo, since a radioactive band with the expected molecular weight of Myc9-Net1 was apparent in immunoprecipitates prepared from ^{32}P-labeled *myc9-NET1* cells but not from untagged cells (Figure 4D). Second,

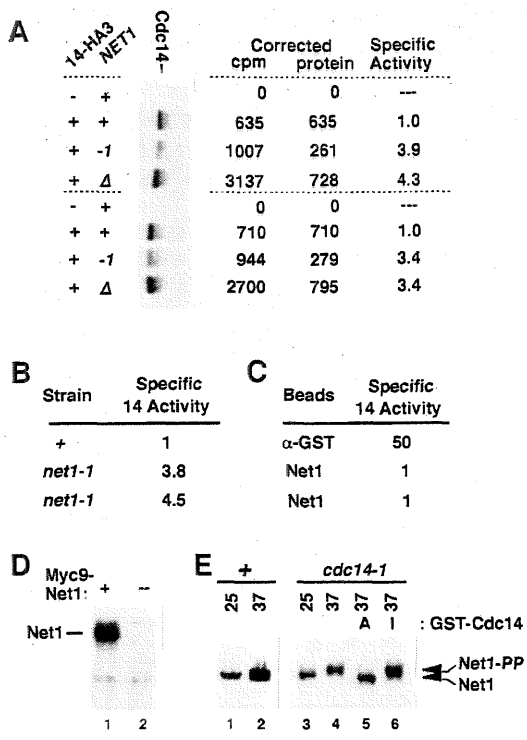

Figure 4. Net1 Is an Inhibitor of and a Candidate Substrate for Cdc14

(A and B) Cdc14 activity is elevated in *net1* mutants. Cdc14-HA3 was retrieved from lysates of the indicated strains (in the "14-HA3" column: −, untagged; +, *CDC14-HA3*; in the "*NET1*" column: +, *NET1*; *−1*, *net1-1*; Δ, *net1Δ*) by immunoprecipitation with 12CA5 antibodies and was incubated with ^{32}P-Sic1 for 20 min at 22°C. The specific activity of Cdc14-HA3 in each reaction was determined by measuring trichloroacetic acid–soluble counts released during the incubation and dividing by the relative amount of Cdc14-HA3 as determined by immunoblotting. All values were corrected by subtracting out background signals obtained with untagged control sample; relative amounts of proteins were normalized such that the specific activity of Cdc14 was 1.0 in wild-type cells. The background signals were ~350 and ~27 in the ^{32}P release and immunoblot assays, respectively. The results of duplicate reactions are presented. In (A), asynchronous cells were used, whereas in (B), cells were synchronized in G1 phase with α factor prior to analysis.

(C) Net1 inhibits Cdc14 phosphatase activity in vitro. Extracts of *myc9-NET1* cells were immunoprecipitated with 9E10 antibodies, and protein A beads were coated with anti-GST antibodies to prepare Net1 and α-GST beads, respectively. Both matrices were washed extensively and incubated with wild-type or mutant GST-Cdc14 purified from *E. coli* (20 ng for GST beads and 60 ng for Net1 beads). The specific activity of bead-bound GST-Cdc14 was evaluated as described above using ^{32}P-Sic1 as the substrate. Levels of GST-Cdc14 recruited to the Net1 and α-GST beads were assessed by immunoblotting with α-GST antibodies. The activity of mutant Cdc14 bound to the α-GST beads was used for background correction. For simplicity, in (B) and (C) only the final values (^{32}P-Sic1 dephosphorylation divided by relative amount of Cdc14 antigen) are shown.

(D and E) Net1 is a candidate substrate for Cdc14. (D) Net1 is a phosphoprotein in vivo. *myc9-NET1* (lane 1) and untagged (lane 2) strains were labeled with ^{32}P-inorganic phosphate. Extracts of labeled cells were immunoprecipitated with 9E10 antibodies, and recovered proteins were fractionated by SDS-PAGE and detected by autoradiography. (E) Net1 can be dephosphorylated by Cdc14 in vitro. *CDC14 myc9-NET1* (+, lanes 1 and 2) and *cdc14-1 myc9-NET1* (*cdc14-1*, lanes 3–6) cells were grown at 25°C or shifted to 37°C for 3 hr, as indicated. Myc9-Net1 was immunoprecipitated from cell extracts with 9E10 antibodies, and portions of the Net1 immunoprecipitate from the 37°C *cdc14-1* culture were either left untreated (lane 4) or incubated with wild-type (A; lane 5) or C283S mutant (I; lane 6) GST-Cdc14 for 60 min at 30°C. All immunoprecipitates were fractionated by SDS-PAGE and immunoblotted with 9E10 to detect Myc9-Net1.

immunoblotting of anti-*myc* immunoprecipitates revealed that Myc9-Net1 isolated from a 37°C *cdc14-1* culture (nonpermissive temperature) migrated slower in SDS-PAGE than that from a 25°C culture (permissive temperature; Figure 4E, lane 3 vs. lane 4). In contrast, no effect of temperature was observed for Myc9-Net1 isolated from wild-type cells (Figure 4E, lanes 1 and 2). The slower migrating form of Myc9-Net1 from the 37°C *cdc14-1* culture was collapsed down to a faster migrating form upon treatment with wild type (A) but not mutant (I) GST-Cdc14 purified from *E. coli* (Figure 4E, lanes 5 and 6). Since Cdc14 modulates the phosphorylation state of Net1 in vivo and in vitro, we conclude that Net1 is most likely one of its physiological substrates. In the Discussion, we consider the possibility that Net1 and Cdc14 reciprocally control each others' activities via a negative feedback loop.

Net1 Resides in the Nucleolus and Is Required for Cdc14 Localization to the Nucleolus

Both Net1 (Straight et al., 1999) and a portion of Sir2 (Gotta et al., 1997) localize to the nucleolus. These data suggest that the entire RENT complex, including Cdc14, might be tethered to the nucleolus. To test this possibility, we compared the localization of Myc9-Net1 and Cdc14-HA3 by indirect immunofluorescence. Myc9-Net1 displayed a crescent-shaped staining pattern characteristic of nucleolar localization (Figure 5A, middle row). A similar pattern was observed for Cdc14-HA3 (Figure 5A, bottom row). To confirm that both proteins do in fact localize to the nucleolus, we probed cells with antibodies directed against the relevant epitope tag and antibodies directed against the RNA polymerase 1 A190 subunit (RPA190), a nucleolar marker (Oakes et al., 1998). A striking overlap in the antibody staining patterns was observed (Figure 5A), indicating that both Net1 and Cdc14 localize to the nucleolus.

Net1 was required for localization of Sir2 to the nucleolus (Straight et al., 1999), which prompted us to examine if Net1 was also required for the nucleolar localization of Cdc14. Cdc14 localization was visualized in wild-type, *net1-1*, and *net1Δ* cells. In wild-type and *net1-1* cells, Cdc14 assumed a sharp nucleolar staining pattern (Figure 5B, center rows). However, in *net1Δ* cells, Cdc14 was diffused throughout the entire cell (Figures 5B and 5C, bottom rows). Although there was 4-fold less Cdc14 protein in *net1Δ* cells (Figure 5D), the level of delocalized Cdc14 staining was clearly greater than that seen in *CDC14-HA3 NET1* cells or in cells that lacked tagged *CDC14*. These data suggest that Net1 anchors the RENT complex to the nucleolus. The significance of the nucleolar localization of Cdc14 in *net1-1* is considered in the Discussion.

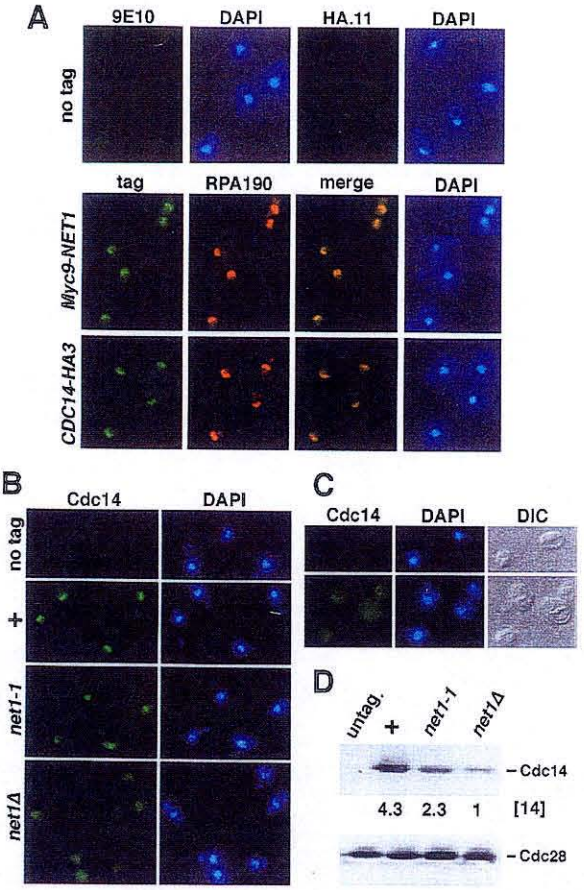

Figure 5. Net1-Dependent Localization of Cdc14 to the Nucleolus

(A) Net1 and Cdc14 both localize to the nucleolus. Top row: untagged wild-type cells were probed with 9E10 antibodies or anti-hemagglutinin monoclonal antibody HA.11 plus the DNA-binding dye DAPI. Center and bottom rows: cells with the indicated genotype were probed with monoclonal antibodies (9E10 or HA.11, column 1) and rabbit anti-RPA 190 antibodies (column 2). The third column shows a merge of the two antibody staining patterns in columns 1 and 2. The fourth column shows the position of nuclei, as revealed by DAPI staining.

(B) Untagged control (top row) and *CDC14-HA3* cells carrying *NET1*, *net1-1*, or *net1*Δ alleles (rows 2–4, respectively) were stained with HA.11 antibodies (column 1) and DAPI (column 2).

(C) Untagged control (top row) and *net1*Δ *CDC14-HA3* (bottom row) cells were stained with HA.11 antibodies (column 1) and DAPI (column 2). DIC images are shown in column 3 to reveal the outline of cells.

(D) The levels of Cdc14-HA3 and Cdc28 proteins in the indicated strains were evaluated by immunoblotting with 12CA5 antibodies. The relative levels of Cdc14-HA3 ([14]) are indicated below the top panel.

Cdc14 Is Released from the Nucleolus during Progression through Mitosis

If Net1 sequesters the bulk of Cdc14 in the nucleolus in a presumably inactive form, how does Cdc14 fulfill its essential role in promoting mitotic exit? To resolve this puzzle, we looked more carefully at the localization of Net1 and Cdc14 during the cell cycle. Asynchronous populations of cells expressing Myc9-Net1 and Cdc14-HA3 were probed with antibodies directed against the relevant epitope tags and with anti-tubulin antibodies to visualize the mitotic spindle. Cells in late anaphase and telophase contain elongated spindles, whereas cells in other stages exhibit either focal tubulin staining (G1 and early S phase cells) or a short spindle (S phase and preanaphase cells). Like the well-characterized nucleolar protein Nop1 (Aris and Blobel, 1988), Net1 exhibited a characteristic nucleolar staining pattern throughout the cell cycle (Figure 6A, upper and middle rows; Straight et al., 1999). Intriguingly, the localization of Cdc14 varied as a function of the cell cycle (Figures 6A, bottom row, and 6B): in cells with short spindles, Cdc14 was localized to the nucleolus (Figure 6B, bottom row). However, in late anaphase/telophase cells with long spindles, Cdc14 was diffused throughout the nucleus (Figure 6B, middle row) or the entire cell (Figure 6B, top row; note the diffuse cytoplasmic staining that extends beyond the nucleus).

To evaluate more rigorously the relationship between long spindles and delocalized Cdc14, we carried out a cell cycle block-release experiment. *myc9-NET1 CDC14-HA3* cells were synchronized in G1 with α factor, and at various time points after release, samples were processed for indirect immunofluorescence. The percentage of cells with long mitotic spindles, delocalized Cdc14-HA3, and delocalized Myc9-Net1 were plotted as a function of time. Although Myc9-Net1 remained localized to the nucleolus throughout the cell cycle, release of Cdc14-HA3 from the nucleolus mirrored the appearance of long spindles (Figure 6C).

The Release of Cdc14 from Nucleolus Requires Tem1

An intriguing possibility is that *tem1* cells fail to exit mitosis due to a failure to dislodge Cdc14 from its Net1 tether in the nucleolus. To test this hypothesis, we examined whether the release of Cdc14 from the nucleolus requires Tem1. *CDC14-HA3 tem1*Δ*::GAL1-UPL-TEM1* cells were either maintained in YPG (*TEM1* expressed) as an exponentially growing culture or were released from α factor–induced G1 arrest into YPD (*TEM1* repressed) to yield a synchronous population of cells arrested in late anaphase/telophase due to a deficit of Tem1 activity. In cells grown in YPG, Cdc14 was largely delocalized in 92% of cells containing a long mitotic spindle (Figure 7B), whereas the nucleolar antigen RPA190 retained a distinctive nucleolar staining pattern (Figure 7A, top row). In contrast, in cells that were arrested in late anaphase/telophase by depletion of Tem1, Cdc14 (Figure 7A, bottom row) and the nucleolar marker RPA190 (data not shown) displayed overlapping focal staining patterns in the vast majority (93%) of cells with long spindles (Figure 7B).

A simple view would argue that *net1-1* bypasses *tem1*Δ by causing ectopic release of Cdc14 from the nucleolus. Surprisingly, Cdc14-HA3 appears correctly localized in *net1-1* cells (Figure 5B). However, it is important to note that the bypass activity of *net1-1* would not necessarily require constitutive delocalization of Cdc14. To test whether Tem1-independent release of Cdc14 from the nucleolus occurred in mitotic cells, we compared Cdc14-HA3 localization in Tem1-depleted *net1-1* and *NET1* cells. Whereas Cdc14-HA3 was localized to the nucleolus in >90% of Tem1-deficient *NET1* cells that contained a long spindle, it was delocalized in ~40% of the equivalently staged Tem1-depleted *net1-1* cells

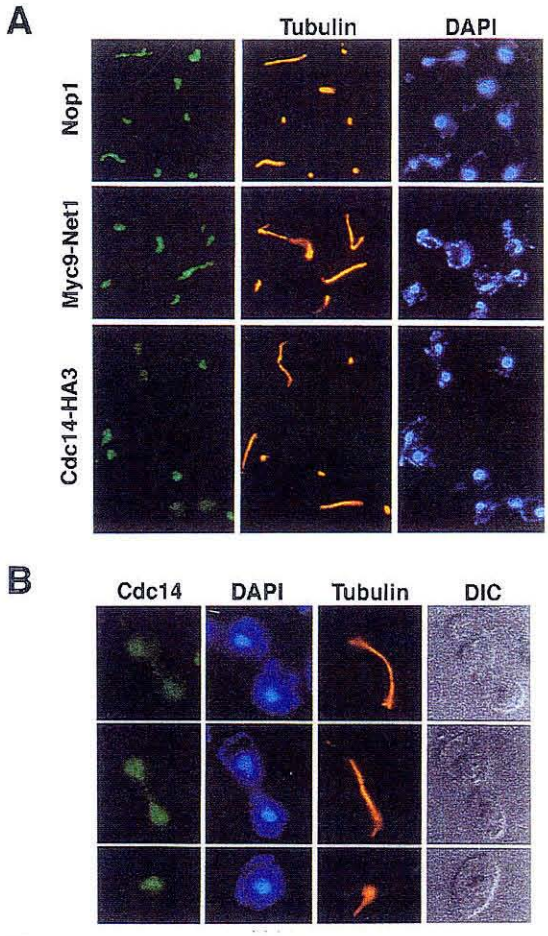

Figure 6. Cdc14 Is Released from the Nucleolus during Anaphase/Telophase

(A) Asynchronous *myc9-NET1 CDC14-HA3* cells were double labeled with rabbit anti-tubulin antibodies (column 2) and one of the following mouse antibodies (column 1): anti-Nop1 (top panel), 9E10 (center panel), or HA.11 (bottom panel). The positions of nuclei, as revealed by DAPI staining, are shown in Column 3.

(B) *Cdc14-myc9/CDC14* diploid cells were probed with 9E10, DAPI, and anti-tubulin antibodies (columns 1–3, respectively). DIC images are shown in column 4. Cdc14 exhibits three different types of staining patterns: delocalized over the entire nucleus (center row), the entire cell (top row) during anaphase/telophase, or restricted to the nucleolus (bottom row) during interphase. Note the absence of extranucleolar Cdc14 in the G1 cell shown in the bottom row.

(C) *myc9-NET1 CDC14-HA3* cells were synchronized with α factor and then released into YPD at time = 0. Samples withdrawn and fixed at the indicated time points were double labeled with anti-tubulin and either 9E10 (to detect Myc9-Net1) or HA.11 (to detect Cdc14-HA3) antibodies. For each sample, more than 200 cells were counted to calculate the percentage of cells with delocalized Cdc14 or Net1 and the percentage of cells with long spindles.

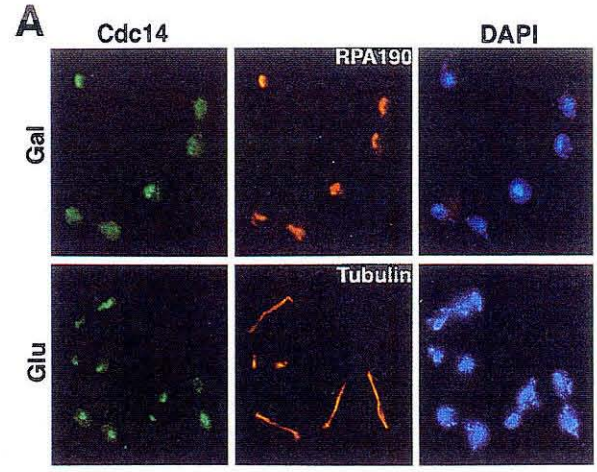

B

Strain	Growth Condition	% long spindles w/ focal Cdc14 1 focus	2 foci	Total
tem1Δ::GAL1-UPL-TEM1 +	Gal	1.9	5.8	7.7
tem1Δ::GAL1-UPL-TEM1 +	Glu	15.1	77.4	92.5
tem1Δ::GAL1-UPL-TEM1 *net1-1*	Glu	5.6	55.5	61.1

Figure 7. Release of Cdc14 from the Nucleolus Requires Tem1

(A) *tem1Δ::GAL1-UPL-TEM1 CDC14-HA3* cells grown in YPG (*TEM1* expressed) were either sampled directly (top panel) or arrested in G1 phase with α factor and subsequently released into YPD (*TEM1* repressed) for 3 hr (bottom panel). Cells were double labeled with HA.11 to visualize Cdc14-HA3 (column 1) and either anti-RPA190 or anti-tubulin antibodies to visualize nucleoli or mitotic spindles, respectively (column 2).

(B) A similar block/release protocol was conducted with a *tem1Δ::GAL1-UPL-TEM1 CDC14-HA3 net1-1* strain, except that samples were processed for indirect immunofluorescence 4–6 hr after release from α factor arrest. A longer release time was required for *net1-1* strains to progress from G1 to anaphase/telophase due to the ~2-fold longer doubling time of this mutant (W. S., data not shown). The percentages of cells with long spindles and focal Cdc14-HA3 staining were quantitated for this sample as well as the samples from (A). More than 50 cells were counted for each sample.

(Figure 7B). These results argue that Tem1 is normally required for release of Cdc14 from the nucleolus during anaphase/telophase and that *net1-1* allows ectopic release of Cdc14 (from at least a fraction of cells) during late mitosis, even in the absence of *TEM1* function.

Discussion

RENT Control: A Model for the Control of Mitotic Exit in Budding Yeast

Tem1, Cdc15, and Cdc14 are required for mitotic exit. These proteins have been implicated in ensuring a rapid and irreversible drop in mitotic cyclin/Cdk activity at the end of mitosis by promoting the proteolysis of the mitotic cyclin Clb2 and the accumulation of the cyclin/Cdk inhibitor Sic1. Despite the appeal of this scenario, it has remained unclear how the activities of these proteins are mobilized at the end of mitosis.

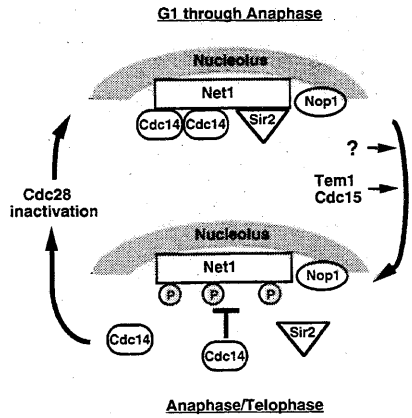

Figure 8. The "RENT Control" Hypothesis
See text for details.

Based on the data presented here, we propose the following model (Figure 8). Throughout G1, S, and early M phase, a pool of Cdc14 is confined to the nucleolus as a subunit of the RENT complex (which also contains Net1 and Sir2). As cells proceed through anaphase, Tem1-dependent signaling impinges on the RENT complex, enabling the release of Cdc14 (and a portion of Sir2; Straight et al., 1999) from Net1. Unfettered Cdc14 diffuses into the nucleus and cytoplasm, where it modulates the phosphorylation state of proteins involved in the proteolysis of Clb2 (Hct1) and transcription of *SIC1* (Swi5) (Visintin et al., 1998; Jaspersen et al., 1999). The RENT complex then reassembles once Clb/Cdk activity is quenched and Tem1-dependent signaling has been terminated, possibly via a negative feedback loop that involves Cdc14-dependent dephosphorylation of Net1.

We present five major lines of evidence in support of this model. First, Net1 and Cdc14 assemble into a complex, and Net1 is required to anchor Cdc14 to the nucleolus throughout interphase. Second, binding of Net1 to Cdc14 inhibits the protein phosphatase activity of Cdc14 in vitro, and *net1* mutants display elevated Cdc14 protein phosphatase activity. Third, Cdc14 is released from its inhibitory nucleolar tether as wild-type cells proceed through mitosis. Fourth, Cdc14 is not released from the nucleolus in cells arrested in late mitosis due to deficiency of *TEM1* function. Fifth, recessive mutations in *NET1* bypass the essential requirement of Tem1 for (1) release of Cdc14 from the nucleolus during late mitosis, (2) destruction of Clb2 and accumulation of Sic1 during late mitosis, and (3) growth.

The "RENT control" model opens up several key questions regarding the function and regulation of RENT. What is the nature of the stimulus that initiates Tem1-dependent signaling? What are the proximal biochemical events that trigger the release of Cdc14 from RENT? How is the RENT complex reestablished as cells return to G1 phase? What functions does the RENT complex perform in the regulation of nucleolar processes? Identification of the dynamic RENT complex provides a focus for exploring the molecular events that culminate in the release of active Cdc14 during anaphase/telophase.

Net1 Is a Multifunctional Protein

Affinity purification of Net1 revealed at least two binding partners—Sir2 and Cdc14—that possess disparate cellular functions. Net1 also appears to associate with the essential nucleolar protein Ypl126w (Nan1), but we do not know whether Nan1 is a component of the RENT complex or part of a distinct Net1-containing complex. Sir2 mediates the silencing of RNA polymerase II–dependent transcription in specific regions of the genome (the rDNA locus, the mating type loci, and telomeres) (Bryk et al., 1997; Fritze et al., 1997; Smith and Boeke, 1997; reviewed by Lustig, 1998). Consistent with the company it keeps, Net1 also participates in the silencing of RNA polymerase II–dependent transcription in the nucleolus (but not at the telomeres or silent mating loci) by tethering Sir2 to rDNA (Straight et al., 1999). In addition, *net1* mutations cause partial delocalization of the nucleolar protein Nop1 and alter the structure of the nucleolus (Straight et al., 1999; W. S. and R. J. D., unpublished data). The nucleolar and cell cycle functions of Net1 are at least partially separable: unlike *net1-1*, *sir2*Δ was not able to bypass *cdc15*Δ, does not cause growth defects, and has no obvious effect on the ultrastructure of the nucleolus (Ivy et al., 1986). Taken together, these observations suggest that the nucleolar functions of Net1 extend beyond its ability to recruit Sir2. Point mutations that specifically disrupt one function at a time will be of great value in dissecting the activities of this multifaceted protein.

On the Relationship between Net1 and Cdc14

Net1 inhibits Cdc14 by two independent mechanisms. First, it physically assembles with Cdc14 and inhibits its protein phosphatase activity, as evidenced by the fact that the specific activity of Cdc14 is elevated in *net1* mutants and Cdc14 recruited to Net1-containing beads is inactive. Multiple protein kinase inhibitors (e.g., p16, p21, p27; reviewed in Xiong, 1996) and serine/threonine protein phosphatase inhibitors (reviewed in Shenolikar, 1995) have been reported. To our knowledge, Net1 is the first known protein inhibitor of a member of the protein tyrosine phosphatase family that does not work by a dominant-negative mechanism. It will be interesting to determine whether human Cdc14 homologs (Li et al., 1997; H. C., unpublished data) and other members of the dual-specificity protein phosphatase family are regulated by Net1-like molecules.

As described in the previous section, Net1 also tethers Cdc14 to the nucleolus from G1 until late mitosis. Whereas Cdc14 is completely delocalized in *net1*Δ cells at all stages of the cell cycle, a nucleolar pool of Cdc14 persists in *net1-1* mutants during interphase. However, Cdc14 is released from the nucleolus in ~40% of Tem1-deficient *net1-1* cells in late anaphase/telophase but is released in only 8% of the equivalent Tem1-deficient *NET1* cells. These observations are consistent with the notion that release of Cdc14 from its nucleolar bonds requires the action of two independent signals: an unknown signal and the Tem1-dependent signal, both of which are active only during mitosis (Figure 8). We suggest that *net1-1* relieves the requirement for the latter but not the former, such that Cdc14 is still localized to the nucleolus in Tem1-depleted *net1-1* cells during

interphase but is delocalized once they proceed through mitosis.

The specific activity of Cdc14 is elevated in *net1-1* to about the same extent as in *net1*Δ, although the majority of Cdc14 is associated with the nucleolus in *net1-1* but not *net1*Δ cells. One explanation for this discrepancy is that the enfeebled Net1-1/Cdc14 protein complex is not stable under our immunoprecipitation conditions such that *net1-1* behaves like a null allele in this assay. Alternatively, the Net1-1 protein could have lost its inhibitory activity, but not its binding affinity, toward Cdc14. It is interesting to note that the level of Cdc14 is reduced in *net1-1* and further reduced in *net1*Δ, suggesting that Cdc14 bound to Net1 is more stable than the released protein. Degradation of free Cdc14 may contribute to the extinction of Cdc14 activity once the exit from mitosis is completed.

Intriguingly, we found that Net1 is a phosphoprotein and can be dephosphorylated by Cdc14. This raises the possibility that there is a negative feedback loop connecting Net1 and Cdc14. We suggest the following scenario. From G1 to anaphase, hypophosphorylated Net1 binds to and sequesters Cdc14 in the nucleolus. In anaphase/telophase, Tem1-dependent signaling activates a Net1 kinase, which in turn hyperphosphorylates Net1, thereby stimulating Cdc14 release. As cells enter G1, Tem1 signaling ceases, the Net1 kinase becomes inactive, and Cdc14 dephosphorylates Net1. The dephosphorylated Net1 subsequently binds Cdc14, thereby resetting Cdc14 activity to the ground state (Figure 8).

Although Net1 influences cell cycle progression by sequestering Cdc14 in the nucleolus, it is not yet clear whether Cdc14 contributes to the assembly or function of this organelle. *cdc14ts* but not *cdc15ts* mutants fail to completely segregate the nucleolar antigen Nop1 (Granot and Snyder, 1991) and the rDNA-bound proteins Net1 and Sir2 (Straight et al., 1999), suggesting that Cdc14 might contribute to the organization or segregation of nucleolar chromatin.

Net1 Provides a Missing Link between Tem1/Cdc15 and Cdc14

Exit from mitosis in *S. cerevisiae* involves an elaborate signaling network consisting of at least seven essential genes: *CDC5*, *CDC14*, *CDC15*, *DBF2/DBF20*, *LTE1*, *MOB1*, and *TEM1*. Since overexpression of the GTP-binding protein Tem1 bypasses the essential requirement (at low temperature) for the nucleotide exchange factor Lte1, and overexpression of the protein kinase Cdc15 bypasses the essential requirement for Tem1 (Shirayama et al., 1994b), it is likely that Lte1 activates Tem1, which in turn activates Cdc15. In support of this model, the *S. pombe* Cdc15 homolog Cdc7 binds to and is genetically downstream of *S. pombe* Tem1 homolog Spg1 (Schmidt et al., 1997). Since the recessive *net1-1* mutation bypasses *cdc15*Δ and *tem1*Δ, *NET1* formally behaves as a mitotic exit inhibitor acting downstream of or parallel to *TEM1* and *CDC15* (W. S. and R. J. D., in preparation). Based on our observation that Net1 binds to and inhibits Cdc14, the most parsimonious model is as follows. During progression through mitosis, an unknown signal activates Lte1, which in turn activates Tem1. Tem1 then activates Cdc15, which in turn relieves the inhibition of Cdc14 by Net1. Although we have yet to test this directly, we suggest that Cdc5, Dbf2/Dbf20, and Mob1 are also required for the release of Cdc14 from RENT. Active Cdc14 then promotes Clb2 degradation and Sic1 accumulation (Visintin et al., 1998; Jaspersen et al., 1999; W. Reynolds, W. S., and R. J. D., unpublished data), which shuts off Cdc28 activity.

Nucleolus as a Sequestration Center?

The nucleolus is a discrete subnuclear area for ribosomal RNA synthesis and preribosome assembly (reviewed in Shaw and Jordan, 1995). Some nucleolar proteins—including nucleolin, B23, and Nopp140—were initially shown to localize to the nucleolus by immunofluorescence and later shown to shuttle between the nucleolus and the cytoplasm (reviewed in Shaw and Jordan, 1995). Therefore, it is possible that Net1 also shuttles between the nucleolus and the cytoplasm to ferry cytoplasmic and nuclear Cdc14 to the nucleolus.

Cdc14 is localized to the nucleolus at times during the cell cycle when it is not needed and is released from the nucleolus when its activity is required for cell cycle progression. Might the nucleolus serve an unappreciated role as a "sequestration center" for proteins that are to be kept inactive? Interestingly, a $p34^{cdc2}$ homolog has been shown to localize to the nucleoli of neurons and glia in the mitotically quiescent murine central and peripheral nervous systems (Ino et al., 1993). This notion raises the possibility that some of the many proteins that have been localized to the nucleolus may not act solely (or even primarily) in the nucleolus but may be stockpiled there in anticipation of their eventual release. It is not clear how many other proteins might be regulated by nucleolar sequestration; only future research can reveal the generality of this mode of regulation.

Experimental Procedures

Yeast Strain Constructions

All yeast strains used in this study are in the W303 background (*can1-100*, *leu2-3*, *-112*, *his3-11*, *-15*, *trp1-1*, *ura3-1*, *ade2-1*). The pRS vector series was described previously (Sikorski and Hieter, 1989). The details of plasmid and strain construction are available upon request. To obtain *tem1*Δ*::TRP1 [GAL1-TEM1, URA3]* (RJD1017), the diploid strain RJD1005 (*tem1*Δ*::TRP1/TEM1, MATa/*α) was transformed with pWS102 *[pRS316: GAL1-TEM1, URA3]* and dissected. To construct *GAL1-UPL-TEM1*, the UPL degron of the UFD (ubiquitin fusion degradation) pathway (Johnson et al., 1992) was amplified by PCR and inserted upstream of *TEM1* in pWS102. The *GAL1-UPL-TEM1* cassette was then excised and cloned into pRS304 (TRP1), which was subsequently digested with both BglII and KpnI, blunt ended with Klenow, and self-ligated to generate pWS103 (*[GAL1-UPL-tem1*Δ*C/TRP1]*). pWS103 was linearized with EcoRI to direct integration at the *TEM1* locus, yielding WY46 (*tem1*Δ*::GAL1-UPL-TEM1, bar1::hisG, MATa*). To construct *net1::myc9-NET1/LEU2* (WY53), pWS104 (containing nucleotides [NT] −293→+3 and +4→+844 of *NET1* flanking Myc9) was linearized with Bsg1 and integrated into a wild-type strain. To construct *cdc14::CDC14-Flag-His6-HA3/HIS3* strain (RJD 1191), pGJR (pRS315 containing NT 1336–1653 of the *CDC14* ORF, followed by Flag-His6-HA3, followed by NT 1654–2095 of *CDC14* 3′ untranslated region) was linearized with EcoRV and transformed into a wild-type strain. To delete *SIR* genes, strains were transformed with *sir*Δ*::LEU2* plasmids (Ivy et al., 1986), and correct transformants were identified based on their sterility. The *NET1* locus was replaced by *S. pombe his5*$^{+}$ using the PCR amplification/transformation method described

previously (Wach et al., 1997). Correct integrants were verified by PCR, sporulated, and dissected (WY 69 and 70).

Cell Growth, Synchronization Procedures, and In Vivo Labeling

Cells were grown on 1% yeast extract/2% peptone (YP) + 2% glucose (YPD) or YP + 2% galactose (YPG) medium. 5-FOA plates were prepared as described (Sikorski and Boeke, 1991). To perform *GAL1-UPL-TEM1* shut-off experiments, exponential phase cells grown in YPG were arrested with α factor (10 μg/ml for *BAR1* and 0.1 μg/ml for *bar1Δ* strains) and released into YPD. In some cases, α factor was added back a few hours after release to trap cells in the subsequent G1 phase. To label cells with [^{32}P]phosphate, 5 × 10^8 exponential phase cells grown in phosphate-free YPD (Warner, 1991) were resuspended in 2.5 ml of phosphate-free YPD and labeled with 0.3 mCi [^{32}P]phosphate (ICN) for 45 min at room temperature. Cells were washed with ice-cold water and harvested. To arrest cells at *cdc* blocks, cells were shifted to 37°C for 2.5–3.5 hr until ≥90% cells were arrested.

Cell Extract Preparation, Immunoprecipitation, and Western Blot

To detect proteins by immunoblotting, 200 μl of SDS sample buffer was added to 8 × 10^7 cells, vortexed for 2 s, and boiled for 3 min. One hundred microliters of acid-washed glass beads (0.5 mm) was added and the mixture was vortexed for 2 min. The samples were boiled again for 2 min, and 8 μl of samples was loaded on SDS-polyacrylamide gels. To prepare extracts for immunoprecipitation (IP), 4–6 × 10^8 cells were pelleted, washed once with HBS (20 mM HEPES [pH 7.2], 150 mM NaCl), and resuspended in 200 μl of lysis buffer (HBS + 2 mM dithiothreitol [DTT], 0.2% Triton, and protease inhibitors) (Shou and Dunphy, 1996). Glass beads (200 μl) were added, and cells were lysed by 12 cycles of vortexing for 30 s followed by a 1 min incubation on ice. Extracts were clarified by two consecutive centrifugations (14,000 g for 5 min). Protein concentration of extracts was typically 5–10 mg/ml. Extracts (80–150 μl) were incubated with 1 μl of 12CA5 (for HA-tagged protein) or 9E10 (for Myc-tagged protein) monoclonal antibodies on ice (1 hr), supplemented with 15–20 μl of either protein A (12CA5 antibodies) or anti-mouse IgG beads (9E10 antibodies), and incubated on a rotator at 4°C for 1 hr. Beads were then washed extensively with lysis buffer lacking protease inhibitors. One-third to one-fourth of the washed immunoprecipitates were subjected to SDS-PAGE and immunoblotting as described (Harlow and Lane, 1988). In the experiment described in Figure 4C, 2 mM Na_3VO_4 was included in the Myc9-Net1 IP reaction (but not the wash buffers) to inhibit the endogenous Cdc14 from binding to Net1 in the extracts. To prepare anti-GST beads, 20 μl of protein A beads was incubated with 1 μl of anti-GST antibodies and washed after 1 hr incubation. Western blot detection relied upon either ^{125}I-labeled secondary antibodies (ICN) or HRP-conjugated secondary antibodies followed by ECL+ (Amersham). The blots were scanned and quantitated using Molecular Dynamics STORM system.

Protein Identification by Mass Spectrometry

Protein bands were excised from a single silver-stained SDS-polyacrylamide gel, reduced with dithiothreitol, alkylated with iodoacetamide, and in gel digested with trypsin (37°C, overnight) as described previously (Shevchenko et al., 1996b). An aliquot (0.3–0.5 μL) of the digest was withdrawn and analyzed by high mass accuracy MALDI peptide mapping on a modified REFLEX mass spectrometer (Bruker Daltonics, Bremen, Germany) essentially as described previously (Shevchenko et al., 1996b). If MALDI peptide mass mapping could not provide a conclusive identification of the protein, the gel pieces were further extracted with 5% formic acid and acetonitrile. The extracts were pooled and lyophilized, and the unseparated mixture of tryptic peptides was sequenced by nanoelectrospray tandem mass spectrometry on an API III triple quadruple instrument (PE Sciex, Concord, ON, Canada) as described previously (Wilm et al., 1996). Database searches were performed against a comprehensive nonredundant protein sequence database using PeptideSearch V. 3.0 software developed in the European Molecular Biology Laboratory. No limitations of protein molecular weight and species of origin were imposed.

Detection of Phospho-Net1 and Treatment with Cdc14

To retrieve ^{32}P-Net1, *myc9-NET1* cells were labeled with [^{32}P]phosphate and disrupted with glass beads in lysis buffer supplemented with phosphatase inhibitors as described (Verma et al., 1997), and clarified extracts were immunoprecipitated with 9E10 antibodies. To assay if phospho-Net1 might be a substrate for GST-Cdc14, GST-Cdc14 and catalytically inactive GST-Cdc14 (C283S) were purified from *E. coli* as described (Taylor et al., 1997). Myc9-Net1 was immunoprecipitated in the presence of phosphatase inhibitors (excluding Na_3VO_4) and washed extensively with the final wash being Cdc14 buffer (50 mM imidazole [pH 6.6], 1 mM EDTA, 1 mM DTT, 0.1 mg/ml BSA, 25 μg/ml aprotinin, 10 μg/ml PLC). Beads were incubated with 1.2 μg of GST-Cdc14 (wild type or mutant) in 50 μl of Cdc14 buffer at 30°C for 1 hr.

Cdc14 Activity Assay

MBP-Sic1-MycHis6 (10 μg) was phosphorylated by GST-Cdc28/Cln2/Cks1/Cak1 kinase in the presence of [γ-^{32}P]ATP (Skowyra et al., 1997), retrieved from the kinase reaction on Ni-NTA resin (Qiagen), and eluted in 120 μl of 200–250 mM imidazole (pH 7.5). To assay bead-bound Cdc14 activity, the beads were incubated with 30 μl of Cdc14 buffer containing 1 μl of ^{32}P-Sic1 and rotated at 22°C for 18–20 min (or 18°C for 15 min; Figure 4C). Control experiments indicated that, at most, 40%–50% of the input substrate was dephosphorylated under these conditions. The supernatant was removed, and the beads were washed two times with 30 μl HBS + 0.1% Triton X-100. The washes were pooled with the supernatant, adjusted to 10% trichloroacetic acid, incubated for 30 min on ice, and centrifuged for 10 min at 14,000 g. Soluble radioactivity was measured by scintillation counting.

Immunofluorescence

Immunofluorescence was carried out essentially as described previously (Pringle et al., 1991). Cells were fixed with 4.5% formaldehyde at room temperature for 0.5 hr for anti-RPA190 and 1 hr for all other antibodies. Primary antibodies included 1:1,000 mouse monoclonal antibodies HA.11 and 9E10 (Babco), 1:1,000 rabbit anti-RPA190, 1:2,000 rabbit-anti-tubulin antibodies, and 1:12,000 mouse-anti-Nop1. Secondary antibodies included 1:1,000 rhodamine-conjugated-donkey-anti-rabbit antibodies (Jackson Lab) and 1:1,000 fluorescein-conjugated-goat-anti-mouse antibodies (Cappel). Images were captured on a Zeiss Axioskop microscope using Fujichrome Provia 400 slide film.

Acknowledgments

W. S. dedicates this paper to her parents, who have supported her unconditionally. We thank D. Kellogg, M. Nomura, F. Solomon, and J. Aris for anti-Clb2, anti-RPA190, anti-tubulin, and anti-Nop1 antibodies, respectively; A. Varshavsky, K. Nasmyth, P. Philippsen, and J. Hicks for the UPL, Myc9, *S. pombe his5*$^+$, and *sirΔ::LEU2* plasmids, respectively; and R. Feldman and R. Verma for the MBP-Sic1 and Sic1 kinase. We thank G. Reynard for constructing CDC14-HA3; J. Archer for sharing immunofluorescence expertise; and R. Verma, R. Feldman, W. Dunphy, and H. Rao for critically reading the manuscript. W. S. thanks B. Hay for insight and encouragement and D. Harrington for assistance with graphics. W. S. is a Howard Hughes Medical Institute predoctoral fellow. H. C. was supported by NIH grant CA59935, and R. J. D. was supported by Junior Investigator Awards from the Searle/Chicago Community Trust and the Beckman Foundation.

Received February 9, 1999; revised March 25, 1999.

References

Aris, J.P., and Blobel, G. (1988). Identification and characterization of a yeast nucleolar protein that is similar to a rat liver nucleolar protein. J. Cell Biol. *107*, 17–31.

Bryk, M., Banerjee, M., Murphy, M., Knudsen, K.E., Garfinkel, D.J.,

and Curcio, M.J. (1997). Transcriptional silencing of Ty1 elements in the RDN1 locus of yeast. Genes Dev. *11*, 255–269.

Charles, J.F., Jaspersen, S.L., Tinker-Kulberg, R.L., Hwang, L., Szidon, A., and Morgan, D.O. (1998). The Polo-related kinase Cdc5 activates and is destroyed by the mitotic cyclin destruction machinery in *S. cerevisiae*. Curr. Biol. *8*, 497–507.

Culotti, J., and Hartwell, L.H. (1971). Genetic control of the cell division cycle in yeast. 3. Seven genes controlling nuclear division. Exp. Cell Res. *67*, 389–401.

Deshaies, R.J. (1997). Phosphorylation and proteolysis: partners in the regulation of cell division in budding yeast. Curr. Opin. Genet. Dev. *7*, 7–16.

Donovan, J.D., Toyn, J.H., Johnson, A.L., and Johnston, L.H. (1994). $p40^{SDB25}$, a putative CDK inhibitor, has a role in the M/G1 transition in *Saccharomyces cerevisiae*. Genes Dev. *8*, 1640–1653.

Fritze, C.E., Verschueren, K., Strich, R., and Easton Esposito, R. (1997). Direct evidence for SIR2 modulation of chromatin structure in yeast rDNA. EMBO J. *16*, 6495–6509.

Gotta, M., Strahl-Bolsinger, S., Renauld, H., Laroche, T., Kennedy, B.K., Grunstein, M., and Gasser, S.M. (1997). Localization of Sir2p: the nucleolus as a compartment for silent information regulators. EMBO J. *16*, 3243–3255.

Granot, D., and Snyder, M. (1991). Segregation of the nucleolus during mitosis in budding and fission yeast. Cell Motil. Cytoskeleton *20*, 47–54.

Hardy, C.F., and Pautz, A. (1996). A novel role for Cdc5p in DNA replication. Mol. Cell. Biol. *16*, 6775–6782.

Harlow, E., and Lane, D. (1988). Antibodies: A Laboratory Manual (Cold Spring Harbor, New York: Cold Spring Harbor Press).

Ino, H., Mochizuki, T., Yanaihara, N. and Chiba, T. (1993). p34cdc2 homologue is located in nucleoli of the nervous and endocrine systems. Brain Res. *614*, 131–136.

Irniger, S., Piatti, S., Michaelis, C., and Nasmyth, K. (1995). Genes involved in sister chromatid separation are needed for B-type cyclin proteolysis in budding yeast. Cell *81*, 269–277.

Ivy, J.M., Klar, A.J., and Hicks, J.B. (1986). Cloning and characterization of four SIR genes of *Saccharomyces cerevisiae*. Mol. Cell. Biol. *6*, 688–702.

Jaspersen, S.L., Charles, J.F., Tinker-Kulberg, R.L., and Morgan, D.O. (1998). A late mitotic regulatory network controlling cyclin destruction in *Saccharomyces cerevisiae*. Mol. Biol. Cell *9*, 2803–2817.

Jaspersen, S.L., Charles, J.F., and Morgan, D.O. (1999). Inhibitory phosphorylation of the APC regulator Hct1 is controlled by the kinase Cdc28 and the phosphatase Cdc14. Curr. Biol. *9*, 227–236.

Johnson, E.S., Bartel, B., Seufert, W., and Varshavsky, A. (1992). Ubiquitin as a degradation signal. EMBO J. *11*, 497–505.

King, R.W., Deshaies, R.J., Peter, J.M., and Kirschner, M. (1996). How proteolysis controls cell division. Science *274*, 1652–1659.

Kitada, K., Johnson, A.L., Johnston, L.H., and Sugino, A. (1993). A multicopy suppressor gene of the *Saccharomyces cerevisiae* G1 cell cycle mutant gene dbf4 encodes a protein kinase and is identified as CDC5. Mol. Cell. Biol. *13*, 4445–4457.

Komarnitsky, S.I., Chiang, Y.C., Luca, F.C., Chen, J., Toyn, J.H., Winey, M., Johnston, L.H., and Denis, C.L. (1998). DBF2 protein kinase binds to and acts through the cell cycle-regulated MOB1 protein. Mol. Cell. Biol. *18*, 2100–2107.

Li, L., Ernsting, B.R., Wishart, M.J., Lohse, D.L., and Dixon, J.E. (1997). A family of putative tumor suppressors is structurally and functionally conserved in humans and yeast. J. Biol. Chem. *272*, 29403–29406.

Luca, F.C., and Winey, M. (1998). MOB1, an essential yeast gene required for completion of mitosis and maintenance of ploidy. Mol. Biol. Cell *9*, 29–46.

Lustig, A.J. (1998). Mechanisms of silencing in *Saccharomyces cerevisiae*. Curr. Opin. Genet. Dev. *8*, 233–239.

Moll, T., Tebb, G., Surana, U., Robitsch, H., and Nasmyth, K. (1991). The role of phosphorylation and the CDC28 protein kinase in cell cycle–regulated nuclear import of the *S. cerevisiae* transcription factor SWI5. Cell *66*, 743–758.

Oakes, M., Aris, J.P., Brockenbrough, J.S., Wai, H., Vu, L., and Nomura, M. (1998). Mutational analysis of the structure and localization of the nucleolus in the yeast *Saccharomyces cerevisiae*. J. Cell Biol. *143*, 23–34.

Parkes, V., and Johnston, L.H. (1992). SPO12 and SIT4 suppress mutations in DBF2, which encodes a cell cycle protein kinase that is periodically expressed. Nucleic Acids Res. *20*, 5617–5623.

Pringle, J.R., Adams, A.E., Drubin, D.G., and Haarer, B.K. (1991). Immunofluorescence methods for yeast. Methods Enzymol. *194*, 565–602.

Schmidt, S., Sohrmann, M., Hofmann, K., Woollard, A., and Simanis, V. (1997). The Spg1p GTPase is an essential, dosage-dependent inducer of septum formation in *Schizosaccharomyces pombe*. Genes Dev. *11*, 1519–1534.

Schwab, M., Lutum, A.S., and Seufert, W. (1997). Yeast Hct1 is a regulator of Clb2 cyclin proteolysis. Cell *90*, 683–693.

Shaw, P.J., and Jordan, E.G. (1995). The nucleolus. Annu. Rev. Cell Dev. Biol. *11*, 93–121.

Shenolikar, S. (1995). Protein phosphatase regulation by endogenous inhibitors. Semin. Cancer Biol. *6*, 219–227.

Shevchenko, A., Jensen, O.N., Podtelejnikov, A.V., Sagliocco, F., Wilm, M., Vorm, O., Mortensen, P., Shevchenko, A., Boucherie, H., and Mann, M. (1996a). Linking genome and proteome by mass spectrometry: large scale identification of yeast proteins from two dimensional gels. Proc. Natl. Acad. Sci. USA *93*, 14440–14445.

Shevchenko, A., Wilm, M., Vorm, O., and Mann, M. (1996b). Mass spectrometric sequencing of proteins from silver stained polyacrylamide gels. Anal. Chem. *68*, 850–858.

Shirayama, M., Matsui, Y., Tanaka, K., and Toh-e, A. (1994a). Isolation of a CDC25 family gene, MSI2/LTE1, as a multicopy suppressor of ira1. Yeast *10*, 451–461.

Shirayama, M., Matsui, Y., and Toh-e, A. (1994b). The yeast TEM1 gene, which encodes a GTP-binding protein, is involved in termination of M phase. Mol. Cell. Biol. *14*, 7476–7482.

Shirayama, M., Matsui, Y., and Toh-e, A. (1996). Dominant mutant alleles of yeast protein kinase gene CDC15 suppress the lte1 defect in termination of M phase and genetically interact with CDC14. Mol. Gen. Genet. *251*, 176–185.

Shou, W., and Dunphy, W.G. (1996). Cell cycle control by Xenopus p28Kix1, a developmentally regulated inhibitor of cyclin-dependent kinases. Mol. Biol. Cell *7*, 457–469.

Sikorski, R.S., and Hieter, P. (1989). A system of shuttle vectors and yeast host strains designed for efficient manipulation of DNA in *Saccharomyces cerevisiae*. Genetics *122*, 19–27.

Sikorski, R.S., and Boeke, J.D. (1991). In vitro mutagenesis and plasmid shuffling: from cloned gene to mutant yeast. Methods Enzymol. *194*, 302–318.

Skowyra, D., Craig, K., Tyers, M., Elledge, S., and Harper, J. (1997). F-box proteins are receptors that recruit phosphorylated substrates to the SCF ubiquitin-ligase complex. Cell *91*, 209–219.

Smith, J.S., and Boeke, J.D. (1997). An unusual form of transcriptional silencing in yeast ribosomal DNA. Genes Dev. *11*, 241–254.

Straight, A.F., Shou, W., Dowd, G.J., Turck, C.W., Deshaies, R.J., Johnson, A.D., and Moazed, D.M. (1999). Net1, a Sir2-associated nucleolar protein required for rDNA silencing and nucleolar integrity. Cell *97*, this issue, 245–256.

Surana, U., Amon, A., Dowzer, C., McGrew, J., Byers, B., and Nasmyth, K. (1993). Destruction of the CDC28/CLB mitotic kinase is not required for the metaphase to anaphase transition in budding yeast. EMBO J. *12*, 1969–1978.

Taylor, G.S., Liu, Y., Baskerville, C., and Charbonneau, H. (1997). The activity of Cdc14p, an oligomeric dual specificity protein phosphatase from *Saccharomyces cerevisiae*, is required for cell cycle progression. J. Biol. Chem. *272*, 24054–24063.

Toyn, J.H., and Johnston, L.H. (1994). The Dbf2 and Dbf20 protein kinases of budding yeast are activated after the metaphase to anaphase cell cycle transition. EMBO J. *13*, 1103–1113.

Toyn, J.H., Johnson, A.L., Donovan, J.D., Toone, W.M., and Johnston, L.H. (1997). The Swi5 transcription factor of *Saccharomyces*

cerevisiae has a role in exit from mitosis through induction of the cdk-inhibitor Sic1 in telophase. Genetics *145*, 85–96.

Verma, R., Annan, R.S., Huddleston, M.J., Carr, S.A., Reynard, G., and Deshaies, R.J. (1997). Phosphorylation of Sic1p by G1 Cdk required for its degradation and entry into S phase. Science *278*, 455–460.

Visintin, R., Prinz, S., and Amon, A. (1997). CDC20 and CDH1: a family of substrate-specific activators of APC-dependent proteolysis. Science *278*, 460–463.

Visintin, R., Craig, K., Hwang, E.S., Prinz, S., Tyers, M., and Amon, A. (1998). The phosphatase Cdc14 triggers mitotic exit by reversal of Cdk-dependent phosphorylation. Mol. Cell *2*, 709–718.

Wach, A., Brachat, A., Alberti-Segui, C., Rebischung, C., and Philippsen, P. (1997). Heterologous HIS3 marker and GFP reporter modules for PCR-targeting in *Saccharomyces cerevisiae*. Yeast *13*, 1065–1075.

Warner, J.R. (1991). Labeling of RNA and phosphoproteins in *Saccharomyces cerevisiae*. Methods Enzymol. *194*, 423–428.

Wilm, M., Shevchenko, A., Houthaeve, T., Breit, S., Schweigerer, L., Fotsis, T., and Mann, M. (1996). Femtomole sequencing of proteins from polyacrylamide gels by nanoelectrospray mass spectrometry. Nature *379*, 466–469.

Xiong, Y. (1996). Why are there so many CDK inhibitors? Biochim. Biophys. Acta *1288*, 1–5.

Zachariae, W., Schwab, M., Nasmyth, K., and Seufert, W. (1998). Control of cyclin ubiquitination by CDK-regulated binding of Hct1 to the anaphase promoting complex. Science *282*, 1721–1724.

Appendix III

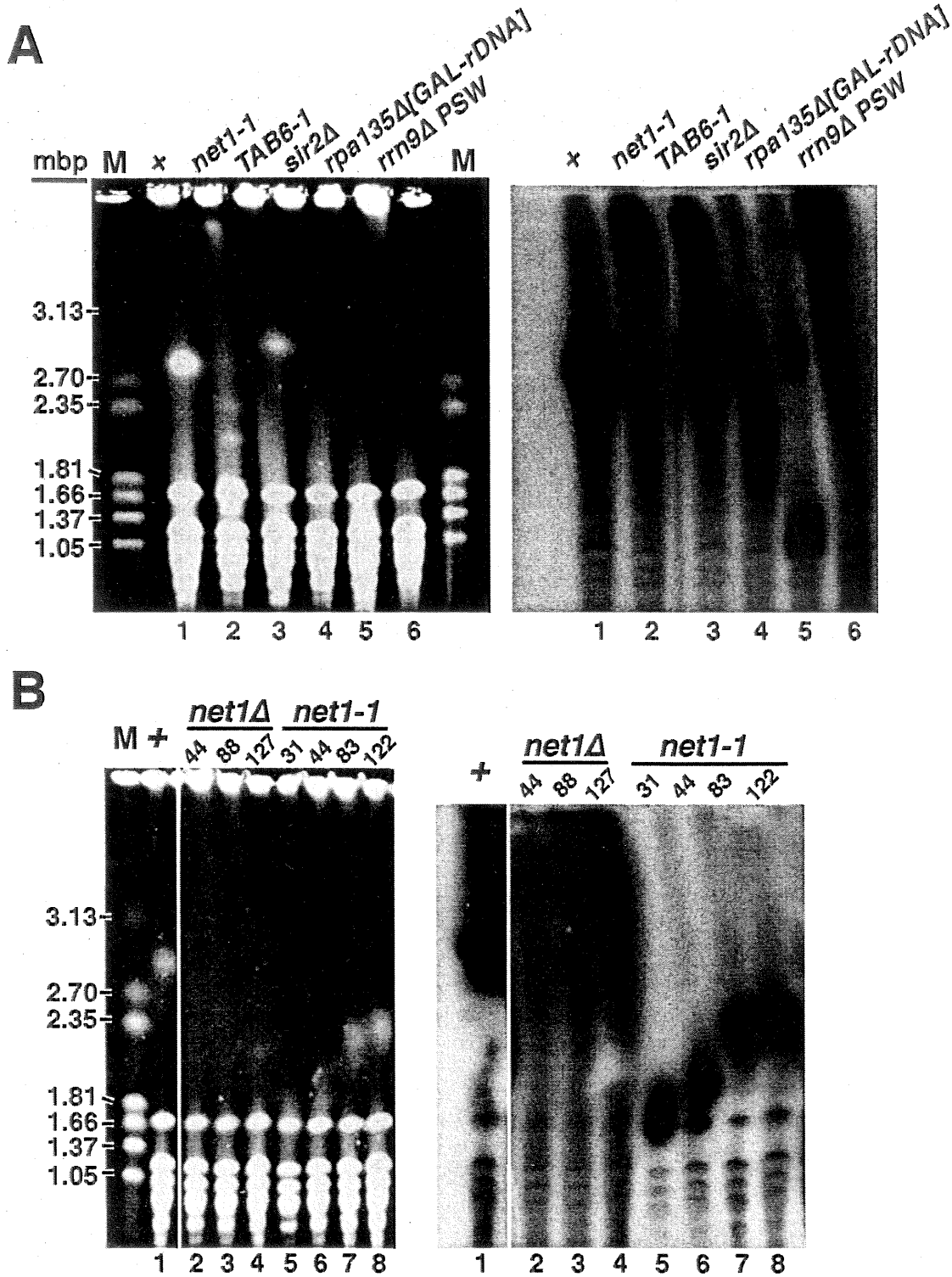
A
mbp
M
+
net1-1
TAB6-1
sir2Δ
rpa135Δ[GAL-rDNA]
rrn9Δ PSW
M
3.13
2.70
2.35
1.81
1.66
1.37
1.05
1 2 3 4 5 6
+
net1-1
TAB6-1
sir2Δ
rpa135Δ[GAL-rDNA]
rrn9Δ PSW
1 2 3 4 5 6
B
M +
net1Δ
44 88 127
net1-1
31 44 83 122
3.13
2.70
2.35
1.81
1.66
1.37
1.05
1 2 3 4 5 6 7 8
+
net1Δ
44 88 127
net1-1
31 44 83 122
1 2 3 4 5 6 7 8

Appendix III: Chromosome XII, which harbors rDNA repeats, has variable length in mutant background.

Chromosome preparations from strains grown at 25°C were separated by contour-clamped homogeneous electric field (CHEF) gel electrophoresis* (A and B). On the left are gels stained with ethidium bromide, and on the right are Southern blots probed with radio-labeled rDNA fragments. The apparent length of Chromosome XII is roughly normal in *TAB6-1*, extremely heterogeneous in *sir2Δ*, and expanded in *net1-1* and *rrn9Δ PSW* strains (A). The length increase in Chromosome XII of *net1* (which presumably resulted from rDNA repeat number expansion) occurred during continuous subculturing (B).

*The method of preparing chromosome plugs and the condition of running CHEF were obtained from M. Nomura lab. Briefly, 0.8% agarose gel in 0.5xTBE was run for 68 hours at 14°C in 0.5xTBE with angle = 120° , initial switch time = 300 sec, final switch time = 900 sec, and voltage = 3V/cm.